Université de Montréal

Regulation of chromosome condensation in *Saccharomyces cerevisiae* during mitosis

Par

Yogitha Thattikota

Département de biologie moléculaire

Institut de Recherche en Immunologie et en Cancérologie (IRIC)

Faculté de Médecine

Thèse présentée à la Faculté des médecine en vue de l'obtention du grade de Ph.D en biologie moléculaire option biologie des systèmes

Mai 2017

Résumé:

La condensation chromosomique est un processus vital nécessaire à la séparation des chromatides sœurs pendant la division cellulaire et au maintien de l'intégrité structurale de la chromatine. L'effecteur central de ce processus est un complexe de protéine pentamérique hautement conservé connu sous le nom de condensine. Le complexe de condensine se trouve dans tous les eucaryotes et est essentiel pour la viabilité. Cependant, on ne sait pas clairement comment cette condensation chromosomique est initiée au début de la mitose. Le complexe condensine est ciblé par diverses kinases du cycle cellulaire pendant la mitose. Nous avons donc émis l'hypothèse que les modifications post-traductionnelles peuvent jouer un rôle important dans l'activation précoce de la condensation en mitose. Conformément à notre hypothèse, nous avons montré que Cdk1 phosphoryle Smc4 dans le complexe de condensine tôt au cours de la mitose et initie le processus de condensation chromosomique. Il est important de noter que les phospho-mutants de *smc4* présentaient des défauts de condensation. Nous avons également découvert une étape intermédiaire au cours de ce processus, *l'intertwist*. Nous montrons en outre que la modification dépendant de CDK de la condensine régule la liaison dynamique du complexe condensine à la chromatine, favorisant ainsi un compactage efficace de la chromatine pendant la division cellulaire. Nous montrons en plus que cette liaison dynamique de condensine est régulée par VCP / p97 / Cdc48 (AAA-ATPase), une chaperone moléculaire connue pour extraire des protéines liées à la chromatine. Soutenant notre idée, nous avons observé des défauts de condensation chromosomique dans trois mutants conditionnels létals de *CDC48* (*cdc48-3, cdc48-6* et *cdc48-9*). Nous avons déterminé que le rôle de Cdc48 dans la condensation des chromosomes nécessite l'activité des cofacteurs Cdc48 Ufd1-Npl4 et que le processus dépend de l'ubiquitilation des protéines. Nous avons également déterminé que la cinétique de mobilité de la condensine sur la chromatine dépend de Cdc48. Ces observations suggèrent que Cdc48 agit comme une chaperone moléculaire pour faciliter l'extraction de condensine de la chromatine, ce qui favorise la condensation des

chromosomes. Pris ensemble, notre travail met en evidence de nouveaux mécanismes de régulation de la morphogenèse chromosomique au cours de la division cellulaire.

Mots-clés: Condensine, Smc4, phosphorylation, Cdk1, cycle cellulaire, Cdc48, Ufd1-Npl4, ubiquitination, chaperone

Abstract:

Chromosomal condensation is a vital process required for sister chromatid separation during cell division and for maintaining the structural integrity of the chromatin. The central effector of this process is a highly conserved pentameric protein complex known as condensin. The condensin complex is found in all eukaryotes and is essential for viability. However, it is not clearly known how condensin initiates chromosome condensation at the onset of mitosis. Condensin is a target for various cell cycle kinases during mitosis. So we hypothesized that post-translational modifications might play an important role in activating condensation in early mitosis. Consistent with our hypothesis, we showed that Cdk1 phosphorylates Smc4 in the condensin complex during early mitosis and initiates chromosomal condensation process. Importantly, the Smc4 phospho-mutant experienced defects in condensation. We have also uncovered an intermediate stage during this process, the intertwist. We further demonstrated that the CDK-dependent modification of condensin regulates the dynamic binding of the complex to chromatin, thereby promoting effective chromatin compaction during cell division. We showed that the dynamic binding of condensin is regulated by VCP/p97/Cdc48 (AAA-ATPase), a molecular chaperon known for extracting chromatin-bound proteins. Supporting this idea, we have observed chromosome condensation defects in three conditional-lethal mutants of *CDC48* (*cdc48-3, cdc48-6* and *cdc48-9)*. We determined that the role of Cdc48 in chromosome condensation requires the activity of Cdc48 co-factors Ufd1-Npl4 and also this process depends on protein ubiquitylation. Finally, we show that the kinetics of condensin mobility on chromatin is dependent on Cdc48. These observations suggest that Cdc48 is acting as a molecular chaperone to facilitate the removal of condensin from chromatin thereby promoting chromosome condensation. Taken together, our work highlights novel regulatory mechanisms responsible for effective chromosome morphogenesis during cell division.

Key words: Condensin, Smc4, phosphorylation, Cdk1, cell cycle, Cdc48, Ufd1-Npl4, ubiquitination, chaperon.

Acknowledgements

First and foremost, I want to thank my academic supervisor, Dr. Damien D'Amours for providing me the opportunity to work in the excellent and exceptional projects in his laboratory. I always appreciated his continuous support, the positive attitude and the free work environment provided during my work in his lab.

I also extend my gratitude to the committee members Dr. Sébastien Carréno, Dr. Gary Brouhard and Dr. Pascal Chartrand for their valuable comments during my annual committee meetings, which helped me to improve the quality of my projects.

I would like to thank all the academic staff at IRIC and UdeM for their constant support during my Ph.D. I am grateful to the FESP for tuition exemption scholarship and Molecular biology program for merit scholarship given to me to support my Ph.D. studies here.

Many thanks to Dr. Erika and Dr. Sylvain for their help in microscopy and comments on manuscripts. I am also thankful to Dr. Claire Brown, Dr. Mike Tyers for the generous support to use experimental setups in their labs and also extending their support and comments on my manuscripts. I am grateful to Dr. Alain Verreault and Dr. Benjamin Kwok for their helpful discussions and comments. I especially thank Dr. Jackie Vogel for allowing me to work in her lab at McGill University for microscopy experiments.

I am thankful to the past and present members of D'Amours lab for many productive scientific and non-scientific discussions. I am grateful to Dr. Xavier, Mirela (best nanny in the world) for teaching me yeast genetics and sharing their expertise. Special thanks to Dr. Julie St-Pierre for providing her help in qPCR analysis and comments given for my manuscripts. I would like to thank Dr. Hery, Dr. Diego, Dhanaraman, Guillaume and Dr. Roger for their constant support and encouragement. I am especially thankful to Justine Vinet for the help in my second

project. I would like to thank all of my friends for all their love and support. Big thanks to you, Rahul, for your support, care and being my family especially when I was far away from them.

Finally, I would like to thank my family members for their unconditional love and support to pursue my career interests. Thank you, Mommy, (Mrs. Kamaleshwari) and Dady (Mr. Venkateswara Rao) for providing me everything and encouraging me in pursuing higher studies. It is you both who made me stronger and confident. I would like to thank my Uncle (Mr. Trinadha Rao), Aunty (Mrs. Malthi), Sister (Mrs. Santoshi) and Brother-in-law (Mr. Venkatachalam) who was there for me supporting at every big step of my life. Thank you all my sweet younger sisters and brothers for your support. Last but not least, thank you Pravy for your love, support, and patience. You are my inspiration to come to research and thank you for being my best friend.

Table of contents:

List of Figures:

Chapter I:

Chapter II:

Chapter III:

List of Tables:

Chapter I:

Chapter II:

Chapter III:

List of abbreviations:

AAA	ATPase associated various cellular activities
ABC	ATP-binding cassette
ADH1	Alcohol dehydrogenase 1
AEBSF	4-(2-aminoethyl)benzenesulfonyl fluoride hydrochloride
AFM	Atomic force microscope
AID	Auxin induced degron
APC	Anaphase promoting complex
Ark1	Aurora related kinase 1
ATM	Ataxia-telangiectasia mutated
ATP	Adenosine triphosphate
ATR	Ataxia-telangiectasia and Rad3 related
BSA	Bovine serum albumin
Brn1	Homologue of Barren
Cak1	Cyclin dependent kinase activating kinase 1
Cdc	Cell division cycle
Cdk	Cyclin Dependent Kinase
Cse4	Chromosome segregation 4
CEN	Centromere
CENP-A	Centromere protein A
ChIP	Chromatin immune precipitation
CK2	Casein kinase 2
Clb	Cyclin B
Cln	Cyclin
CMG	Cdc45-MCM2-7-GINS
Csm4	Chromosome segregation meiosis 4
CycBox	Cyclin binding box
Cyt	Cytoplasmic
DAPI	4',6-diamidino-2-phenylindole

DIC	Differential interference contrast
Dm	Drosophila melanogaster
DNA	Deoxyribonucleic acid
DTT	Dithiothreitol
E-64	Trans-Epoxysuccinyl L-leucylamido(4-guanido) butane
ECL	Enhanced chemiluminescence
EDTA	Ethylene-diamine-tetra-acetic acid
EGFP	Enhanced green fluorescent protein
Esa1	Essential SAS 1
Esp1	Extra spindle pole bodies
EXP	Exponential
FEAR	Cdc Fourteen Early Anaphase Release
FISH	Fluorescence in situ hybridization
FITC	Fluorescein isothiocyanate
FOV	Field of view
G1-phase	Gap 1-phase
G2-phase	Gap 2-phase
GAL1	Galactose metabolism 1
GFP	Green Flurescent protein
Glc7	Glycogen 7
H1	Histone 1
H2A	Histone 2A
H2B	Histone 2B
H3	Histone 3
H4	Histone 4
HA	Human influenza Hemagglutinin
HAT	Histone acetyl transferase
HCl	Hydrochloric acid
HEAT	Huntingtin-elongation factor 3-protein phosphatase 2A -yeast kinase TOR1

HeLa	Henrietta Lacks
HEPES	4-(2-hydroxyethyl)-1-piperazine ethane sulfonic acid
HIS3	Histidine 3
HR	Homologous recombination
HRP	Horse radish peroxidase
Hs	Homo sapiens
HTA1	Histone h two A 1
HU	Hydroxyurea
IAA	Indole-3-acetic acid
INO80	Inositol requiring 80
IP	Immuno precipitate
Ipl1	Increase in ploidy
KCl	Potassium chloride
kDa	Kilo Dalton
NaF	Sodium fluoride
LC-MS	Liquid chromatography-mass spectrometry
Li	*Leishmania infantum*
LiCl	Lithium Chloride
Lrs1	Loss of RDNA silencing
M-phase	Mitotic phase
MCC	Mitotic checkpoint complex
Mcd1	Mitotic chromosome determinant
MCM	Mini-chromosome maintenance
MEN	Mitotic Exit Network
MWW	Mann-Whitney-Wilcoxon
Ni-NTA	Nickle-Nitrylo tri acetic acid
NLS	Nuclear localization signal
NM-PP1	1-(1,1-dimethylethyl)-3-(1-naphthalenylmethyl)-1H-pyrazole(3,4-d) pyrimidin-4-amine
Npl4	Nuclear protein localization 4

NT	N (Amino)-terminal
oriC	Origin of replication
ORF	Open reading frame
Otu1	Ovarian tumor 1
Os	Oriza sativa
PAGE	Polyacrylamide gel electrophoresis
PBS	Phosphate buffer saline
PCR	Polymerase chain reaction
Pds1	Precocious dissociation of sisters
Pgal1	Promoter Galactose 1
Pgk1	3-PhosphoGlycerate kinase 1
pH	Potential of hydrogen
PI	Propidium iodide
Plk1	Polo-like kinase 1
PP2A	Protein Phosphatase 2A
PPH	Protein Phosphatase
PSF	Point spread function
qPCR	Quantitative PCR
Rad52	Radiation sensitive
RDN	Ribosomal DNA
rDNA	Ribosomal DNA
RICS	Raster image correlation spectroscopy
Rvb2	RuvB like 2
S	Serine
S	Svedberg (Sedimentation coefficient unit)
S-phase	Synthetic-phase
SAC	Spindle assembly checkpoint
SAGA	Spt-Ada-Gcn5 acetyl transferase
San1	Sir Antagonist 1
Sc	Saccharomyces cerevisiae

Scc	Sister chromatid cohesion
SD	Standard deviation
SDS	Sodium dodecyl sufate
Si	*Setaria italica*
Sic1	Substrate/Subunit inhibitor of cyclin-dependent protein kinase
SMC	Structural maintenance chromosomes
Smc	Structural maintenance chromosomes
Sp	Schizosaccharomyces pombe
SPB	Spindle pole bodies
Swr1	Swi/snf2 related
STII	Strep tag II
SSB	Single strand break
SUMO	Small ubiquitin like modifier
Swe1	Saccharomyces WEe1
Tb	*Trypanosoma brucei brucei*
TCA	Tricholo acetic acid
TE	Tris-EDTA
TFIIIC	Transcription factor complex
TIR1	Tip 1 related
Topo II	Topoisomerase II
ts	Thermo sensitive
tetO	Tetracyclin operator
tetR	Tetracyclin repressor
Ub	Ubiquitin
Uba 1	Ubiquitin activating 1
Ubc 9	Ubiquitin conjugating 9
Ubx	Ubiquitin regulatory X
Ufd1	Ubiquitin degradation 1
URA3	Uracil requiring 3
VCP	Vasoline containing protein

Vms1	VCP/Cdc48-associated mitochondrial stress-responsive 1
WB	Western blot
Wss1	Weak suppressor of Smt3
Ycg1	Yeast cap G
YCp	Yeast centromeric plasmid
Ycs4	Yeast condensin subunit 4
YES-A	Yeast extract sucrose-agar
YIp	Yeast replicating plasmid

Dedicated to my Mom, Dad

&

to my great teachers who taught me during

my journey

from alphabets to Yeast genetics….

Chapter I: General Introduction

1.1 The cell division cycle:

The cell is the fundamental unit of life. In the 17th century, Robert Hooke for the first time observed cells under his simple microscope. Two hundred years after the discovery of cells, Walter Flemming observed thread-like structures under the microscope and named them as "chromatin" (Flemming, 1882). He observed that these thread-like structures divided inside the nucleus and named this process of nuclear division as "mitosis" after the Greek word for thread. Wilhelm von Waldeyer-Hartz named these thread like structures as chromosomes. Later it was shown that chromosomes that carry the genetic material are composed of DNA and proteins. Faithful transmission of this genetic material during cell division from generation to generation forms the basis for continuity of life (Morgan, 1915). It has been centuries since the discovery of cells, but still, the cell division cycle continues to fascinate the scientists.

1.2 The model organism:

Saccharomyces cerevisiae, which I have used for my studies, is well known for many centuries for making bread and beer. It is commonly known as bakers yeast or brewers yeast. It is also an excellent model organism to study many eukaryotic processes. Leland Hartwell first identified many genes responsible for cell cycle using this amazing model system. Yeast is an unicellular eukaryote, which can exist in haploid (one copy of each gene) or diploid (two copies of each gene) state. *Saccharomyces cerevisiae* undergoes both asexual and sexual life cycles. The asexual life cycle proceeds through budding (a small bleb or bud formed from the parent cell), which is how the budding yeast got its common name. The sexual life cycle involves mating of two haploid cells **a** and **α** to form a diploid cell. Under poor nutrient conditions, this diploid goes through meiosis and sporulation to form four haploid spores (Figure 1) (Herskowitz, 1988). These genetic features enable a scientist to delete genes or integrate markers and transform plasmids

making yeast a powerful genetic tool to study different aspects of eukaryotic cellular processes. Having these advantages also enable us to study the genetic interaction between various genes. Another unique feature of yeast is to have temperature sensitive mutants to study essential genes involved in different processes, which made it as a premier model system.

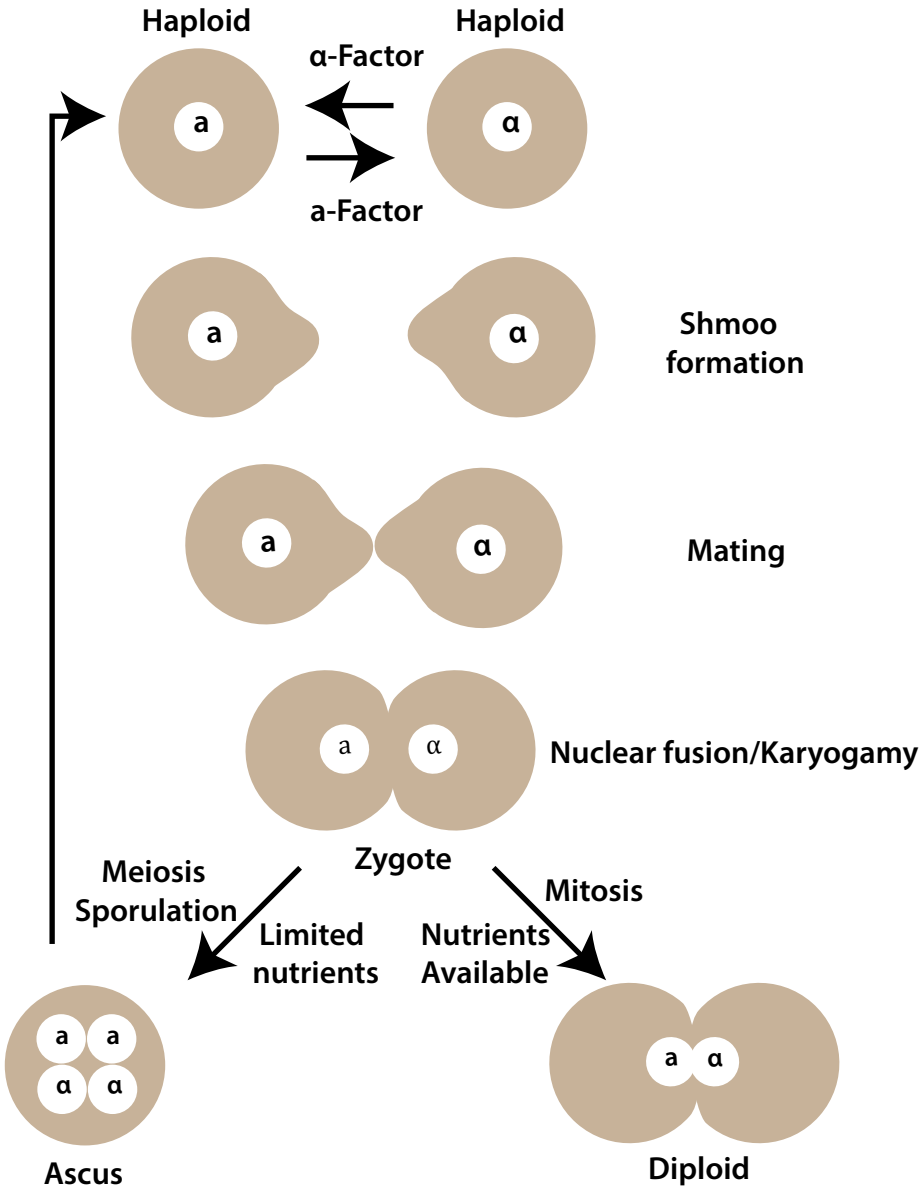

Figure 1: ***Saccharomyces cerevisiae*** **life cycle.** The graphical representation showing budding yeast mating type a or α recognizes pheromone release by opposite mating type and this initiate shmoo formation. Mating between a and α cells leads to nuclear fusion forming a zygote which can form haploid cells via sporulation or diploid cells via mitotic division.

1.3 Stages of eukaryotic cell cycle:

The cell division cycle is a highly organized and tightly regulated sequence of events (Nurse et al., 1998). In eukaryotes, the cell division is comprised of two phases: interphase and mitosis (Figure 2). Budding yeast divides asymmetrically to produce two distinct types of cells. Its cell division cycle is similar to that of higher eukaryotes with some exceptions.

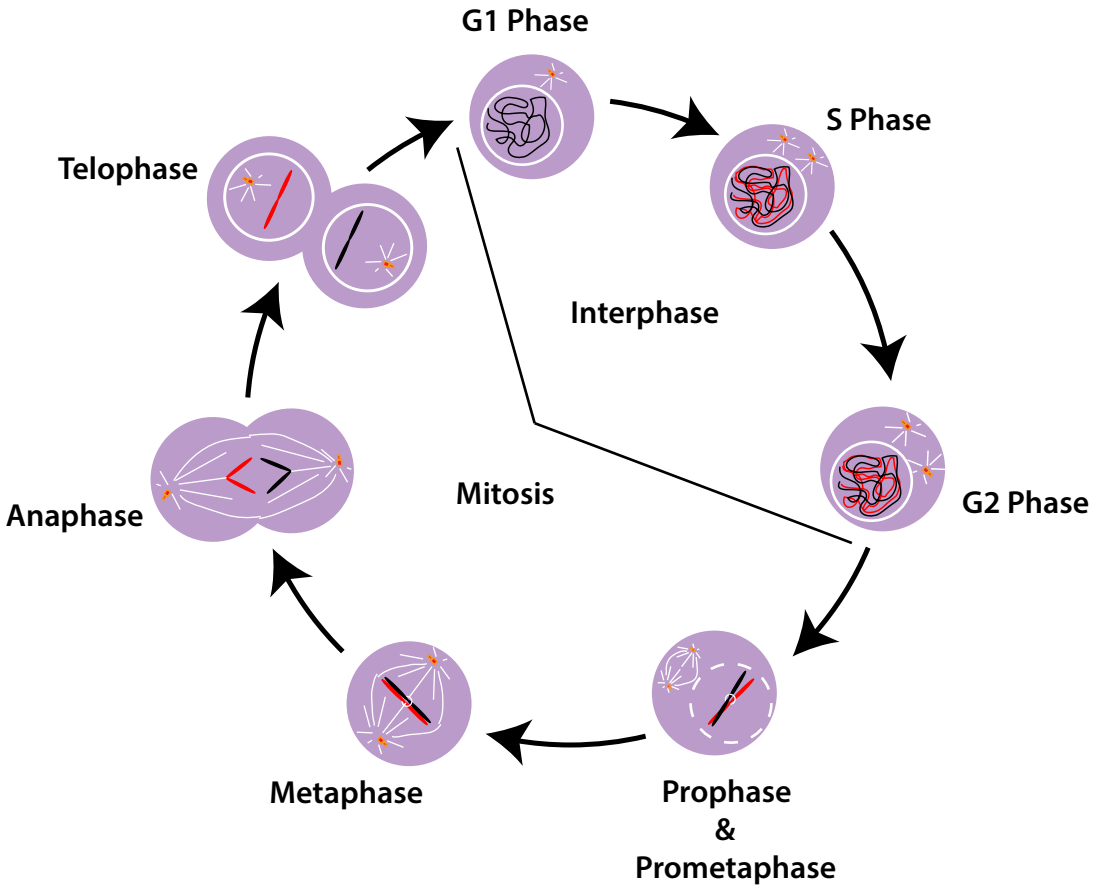

Figure 2: The cell division cycle. Graphical representation of different stages in the eukaryotic cell cycle is shown.

1.3.1 Interphase:

Interphase comprised of G1 (Gap1), S (synthesis) and G2 (Gap2) phases. During G1, the cell rapidly grows and synthesizes cellular components required for subsequent cell cycle progression. The G1 phase is followed by S-phase where DNA replicates to double the genome content. Replication should occur once per cell cycle and in yeast, initiation of DNA synthesis involves assembly of the pre-replication complex at an origin of replication during G1 phase (Diffley, 2004). In early S-phase, centrosomes/spindle pole bodies (SPB in yeast) duplication occurs (Winey & O'Toole, 2001). During S-phase, canonical histones (H3, H4, H2A and H2B) are deposited onto chromatin and cohesion is established (Marston, 2014; Weber & Henikoff, 2014). In yeast, spindle formation starts during early S-phase compared to other higher eukaryotes. After DNA replication, cells enter G2-phase where it continues to grow and make sure it is ready to enter mitosis. In yeast, G2-phase is very short or inexistent. In eukaryotes, three major events like spindle formation, nuclear envelope breakdown and chromosome condensation have to happen upon entry into mitosis.

1.3.2 Mitosis:

During mitosis, the chromatin divides equally into two sister chromatids. Mitosis starts after the G2 checkpoint has been satisfied. Mitosis is comprised of five important phases: prophase, prometaphase, metaphase, anaphase and telophase. After the mitosis, two daughter cells separate as a result of cytokinesis (Morgan, 2007).

Prophase: This phase is characterized by condensation of chromosomes with the help of histone and non-histone proteins. Chromosome condensation is the first visible step

during mitosis. Centrosomes/SPB moves towards opposite poles to form mitotic spindles. Centrosomes/SPB are microtubule-organizing centers for mitotic spindles.

Prometaphase: The next step after prophase is prometaphase where the nuclear envelope breakdown happens and microtubules attach to the kinetochores on chromosomes. Unlike higher eukaryotes, in budding yeast nuclear envelope breakdown does not occur, hence it is called a closed mitosis (Smoyer & Jaspersen, 2014).

Metaphase: In metaphase, the sister chromatids are attached to microtubules from opposite poles of the cells ensuring bipolar attachment. Then these microtubules pull two sister chromatids, which are, held together by cohesion. This creates tension between chromatids, which results in the proper alignment of spindles on the metaphase plate between the two poles (Winey & O'Toole, 2001). Metaphase plate formation is observed in higher eukaryotes. However, in live yeast cells metaphase formation is not observed (Straight et al., 1997)

Anaphase: This phase includes anaphase-A (movement of kinetochores towards poles) and anaphase-B (increase in the distance between the two poles). In budding yeast, both anaphase-A and -B exists (Winey & O'Toole, 2001). Once the chromosomes are condensed and aligned properly on the metaphase plate, the spindle tension triggers the action of the anaphase-promoting complex (APC) to dissolve cohesion links holding the two sister chromatids. This action allows the separation of two sister chromatids. At the metaphase-anaphase transition, inactivation of Cdk1 is also initiated. Later, exit from mitosis is activated by dephosphorylation of many Cdk1 substrates by PP2A in higher eukaryotes and Cdc14 phosphatase in yeast. Cdc14 is bound to its inhibitor Net1 and localized to the nucleolus. During anaphase, two important pathways; FEAR (Cdc Fourteen Early Anaphase Release) and MEN (Mitotic Exit Network), trigger the release of Cdc14 from Net1 (Bardin & Amon, 2001; D'Amours et al., 2004; Stegmeier & Amon, 2004).

Telophase: During telophase, the sister chromatids are fully separated into two nuclei. Cdc14 phosphatase triggers the complete inactivation of Cdk1 by ubiquitin dependent APC system. Chromosomes start to decondense at this stage. Nuclear envelope reformation and microtubule dissolution occurs around the newly formed nucleus and leads the cells to exit from mitosis and enter the cytokinesis stage.

Cytokinesis: The nuclear division (mitosis) is followed by the separation of cellular components to form two individual cells during cytokinesis. In higher eukaryotes, cleavage furrow appears at the cell equator followed by the assembly of a actomyosin contractile ring. Further contraction of this ring followed by abscission leads to the separation of two daughter cells with equal distribution of cytoplasmic contents (Guertin et al., 2002). In budding yeast, cytokinesis comprises: the actomyosin ring formation at the bud neck and chitinous cell wall as well as septum formation. Later this septum is degraded by a sequence of digestive enzymes to separate the two individual cells (Bhavsar-Jog & Bi, 2016).

1.4 Cell cycle checkpoints/transitions:

Checkpoints are surveillance mechanisms that ensure proper sister chromatid segregation during the cell cycle. There are several checkpoints, which transiently arrest cells in G1, S, G2 and M phase if the cellular machinery senses any alteration in cell size, DNA replication and spindle assembly during cell division.

G1 checkpoint: Prior to G1-S transition, cells go through START (the commitment to replication) and it allows the cells to commit to cell cycle based on the availability of nutrients, the presence of mating pheromones and absence of DNA damage. The alternative fate of cells before START is mating, but after START, the cell must undergo replication and cell division (Cross, 1995).

Replication checkpoint: This checkpoint ensures the fidelity and progression of DNA replication in response to stalled replication forks. The replication checkpoint delays the origin of replication (oriC) firing and helps in the proper progression of replication (Nyberg et al., 2002; Rhind & Russell, 1998).

G2 checkpoint: It is the next major checkpoint to monitor DNA damage. Any damage to DNA initiates the activation of signaling events that inhibits mitotic entry. Important early responsive protein kinases for damage such as ATM/ATR family kinases that phosphorylate different proteins, which regulate cell cycle progression, and damage repair processes. Checkpoint kinases (Chk1 and Chk2) works downstream of ATM/ATR kinases. In higher eukaryotes, Chk1 and Chk2 negatively regulate Cdc25C and also phosphorylate Wee1 kinase. This Wee1 kinase further increases inhibitory phosphorylation of Cdc2 thereby arresting cells in G2 phase. In budding yeast, Chk1 phosphorylates Pds1 preventing its degradation thereby maintaining an efficient G2 checkpoint arrest (Callegari & Kelly, 2007; Nyberg et al., 2002).

Spindle assembly checkpoint (SAC): SAC ensures that one sister chromatid of each pair is attached to microtubules from opposite poles. The onset of anaphase is delayed until all chromosomes are attached in a bipolar fashion. SAC ensures this delay prior to anaphase in the case of improper attachment of spindle during mitosis (Amon, 1999). In addition to microtubule attachment to kinetochores, spindle tension also plays a role in regulating SAC. Stretching the chromatids at the centromere in bi-oriented condition creates tension and inactivates SAC (also in case of merotelic attachment – one kinetochore attached to microtubules coming from opposite poles). Low tension leads to destabilization of microtubule kinetochore attachment (in case of syntelic attachment – both sister kinetochore attached to microtubules from same pole). Mitotic checkpoint complex (Guertin et al., 2002) proteins like Mad2, Mad3, Bub3 and Cdc20 are involved in the regulation of SAC activation (Joglekar, 2016).

1.5 Cell cycle regulation by Cdk1:

Cdk1 is the major protein kinase in mitosis, which is involved in the regulation of different cell cycle stages by associating with various cyclins. *S. cerevisiae* has a single Cdk1 (Cdc28 – Cell division cycle 28). The typical consensus site for Cdk1 phosphorylation is S/T-P-X-K/R (where S/T – serine/threonine; X represents any amino acid; K/R – lysine/arginine) and sometimes, a minimal site (S/T-P) is enough to promote phosphorylation (Moreno & Nurse, 1990; Nigg, 1993). Cyclin binding to Cdk1, however, is not sufficient to activate Cdk1; it requires activating phosphorylation at important residues. In budding yeast, Cak1 (cyclin-dependent kinase activating kinase) phosphorylate Cdk1 (at Threonine-169 located in T-loop) and activate its binding to different substrates and its kinase activity (Espinoza et al., 1996; Kaldis et al., 1996). Cdk1 activity is further regulated by its phosphorylation at tyrosine-19 by Swe1 kinase (Booher et al., 1993). In G1, Cdk1 associates with three cyclins Cln1, 2 and 3. Cln2 and Cln3 are important for G1 to S transition. As cells progress through G1, Cln-Cdk1 complex phosphorylates Sic1, leading to its degradation. As Sic1 is an inhibitor of the kinase activity of Clb5-6 /Cdc28 complex, its degradation during late G1 facilitates G1-S transition (Verma et al., 1997). Late G1-phase is also marked with low Cln levels which initiate START and subsequently, licensing factors (MCM2-7 helicases) are loaded onto replication origins to initiate the DNA replication process (Diffley, 2004). After completion of S-phase, activation of mitotic cyclin-Cdk1 complex leads to entry into mitosis. Clb1, 2, 3 and 4 are the cyclins associate with Cdk1 during mitosis. At the end of mitosis, mitotic cyclins are degraded by ubiquitin-mediated proteolysis through APC and proteasome. The APC (an E3 ubiquitin ligase) associates with its regulatory subunits (Cdc20 at anaphase onset, Cdh1 later in mitotic exit) to trigger cascades of protein degradation (King et al., 1995). Two different models: quantitative and substrate specificity models were proposed to describe cell cycle regulation by Cdk1 activity. In the quantitative model, different levels of cyclin–Cdk1 trigger the activation of different stages of cell cycle (Coudreuse & Nurse, 2010; Stern & Nurse, 1996). Whereas, in the substrate specificity model, cyclin-Cdk1 recognizes different substrates based on their specific binding sites and thereby regulate different stages of the cell cycle (Koivomagi et al., 2011).

1.6 Sister chromatid cohesion:

The end product of DNA replication is the formation of two sister chromatids and it is important that they remain connected until the anaphase-metaphase transition. This physical connection is known as sister chromatid cohesion (Nasmyth & Haering, 2009) and it is maintained by a well-conserved protein complex called cohesin (Guacci et al., 1994; Michaelis et al., 1997; Peters et al., 2008). Cohesion is established during replication by cohesin deposition on DNA. Cohesin is made up of two SMC (Structural Maintenance Chromosomes) proteins, Smc1 and Smc3 as well as two non-SMC proteins, Scc1 and Scc3 (Nasmyth & Haering, 2005). Cohesin binds to DNA topologically in a ring shaped structure (Anderson et al., 2002; Haering et al., 2002). In budding yeast, cohesion destruction happens at the onset of anaphase. Once the spindle assembly checkpoint is satisfied, APC-mediated degradation of securin (Pds1) releases the separase (Esp1), which cleaves the cohesin subunit Scc1 (Uhlmann et al., 1999). This cleavage of cohesin leads to anaphase onset for the proper separation of sister chromatids. However, sister chromatid cohesion at the rDNA (ribosomal DNA) locus is independent of cohesin and it is dissolved later during anaphase in a Cdc14 and condensin dependent manner (D'Amours et al., 2004).

1.7 Chromosome condensation:

At the onset of mitosis, chromosomes undergo major compaction and re-organization to form mitotic chromosomes. This process of chromosome organization is known as chromosome condensation. It is an essential process and is required for faithful segregation of sister chromatids during mitosis. During replication, the DNA content is doubled and this DNA needs to be compacted in a way to confine it to the nuclear compartments. The chromosomal organization is not simply compaction of linear DNA but a sequential hierarchical organization by removing topological tangles between sister chromatids and maintaining chromosome rigidity. These features of condensed

chromosomes are important to withstand the mechanical force created by sister chromatid separation.

The first level of chromosome organization is achieved with 140bp of DNA wrapping around core histone proteins (H2A, H2B, H3 and H4) to form the nucleosome. These nucleosomes are connected with linker histone H1. The second level of organization occurs with the coiling of these nucleosomes to create a helical structure (30 nm fiber) and further folding of these structures results into higher order structures such as scaffolds and loops. However, the existence of 30 nm fiber structures *in vivo* was not observed (Maeshima et al., 2010). Several models were proposed to explain the mitotic chromosome organization like loops-on-a scaffold model (DNA form loop structures on top of the nucleosome and it forms scaffold like structure with non-histone proteins), hierarchical model (different levels of nucleosome folding) and chromatin network model (chromosomes formed by crosslinking of distant DNA fibers and proteins) (Maeshima & Eltsov, 2008; Swedlow & Hirano, 2003). However, it is not completely understood how chromosome condensation is orchestrated to achieve this hierarchical folding. Multiple factors like condensin complex, histones and DNA topoisomerase II (Topo II) are involved in the regulation of this essential process. Among these, condensin is the main protein complex involved in chromosome condensation.

1.7.1 Condensin:

The condensin complex belongs to a group of protein complexes containing unique subunits of the SMC family along with cohesin and Smc5-6 complex. SMC members play major roles in chromosome condensation, sister chromatid cohesion and DNA repair processes (Uhlmann, 2016). The condensin complex was first isolated from *Xenopus laevis* egg extracts as two major forms with sedimentation coefficients 13S and 8S (Hirano & Mitchison, 1994) and later also found in yeast and vertebrates (Csankovszki et al., 2009; Freeman et al., 2000; Hirano et al., 1997; Lavoie et al., 2000; Ouspenski et al.,

2000; Saka et al., 1994; Strunnikov et al., 1995). The condensin complex is composed of two SMC subunits and three non-SMC regulatory subunits (Bazile et al., 2010; Hirano, 2016).

Both budding and fission yeast contain only one condensin complex, but in higher eukaryotes, second type of condensin complex is also present (condensin-II). In *Caenorhabditis elegans,* a third type of condensin complex (condensin I_{DC}) is present, which is involved in dosage compensation (Csankovszki et al., 2009). Condensin-I & II have identical SMC subunits but use different regulatory non-SMC subunits (Table I). Bacteria and archaea also have condensin-like complexes composed of SMC/MukB, ScpA/MukF, ScpB/MukE (Graumann & Knust, 2009; Hiraga, 2000).

Complex	*Saccharomyces cerevisae*	*Schizosaccharomyces pombe*	*Caenorhabditis elegans*	*Drosophila melanogaster*	*Xenopus laevis*	Human
Condensin I	Smc2	Smc2	MIX-1	DmSmc2	XCAP-E	hCAP-E
	Smc4	Smc4	SMC-4	DmSmc4/ glucon	XCAP-C	hCAP-C
	Brn1	Cnd3	DPY-26	barren	XCAP-H	hCAP-H
	Ycs4	Cnd1	DPY-28	Cap-D2	XCAP-D2	hCAP-D2
	Ycg1	Cnd2	CAP-G1	Cap-G	XCAP-G	hCAP-G
Condensin II	—	—	MIX-1	Smc2	XCAP-E	hCAP-E
			SMC-4	Smc2	XCAP-C	hCAP-C
			KLE-2	Cap-H2	XCAP-H2	hCAP-H2
			HCP-6	Cap-D3	XCAP-D3	hCAP-D3
			CAP-G2	—	XCAP-G2	hCAP-G2
Condensin I_{DC}	—	—	MIX1	—	—	—
			DPY-27			
			DPY-26			
			DPY-28			
			CAP-G1			

Table 1: List of condensin complexes and their subunits in different eukaryotes.

1.7.1.1 Architecture of condensin:

SMC proteins are characterized by the presence of conserved amino-terminal (N-terminus) and carboxy-terminal (C-terminus) head domains and a middle hinge domain. Each SMC subunit contains N-terminal Walker-A and C-terminal Walker-B motifs, which folds back to form a long antiparallel coiled-coil that connects to the globular hinge domain (Anderson et al., 2002). The two SMC subunits combine to form a heterodimer by association at their hinge domain that results in a V- shaped molecule, forming an ABC type ATPase (Saitoh et al., 1994). The V-shaped ATPase heterodimer is predicted to hold 2 ATP molecules (Lammens et al., 2004). The regulatory subunits Brn1, Ycs4 and Ycg1 binds to the SMC heterodimer forming a pentameric complex. The kleisin subunit (Brn1) binds to N- and C-terminus of Smc2 and Smc4, respectively. The two HEAT repeat containing subunits (Ycs4 & Ycg1) bind to the kleisin subunit. Previous studies proposed that this pentameric condensin complex binds as a ring like structure around the DNA (Cuylen et al., 2011), but so far the mechanistic details are poorly understood.

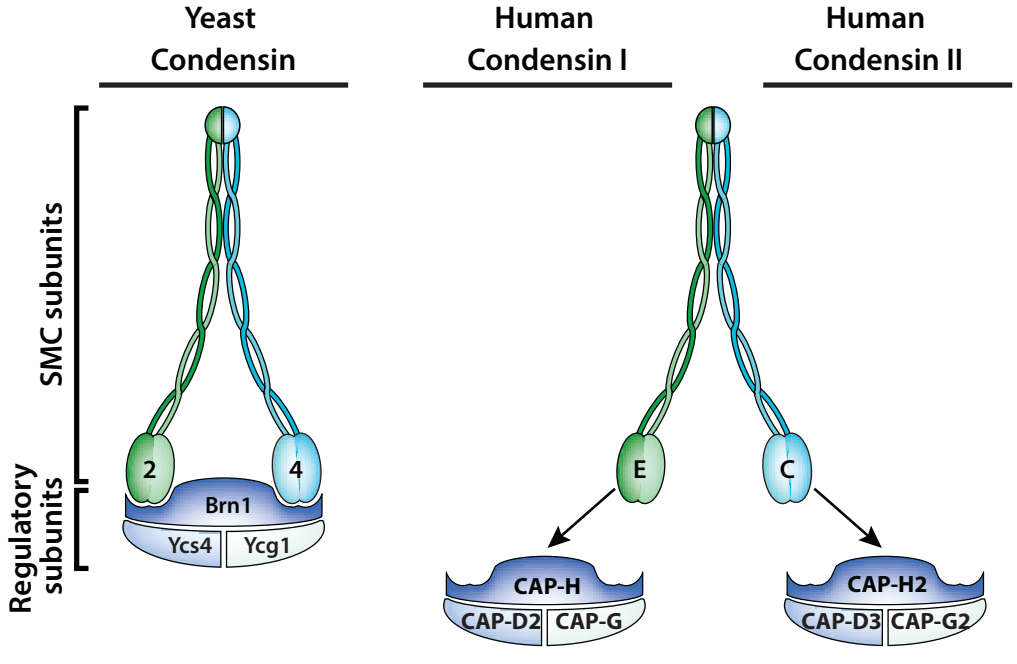

Adapted from Bazile *et al.* 2010

Figure 3: Schematic representation of condensin complex in yeast and human.

Electron microscopy studies on Smc2-4 dimers revealed different conformations including "V", "O", "B" or "P" shaped structures (Figure 4) (Anderson 2002, Eeftens 2016). These conformations help to predict molecular mechanism of condensin action on chromosome condensation.

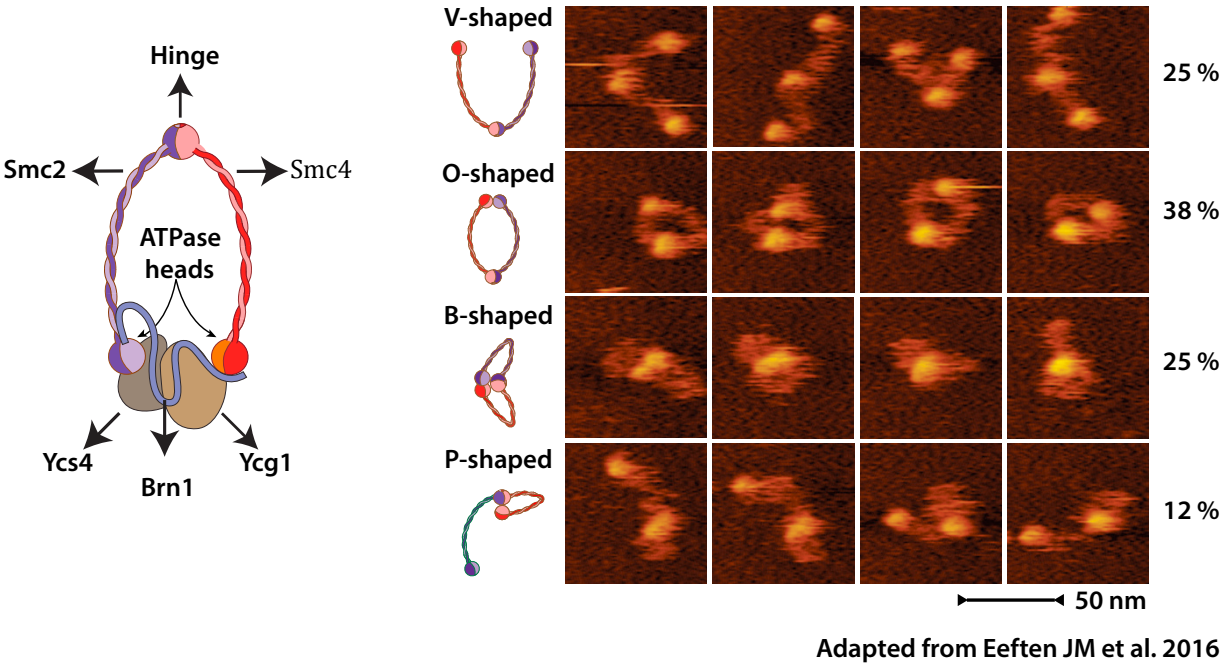

Figure 4: Different conformations of yeast condensin complex. On the left, graphical representation of the condensin complex with different subunits is shown. On the right, images from AFM along with the percentage of observed shapes and graphical representation of the corresponding conformation are shown.

1.7.1.2 Subcellular localization of condensin complex:

The subcellular localization pattern of condensin varies according to cell cycle events in

different organisms. In *Saccharomyces cerevisiae*, condensin always localizes in the nucleus (Bhalla et al., 2002; D'Ambrosio et al., 2008; Freeman et al., 2000), but in *S. pombe* condensin localizes to the cytoplasm during interphase and translocate into the nucleus in a Cdk1 phosphorylation-dependent manner during mitosis. (Sutani et al., 1999). Similarly, in vertebrates, condensin-I is localized to the cytoplasm and translocates onto the chromatin after nuclear envelope break down. In contrast, the localization of condensin-II is always restricted to the nucleus (Collette et al., 2011; Gerlich et al., 2006; Oliveira et al., 2007).

1.7.1.3 Condensin binding onto chromatin:

Condensin binding onto chromatin is important to mediate the folding of chromatin fibers into the hierarchical state. It has been shown earlier that condensin association with chromatin is highly dynamic (Gerlich et al., 2006). In budding yeast, condensin loading is facilitated by Scc2-4, TFIIIC and monopolin subunits: Csm1 and Lrs4 (D'Ambrosio et al., 2008; Johzuka & Horiuchi, 2009). In *S. pombe*, condensin loading is facilitated by monopolin subunits Pcs1 and Mde4 (Tada et al., 2011). Various *in vitro* studies have demonstrated that ATP is required for condensin binding onto DNA and ATPase-defective mutants shown to be impaired in DNA binding (Hirano et al., 2001; Hudson et al., 2008; Kinoshita et al., 2015). Condensin binding sites on chromatin includes highly transcribed regions, centromeres, rDNA locus and along the chromosome arms (D'Ambrosio et al., 2008).

1.7.1.4 Functions of condensin complex:

Condensin is one of the main players in chromosome condensation process. It was first described from *Xenopus* cell free extracts as a major component that assembles chromosomes. Condensin is proposed to induce compaction of DNA based on two of its functions characterized *in vitro*: the role of inducing ATP-dependent positive supercoils and ATP independent DNA reannealing activity (Hirano, 2005; Kimura & Hirano, 1997;

St-Pierre et al., 2009; Sutani & Yanagida, 1997). Condensin also helps in decatenation of positive supercoils in the presence of Topo II (Baxter et al., 2011). Recent evidence also shows that condensin loading on reconstituted chromatid is dependent on ATP (Kinoshita et al., 2015; Shintomi et al., 2015). Condensin I is important for lateral compaction and condensin II for axial compaction (Shintomi & Hirano, 2011). Together, the studies described above suggests the condensin role in the compaction of DNA but the precise mechanism underlying this process is yet to be determined.

There are different models proposed to explain the mechanism of action of condensin such as the loop extrusion model and the chromatin folding or supercoiling model (Elnaz alipour 2002, Hirano 2006, Hirano 2016). In loop extrusion model, DNA passes through the condensin ring forming a loop structure. In chromatin folding or supercoiling model, multiple condensin molecules bring the chromatin together by supercoiling activity and thus forming chiral loops (Figure 5). Further folding of these loop structures leads to more compacted chromatin. These two models favour the formation of loop collision between lateral loops, which leads to the formation of tangles and it is proposed that Topo II may be involved in resolving these tangles.

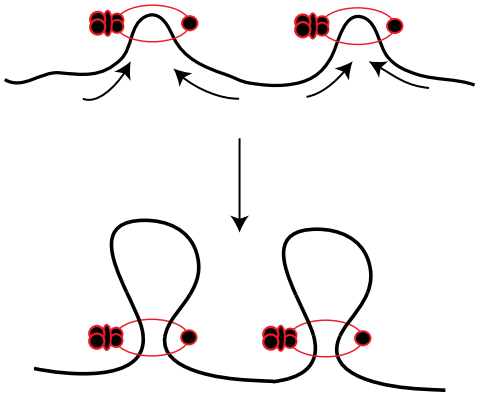

Loop extrusion model

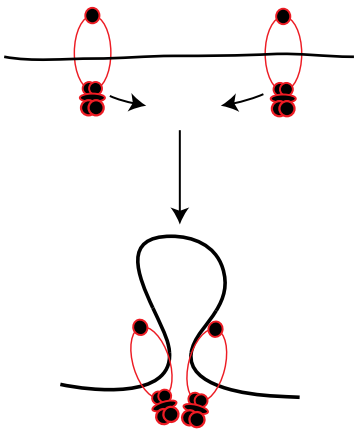

Chromatin folding/supercoil model

Figure 5: Models to explain the molecular mechanism of chromosome condensation by condensin complex. The graphical representations of loop extrusion (left) and chromatin folding/supercoiling models (right) are shown.

In addition to chromosome condensation, the condensin complex also mediates other cellular processes. Condensin is important for rDNA segregation in yeast. rDNA locus in yeast is composed of 150-200 repeats of ~9.1kb each (Venema & Tollervey, 1999) and it is known as a late replicating locus. It has been shown that the condensin subunit, Ycs4, is SUMOylated in a Cdc14 dependent manner to promote rDNA segregation during anaphase (D'Amours et al., 2004). Condensin also regulates gene expression. In yeast, it has been shown that condensin regulates the HMR locus (mating locus) silencing (Bhalla et al., 2002) and in *Drosophila* kleisin subunit (Barren) along with Topo II regulates epigenetic gene expression (Lupo et al., 2001). Further, Ycs4 analog in *C. elegans* is important for dosage compensation (Csankovszki et al., 2009).

Another interesting role of condensin is its involvement in DNA repair processes such as excision repair (Aono et al., 2002), single strand break repair (SSB) and homologous directed repair (HR) (Heale et al., 2006; Kong et al., 2011; Wood et al., 2008). Also, it has been shown that condensin prevents unwanted intrachromosomal recombination at rDNA locus by excluding Rad52 thereby maintaining rDNA stability and genome integrity (Tsang & Zheng, 2009). Another important role of condensin complex is its involvement in microtubule kinetochore attachment during mitosis to facilitate sister chromatid segregation. It has been shown that NCAPG2 of condensin II complex interacts with Plk1 for proper microtubule-kinetochore attachment (Kim et al., 2014). In yeast, condensin is important for proper microtubule attachment (Burrack et al., 2013; Johzuka & Horiuchi, 2009; Tada et al., 2011).

1.7.2 Histones:

Histones are most abundant proteins that compose the nucleosome. Two copies of each

H2A, H2B, H3 & H4 form an octamer. Each nucleosome is connected with a linker histone H1 (Kornberg, 1974; Kornberg & Thomas, 1974). At the centromere, histone H3 is replaced by centromere H3 (CENP-A in humans/Cse4 in yeast) (McKinley & Cheeseman, 2016). Histones play an important role in the maintenance of genomic integrity and mitotic chromosome structure. Nucleosome is a basic unit in higher order genome organization. Post-translational modifications of histone proteins also known as the "histone code", are important regulatory events for various cellular activities (Jenuwein & Allis, 2001). Previous studies suggested that histone H3 phosphorylation is important for chromosome condensation (Gurley et al., 1978; Paulson & Taylor, 1982; Van Hooser et al., 1998; Wei et al., 1999). Also, it has been shown that H4K20 methylation is implicated in condensin recruitment onto chromatin (Liu et al., 2010).

1.7.3 Topoisomerase II:

DNA topoisomerase II (Topo II) is an evolutionarily conserved protein that plays a critical role in mitotic chromosome organization and genome integrity (Uemura et al., 1987). Topo II introduces a double-strand break in one double stranded DNA and allows the passage of other double stranded DNA through it and subsequently ligate the ends in an ATP dependent manner (Nitiss, 2009). Topo II is major component isolated as a chromosome scaffold protein (Earnshaw et al., 1985; Gasser et al., 1986). Condensin interacts with Topo II in *Drosophila* and the loading of Topo II on chromatin is dependent on condensin in yeast (Bhalla et al., 2002; Bhat et al., 1996). The most important function of Topo II is to decatenate the intertwine DNA tangles generated during DNA replication. It has also been shown that condensin induces positive supercoils in DNA in a Topo II dependent manner (Baxter et al., 2011).

1.8 Regulation of condensin complex by kinases:

Post-translational modifications of proteins play a crucial role in the regulation of various biological processes like subcellular localization, protein-protein interactions,

loading and unloading at a target site on chromatin (Karve & Cheema, 2011). These modifications involve the addition of a functional group covalently to a protein by a group of enzymes. One such important post-translational modification of proteins is phosphorylation. It is well known that condensin complex is a target of various kinases during the cell cycle. It has been proposed that a single dominant kinase is not sufficient to regulate condensin complex, rather a set of kinases might sequentially phosphorylate condensin to assist the chromosome condensation during mitosis (Bazile et al., 2010). Three major kinases, which regulate condensin, are Cdk1, Aurora B and polo-like kinase.

Cdk1: First, in *Xenopus* cell free extracts, it was shown that the supercoil formation by condensin is dependent of Cdk1 (Kimura et al., 1998). In human cells, Cdk1 phosphorylates the condensin II subunit CAP-D3 and it is important for polo-like kinase (Plk1) localization to chromosomes (Abe et al., 2011). In *S. pombe*, condensin is localized in the cytoplasm during interphase and it is transported to the nucleus upon Cdk1 phosphorylation of Cut14/Smc4 on T19 (threonine) residue at the onset of mitosis (Sutani et al., 1999). In budding yeast, Cdk1 phosphorylates purified condensin *in vitro* and it is important for its supercoiling activity (St-Pierre et al., 2009).

Aurora B kinase: Aurora B kinase depletion in *Drosophila* leads to loss of condensin I (Kleisin/Barren) loading onto mitotic chromosomes (Giet & Glover, 2001). In HeLa cells, Aurora B depletion cause reduction in binding of condensin I complex but it does not affect binding of condensin II complex (Lipp et al., 2007). *C. elegans* condensin subunit, Smc2/MIX1 binding to chromatin is also disrupted in Aurora B depletion (Kaitna et al., 2002). In budding yeast, Aurora B/Ipl1 has no role in metaphase chromosome condensation, but it is important during anaphase (Lavoie et al., 2004; St-Pierre et al., 2009). In *S. pombe*, Aurora B/Ark1 phosphorylates Cnd2 subunit of condensin complex (Nakazawa et al., 2011).

Polo-like kinase (Plk1): Plk1 in yeast phosphorylates all three non-SMC subunits of condensin and this phosphorylation is required for supercoiling activity and the

maintenance of chromosome condensation during late mitosis (St-Pierre et al., 2009). However, Plk1 phosphorylation alone is not sufficient for supercoiling activity of condensin and it also requires Cdk1 activity. Condensin II subunit CAP-D3 is a target of Plk1 in human cells (Abe et al., 2011).

Other kinases like Mps1 kinase, Casein kinase II (CK2) and are also shown to phosphorylate condensin complex (Kagami et al., 2014; Takemoto et al., 2006). CK2 phosphorylates at serine-570 residue of Cap-H subunit of human condensin I complex. This phosphorylation during interphase by CK2 reduces the supercoiling activity thereby negatively regulating condensin complex (Takemoto et al., 2006). Mps1 kinase phosphorylates at the serine-492 residue of Cap-H2 subunit of human condensin II and helps in the chromosome condensation at the onset mitosis (Kagami et al., 2014).

1.8 Hypothesis and Objectives:

Since the discovery of condensin, many studies have come to understand its role in chromosome condensation. Nevertheless, how this pentameric complex is involved in the compaction of chromatin into highly organized metaphase chromosomes is poorly understood. There are many unanswered questions in this field of chromosome condensation. Our study mainly focused on a few interesting questions such as: how chromosome condensation process is initiated at the onset of mitosis? What is the driving force responsible for this initiation of compaction and how it is regulated to achieve full chromatin compaction in metaphase? In this thesis, I attempted to answer these questions. An important regulator of chromosome condensation during early mitosis is the Cdk1 kinase. Previous studies on the role of Cdk1 in chromosome condensation showed that it is important for transport of the condensin complex from the cytoplasm to the nucleus and is essential for condensin function. But these studies do not show how chromosome condensation is initiated during early mitosis. Hence, we studied the role of Cdk1 in chromosome condensation process, as it is the major kinase required for mitosis. Importantly, we focused on whether Cdk1 regulate condensin complex to induce the initiation of chromosome condensation.

Our hypothesis is that Cdk1 phosphorylates condensin in early mitosis to initiate the process of chromosome condensation. To test this, we have the following objectives in this study.

Objective I: To understand the role of Cdk1 in chromosome condensation in budding yeast.
Objective II: To determine the consequences of Cdk1 dependent phosphorylation on condensin activity
Objective III: To identify novel chromatin factors required for the maintenance of chromosome condensation in metaphase.

Chapter II: A high sensitivity phospho-switch triggered by Cdk1 governs chromosome morphogenesis during cell division

Xavier Robellet[1,2], Yogitha Thattikota[1,2], Fang Wang[1,2], Tse-Luen Wee[3], Mirela Pascariu[1,2], Sahana Shankar[1,2], Éric Bonneil[1], Claire M. Brown[3], & Damien D'Amours[1,2*]

[1]Institute for Research in Immunology and Cancer (IRIC)
and [2]Département de Pathologie et biologie cellulaire
Université de Montréal, P.O. Box 6128, Succursale Centre-Ville
Montréal, QC, H3C 3J7, CANADA
[3]Advanced BioImaging Facility (ABIF)
Department of Physiology, McGill University
3649 Promenade Sir William Osler
Montréal, QC, H3G 0B1, CANADA

Running head: Regulation of chromosome assembly in mitosis
Keywords: Chromosome, morphogenesis, Cdk1, Smc4, multi-site phosphorylation
These authors contributed equally to this work: Xavier Robellet, Yogitha Thattikota
**Corresponding author:* Damien D'Amours

2.1 Abstract

The initiation of chromosome morphogenesis marks the beginning of mitosis in all eukaryotic cells. Although many effectors of chromatin compaction have been reported, the nature and design of the essential trigger for global chromosome assembly remains unknown. Here we reveal the identity of the core mechanism responsible for chromosome morphogenesis in early mitosis. We show that the unique sensitivity of the chromosomes condensation machinery for the activity of Cdk1 acts as the main driving force for the compaction of chromatin at mitotic entry. This sensitivity is imparted by multi-site phosphorylation of a conserved chromatin-binding sensor, the Smc4 protein. The multi-site phosphorylation of this sensor integrates the activation state of Cdk1 with the dynamic binding of the condensation machinery to chromatin. Abrogation of this event leads to chromosome segregation defects and lethality, while moderate reduction reveals the existence of a novel chromatin transition state specific to mitosis, the intertwist configuration. Collectively, our results identify the mechanistic basis governing chromosome morphogenesis in early mitosis and how distinct chromatin compaction states can be established via specific thresholds of Cdk1 kinase activity.

2.2 Introduction

In his seminal description of mitosis, Flemming recognized that the formation of visible chromosomes is one of the earliest cytological landmarks of the cell division program (Flemming, 1882). Since then, much efforts has been devoted to unraveling the structural and regulatory mechanisms that underpin the formation of mitotic and meiotic chromosomes (Baxter & Aragon, 2012; Hirano, 2012; Maeshima & Eltsov, 2008). A number of independent steps, such as chromosome replication, condensation, and the establishment of sister chromatid cohesion are required for the formation of mature and functional chromosomes during cell division. The morphological changes that associate with these steps are collectively referred to as the process of chromosome morphogenesis (van Heemst et al., 1999; Yu & Koshland, 2005).

The compaction of amorphous chromatin into visible chromosomes is one of the earliest and most extensive change in the morphogenetic process (Flemming, 1882). Given the physical challenges associated with the assembly of micrometer-scale chromosomes in the crowed cellular environment (Marko, 2008), it is not surprising that many chromatin and cell cycle effectors have been suggested as possible regulators of the process. Chief among those is the condensin complex, a pentameric ATPase that binds to chromatin and alter its configuration and/or association status with distant chromatin regions (Baxter & Aragon, 2012; Bazile et al., 2010; Hirano, 2012). Other factors, such as cell cycle kinases and histone modifying enzymes, have also been proposed as possible regulators of chromosome condensation during mitosis (Abe et al., 2011; Morishita et al., 2001; Neurohr et al., 2011; St-Pierre et al., 2009; Wilkins et al., 2014). Although it is clear that these enzymes impact chromatin compaction at specific genomic locations and/or during specific stages of mitosis, it is remarkable that the chromosome condensation process as a whole remains largely operational when these enzymes are fully inhibited in mammalian cells (Abe et al., 2011; Cimini et al., 2003; Ditchfield et al., 2003; Hauf et al., 2003; Lenart et al., 2007; Ono et al., 2004). The fact that no specific mutation and/or inhibitory condition prevent the formation of condensed chromosomes during metaphase in mammalian cells suggests that the fundamental

nature of the mechanism responsible for global chromosome assembly is still unknown.

Another key issue about chromosome morphogenesis relates to the timing of the process in relationship to other mitotic events. It has been established several decades ago that mitosis is initiated by a sudden increase in cyclin-dependent kinase (Cdk1) activity (Morgan, 2007). The fact that the early assembly of mitotic chromosomes correlates well with the early increase in Cdk1 activity in prophase (Gavet & Pines, 2010) suggests that Cdk1 may regulate early chromosome assembly directly. However, the dependency of the chromosome morphogenesis process on mitotic entry (Ferrell, 1996; Gong & Ferrell, 2010; Paulson, 2007; Vassilev et al., 2006) makes it difficult to determine whether the impact of Cdk1 on chromosome morphology reflects a direct role in this process or, alternatively, a need to establish a mitotic state prior to initiating chromosomes assembly. Moreover, given that a requirement for Cdk1 activity is shared between many mitotic processes, it is unclear why the establishment of chromosome condensation should precede other mitotic landmarks if all mitotic processes respond to the same Cdk1 signal. The temporal primacy of condensation in the mitotic program could be due to heightened sensitivity to Cdk1 phosphorylation, higher specificity for specific cyclin-Cdk1 complexes, or a yet unknown Cdk1-independent mechanism. In this study, we test those possibilities and show how Cdk1 can initiate chromosome morphogenesis directly using quantitative multisite phosphorylation of the Smc4 protein. Moreover, we identify a novel two-step mechanism necessary for the folding of chromatin and subsequent assembly of functional chromosome during mitosis.

2.3 Results

2.3.1 Regulation of chromosome morphology by Cdk1

To investigate the mechanistic basis for chromosome morphogenesis, we first determined whether the process was under direct Cdk1 control in *Saccharomyces cerevisiae*. Yeast cells carrying a Cdk1 temperature-sensitive (ts) mutation, *cdc28-4*, were arrested in mitosis and the morphology of the ribosomal DNA (rDNA) locus was evaluated in these cells. The shape of the rDNA locus is dramatically reorganized during

mitosis, which provides a sensitive assay to monitor chromosome morphogenesis in yeast (Guacci et al., 1994). Whereas wild-type cells arrested in mid-mitosis showed the typical condensed “loop” configuration of the rDNA locus at both 23°C and 37°C, inactivation of Cdk1 resulted in the formation of an uncondensed "puff" rDNA signal at 37°C (Fig. 1A) (Guacci et al., 1994). Having established the Cdk1-dependency of the chromosome morphogenetic process in yeast, we next asked whether chromosome condensation could be quantitatively modulated by down-regulation of Cdk1 activity using conditional B-type cyclin mutations (*i.e.*, *clb1 clb3 clb4 clb2-VI*; *clb-ts* mutant henceforth). Although able to enter mitosis, *clb-ts* cells are incapable of executing subsequent mitotic events (Amon et al., 1993). Analysis of chromosome morphology in this mutant revealed the existence of a novel intertwined rDNA configuration distinct from the uncondensed "puff" signal (Fig. 1B) or from the fully condensed loop signal (Fig. 1A). Specifically, under low Cdk1 activity, individual chromosomal "threads" are clearly visible at the rDNA locus and appear to follow an elaborate intertwined path distinct from the non-overlapping path of chromosome threads in the loop configuration (Figs. 1A–B, S1). We will therefore refer to this novel stage in chromosome condensation as the intertwist configuration. Interestingly, chromatin folding within the intertwist configuration is consistent in shape with the early condensation intermediates that were recently proposed to exist based on polymer simulation models (Naumova et al., 2013). Cytological characterization of *clb-ts* mutants confirmed that other mitotic events, such as bipolar spindle formation and chromosome segregation, do not occur in these cells (Fig. S1)(Amon et al., 1993).

To exclude the possibility that rDNA intertwist formation is a consequence of a change in Cdk1 specificity in *clb-ts* mutants, we monitored chromosome morphology in the *cdc28-as1* mutant. This mutant, when treated with low concentrations of 1NM-PP1 inhibitor, experiences a cell cycle arrest at mitotic entry (*i.e.*, after DNA replication but prior to mitotic spindle formation) (Bishop et al., 2000), similar to the point of arrest of *clb-ts* mutants. Examination of chromosome morphology in *cdc28-as1* cells treated with the inhibitor revealed a striking enrichment in the number of cells carrying the intertwist configuration at the rDNA, whereas untreated cells formed mostly loops at this locus

under identical conditions (Fig. 1C). Interestingly, the intertwist configuration appears to be stabilized at low temperature and could be readily observed in wild-type cells progressing synchronously into mitosis at 16 °C (Fig. S2). As previously observed with the fully condensed loop configuration (Lavoie et al., 2004), formation of the intertwist rDNA intermediate also requires cohesin activity, since inactivation of *mcd1-1* prevented the appearance of this rDNA configuration in mitosis (Fig. S3). Taken together, our results indicate that chromosome condensation is initiated at levels of Cdk1 activity that are too low to induce other mitotic events. Moreover, conditions of low Cdk1 activity revealed the existence of a *hitherto* unknown early chromatin-folding step in the formation of mitotic chromosomes.

2.3.2 The Smc4 subunit of condensin is a target for Cdk1 in early mitosis

What is the target of Cdk1 in the induction of chromosome morphogenesis? A likely candidate is the condensin complex, a central effector of chromosome condensation in eukaryotes(Baxter & Aragon, 2012; Hirano, 2012). To test this possibility, we removed all the core Cdk1 consensus sites (*i.e.*, Ser/Thr-Pro) (Holt et al., 2009) from condensin subunits and determined the effect of these mutations on cell proliferation (Fig. 2A–B). Only *smc4-10A* showed detectable growth defects in the absence of Cdk1 phosphorylation (Fig. 2B). Combining all mutations in one yeast strain only had modest additive effects on cell proliferation relative to the *smc4-10A* single mutant (Fig. 2B). These results indicate that the Smc4 subunit of condensin is a likely target of Cdk1 *in vivo*. To further substantiate this possibility, we immunopurified the condensin complex from metaphase-arrested cells and subjected the immunoprecipitate to mass spectrometry analysis to identify possible *in vivo* phosphorylation sites. This analysis revealed the existence of 5 phosphorylation sites that conform to the Cdk1 consensus in Smc4 (Figs. 2C, S4A) and none in the other subunits of condensin. An additional Cdk1 phospho-site, Ser117, was uncovered in Smc4 in a proteome-wide analysis of mitotic cells (Holt et al., 2009; Kao et al., 2014). Interestingly, all these Cdk1 phospho-sites were clustered in the N-terminal extension of Smc4, a region of the protein that is conserved

among eukaryotic Smc4 family members but absent in Smc1-3 families (Fig. S4B–C). Deletion of the N-terminal extension of Smc4 results in a stable but inactive protein, thereby revealing the essential role played by this part of Smc4 in condensin function (Fig. 2D). Finally, we asked whether Cdk1 is directly responsible for condensin phosphorylation. To test this possibility, we purified condensin from yeast and exposed it to purified Cdk1-Clb2 in the presence of radiolabeled ATP. We observed that a single band corresponding to the molecular mass of Smc4 became phosphorylated following the kinase reaction (St-Pierre et al., 2009) (Fig. 2E). Performing a similar experiment using only the N-terminal fragment of Smc4 (residues 1-163) resulted in a Cdk1 phosphorylation-induced gel retardation of the substrate after electrophoresis (Fig. 2F). Taken together, these experiments demonstrate that Cdk1 phosphorylates Smc4 *in vitro* and *in vivo*.

We next characterized the timing of Smc4 phosphorylation during the cell cycle. Since phosphorylation of the N-terminal part of Smc4 by Cdk1 causes a gel shift after electrophoresis (Fig. 2F), we used cells expressing the N-terminal extension of Smc4 fused to an epitope tag (henceforth, Smc4-NT) to monitor *in vivo* phosphorylation. As expected, the electrophoretic behavior of Smc4-NT changes dramatically during the cell cycle, starting as a single band in G1 and acquiring at least 2 retarded species as cells progressed towards mitosis (Fig. 3A). Phosphatase treatment of Smc4-NT confirmed that the retarded species were due to phosphorylation (Fig. 3B). Importantly, Smc4-NT became phosphorylated simultaneously with/or slightly prior to Swe1, an early Cdk1 substrate during mitosis (Harvey et al., 2005), and much earlier than Ycg1, a condensin subunit phosphorylated in anaphase (St-Pierre et al., 2009) (Fig. 3A). These results indicate that Smc4 phosphorylation occurs at, or very close to mitotic entry. Consistent with this interpretation, monitoring the phosphorylation of two of the Cdk1 sites – Ser4 and Ser128– on Smc4 using phospho-specific antibodies confirms that these residues are also modified early in mitosis (Figs. 3C–D, S5A-B). The *in vivo* kinetics of Smc4 phosphorylation revealed by the Smc4-NT construct and the phospho-specific Ser128 antibody were essentially identical (Fig. 3D), thereby validating Smc4-NT as en effective reporter to monitor Smc4 phosphorylation status. Importantly, removal of the 7 Cdk1

sites in the Smc4-NT fragment completely abrogated its phosphorylation-induced gel retardation in live cells (Figs. 3E, S5C). These results strongly suggest that Cdk1 is the kinase that targets Smc4 for phosphorylation in early mitosis. Consistent with this prediction, cells defective in early (*clb5, clb6)* and late cyclin (*clb1, clb3, clb4, clb2-ts*) subunits showed marked reductions in the extent of Smc4 phosphorylation *in vivo* (Figs. 3F, S5D–E). Moreover, removal of the Clb5-targetting RxL motifs (Koivomagi et al., 2011; Loog & Morgan, 2005; Morgan, 2007) in the N-terminus of Smc4 caused a substantial reduction in the extent of its phosphorylation (Figs. 3G, S5F). Finally, we wanted to test the possibility that Smc4 phosphorylation might be mediated by Cdc5 since this kinase is known to be activated by Cdc28 in mitosis (Mortensen et al., 2005). However, the fact that Smc4-NT phosphorylation remained normal in *cdc5-99* mutant cells entering mitosis (Fig. S5G), or in cells already arrested at this stage of the cell cycle (Fig. S5H) argues against a role for this kinase as the major or sole Smc4 kinase in early mitosis (Fig. S5G-H). Taken together, our results show that effective phosphorylation of Smc4 in early mitosis requires direct targeting of condensin by cyclin-Cdk1 complexes.

2.3.3 Smc4 phosphorylation activates chromosome morphogenesis

What is the physiological significance of Smc4 phosphorylation by Cdk1? To answer this question, we introduced in the yeast genome mutations that either prevent or mimic the phosphorylation of the 7 Cdk1 sites in the N-terminal extension of Smc4. Whereas removal of individual Cdk1 sites resulted in little to no effect on growth properties or on chromosome condensation (Fig. S6A–B), cells carrying a *SMC4* allele that lacks all N-terminal Cdk1 sites exhibited a strong growth defect at non-permissive temperature (*i.e.*, *smc4-7A*; Fig. 4A). We noticed that the Smc4-7A protein was less abundant than its wild-type counterpart in immunoblot analysis (Fig. 4B, first two lanes). This reduction in Smc4-7A protein levels is not responsible for its growth defect since down-regulation of wild-type Smc4 abundance using the auxin-inducible degron (*i.e.*, Smc4-AID) did not result in detectable growth defect at Smc4 protein levels comparable to, or lower than those of the Smc4-7A mutant (compare 40 μM auxin/IAA and *smc4-7A* lanes in Fig. 4B,C).

Consistent with this, inactivation of the pathway responsible for the degradation of unstable nuclear proteins did not suppress the ts phenotype of *smc4-7A* cells (Fig. S7A), and no defect in condensin complex formation was detected in *smc4-7A* mutants (Fig. 4D). Collectively, these results indicate that the conditional lethality phenotype of the *smc4-7A* mutant is specifically due to the loss of Cdk1-mediated phosphorylation of condensin.

Microscopic examination of *smc4-7A* mutants at non-permissive temperature provided critical insights on the nature of the cellular defect responsible for the lethality of this mutant. We noticed that there was a significant fraction of dividing cells in the mutant population that contained unequal amounts of nuclear material and/or connecting threads of chromosomal DNA between separating nuclei (see arrowheads; Fig. 4E). This phenotype was much less frequent in wild-type cells (Fig. 4F), and is indicative of severe chromosome segregation defects in the absence of Smc4 phosphorylation. The root cause for the segregation defect of condensin mutants has been ascribed to their inability to promote chromosome condensation (Hirano, 2012). To test this notion, we examined the rDNA condensation proficiency of the *smc4-7A* mutant in relationship to that of *SMC4* and *smc4-82* cells (*i.e.*, a strong ts mutant of condensin; see below). Whereas wild-type cells were able to condense the rDNA effectively at 37°C, both *smc4-7A* and *smc4-82* mutant were completely defective in rDNA loop formation at non-permissive temperatures (Fig. 4G,H). These results indicate that Cdk1 phosphorylation is absolutely necessary to activate condensin and initiate chromosome condensation *in vivo*.

A previous study using the fission yeast *Schizosaccharomyces pombe* suggested that Cdc2 might regulate condensin by phosphorylation *in vivo* (Sutani et al., 1999). The authors showed that overexpression of the *cut3-T19A* phosphomutant caused a dominant-negative chromosome segregation defect in this organism (however, no chromosome condensation defects were observed in this study). Since the phenotype of the *cut3-T19A* mutant expressed at its natural level was not reported by Sutani and colleagues, and protein overexpression can often obscure the physiological relevance of

natural regulatory processes (Robbins & Cross, 2010), we wondered what might be the phenotype associated with loss of Thr19 phosphorylation when Cut3 is expressed at physiological levels. To address this, we integrated the *cut3-T19V* phosphomutant at its natural locus in diploid *S. pombe*. The valine substitution was used in *cut3* instead of alanine since valine is structurally more similar to threonine, thus precluding destabilizing effects not related to loss of phosphorylation. Dissection of a sporulated heterozygous diploid yeast carrying the *cut3-T19V* allele revealed that loss of Thr19 phosphorylation is lethal in haploid cells when the mutant is expressed from its physiological locus (Fig. S7B). Interestingly, the heterozygous diploid carrying *cut3-T19V* grew normally (Fig. S7C), thereby suggesting that the dominant lethal effects previously observed with the *cut3-T19A* mutant might be specific to the alanine substitution and/or to the overexpression of the protein (Sutani et al., 1999). Taken together, these results further strengthen the conclusion that Cdk1 phosphorylation of the N-terminal extension of Smc4 family members plays a critical role in the regulation of condensins in eukaryotes.

2.3.4 Cdk1 phosphorylation sites activate condensin by altering its charge

We next examined the phenotype of a *SMC4* allele carrying phospho-mimetic residues (*i.e.*, negatively-charged glutamates) at the position of Cdk1 sites. Constitutive activation of condensin by such mutations is expected to create a lethal form of the enzyme because it would permanently alter chromatin structure in yeast. However, replacement of phosphorylated residues by glutamates in Smc4 did not result in an obvious activation of condensin or any detectable growth defect in the *smc4-7E* mutant (Fig. 4A). This is not completely unexpected since a single negatively-charged residue does not accurately mimic the structure or net charge of a phosphorylated residue, as previously observed (Lyons & Morgan, 2011; Pearlman et al., 2011). Based on the fact that the N-terminal extension of Smc4 is predicted to be highly unstructured (Fig. S8A–C), we considered the possibility that the change in charge imparted by phosphorylation of this domain would be more relevant as a regulatory mechanism than a possible change in structure. We

therefore created a *smc4-7EE* allele where the phosphorylated residues and adjacent prolines (+1 position of the CDK motif) were mutated to double-glutamates to more accurately mimic phosphate charges (Pearlman et al., 2011) (Fig. 5A–B). It was recently shown that this approach is more effective at mimicking an "activated" state than single glutamate/aspartate substitutions in substrates targeted by proline-directed kinases (Li et al., 2014; Strickfaden et al., 2007). The charge-mimetic allele, together with additional control mutations, were integrated at the *SMC4* locus in a diploid yeast strain and the resulting heterozygous mutants were sporulated and dissected to reveal the phenotypes of the mutations in haploid spores. Remarkably, introducing dual charge-mimetic mutations at the seven phosphosites and adjacent positions (*i.e.*, Ser/Thr-Pro motif) of Smc4 led to lethality in all spores inheriting those mutations, whereas altering simultaneously the seven phosphosites with single glutamates at either position of the Ser/Thr-Pro motifs had no detectable effect on viability (*i.e.*, 4 viable spores per tetrad; Fig. 5B). Moreover, a mutant carrying dual glutamines –an amino acid approximately isosteric with glutamate but lacking the negative charge (Fig. 5A)– did not result in obvious viability defects (Fig. 5B). These results demonstrate that the lethality of the *smc4-7EE* mutant is due to the presence of negative charges that effectively mimic the phosphorylated state of the active protein. Immunoblot analysis of heterozygote diploids confirmed that the Smc4-7EE mutant is expressed at normal levels in yeast (Fig. S8D).

To further strengthen our previous interpretation, we asked whether an alternative means of imposing a constitutive state of phosphorylation on Smc4 would recapitulate the phenotype of the *smc4-7EE* allele. To achieve this, we fused the B-type cyclin Clb2 to the N-terminus of Smc4 in order to target Cdk1 to Smc4 throughout the cell cycle, an experimental approach previously described (Lyons & Morgan, 2011). Dissecting a sporulated heterozygous diploid strain carrying the *CLB2-SMC4* fusion gene led to lethality or severe growth defects in most of the spores inheriting the fusion construct (Fig. 5B). Preventing phosphorylation of Smc4 by removal of its phosphosites or by deletion of Clb2's cyclin box, the part of the protein responsible for interaction with Cdk1, largely suppressed the lethality associated with the cyclin-Smc4 fusion protein (Figs. 5B, S9A). These results are consistent with the phenotype of the *smc4-7EE* allele,

and indicate that inducing a permanent state of phosphorylation in Smc4 is incompatible with viability in yeast. Since the phenotype associated with mimicking phosphorylation is much stronger than that caused by loss of phosphorylation, we posit that the *smc4-7EE* and *CLB2-SMC4* mutants behave as gain-of-function alleles *in vivo*.

We envision two possible regulatory modes that can account for the lethality of *smc4-7EE* and *CLB2-SMC4* mutants. First, constitutive phosphorylation of condensin may simply activate the enzyme and result in a permanent state of chromosome condensation that is not compatible with viability. Alternatively, preventing phosphate removal in phospho-mimetic mutants may abrogate iterative phosphorylation/dephosphorylation cycles that are normally required to maintain full enzyme activity during mitosis (De Wulf et al., 2009). Overexpression of *smc4-7EE* can distinguish between these two regulatory modes since a version of condensin that is fully activated by static phosphorylation (*i.e.*, no turnover model) would be expected to induce unscheduled condensation following overexpression, whereas a version of this enzyme that is engaged into its activation cycle by phosphorylation but not allowed to complete it by dephosphorylation (*i.e.*, dynamic phosphorylation model) would act as a dominant-negative inhibitor. To test these hypotheses, we expressed ectopically *smc4-7EE* in wild-type and *clb2-ts*-arrested cells. Remarkably, ectopic expression of *smc4-7EE* was not able to induce unscheduled condensation of the rDNA locus in G1 cells or full rDNA condensation in G2/early mitotic cells (Fig. S9B–E, S10A), which suggests a need for dynamic phosphorylation in the regulation of condensin *in vivo*. Consistent with this, overexpression of *smc4-7EE* led to dominant-negative lethality in both wild-type and *smc4-82* mutants (Fig. 5C). This lethality is not due to unspecific loss-of-function in *smc4-7EE* or subunit imbalance in condensin since overexpression of *smc4-1* (Freeman et al. 2000), *smc4-7A,* or *SMC4* complemented the lethality of the *smc4-82* mutant at 37 °C, without causing dominant-lethal effects in wild-type cells (Fig. 5C). We note however that overexpression of *SMC4* in wild-type cells caused a weak proliferation delay at 23 °C.

It has been previously demonstrated that the effects of mutations that confer a gain of activity on a protein can be abrogated by fusion with known inactivating

mutations (Schott & Hoyt, 1998). To formally test the gain-of-function nature of the charge mimetic mutations in *SMC4*, we combined the *7EE* substitutions with the inactivating mutations in the *smc4-1* allele and monitored the ability of the chimeric mutant to behave in a dominant-negative manner. As expected, overexpression of the *smc4-7EE-1* chimeric mutant in condition where its charge-mimetic mutations are not counteracted by the *smc4-1* mutations (*i.e.*, 23°C; the permissive temperature for *smc4-1*) led to a dominant-negative lethality similar to that of the *smc4-7EE* single mutant (Fig. 5D *vs* 5C,E). In contrast, overexpression of the chimeric mutant at 37°C (*i.e.*, the inactivating condition for *smc4-1* and, by extension, *smc4-7EE*) suppressed the lethal gain-of-function associated with the charge mimetic substitutions (Fig. 5D). Since Smc4-7EE must be endowed with an activity to be able to lose it, we conclude from this experiment that the charge mimetic mutations impart a new activity on Smc4 that requires otherwise normal protein function to mediate its effect. Importantly, this new activity can be induced equally well by fusion of *SMC4* with *CLB2* or by charge-mimicking mutations, which indicates that Cdk1 phosphorylation activates condensin by altering its charge in living cells and that preventing Smc4 dephosphorylation is lethal *in vivo*. Consistent with this interpretation, inactivation of a major mitotic phosphatase and known condensin interactor, PP2A (encoded by the *PPH3*, *PPH21*, and *PPH22* genes in budding yeast; (Peplowska et al., 2014; Takemoto et al., 2009; Yeong et al., 2003)), caused a large reduction in the ability of phosphatase-defective cells to maintain chromosome condensation in metaphase (Fig. S10B). Collectively, our results indicate that dynamic turnover of Cdk1 phosphorylation events on condensin is important for mitotic chromosome condensation.

2.3.5 Hypersensitivity of Smc4 to Cdk1 phosphorylation

How might charge-driven activation of condensin promote early mitotic appearance of condensed chromosomes? One likely possibility would be that condensin is hypersensitive to low levels of Cdk1 activity because phosphorylation of any individual Cdk1 site is functionally equivalent for enzyme activation and only a few of them need to

be modified (in any combination) to fully activate the enzyme. The dominant effects of charge-mimetic mutations provide a unique means to test this hypothesis. Indeed, one would expect that progressive removal of the 7 dual glutamates in Smc4 would eventually reverse the partial gain-of-function of the *smc4-7EE* allele, thereby revealing the minimal number of phospho-sites that are required to activate condensin *in vivo*.

Prompted by this rationale, we created a series of heterozygous *SMC4/smc4-EE* mutants carrying progressively smaller numbers of dual glutamate mutations and tested their phenotypes after sporulation of diploid cells. Remarkably, diploid strains carrying as few as 3-4 charge-mimetic mutations gave rise to tetrads with a very penetrant 2:2 lethality phenotype co-segregating with *smc4* mutations (Fig. 6, rows 5–6). This is identical to the phenotype of the original *smc4-7EE* or *-10EE* alleles (Fig. 6, rows 2–3), but is in contrast to the absence of phenotype of mutations affecting the first 3 Cdk1 sites at the N-terminus of the protein (Fig. 6, row 4). This result suggests that 3-4 phosphorylation events in the middle or C-terminal clusters of Cdk1 sites may be sufficient to activate Smc4. To further refine this conclusion, we focused our analysis of charge-mimetic mutations to those in the middle cluster of phospho-sites (*i.e.*, positions 109, 113, 117, 128). Removing a single dual-glutamate mutation from the 4 present in this cluster did not fully suppress the lethality of the remaining charge-mimetic mutations (Fig. 6, rows 7–8). However, loss of any additional site either reduced the penetrance of the lethality phenotype (Fig. 6, rows 8–9) or allowed complete recovery of spore viability (Fig. 6, rows 10–14). Importantly, preventing phosphorylation of the Cdk1 sites away from the middle cluster of dual glutamates (*i.e.*, *smc4-3A-4EE-3A* mutant) did not suppress the effect of the *smc4-4EE* mutant (*i.e.*, Fig. 6, compare rows 5 and 17), thereby indicating that the lethality of this strain was not due to phosphorylation of the remaining Cdk1 sites in Smc4-4EE. Taken together, these results indicate that a threshold of 2-3 phospho-mimicking charges is sufficient to stimulate condensin activity *in vivo* (Fig. 6, rows 7, 16). Moreover, our data reveal a degree of functional equivalency (or redundancy) in Cdk1 phosphosites, thereby explaining how condensin activation in early mitosis can be hypersensitive to Cdk1 levels.

2.3.6 Cdk1 controls condensin binding to chromatin

Finally, we wished to identify the specific aspect of condensin behavior that was regulated by Cdk1 phosphorylation. Multiple events have been previously shown to be required for full activation of condensin in eukaryotes, including nuclear import (Sutani et al., 1999), recruitment on chromatin (Freeman et al. 2000), and enzymatic activation (Kimura et al., 1998). The fact that budding yeast condensin and mammalian condensin II are constitutively located in the nucleus (Freeman et al., 2000; Gerlich et al., 2006; Ono et al., 2004) suggests that the Cdk1 regulation of these enzymes may not occur at the level of nuclear import. Interestingly, previous studies in human cells showed that condensin II binding to chromatin is very dynamic prior to chromosome condensation, but then becomes much more stable as cells enter mitosis (Gerlich et al., 2006). The mechanistic basis for this change in chromatin binding dynamics is unknown, but it seems likely that increasing the duration of condensin interactions with chromatin would stimulate chromosome condensation (Gerlich et al., 2006). To evaluate whether condensin phosphorylation by Cdk1 could affect its chromatin-binding dynamics, we used photobleaching confocal laser scanning microscopy. A subdomain in the nucleus of live yeast cells expressing GFP-fused Smc4 was photobleached using the line scan feature of the microscope and the kinetics of fluorescence decay were determined over time at the region of interest in the cell (*i.e.*, red rectangle in Fig. 7A). In this experiment, the Smc4-3xGFP contained within the unbleached area is expected to replenish the fluorescence in the photobleached area of the cell at a rate that is directly proportional to the exchange of condensin complexes between the two regions within the nucleus. As expected, preventing exchange by fixation of cells with paraformaldehyde led to a very rapid loss of Smc4-3xGFP fluorescence signal in the photobleached area, while leaving the fluorescence in the rest of the nucleus unaffected (Fig. 7A). In contrast, photobleaching a subdomain of the Smc4-3xGFP signal in live cells resulted in a rapid decay of fluorescence signal throughout the entire yeast cell (Fig. 7A–B). This rapid loss of fluorescence is consistent with highly dynamic exchange of condensin complexes

between the site of photobleaching and the rest of the nucleus, a behavior consistent with that of condensin I in higher eukaryotes (Gerlich et al., 2006). Remarkably, performing the same experiment in cells expressing Smc4-7A revealed that the fluorescence decay of the phospho-mutant is significantly slower than that of the wild-type (Fig. 7B). This result is consistent with Smc4-3xGFP residing in the bleaching volume for longer periods of time while it is bound to chromatin, thereby causing it to bleach more quickly. The rapidly-exchanging Smc4-7A still binds to DNA but does not reside in the bleaching region as long, so it takes a longer time to photobleach. To quantify this difference, decay curves were fit with a two-component exponential decay model with a short (*d*) and a long (*b*) time decay constant (*cf*., Equation 1 in Materials and Methods). Both decay constants were significantly longer for the highly dynamic Smc4-7A or cytosolic GFP protein than that of wild-type Smc4 (Fig. 7B–C; $p \leq 0.001$; decay constant *d* is shown in Fig. S11A). Taken together, these results reveal that Cdk1 phosphorylation extends the duration of condensin's interaction with chromatin, thereby providing an explanation as to how this post-translational modification regulates chromosome condensation during mitosis. These rapid protein dynamics in the yeast nucleus are consistent with other studies done using fluorescence correlation spectroscopy in yeast (Slaughter et al., 2007).

2.4 Discussion

2.4.1 Quantitative activation of chromosome condensation in early mitosis

The central prediction from the quantitative model of Cdk1 action is that cellular events occurring early in the cell division program must be more readily activated by Cdk1 than later events of the cell cycle (Stern & Nurse, 1996). Although differential susceptibility to Cdk1 activation explains the directionality of S and M phases (Coudreuse & Nurse, 2010), the notion that a similar process would also explain the specific order of events in the mitotic program is currently unknown. Here, we show that initiation of chromosome condensation can be achieved at levels of Cdk1 activity that are too low to activate other mitotic processes. This result demonstrates that the order of cellular events in early

mitosis is dictated by quantitative difference in substrate susceptibility to Cdk1 activation. Mechanistically, we show that the temporal kinetics of chromosome condensation in mitosis can be explained by functional redundancy in the phosphorylation sites that Cdk1 uses to activate condensin *in vivo*. Multisite redundancy in phospho-regulatory events is known to enable quantitative activation of effectors at very low levels of kinase activity in signaling cascades (Ferrell, 1996).

2.4.2 Identification of a novel chromosome-folding state in early mitosis

The nature of the individual steps leading to the formation of condensed mitotic chromosomes has been a topic of much debate over the years. Previous attempts to define the architecture of mitotic chromosomes have been frustrated by the absence of cytologically-defined chromatin-folding intermediates in the process of condensation. More recently, a study has proposed a two-stage mechanism of chromosome condensation that involves longitudinal compression of arrays of consecutive chromatin loops (Naumova et al., 2013). This model was generated using *in silico* polymer simulations and predicts that the formation of local loops of chromatin would represent the initial stage of chromosome condensation. Our identification of rDNA condensation intermediates containing intertwined loops of thin chromatin threads –the intertwist configuration– gives credence to this *in silico* model. Moreover, the resolution of the intertwist configuration into a thicker thread of rDNA chromatin later in mitosis indicates that intertwined loops of rDNA are eventually resolved by compaction into a linear organization in yeast, as previously suggested for human chromosomes (Naumova et al., 2013). Taken together, our results provide the first direct observation of a two-step process involving distinct chromatin folding-states as intermediates in the process of chromosome condensation.

2.4.3 Mechanistic basis for condensin activation in early mitosis

Our study reveals that the unique N-terminal extension of Smc4 family members acts as modulator of condensin's ability to bind on chromatin. Upon phosphorylation by Cdk1, condensin binding to the bulk of chromatin becomes less dynamic relative to the

unphosphorylated enzyme and thus allows extended interactions with mitotic recruiters to promote condensation (Figs. 7D, S11B). It is tempting to speculate that Cdk1 phospho-sites on Smc4 could enhance –by virtue of their negative charges– the stability of the interaction between condensin and the positively-charged residues in the N-terminal tails of histone H2A and H2A.Z on chromosomes (Tada et al., 2011). Such stabilization would nicely explain the observed Cdk1-dependent reduction in the dynamic binding of condensin to chromatin in yeast and human cells (Gerlich et al., 2006). Importantly, this model explains how condensin can associate with chromatin throughout interphase without actually inducing chromosome condensation before mitosis (Freeman et al., 2000).

From an evolutionarily perspective, the mechanisms that we have unraveled in budding yeast are likely to be conserved in a wide range of eukaryotes. Notably, the Cdk1 consensus sites within the N-terminal extension of Smc4 homologs are modified by phosphorylation in several organisms, including fission yeast, budding yeast, and humans (Fig. S4C) (Bazile et al., 2010). We envision that these Smc4 phosphorylation events collaborate with other regulatory events, such as Aurora B, Polo kinase, and Cdk1 phosphorylation of non-SMC subunits, to establish a chromosome architecture that is sufficiently condensed and yet adaptable to the unique cellular conditions experienced during mitosis (Bazile et al., 2010; Hirano, 2012). In particular, it is conceivable that the appearance of a second condensin complex during evolution has resulted in a "division of labor" and sharing of Cdk1 phospho-sites between Smc4 and CapD subunits (Fig. S12) to allow a regulation that is highly specific to either condensin I or II complexes. In organisms where condensin is monomorphic, such as in yeast, current data indicate that this regulation would occur solely at the level of Smc4. This simplified regulation has enabled us to reveal how Cdk1 can act as an essential and high-sensitivity trigger for the initiation of chromosome morphogenesis during mitosis.

2.5 Materials and Methods

2.5.1 Yeast genetics and molecular biology

All *S. cerevisiae* strains used in this study are isogenic with K699 and K700. Yeast growth conditions, media composition, and procedures for genetic analysis were as described previously (Gutherie, 1991). The genotypes of yeast strains used in this study are listed in Supplemental Table 1. Additional details relating to mutant yeast construction and molecular biology procedures are also included in Supplemental Material.

2.5.2 Microscopy

For FISH analyses, cells were fixed in 0.1M KPO4 buffer pH 6.4 containing 3.7% formaldehyde for 2 hours at 23 °C. Probe preparation and hybridization were performed as described previously (Guacci et al., 1994; Lavoie et al., 2004). Images of rDNA morphology were acquired on a DeltaVision microscope equipped with the softWoRx software (Applied Precision). For photobleaching experiments, cells were grown at 25 °C, and images were acquired on a Zeiss 710 confocal laser-scanning microscope (Carl Zeiss, Jena, Germany) after photobleaching. See Supplemental Material for a detailed description of specific conditions used for microscopy experiments.

2.5.3 Electrophoresis and immunoblotting

8% Phos-tag acrylamide gels (Wako Chemicals USA) were used to resolve Smc4-NT phosphorylated species (Kinoshita et al., 2006), whereas gels containing 7.5 % Next gel acrylamide (Amresco) were used to monitor Smc4 abundance and Ycg1 phosphorylation (St-Pierre et al., 2009). All gels were transferred using the iBlot apparatus (Invitrogen). Antibodies and conditions used for immunoblotting are listed in Supplemental Material.

2.5.4 Mass spectrometry analysis of Smc4 phosphorylation

To identify the Cdk1 phosphorylation sites on Smc4, condensin was immunopurified from protein extracts prepared from cells arrested in metaphase using nocodazole. LC-MS/MS analysis was performed on immunoprecipitated condensin, as described

previously (St-Pierre et al., 2009). An extended description of all methods used in this study is provided in Supplemental Material.

2.6 Acknowledgements

We thank Julie St-Pierre and members of the D'Amours laboratory for their comments on the manuscript; Adam Rudner, Pascal Bernard, Alain Verreault, Angelika Amon, Michael Stark, and Fred Cross for antibodies and/or yeast strains; as well as David Morgan for communicating unpublished results. Research in D.D. laboratory is supported by grants from CIHR (MOP–136788, MOP–82912) and CCSRI (#20304). X.R. is supported by a fellowship from the Cole Foundation. D.D. is recipient of a Canada Research Chair in Cell Cycle Regulation and Genomic Integrity. Photobleaching experiments were performed in the McGill Life Sciences Complex Advanced BioImaging Facility (ABIF).

2.7 Author Contributions

Conceived and designed the experiments: XR, YT, DD, CB. Performed experiments: XR, YT, MP, SS, FW; Photobleaching analysis – TW, CB; Mass spectrometry analysis – EB. Wrote the paper: DD, XR, YT, CB.

2.8 Figures and Legends

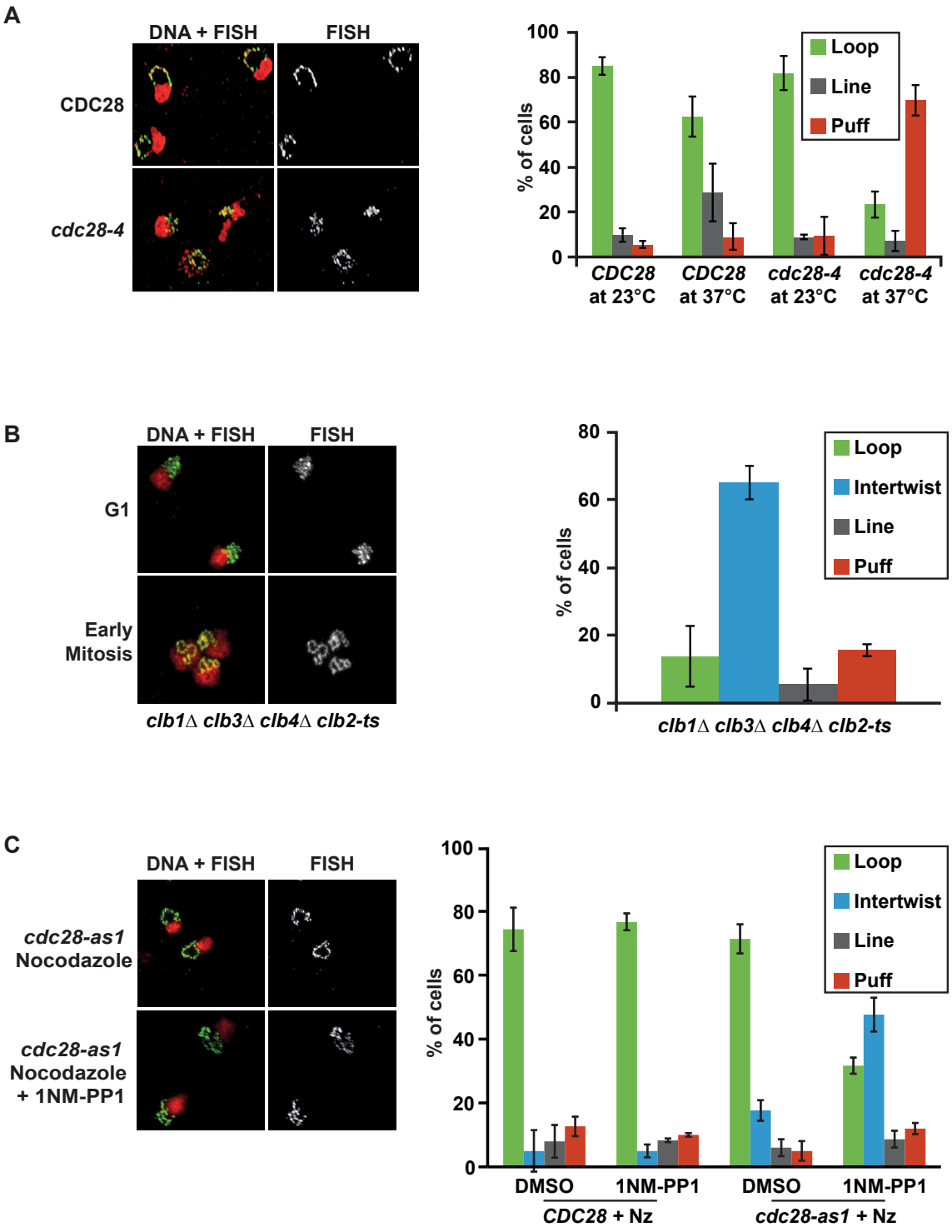

Figure 1 Modulation of Cdk1 activity reveals distinct steps in the process of chromosome morphogenesis.

(**A–C**) Morphology of the yeast rDNA locus revealed by fluorescence *in situ* hybridization (FISH). Representative micrographs of the most prominent rDNA morphology observed for each condition is shown on the left. Propidium iodide (PI; red) and fluorescein isothiocyanate (FITC; green) were used to label the nucleus and rDNA locus, respectively. Quantification of each rDNA species is shown on the right. At least one hundred nuclei were counted per condition. (n=3 for all experiments and error bars represent S.D.) (**A**) *cdc28-4* mutants exhibit classic condensation defects. Cells were blocked in metaphase at 23°C using nocodazole and shifted at 37°C for 1hr before processing samples for FISH analysis. To ensure that the quantification reflects loss of condensation in mitotic cells, rather than a return into interphase due to the loss of *cdc28-4* activity (Sanchez-Diaz et al., 2012), we normalized the rDNA quantification according to the budding index of cells during the arrest. (**B–C**) Reducing Cdk1 activity uncovers a novel condensation intermediate at the rDNA. (**B**) *clb-ts* cells growing asynchronously at 23°C were arrested in G1 or in early mitosis by incubation with alpha-factor or by shifting the culture at 37°C for 135 min, respectively. Cells were subsequently harvested and their rDNA morphology was revealed by FISH. (**C**) *cdc28-as1* cells growing asynchronously at 25°C were arrested in early mitosis by incubation with nocodazole with or without the kinase inhibitor NM-PP1 for 150 min. Samples were then fixed and the morphology of the rDNA locus was monitored as above.

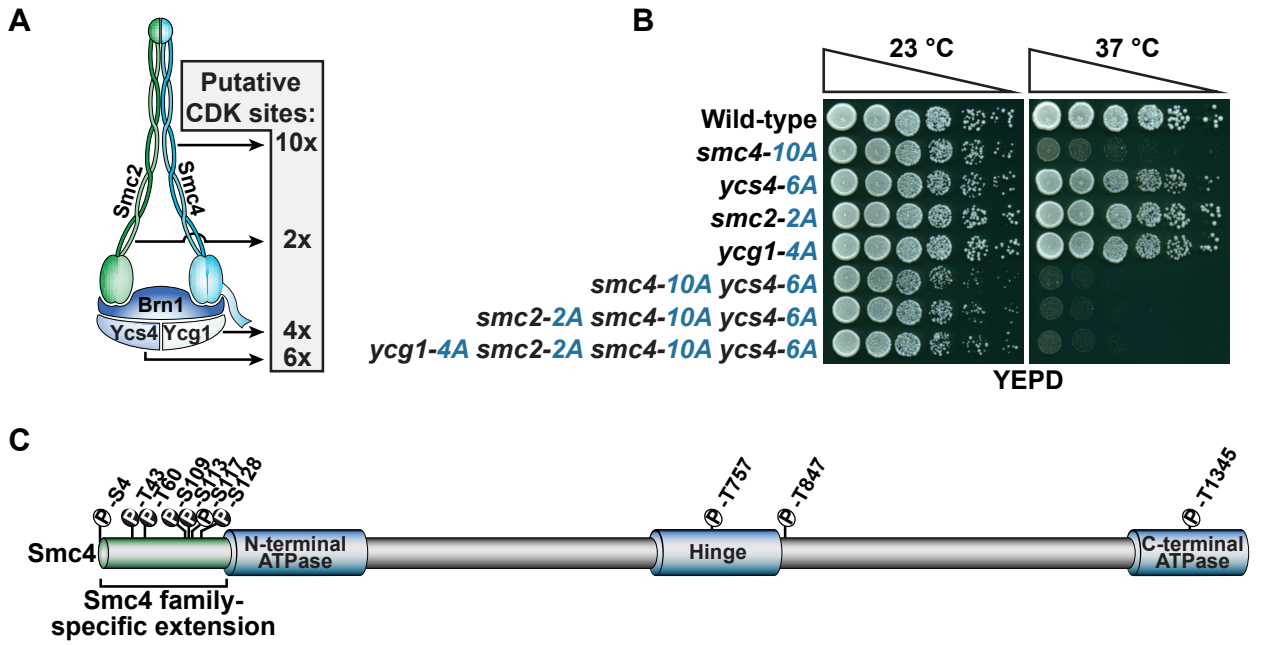
A
Putative CDK sites:
10x
2x
4x
6x
Smc2
Smc4
Brn1
Ycs4
Ycg1
B
23 °C
37 °C
Wild-type
smc4-10A
ycs4-6A
smc2-2A
ycg1-4A
smc4-10A ycs4-6A
smc2-2A smc4-10A ycs4-6A
ycg1-4A smc2-2A smc4-10A ycs4-6A
YEPD
C
S4
T43
T60
S109
S113
S117
S128
T757
T847
T1345
Smc4
N-terminal ATPase
Hinge
C-terminal ATPase
Smc4 family-specific extension
D
SMC4/smc4-ΔNT-3xSTII
Spores
Viability
Genotype
YEPD
SMC4/smc4-ΔNT-3xSTII
SMC4/SMC4-3xSTII
SMC4/smc4-ΔNT-3xSTII
180 kDa
Smc4-3xSTII
Smc4-ΔNT-3xSTII
Pgk1
E
ATP
Cdk1-Clb2
Condensin
Histone H1
245
135
75
48
25
Smc4
Smc2/Ycs4
Ycg1
Brn1
Clb2
Cdc28
Histone H1
F
Smc4-NT
ATP
Cdc28-Clb2
Clb2
Cdc28
Smc4-NT

Figure 2. Smc4 is a key target of Cdk1 in the yeast condensin complex.

(**A**) Schematic representation of the number of putative CDK site (*i.e.,* Ser/Thr-Pro) (Holt et al., 2009) in the subunits of the yeast condensin complex. (**B**) Growth phenotype of condensin subunits lacking putative Cdk1 sites. Five-fold serial dilution of wild-type and phospho-mutants were spotted on solid medium to evaluate growth at 23°C and 37°C. (**C**) Schematic representation of Smc4 domain organization. The positions of Cdk1 phosphorylation sites are marked above the protein schematic. Sites identified by mass spectrometry are labeled with a white P, while other consensus Cdk1 sites were marked with a black P. (**D**) Deletion of the N-terminal extension of Smc4 is lethal in *S. cerevisiae*. Dissection of a sporulated heterozygous diploid strain carrying an allele of Smc4 that has lost its N-terminal extension is shown on the left. The sequence of this particular allele starts at the position of the blue arrow in the sequence shown in Figure S4C, which corresponds to the start site of other SMC family members. On the right, an immunoblot shows that loss of the N-terminal extension of Smc4 does not affect its protein abundance in heterozygous diploid cells. (**E**) *In vitro* kinase assay showing that Smc4 is a direct substrate for Cdk1. Purified condensin was incubated alone (lane 1), with ^{32}P-ATP (lane 2), or in the presence of purified Cdc28-Clb2 complex and ^{32}P-ATP (lane 3). Purified histone H1 was used as positive control for Cdk1 phosphorylation (lane 4). After incubation, proteins were separated on a 4-12% SDS-polyacrylamide gel and revealed by Coomassie staining (left part). An autoradiograph of the same gel is shown on the right. Bullets indicate the different subunits of condensin. Asterisks correspond to the Cdk1-Clb2 complex and the open circle marks the position of histone H1. (**F**) The N-terminal extension of Smc4 is phosphorylated by Cdk1 *in vitro*. Purified Smc4-NT was incubated with ATP or with purified Cdc28-Clb2 complex and ATP. After the kinase reaction, proteins were resolved by SDS-PAGE and stained with Coomassie.

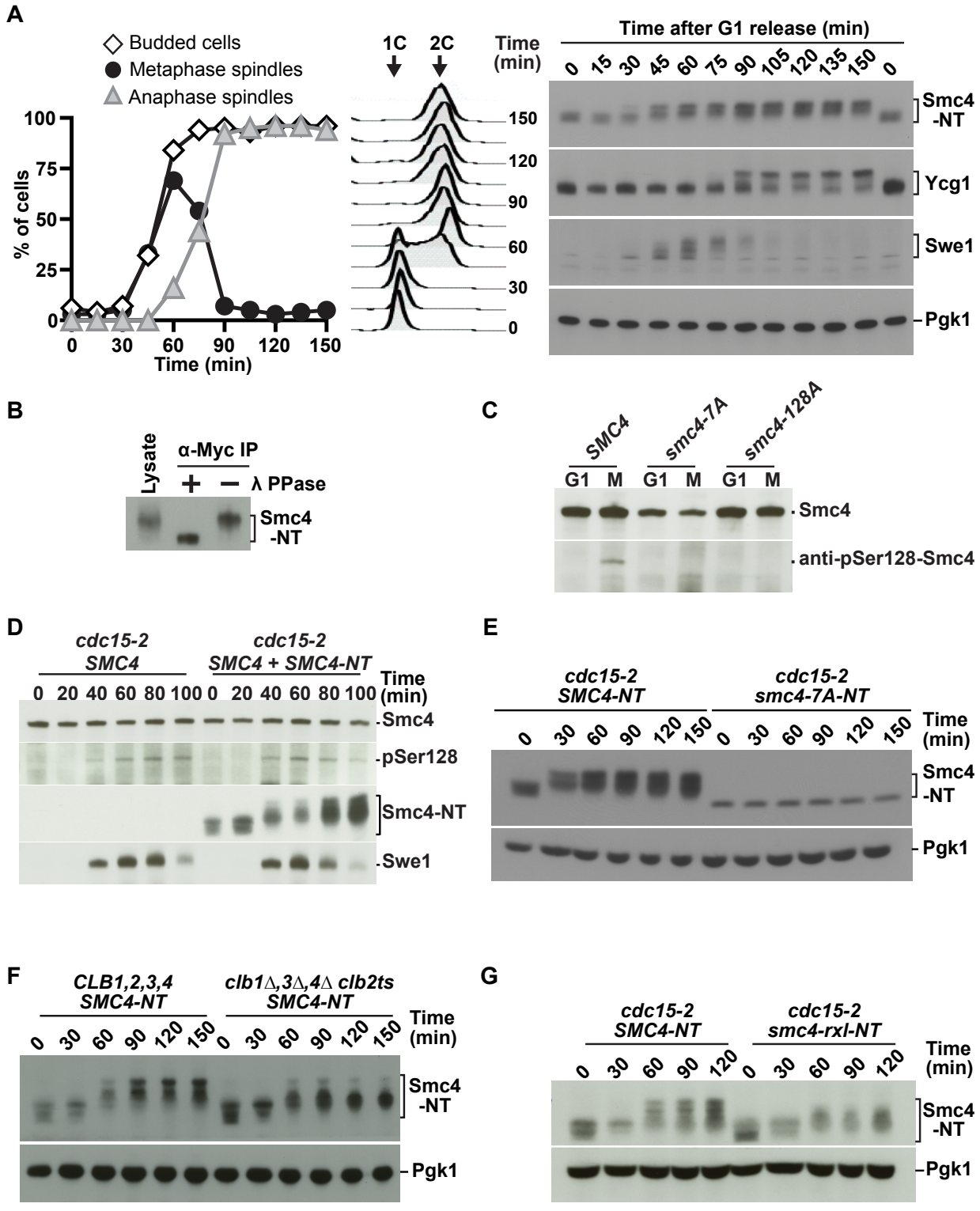

Figure 3. Cdk1 phosphorylates Smc4 in early mitosis.

(**A**) Kinetics of Smc4 modification during the cell cycle. Cells expressing the Smc4-NT fragment were released from a G1 arrest into fresh medium at 37°C. Samples were collected every 15 minutes and processed for visualization of the budding index and mitotic spindle length (left panel), DNA content analysis (middle panel) and immunoblot analysis (right panel). Pgk1 serves as loading control, while changes in the electrophoretic behavior of Swe1 and Ycg1 mark early and late mitotic events, respectively (Harvey et al., 2005). (**B**) λ-phosphatase treatment of Smc4 isolated from mitotic cells. Following dephosphorylation, samples were processed as in panel A. (**C**) Validation of antibodies against phosphoserine 128 (pSer128) of Smc4. Protein samples from interphase (G1) and mitotic (M) cells of the indicated genotypes were probed by immunoblot analysis for the presence of phosphorylated Smc4. (**D**) The appearance of the pSer128 signal parallels that of the phosphorylation-induced gel retardation of Smc4-NT during mitosis. *cdc15-2* mutants carrying *SMC4-3xSTII* with and without the Smc4-NT fragment were released from a G1 arrest into fresh medium at 37°C, and treated for immunoblot analysis as in panel A. The Smc4-3xSTII signal serves as loading control, while the appearance of Swe1 marks mitotic entry, respectively. Note the concurrent appearance of the pSer128 and Swe1 signals, as well as the gel retardation of Smc4-NT at 40 min post-release. The budding index of the cultures is shown in Figure S5A. (**E**) Time course analysis of Smc4 phosphorylation in the presence and absence of Cdk1 sites. Cells expressing wild-type Smc4-NT or the Smc4-7A-NT phospho-mutant were released from a G1 block at 37°C and samples were taken every 30 minutes to evaluate phosphorylation-induced gel retardation. The spindle morphology of cells during the time course experiment is shown in Figure S5C. (**F**) Time course analysis of Smc4-NT phosphorylation in cells carrying *clb1Δ clb3Δ clb4Δ clb2-ts* mutations. The experiment was performed as described in panel E, except that cells were released from G1 arrest in nocodazole-containing medium. The budding index of the cultures is shown in Figure S5E. (**G**) Removal of RxL docking sites leads to a partial loss of Smc4 phosphorylation. *cdc15-2* mutant cells expressing wild-type *SMC4-NT* or the *smc4-rxl-NT* mutant were released from a G1 block at 37°C and treated as in panel E. Percentages of budded cells are shown in Figure S5F.

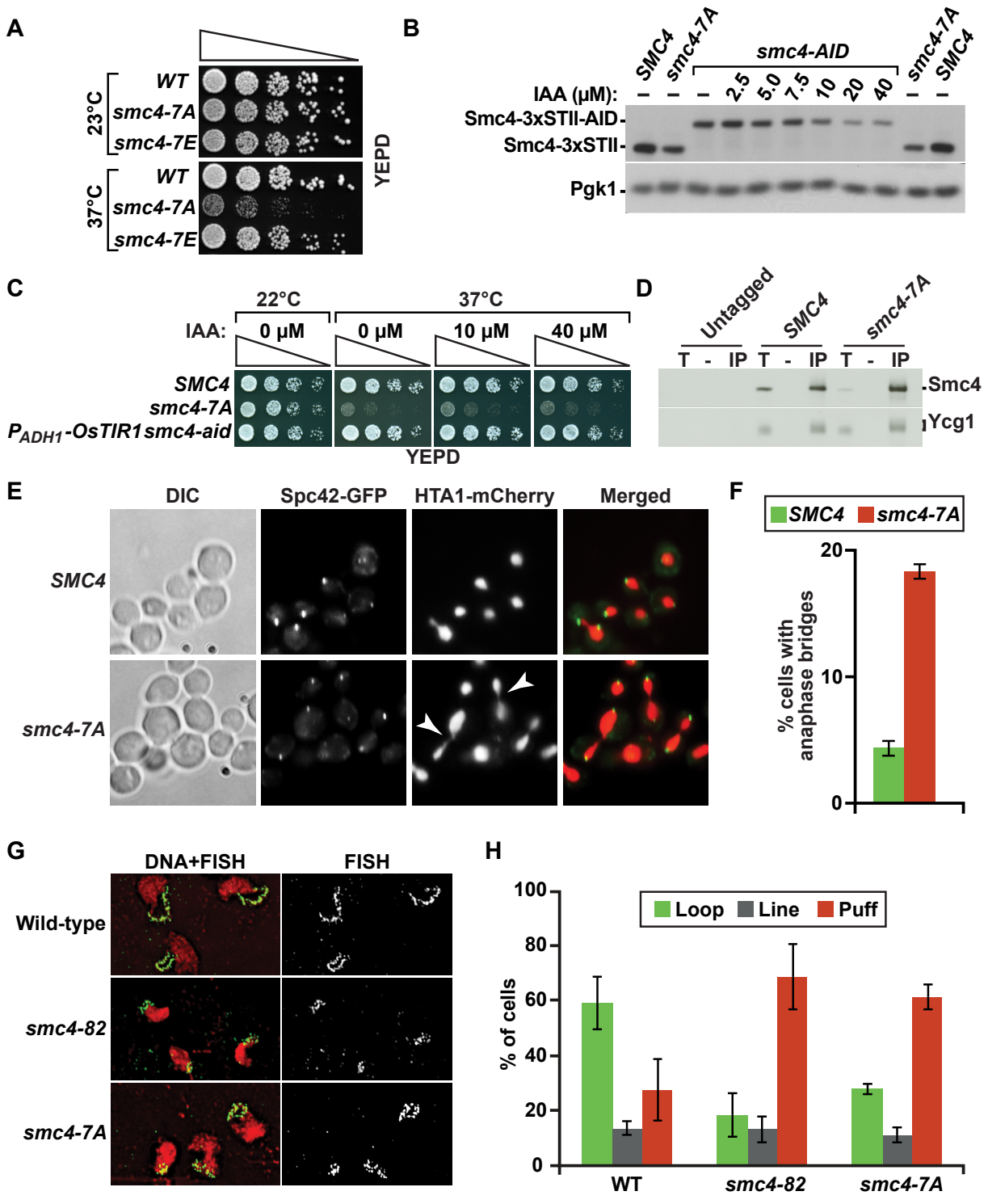

Figure 4. Cdk1-mediated phosphorylation of Smc4 is required for chromosome condensation.

(**A**) Growth properties of phospho-mimetic and phospho-mutant forms of Smc4. Five-fold serial dilution of *smc4* phospho-mutants were spotted on solid medium to evaluate growth at 23°C and 37°C. (**B**) Regulation of Smc4-AID protein abundance by auxin/IAA. Cells were grown asynchronously at 23°C until exponential phase and exposed to different concentrations of auxin for 2 hrs at 30°C. Smc4-AID abundance was evaluated by immunoblot analysis using the 3x StrepTagII epitopes at the C-terminus of the protein. (**C**) Effects of reduced Smc4-AID abundance on yeast growth properties. Strains carrying *SMC4* or *smc4-7A* were included as controls to show normal and ts growth phenotypes in the presence of auxin. (**D**) The *smc4-7A* mutant is competent for condensin complex formation. Smc4 was immunoprecipitated from whole cell extracts using anti-STII antibodies and its ability to associate with Ycg1-3xFLAG was determined by immunobloting. Whole cell extracts (T) and beads only (–) were loaded as controls. Approximately equal amounts of immunoprecipated (IP) Smc4 were loaded in each lane to allow effective comparison of the levels of Ycg1 interacting with Smc4. (**E**) *smc4* phospho-mutants show cytological markers associated with chromosome segregation defects. A high proportion of anaphase nuclei connected with lagging genetic material (arrowheads) and having an elongated morphology can be seen in a culture of *smc4-7A* mutants growing at non-permissive temperature. Chromatin and spindle pole bodies were visualized using HTA1 fused with mCherry and Spc42 fused to GFP, respectively. (**F**) Quantification of anaphase bridges in wild-type and *smc4* phospho mutant (n=3; error bars are S.D.). (**G**) Chromosome condensation defects in *smc4* phospho-mutant. For each genotype, a representative micrograph of the most prominent rDNA species detected by FISH is shown. Cells were grown asynchronously at 23°C until exponential phase and shifted at 37°C for 2h30. Nocodazole was used to block cells in metaphase**.** Nuclei and rDNA were stained with PI (red) and FITC (green), respectively. (**H**) Quantification of rDNA condensation in *SMC4*, *smc4-7A* and *smc4-82* mutants grown at non-permissive temperature. At least 100 cells have been counted for each genotype in 3 independent experiments (error bars are S.D.).

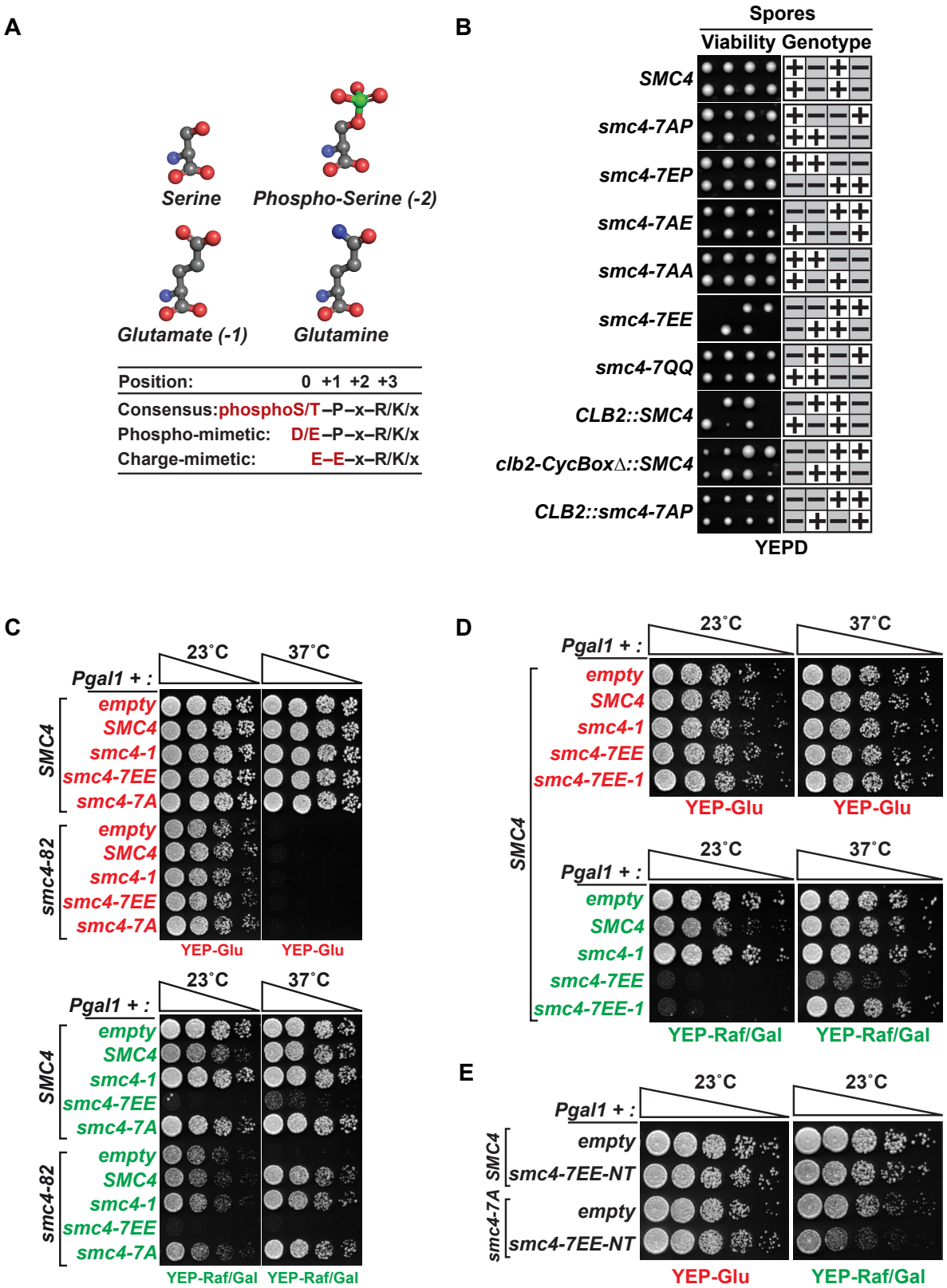
A
Serine
Phospho-Serine (-2)
Glutamate (-1)
Glutamine
Position: 0 +1 +2 +3
Consensus: phosphoS/T–P–x–R/K/x
Phospho-mimetic: D/E–P–x–R/K/x
Charge-mimetic: E–E–x–R/K/x
B
Spores
Viability Genotype
SMC4
smc4-7AP
smc4-7EP
smc4-7AE
smc4-7AA
smc4-7EE
smc4-7QQ
CLB2::SMC4
clb2-CycBoxΔ::SMC4
CLB2::smc4-7AP
YEPD
C
23˚C
37˚C
Pgal1 + :
SMC4
smc4-82
empty
SMC4
smc4-1
smc4-7EE
smc4-7A
YEP-Glu
YEP-Raf/Gal
D
SMC4
empty
SMC4
smc4-1
smc4-7EE
smc4-7EE-1
YEP-Glu
YEP-Raf/Gal
E
23˚C
Pgal1 + :
SMC4
smc4-7A
empty
smc4-7EE-NT
YEP-Glu
YEP-Raf/Gal

Figure 5. Constitutive phosphorylation creates a dominant-negative form of Smc4.
(**A**) Structural basis of phospho-mimicking mutations in *SMC4*. Ball-and-stick representation of different amino-acids used to substitute the phosphorylated residues in Smc4 (top). Positions of the mutagenic substitutions used in this study relative to the Cdk1 optimal consensus for phosphorylation (bottom). (**B**) Physiological effect of charge-mimetic mutations in *SMC4*. Diploid strains carrying *smc4* phospho-mimetic, charge-mimetic, and phospho-constitutive mutations were induced to sporulate and the viability of the resulting haploid spores was determined after 3 days of growth on solid medium. Two typical tetrads of spores are shown per genotype. The genotype of spores was ascertained using the *HIS3* marker associated with the mutant alleles of *SMC4* (*i.e.*, + sign means wild-type *SMC4*). Phospho-defective substitutions are included as controls. (**C**) Overexpression of *smc4-7EE* leads to dominant lethality in cells. Five-fold dilution series of wild-type and *smc4-82* mutant harbouring galactose-inducible versions of *SMC4* integrated at the *URA3* locus were spotted on solid medium to evaluate growth at 23°C and 37°C. Unlike *smc4-1* or *smc4-7A* alleles, expression of *smc4-7EE* induced strong dominant-negative lethality irrespective of the genetic background or temperature used for overexpression. (**D**) The *smc4-7EE* allele encodes a gain-of-function mutant. Five-fold dilution series of wild-type cells expressing a galactose-inducible *smc4-7EE-1* chimeric mutant (or *SMC4*, *smc4-1, smc4-7EE* controls) integrated at the *URA3* locus were spotted on solid medium to evaluate growth as in panel C. (**E**) The charge-mimetic mutations can act in trans. Wild-type or *smc4-7A* mutant cells expressing a galactose-inducible *smc4-7EE-NT* construct were spotted on solid medium, as in panel C.

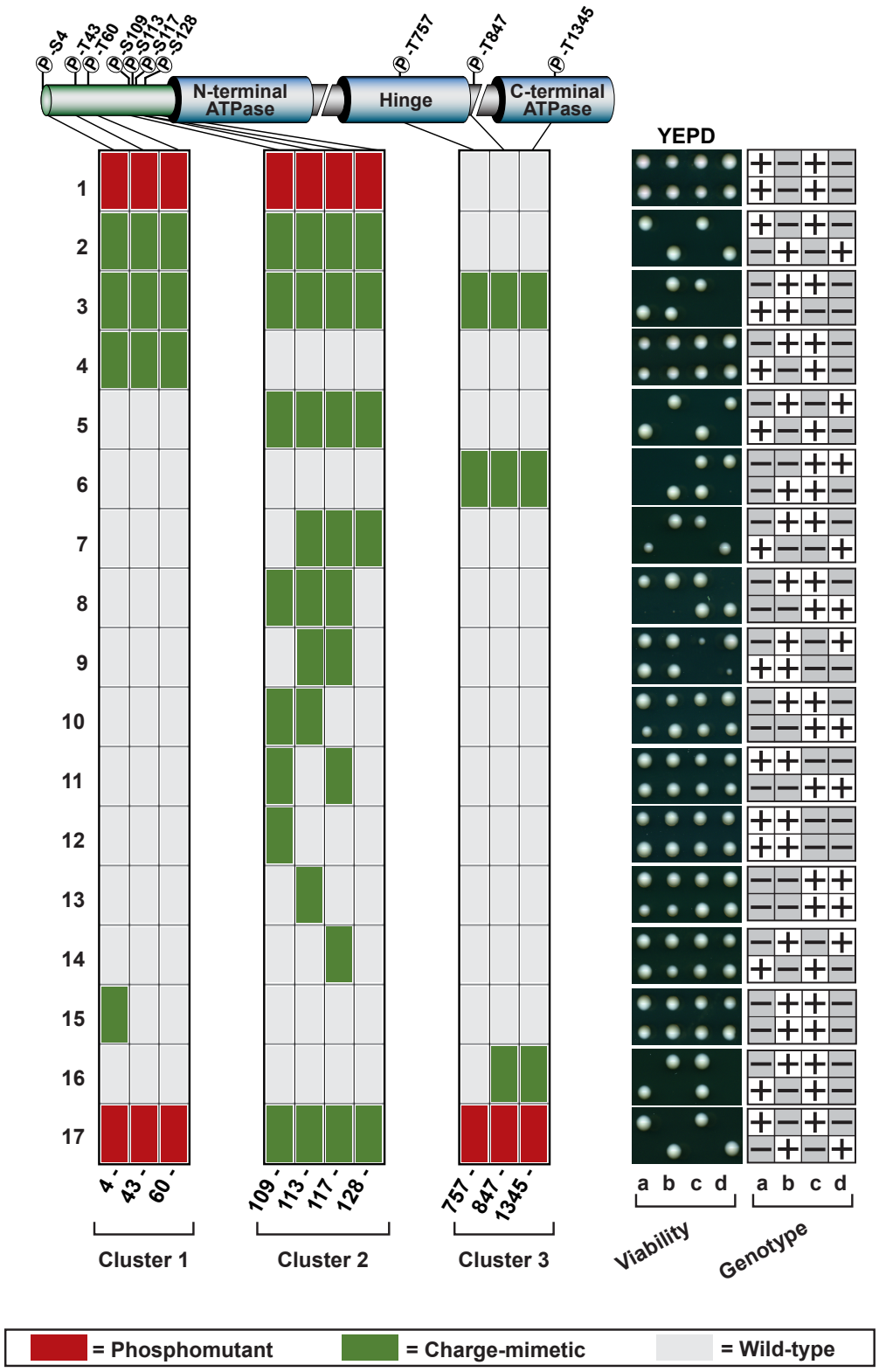
P-S4
P-T43
P-T60
P-S109
P-S113
P-S117
P-S128
P-T757
P-T847
P-T1345
N-terminal ATPase
Hinge
C-terminal ATPase
YEPD
1
2
3
4
5
6
7
8
9
10
11
12
13
14
15
16
17
4 -
43 -
60 -
109 -
113 -
117 -
128 -
757 -
847 -
1345 -
a b c d
a b c d
Cluster 1
Cluster 2
Cluster 3
Viability
Genotype
= Phosphomutant
= Charge-mimetic
= Wild-type

Figure 6. Determining the minimal number of charge-mimetic mutations required to activate condensin.

A schematic representation of Smc4 domains showing the positions of the phosphorylated residues modified in this analysis is shown on top. The combinations of dual charge-mimetic substitutions used in the various mutants are shown in the chart on the left. Phosphorylated residues are represented in the chart by small rectangles that are color-coded according to their mutagenic status (*i.e.*, grey is wild-type; red corresponds to single alanine; and green represents dual charge-mimetic). The viability and genotypes of two typical tetrads of spores resulting from the dissection of diploid strains carrying the various *smc4* mutations are shown on the right of the chart.

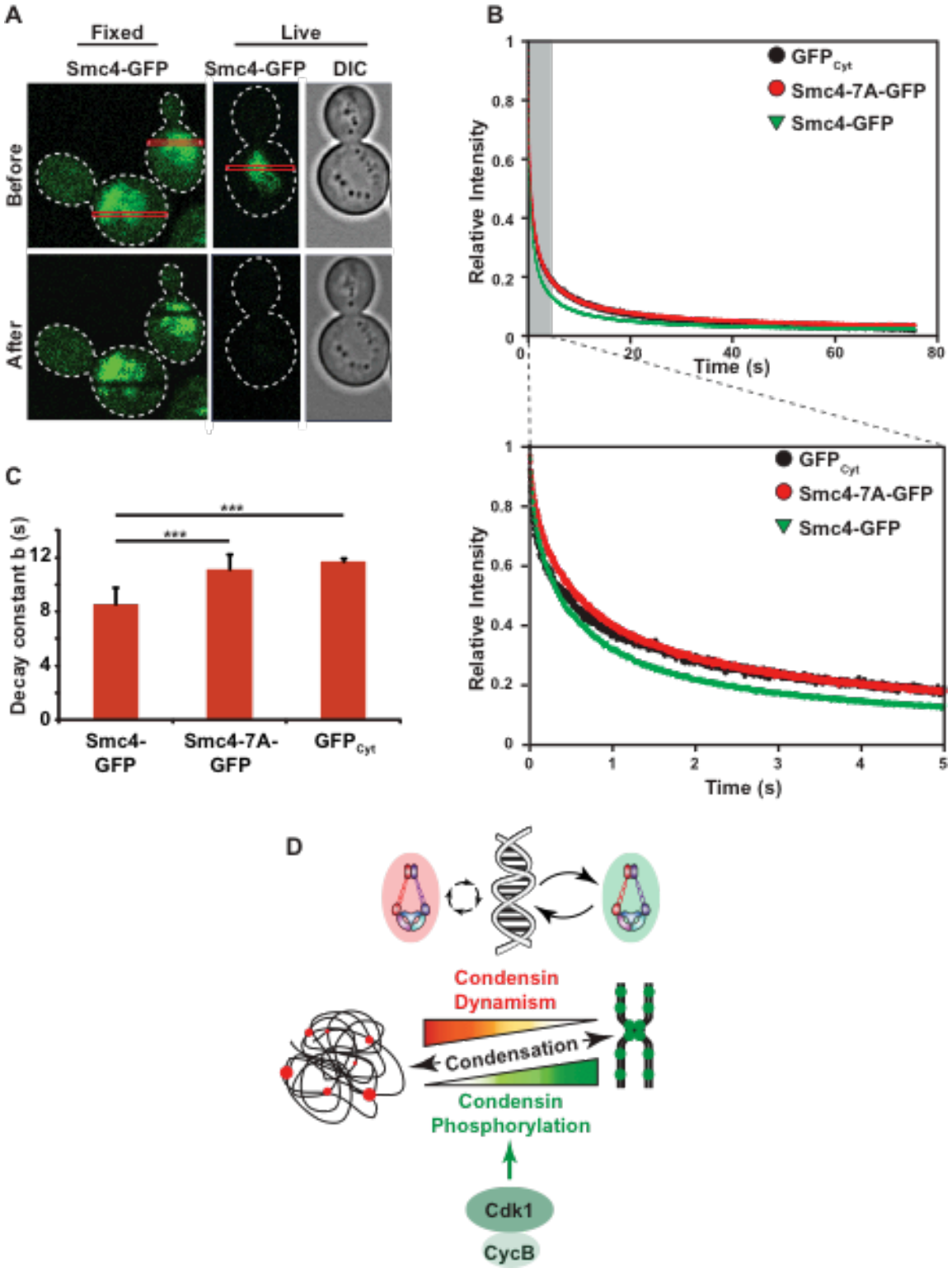
A
Fixed
Live
Smc4-GFP
Smc4-GFP
DIC
Before
After
B
GFP Cyt
Smc4-7A-GFP
Smc4-GFP
Relative Intensity
Time (s)
C
Decay constant b (s)
Smc4-GFP
Smc4-7A-GFP
GFP Cyt
D
Condensin Dynamism
Condensation
Condensin Phosphorylation
Cdk1
CycB

Figure 7. Cdk1 phosphorylation regulates the dynamics of condensin interaction with chromatin.

(**A**) Decay of fluorescence after photobleaching of cells expressing Smc4-3xGFP. Images were collected and photobleaching was performed using a 63x/1.4 NA plan-apochromat oil immersion objective lens. Single DIC and fluorescence images of cells in metaphase were collected before and after each photobleaching experiment. Photobleaching was performed using 20,000 line scans of 512 pixels across the center of the cell with a 488 nm laser at 20% power. Emission from the sample was collected from 493 nm to 598 nm. Photobleaching was performed on fixed cells (left) or live cells (right). Upper panels show Smc4-3xGFP fluorescence prior to treatment, whereas bottom panels show remaining fluorescence after line scan photobleaching. The region of interest in each cell is labelled with a red rectangle, whereas the cell outline is labelled with a dashed line. DIC micrographs are shown for live cells. (**B**) Graphs representing the kinetics of GFP fluorescence decay over time after line scan photobleaching of cells expressing *SMC4-3xGFP*, *smc4-7A-3xGFP* mutant, or cytosolic GFP. Details of the data analysis are in the Materials and Methods section. The bottom graph shows data corresponding to the first five-second interval of the experiment. (**C**) Histogram showing the calculated decay constant b of wild-type Smc4, Smc4-7A mutant and cytosolic GFP. Triple star symbols indicate a significant difference in decay constant for cells expressing different versions of Smc4-3xGFP (***$p<0.001$). Error bars indicate S.D. over three independent experiments ($n\geq12$ cells per experiment). (**D**) Model for the role of Cdk1 in the regulation of chromosome morphogenesis (see text for details).

2.9 References

Abe, S., Nagasaka, K., Hirayama, Y., Kozuka-Hata, H., Oyama, M., Aoyagi, Y., Obuse, C., & Hirota, T. (2011). The initial phase of chromosome condensation requires Cdk1-mediated phosphorylation of the CAP-D3 subunit of condensin II. *Genes Dev, 25*(8), 863-874. doi:10.1101/gad.2016411

Amon, A., Tyers, M., Futcher, B., & Nasmyth, K. (1993). Mechanisms that help the yeast cell cycle clock tick: G2 cyclins transcriptionally activate G2 cyclins and repress G1 cyclins. *Cell, 74*(6), 993-1007.

Baxter, J., & Aragon, L. (2012). A model for chromosome condensation based on the interplay between condensin and topoisomerase II. *Trends Genet, 28*(3), 110-117. doi:10.1016/j.tig.2011.11.004

Bazile, F., St-Pierre, J., & D'Amours, D. (2010). Three-step model for condensin activation during mitotic chromosome condensation. *Cell Cycle, 9*(16), 3243-3255. doi:10.4161/cc.9.16.12620

Bishop, A. C., Ubersax, J. A., Petsch, D. T., Matheos, D. P., Gray, N. S., Blethrow, J., Shimizu, E., Tsien, J. Z., Schultz, P. G., Rose, M. D., Wood, J. L., Morgan, D. O., & Shokat, K. M. (2000). A chemical switch for inhibitor-sensitive alleles of any protein kinase. *Nature, 407*(6802), 395-401. doi:10.1038/35030148

Cimini, D., Mattiuzzo, M., Torosantucci, L., & Degrassi, F. (2003). Histone hyperacetylation in mitosis prevents sister chromatid separation and produces chromosome segregation defects. *Mol Biol Cell, 14*(9), 3821-3833. doi:10.1091/mbc.E03-01-0860

Coudreuse, D., & Nurse, P. (2010). Driving the cell cycle with a minimal CDK control network. *Nature, 468*(7327), 1074-1079. doi:10.1038/nature09543

De Wulf, P., Montani, F., & Visintin, R. (2009). Protein phosphatases take the mitotic stage. *Curr Opin Cell Biol, 21*(6), 806-815. doi:10.1016/j.ceb.2009.08.003

Ditchfield, C., Johnson, V. L., Tighe, A., Ellston, R., Haworth, C., Johnson, T., Mortlock, A., Keen, N., & Taylor, S. S. (2003). Aurora B couples chromosome alignment with

anaphase by targeting BubR1, Mad2, and Cenp-E to kinetochores. *J Cell Biol, 161*(2), 267-280. doi:10.1083/jcb.200208091

Ferrell, J. E., Jr. (1996). Tripping the switch fantastic: how a protein kinase cascade can convert graded inputs into switch-like outputs. *Trends Biochem Sci, 21*(12), 460-466.

Flemming, W. (1882). Zellsubstanz, kern und zelltheilung. *F.C.W Vogel, Leipzig*.

Freeman, L., Aragon-Alcaide, L., & Strunnikov, A. (2000). The condensin complex governs chromosome condensation and mitotic transmission of rDNA. *J Cell Biol, 149*(4), 811-824.

Gavet, O., & Pines, J. (2010). Progressive activation of CyclinB1-Cdk1 coordinates entry to mitosis. *Dev Cell, 18*(4), 533-543. doi:10.1016/j.devcel.2010.02.013

Gerlich, D., Hirota, T., Koch, B., Peters, J. M., & Ellenberg, J. (2006). Condensin I stabilizes chromosomes mechanically through a dynamic interaction in live cells. *Curr Biol, 16*(4), 333-344. doi:10.1016/j.cub.2005.12.040

Gong, D., & Ferrell, J. E., Jr. (2010). The roles of cyclin A2, B1, and B2 in early and late mitotic events. *Mol Biol Cell, 21*(18), 3149-3161. doi:10.1091/mbc.E10-05-0393

Guacci, V., Hogan, E., & Koshland, D. (1994). Chromosome condensation and sister chromatid pairing in budding yeast. *J Cell Biol, 125*(3), 517-530.

Gutherie, G. R. F. a. C. (1991). Guide to yeast Genetics and Molecular Biology. *Acedemic Press, San Diego*.

Harvey, S. L., Charlet, A., Haas, W., Gygi, S. P., & Kellogg, D. R. (2005). Cdk1-dependent regulation of the mitotic inhibitor Wee1. *Cell, 122*(3), 407-420. doi:10.1016/j.cell.2005.05.029

Hauf, S., Cole, R. W., LaTerra, S., Zimmer, C., Schnapp, G., Walter, R., Heckel, A., van Meel, J., Rieder, C. L., & Peters, J. M. (2003). The small molecule Hesperadin reveals a role for Aurora B in correcting kinetochore-microtubule attachment and in maintaining the spindle assembly checkpoint. *J Cell Biol, 161*(2), 281-294. doi:10.1083/jcb.200208092

Hirano, T. (2012). Condensins: universal organizers of chromosomes with diverse functions. *Genes Dev, 26*(15), 1659-1678. doi:10.1101/gad.194746.112

Holt, L. J., Tuch, B. B., Villen, J., Johnson, A. D., Gygi, S. P., & Morgan, D. O. (2009). Global analysis of Cdk1 substrate phosphorylation sites provides insights into evolution. *Science, 325*(5948), 1682-1686. doi:10.1126/science.1172867

Kao, L., Wang, Y. T., Chen, Y. C., Tseng, S. F., Jhang, J. C., Chen, Y. J., & Teng, S. C. (2014). Global analysis of cdc14 dephosphorylation sites reveals essential regulatory role in mitosis and cytokinesis. *Mol Cell Proteomics, 13*(2), 594-605. doi:10.1074/mcp.M113.032680

Kimura, K., Hirano, M., Kobayashi, R., & Hirano, T. (1998). Phosphorylation and activation of 13S condensin by Cdc2 in vitro. *Science, 282*(5388), 487-490.

Kinoshita, E., Kinoshita-Kikuta, E., Takiyama, K., & Koike, T. (2006). Phosphate-binding tag, a new tool to visualize phosphorylated proteins. *Mol Cell Proteomics, 5*(4), 749-757. doi:10.1074/mcp.T500024-MCP200

Koivomagi, M., Valk, E., Venta, R., Iofik, A., Lepiku, M., Morgan, D. O., & Loog, M. (2011). Dynamics of Cdk1 substrate specificity during the cell cycle. *Mol Cell, 42*(5), 610-623. doi:10.1016/j.molcel.2011.05.016

Lavoie, B. D., Hogan, E., & Koshland, D. (2004). In vivo requirements for rDNA chromosome condensation reveal two cell-cycle-regulated pathways for mitotic chromosome folding. *Genes Dev, 18*(1), 76-87. doi:10.1101/gad.1150404

Lenart, P., Petronczki, M., Steegmaier, M., Di Fiore, B., Lipp, J. J., Hoffmann, M., Rettig, W. J., Kraut, N., & Peters, J. M. (2007). The small-molecule inhibitor BI 2536 reveals novel insights into mitotic roles of polo-like kinase 1. *Curr Biol, 17*(4), 304-315. doi:10.1016/j.cub.2006.12.046

Li, Y., Cross, F. R., & Chait, B. T. (2014). Method for identifying phosphorylated substrates of specific cyclin/cyclin-dependent kinase complexes. *Proc Natl Acad Sci U S A, 111*(31), 11323-11328. doi:10.1073/pnas.1409666111

Loog, M., & Morgan, D. O. (2005). Cyclin specificity in the phosphorylation of cyclin-dependent kinase substrates. *Nature, 434*(7029), 104-108. doi:10.1038/nature03329

Lyons, N. A., & Morgan, D. O. (2011). Cdk1-dependent destruction of Eco1 prevents cohesion establishment after S phase. *Mol Cell, 42*(3), 378-389. doi:10.1016/j.molcel.2011.03.023

Maeshima, K., & Eltsov, M. (2008). Packaging the genome: the structure of mitotic chromosomes. *J Biochem, 143*(2), 145-153. doi:10.1093/jb/mvm214

Marko, J. F. (2008). Micromechanical studies of mitotic chromosomes. *Chromosome Res, 16*(3), 469-497. doi:10.1007/s10577-008-1233-7

Morgan, D. O. (2007). The Cell Cycle: Principles of Control. *New Science Press, London*.

Morishita, J., Matsusaka, T., Goshima, G., Nakamura, T., Tatebe, H., & Yanagida, M. (2001). Bir1/Cut17 moving from chromosome to spindle upon the loss of cohesion is required for condensation, spindle elongation and repair. *Genes Cells, 6*(9), 743-763.

Mortensen, E. M., Haas, W., Gygi, M., Gygi, S. P., & Kellogg, D. R. (2005). Cdc28-dependent regulation of the Cdc5/Polo kinase. *Curr Biol, 15*(22), 2033-2037. doi:10.1016/j.cub.2005.10.046

Naumova, N., Imakaev, M., Fudenberg, G., Zhan, Y., Lajoie, B. R., Mirny, L. A., & Dekker, J. (2013). Organization of the mitotic chromosome. *Science, 342*(6161), 948-953. doi:10.1126/science.1236083

Neurohr, G., Naegeli, A., Titos, I., Theler, D., Greber, B., Diez, J., Gabaldon, T., Mendoza, M., & Barral, Y. (2011). A midzone-based ruler adjusts chromosome compaction to anaphase spindle length. *Science, 332*(6028), 465-468. doi:10.1126/science.1201578

Ono, T., Fang, Y., Spector, D. L., & Hirano, T. (2004). Spatial and temporal regulation of Condensins I and II in mitotic chromosome assembly in human cells. *Mol Biol Cell, 15*(7), 3296-3308. doi:10.1091/mbc.E04-03-0242

Paulson, J. R. (2007). Inactivation of Cdk1/Cyclin B in metaphase-arrested mouse FT210 cells induces exit from mitosis without chromosome segregation or cytokinesis and allows passage through another cell cycle. *Chromosoma, 116*(2), 215-225. doi:10.1007/s00412-006-0093-1

Pearlman, S. M., Serber, Z., & Ferrell, J. E., Jr. (2011). A mechanism for the evolution of phosphorylation sites. *Cell, 147*(4), 934-946. doi:10.1016/j.cell.2011.08.052

Peplowska, K., Wallek, A. U., & Storchova, Z. (2014). Sgo1 regulates both condensin and Ipl1/Aurora B to promote chromosome biorientation. *PLoS Genet, 10*(6), e1004411. doi:10.1371/journal.pgen.1004411

Robbins, J. A., & Cross, F. R. (2010). Requirements and reasons for effective inhibition of the anaphase promoting complex activator CDH1. *Mol Biol Cell, 21*(6), 914-925. doi:10.1091/mbc.E09-10-0901

Sanchez-Diaz, A., Nkosi, P. J., Murray, S., & Labib, K. (2012). The Mitotic Exit Network and Cdc14 phosphatase initiate cytokinesis by counteracting CDK phosphorylations and blocking polarised growth. *EMBO J, 31*(17), 3620-3634. doi:10.1038/emboj.2012.224

Schott, E. J., & Hoyt, M. A. (1998). Dominant alleles of Saccharomyces cerevisiae CDC20 reveal its role in promoting anaphase. *Genetics, 148*(2), 599-610.

Slaughter, B. D., Schwartz, J. W., & Li, R. (2007). Mapping dynamic protein interactions in MAP kinase signaling using live-cell fluorescence fluctuation spectroscopy and imaging. *Proc Natl Acad Sci U S A, 104*(51), 20320-20325. doi:10.1073/pnas.0710336105

St-Pierre, J., Douziech, M., Bazile, F., Pascariu, M., Bonneil, E., Sauve, V., Ratsima, H., & D'Amours, D. (2009). Polo kinase regulates mitotic chromosome condensation by hyperactivation of condensin DNA supercoiling activity. *Mol Cell, 34*(4), 416-426. doi:10.1016/j.molcel.2009.04.013

Stern, B., & Nurse, P. (1996). A quantitative model for the cdc2 control of S phase and mitosis in fission yeast. *Trends Genet, 12*(9), 345-350.

Strickfaden, S. C., Winters, M. J., Ben-Ari, G., Lamson, R. E., Tyers, M., & Pryciak, P. M. (2007). A mechanism for cell-cycle regulation of MAP kinase signaling in a yeast differentiation pathway. *Cell, 128*(3), 519-531. doi:10.1016/j.cell.2006.12.032

Sutani, T., Yuasa, T., Tomonaga, T., Dohmae, N., Takio, K., & Yanagida, M. (1999). Fission yeast condensin complex: essential roles of non-SMC subunits for condensation and Cdc2 phosphorylation of Cut3/SMC4. *Genes Dev, 13*(17), 2271-2283.

Tada, K., Susumu, H., Sakuno, T., & Watanabe, Y. (2011). Condensin association with histone H2A shapes mitotic chromosomes. *Nature, 474*(7352), 477-483. doi:10.1038/nature10179

Takemoto, A., Maeshima, K., Ikehara, T., Yamaguchi, K., Murayama, A., Imamura, S., Imamoto, N., Yokoyama, S., Hirano, T., Watanabe, Y., Hanaoka, F., Yanagisawa, J., & Kimura, K. (2009). The chromosomal association of condensin II is regulated by a noncatalytic function of PP2A. *Nat Struct Mol Biol, 16*(12), 1302-1308. doi:10.1038/nsmb.1708

van Heemst, D., James, F., Poggeler, S., Berteaux-Lecellier, V., & Zickler, D. (1999). Spo76p is a conserved chromosome morphogenesis protein that links the mitotic and meiotic programs. *Cell, 98*(2), 261-271.

Vassilev, L. T., Tovar, C., Chen, S., Knezevic, D., Zhao, X., Sun, H., Heimbrook, D. C., & Chen, L. (2006). Selective small-molecule inhibitor reveals critical mitotic functions of human CDK1. *Proc Natl Acad Sci U S A, 103*(28), 10660-10665. doi:10.1073/pnas.0600447103

Wilkins, B. J., Rall, N. A., Ostwal, Y., Kruitwagen, T., Hiragami-Hamada, K., Winkler, M., Barral, Y., Fischle, W., & Neumann, H. (2014). A cascade of histone modifications induces chromatin condensation in mitosis. *Science, 343*(6166), 77-80. doi:10.1126/science.1244508

Yeong, F. M., Hombauer, H., Wendt, K. S., Hirota, T., Mudrak, I., Mechtler, K., Loregger, T., Marchler-Bauer, A., Tanaka, K., Peters, J. M., & Ogris, E. (2003). Identification of a subunit of a novel Kleisin-beta/SMC complex as a potential substrate of protein phosphatase 2A. *Curr Biol, 13*(23), 2058-2064.

Yu, H. G., & Koshland, D. (2005). Chromosome morphogenesis: condensin-dependent cohesin removal during meiosis. *Cell, 123*(3), 397-407. doi:10.1016/j.cell.2005.09.014

2.10 Supplemental Materials and Methods:

2.10.1 Yeast strains and growth conditions

Standard yeast culture conditions have been used (Gutherie, 1991). *Saccharomyces cerevisiae* strains used in this study are derivative of K699 and K700 strains (Nasmyth et al., 1987) and their genotype is summarized in Table S1. Synchronization of cell cultures was performed using α-factor (50 ng/ml for 180 min; G1 arest), nocodazole (30 μg/ml for 150 min; metaphase arrest), NM-PP1 (500 nM for 150 min; G2/M arrest in *cdc28-as1* background), or hydroxyurea (0.2 M for 120 min; S phase arrest) at 23 °C, 25 °C or 37.5 °C (Bishop et al., 2000; St-Pierre et al., 2009). Treatment of yeast with indole-3-acetic acid (IAA) was performed according to published procedures (Nishimura et al., 2009). The growth properties of yeast mutants were determined by serial dilution on solid medium, as described previously (Ratsima et al., 2011). For photobleaching experiments, yeast cultures were grown in low fluorescence synthetic media (*i.e.*, using yeast nitrogen base without folic acid and riboflavin) (Sheff & Thorn, 2004). The cyclin-defective yeast mutant (*clb1Δ clb3Δ clb4Δ clb2-ts* and *clb5Δ clb6Δ*), and the strain carrying *mCherry*-tagged *HTA1* were kind gifts from A. Amon and F.R. Cross, respectively. *Schizosaccharomyces pombe* culture conditions were as described previously (Moreno et al., 1991).

2.10.2 Plasmid and mutant construction

Phospho-site mutations in *SMC4* were incorporated into *YCplac111*-derived plasmids carrying a *SMC4::3xSTII::*T_{ADH1}*:: HIS3 MX6* insert. The following alleles of *SMC4* and of *YCS4* were created in part by custom gene synthesis (Bio Basic Inc.): *smc4-7A(601)*; *smc4-7E(757)*; *smc4-7EE(879)*; *smc4-7AA*(969); *smc4-7AE(1061)*; *smc4-7QQ(1075);* and *ycs4-6A*. Manual site-directed mutagenesis (using Quickchange Multi-Mutagenesis kit, Stratagene) and/or subcloning strategies were used to create other combinations of mutations in the *YCplac111-smc4-x::3xSTII::*T_{ADH1}*::HIS3MX6* plasmid backbone, as well as

in *YCplac33-YCS4::13MYC::T_{ADH1}::kanMX6*, *YCplac111-YCG1::T_{ADH1}::TRP1*, *YCplac22-SMC2::T_{ADH1} ::caURA3MX6* plasmids. Condensin alleles created in this study carry the following mutations: *smc4-7A(601)*: S4A, T43A, T60A, S109A, S113A, S117A and S128A; *smc4-7E(757)*: S4E, T43E, T60E, S109E, S113E, S117E and S128E; *smc4-7EE(879)*: SP[4-5]EE, TP[43-44]EE, TP[60-61]EE, SP[109-110]EE, SP[113-114]EE, SP[117-118]EE and SP[128-129]EE; *smc4-7AA(969)*: SP[4-5]AA, TP[43-44]AA, TP[60-61]AA, SP[109-110]AA, SP[113-114]AA, SP[117-118]AA and SP[128-129]AA; *smc4-7AE(1061)*: SP[4-5]AE, TP[43-44]AE, TP[60-61]AE, SP[109-110]AE, SP[113-114]AE, SP[117-118]AE and SP[128-129]AE; *smc4-7QQ(1075)*: SP[4-5]QQ, TP[43-44]QQ, TP[60-61]QQ, SP[109-110]QQ, SP[113-114]QQ, SP[117-118]QQ and SP[128-129]QQ; *smc4-10A(702)*: S4A, T43A, T60A, S109A, S113A, S117A, S128A, T757A, T847A and T1345A; *smc4-10EE(927)*: SP[4-5]EE, TP[43-44]EE, TP[60-61]EE, SP[109-110]EE, SP[113-114]EE, SP[117-118]EE, SP[128-129]EE, TP[757-758]EE, TP[847-848]EE and TP[1345-1346]EE; *smc4-983*: SP[4-5]EE, TP[43-44]EE and TP[60-61]EE; *smc4-928**: SP[109-110]EE, SP[113-114]EE, SP[117-118]EE and SP[128-129]EE; *smc4-929**: TP[757-758]EE, TP[847-848]EE and TP[1345-1346]EE; *smc4-1051*: SP[113-114]EE, SP[117-118]EE and SP[128-129]EE; *smc4-988*: SP[109-110]EE, SP[113-114]EE and SP[117-118]EE; *smc4-1002*: SP[113-114]EE and SP[117-118]EE; *smc4-986*: SP[109-110]EE and SP[113-114]EE; *smc4-997*: SP[109-110]EE and SP[117-118]EE; *smc4-982*: SP[109-110]EE; *smc4-995*: SP[113-114]EE; *smc4-996*: SP[117-118]EE; *smc4-984**: SP[4-5]EE; *smc4-930**: TP[847-848]EE and TP[1345-1346]EE; *smc4-1013*: S4A, T43A, T60A, SP[109-110]EE, SP[113-114]EE, SP[117-118]EE, SP[128-129]EE, T757A, T847A and T1345A; *smc4-82*: S40P, T43A, S54A, T60A, S67A, S68A, Y106F, S109A, S113A, S117A, L525F, L526P, E557G, V697D, L744V, and L1240P; *smc4-7EE-1*: SP[4-5]EE, TP[43-44]EE, TP[60-61]EE, SP[109-110]EE, SP[113-114]EE, SP[117-118]EE and SP[128-129]EE, L526P, E557G, V697D, L744V; *smc4-ΔNT(1011)*: *[1-153]Δ*-L154M; *ycs4-6A*: S41A, S48A, T66A, T186A, S305A and S988A; *ycg1-4A*: S128A, T591A, T608A and S734A; *smc2-2A*: S91A and S98A. To insert the phospho-mutant alleles of condensin subunits at their endogenous loci, diploid yeast strains were transformed with linearized plasmids containing the appropriate mutations. Integration of the desired mutations was subsequently confirmed by

sequencing the relevant genomic loci. Some alleles of *smc4* (marked with an asterisk above) were obtained through partial integration of phospho-mutations contained within mutagenic constructs. Yeast strains carrying mutations in multiple genes were created by conventional mating and dissection of sporulated heterozygous diploid strains.

To create the *S. pombe cut3-T19V* allele, the open reading frame (ORF) of the gene plus 200 bp of its promoter sequence were subcloned into a pFA6a-kanMX6 series plasmid (Bahler et al. 1998) to create the pFA6a-P_{cut3}-*cut3*::T_{ADH1}::*kanMX6* vector. Site-directed mutagenesis was used to create the pFA6a-P_{cut3}-*cut3-T19V*::T_{ADH1}::*kanMX6* mutant plasmid. Both plasmids were subsequently used as templates to amplify *cut3*-targeting constructs (encompassing the entire ORF plus 200 bp of adjacent sequence) by PCR. The amplification products were transformed into a wild-type diploid yeast strain, and transformants were selected for their ability to grow on solid YES-A medium containing G418. Homologous integration at the *cut3* locus was confirmed by PCR and the entire ORF of the mutant and wild-type alleles were sequenced to confirm the absence of unexpected mutation.

Strains expressing *SMC4* from an ectopic locus were generated by integration at the *URA3* locus of a linearized plasmid carrying the appropriate allele of *SMC4* under the control of the *GAL1* promoter (overexpression) or its own promoter. For each strain, we confirmed by PCR that the *URA3* locus contained a single copy of the integrative plasmid. To create the *CLB2::SMC4* fusion construct, we amplified a version of *CLB2* lacking its destruction and KEN boxes and subcloned it upstream of *SMC4* coding sequence in *YCplac111-SMC4::3xSTII::*T_{ADH1}*:: HIS3MX6* plasmid, thereby creating *YCplac111-*P_{SMC4}*-CLB2::SMC4::3xSTII::*T_{ADH1}*::HIS3MX6*. This cloning step also introduced a flexible linker between *CLB2* and *SMC4*. The *CLB2::smc4-7A* fusion construct was obtained by subcloning the N-terminal part of *smc4-7A* from *YIplac211-*P_{GAL1}*-smc4-7A::3xSTII::*T_{ADH1}*::URA3* plasmid into the *YCplac111-*P_{SMC4}*-CLB2 ::SMC4::3xSTII::*T_{ADH1}*::HIS3MX6*. To create the *CycBoxΔ* variant of this construct, we introduced 2 new *Stu*I restriction sites in the nucleotide sequence encoding residues RF291-292 and MN362-363 of *CLB2*. *YCplac111-*P_{SMC4}*-clb2-CycBoxΔ:: SMC4 ::3xSTII::*

T_{ADH1}::HIS3MX6 was obtained after removal of the *Stu*I-fragment and re-ligation of the plasmid. This removes the sequence encoding residues F292 to N363 (inclusively), thereby creating a version of Clb2 analogous to the *Δ241-313* mutant of human Cyclin A2, which is incapable of binding to Cdc2/Cdk1 (Lees & Harlow, 1993). Wild-type, *smc4-7A* and *CycBoxΔ* versions of the *CLB2::SMC4* plasmids were then linearized and transformed into a wild-type diploid strain. To create the *smc4-ΔNT(1011)*- targeting construct, we introduced a new BamHI restriction site at the sequence encoding L154 of *SMC4* in *YCplac111-P_{SMC4}-BamHI-SMC4::3xSTII::T_{ADH1}::HIS3MX6*. The *YCplac111-P_{SMC4}-BamHI-smc4-ΔNT::3xSTII::T_{ADH1}::HIS3MX6* construct was obtained after removal of the BamHI fragment and re-ligation of the parental plasmid. This removes the sequence M1 to R153 (inclusively) and substitutes the L154 into a start codon. To create strains expressing *smc4-AID*, we subcloned the auxin-inducible degron sequence (Nishimura et al., 2009) downstream of *SMC4* coding sequence in *YCplac111-SMC4::3xSTII::T_{ADH1}::HIS3MX6*, thereby creating *YCplac111-SMC4::3xSTII:: AID::HIS3MX6.* This plasmid was then linearized and transformed into a strain expressing *Oryza sativa* (*Os*) *TIR1* gene (Nishimura et al., 2009). Selection of the transformed yeast on SC-histidine medium and PCR screening revealed clones with *smc4-AID* integrated at its endogenous locus. Single copy integration of *smc4-aid* was confirmed by qPCR analysis of the amplification signal obtained from genomic DNA isolated from a control wild-type strain and from the *smc4-aid* strain. The *SMC4* amplification signal was essentially identical (relative to *TRP1*) in both strains, thereby indicating the presence of a single copy of *SMC4* gene in the *smc4-aid* strain (data not shown). The plasmid containing the AID degron and the yeast strain expressing *OsTIR1* were obtained from the Yeast Genetic Resource Center (YCGR, Japan). Strains expressing Smc4-NT/Smc4-7A-NT/Smc4-rxl-NT from centromeric plasmids were constructed as follows. A new restriction site was introduced by site-directed mutagenesis into *YCplac111-SMC4::13MYC::T_{ADH1}::HIS3MX6* to allow removal of the C-terminal part of Smc4 (*i.e.*, from residue 143 to 1418). After the removal was completed, the sequence encoding SV40 large T antigen nuclear localization signal (PKKKRK) (Kalderon et al., 1984) was inserted between the sequence encoding *SMC4-[1–142]* and the *13xMYC* tag to ensure the correct localization of the reporter

construct. *YCplac111-smc4-7A(601)[1-142]::NLS::13MYC::T_{ADH1}::HIS3MX6* was obtained by subcloning the N-terminal part of *YCplac111-smc4-7A(601)::13MYC::T_{ADH1}::HIS3MX6* into *YCplac111-SMC4[1-142]::NLS::13MYC::T_{ADH1}::HIS3MX6*. *YCplac111-smc4[1-142]-[RxL#1/2->AAA]::NLS:: 13MYC::T_{ADH1}::HIS3MX6* was obtained by site-directed mutagenesis of *SMC4* sequence in *YCplac111-SMC4[1-142]::NLS::13MYC::T_{ADH1}::HIS3MX6* plasmid (using Quickchange Multi-Mutagenesis kit, Stratagene). These single-copy plasmids were transformed into *cdc15-2*, *clb1Δ clb3Δ clb4Δ clb2-VI*, *clb5Δ clb6Δ*, *cdc5-99*, and *cdc28-4 cdc5-99* mutants, or in a wild-type strain and maintained in yeast using selective medium. The plasmid expressing *SMC4-7EE-NT* from the *GAL1* promoter was obtained by subcloning the N-terminal part of *YCplac111-smc4-7EE-[1–142]::13MYC::TADH1::HIS3MX6* into *YIplac211-smc4-7EE::3xSTII::T_{ADH1}*. The plasmid used to express and purify the N-terminal extension of Smc4 in bacteria was created by subcloning a PCR-amplified fragment encoding the first 163 amino-acid residues of *SMC4* into the pET30a plasmid. The resulting construct expresses Smc4-[1-163] as a fusion protein with a C-terminal hexahistidine tag. In all plasmid constructs, the sequences of condensin subunits correspond to those present in the wild-type K699 strain background. For the overexpression and purification of the Cdc28-Clb2 complex, *P_{GAL1}-2xStreptagII-CLB2* and *P_{GAL10}-9xHIS-CDC28* were subcloned in a 2µ *URA3 leu2-d* plasmid, resulting in p711. Key residues within the destruction box of *CLB2* were removed (*i.e.*, R25A, L28A) to ensure maximal expression of the protein in yeast. Maps of most plasmids used in this study are available and will be provided upon request.

2.10.3 Western blotting

Cell lysates were prepared using the TCA/glass bead method (Foiani et al., 1994). To visualize the phosphorylation-induced gel shift of Smc4-NT, lysates were separated on 8% Phos-tag gels (Kinoshita et al., 2006) following the manufacturer's instructions. Note that Smc4-NT and Smc4-7A-NT migrate at nearly identical positions on gel after phosphatase treatment (data not shown). To detect full-length Smc4, yeast lysates were separated by SDS-PAGE using gels containing 7.5% Next Gel acrylamide (St-Pierre et al.,

2009) (Amresco). All gels were transferred using the iBlot system (Invitrogen). Membranes were probed with the following antibodies: mouse monoclonal 9E-10 (from GeneTex; at 1:1000 dilution) or 9E-11 (gift from A. Verreault; at 1:1000 dilution); rabbit polyclonal anti-Swe1 (gift from A.D. Rudner; at 1:1000 dilution in Fig. 3A); rat monoclonal 18D9 and 15F2 antibodies against Swe1 (from Medimabs; both at 1:150 dilution in Fig. 3D); mouse monoclonal anti-StrepTagII (from Qiagen; at 1:1000 dilution); mouse monoclonal 11H12 and 4F10 against Cdc5 (from Medimabs; both at 1:500 dilution); and mouse monoclonal 22C5 (from Abcam; at 1:10,000 dilution) in 2% milk and 1% BSA. The rabbit polyclonal anti-phospho-serine 128 and anti-phospho-serine 4 antibodies were generated by Genscript using a phosphorylated peptide covering the amino-acid sequence surrounding Ser128 or Ser4 in Smc4 and used at a 1:250 and 1:1000 dilutions in 5% BSA respectively. The rat monoclonal antibodies 18D9 and 15F2 were generated against full-length recombinant Swe1 expressed in bacteria and recognize different epitopes on the protein. Secondary antibodies used were HRP-conjugated anti-mouse or anti-rabbit IgG antibodies (1:10,000, Amersham/GE Healthcare). Protein-antibody conjugates were revealed by chemiluminescence (Western Lightning *Plus* ECL; Perkin-Elmer).

2.10.4 Fluorescent *in situ* hybridization (FISH)

For all experiments, cells were fixed and harvested in 0.1M KPO_4 buffer pH 6.4 containing 3.7% formaldehyde for 2hrs at 23 °C. We used published procedures to reveal the morphology of the rDNA locus by FISH (Guacci et al., 1994; Lavoie et al., 2004). Probes were generated by PCR amplification of a section of the rDNA locus cloned within plasmid p333, which contains a ~9.1 kb XmaI fragment encompassing a complete rDNA repeat. The amplified fragment was purified after electrophoretic separation using Qiagen's Gel Extraction kit and labelled with digoxigenin using the BioNick Labelling System (Invitrogen). The digoxigenin labelling protocol is similar to that described for biotin labelling, except that 1 µl digoxigenin DNA labelling mixture (Gasser et al.) and 5 µl 10X nick translation buffer (0.5 M Tris-HCl pH 7.8, 50 mM MgCl, 100 mM beta-

mercaptoethanol, 100 µg/ml Bovine Serum Albumin [BSA]) are substituted for 5 µl 10X dNTP mix from the BioNick Labelling kit. The digoxigenin-labelled probe was detected using a mouse anti-DIG antibody from Roche, and FITC-conjugated goat anti-mouse IgG (Jackson Immunoresearch) and Alexa Fluor 488-conjugated rabbit anti-goat IgG antibodies (Jackson Immunoresearch). All three antibodies were diluted 1:250 using 10% horse serum immediately prior to use. Nuclei were counterstained with propidium iodide (PI; Sigma) in 5 mg/ml of p-phenylenediamine (Sigma).

2.10.5 Microscopy

Procedures to monitor mitotic spindle length, nucleus morphology and spindle pole body position in cells have been described previously (Ratsima et al. 2011). Live cell imaging and visualization of rDNA morphology were performed on a DeltaVision microscope using the softWoRx software (Applied Precision). The microscope was equipped with a 100X/NA 1.4 Plan APO objective (Olympus) and a CoolSnap HQ2 camera (Photometrics). Images were acquired at 1x1 binning. Final images represent maximum intensity projections of multiple image stacks taken at 0.2 µm intervals. Deconvolution (softWoRx) was applied to images shown in Figures 1A and 4G to represent accurately the morphology of the rDNA loops observed under the microscope.

2.10.6 Photobleaching

Cells were grown until exponential phase at 25 °C in modified synthetic medium. Photobleaching experiments were performed on a Zeiss 710 confocal laser scanning microscope (Carl Zeiss, Jena, Germany) attached to an AxioObserver inverted microscope stand. Images were collected and photobleaching was performed using a 63x/1.4 NA plan-apochromat oil immersion objective lens. Single images of cells in metaphase (*i.e.*, with a large bud and the nucleus close to the bud neck) were collected at 10x zoom and at low laser power (2% of the 488 nm laser line of a 25 mW argon ion laser) in DIC and in fluorescence before and after each photobleaching experiment. Cells were then centered

in the field of view. Photobleaching was performed using the line scan feature and a bleach line of 512 pixels across the center of the cell was selected. Total of 20,000 line scans were collected with 3.15 µs pixel dwell times for each cell, PMT gain at 700 digital gain at 1, digital offset at 10, pinhole at 2 Airy unit, no line averaging and 20% laser power. Emission from the sample was collected from 493 nm to 598 nm. Experiments were done on at least twelve budded cells for each strain. Fixed cell experiments were performed the same way on cells fixed with 3.7% formaldehyde for 5 min at room temperature. Two rectangular regions of interest were selected on XT line scan plots, one for background intensity and one for EGFP fluorescence intensity measurements. Intensity measurements were then corrected line-by-line for the background intensity (from an area of the XT line scan image where no cell was located). Corrected intensities were normalized to maximal for each photobleaching trace. Normalized data from three separate experiments were averaged and standard deviations were calculated from the three experimental averages. Final normalized curves for each strain were plotted and fit to a double exponential decay with an offset (*i.e.*, Equation 1). Graphs were generated and fit using SigmaPlot software (Systat Sofware Inc., Chicago, Il). Equation 1: $y = y_0 + a * e^{(-x/b)} + c * e^{(-x/d)}$.

2.10.7 Protein purification

To identify Cdk1 phosphorylation sites on condensin, the complex was immunopurified from nocodazole-arrested cell lysates and processed for mass spectrometry analysis, as previously described (St-Pierre et al., 2009). For the purification of Smc4 N-terminus from bacteria, plasmid p792 expressing the first 163 residues of Smc4 fused to a hexahistidine tag was transformed into *Escherichia coli* BL21 strain. Cells were inoculated at an optical density (A_{600}) of 0.225 in LB medium containing all the necessary antibiotics and grown for 2 hr at 30 °C. Overexpression was induced by the addition of 1mM IPTG for 1 hr. Cells were collected by centrifugation and suspended in buffer A (50 mM KPO_4 pH 8.0, 500 mM NaCl, 10 mM imidazole, plus protease inhibitor cocktail [0.5 mM 4-(2-aminoethyl) benzenesulfonyl fluoride hydrochloride (AEBSF), 10 µM Pepstatin

A and 7.5 µM E64]) containing 300 µg/ml lysozyme. After a 30 min incubation at 4 °C, cells were lysed by sonication using a Misonix sonicator 3000 (3 pulses of 10 sec at output level 3) and centrifuged 15 min at 13000 rpm. The supernatant was further clarified by filtration with a 0.45 µm syringe-filter. The recombinant Smc4-[1-163] protein was purified on a FPLC system equipped with a HisTrap column (GE Healthcare) and fractions containing the purified protein were concentrated by ultrafiltration using Amicon Ultra filtration units (3K Nominal Molecular Weight Limit [NMWL]; Millipore). All purification steps were carried out at 4 °C. For kinase assays, condensin and Cdc28-Clb2 were purified according to published procedures (Ratsima et al., 2011; St-Pierre et al., 2009).

2.10.8 *In vitro* kinase assay

3 µg of purified condensin or 0.5 µg of histone H1 were diluted into a final volume of 15 µl of kinase reaction buffer (25 mM Tris-HCl pH 7.5, 2 mM DTT, 10 mM $MgCl_2$, 0.5 mM EDTA, 100 µM ATP) supplemented with protease/phosphatase inhibitors (1 mM AEBSF, 10 µM E-64, 10 µM pepstatin A and 200 µM tungstate), and 2 µCi [γ32P] ATP, and 1.86 µg purified Cdc28-Clb2. Phosphorylation reactions were performed for 30 minutes at 30 °C and stopped by addition of SDS-PAGE sample loading buffer. Proteins were denatured 5 minutes at 100 °C and separated on a 4-12% gradient gel (Biorad) before being revealed byCoomassie staining (Biorad). ^{32}P-labelled bands were detected in dried gels by autoradiography using Amersham Hyperfilm ECL films (GE Healthcare). For kinase reactions with Smc4-[1-163], 0.5 µg of purified substrate was phosphorylated using the same conditions as described above, except that radio-labelled ATP was omitted from the reaction. Phosphorylated proteins were separated on 14% SDS-polyacrylamide gels and revealed by coomassie staining.

2.10.9 Immunoprecipitation and dephosphorylation

Cell lysates were prepared in lysis buffer (50 mM Tris-HCl pH7.5, 100 mM KCl, 100 mM

NaF, 10% glycerol, 0.1% tween 20, 1 mM tungstate, 1 mM DTT, 10 μM AEBSF, 10 μM pepstatin A, 10 μM E-64), as previously described (St-Pierre et al., 2009). For each immunoprecipitation reaction, 5 μg of anti-Myc 9E-10 or anti-Strep-tag antibody were bound to GammaBind Plus Sepharose beads (GE Healthcare). Dephosphorylation reactions were performed at 30 °C for 30 minutes in λ-phosphatase buffer (NEB) in presence or absence of purified λ phosphatase.

2.10.10 Other experimental procedures and statistical analyses

Determination of budding index by light microscopy and DNA content by flow cytometry were performed using standard procedures (Ratsima et al., 2011). For budding index, 100 cells were scored per time-point. Except for mass spectrometry analysis of purified condensin subunits (*i.e.*, Supplementary Fig. 2a), all experiments described in this study have been performed 3 (or more) independent times. Error bars in graphs represent standard deviation (S.D.). Triple star symbols in graphs indicate statistically significant differences, as determined by *t*-test (paired, one tailed distribution). *P*-values are provided in the legend of figures.

2.10.11 Table S1: Yeast strains used in this study

Relevant parts of the genotypes of yeast strains used in this study are described next to yeast designations.

Figure	Name	Relevant genotype
Fig 1A	D2	*MATα CDC28*
	D1483	*MATα cdc28-4*
Fig 1B	D390	*MATa clb1Δ clb3Δ::TRP1 clb4Δ::HIS3 clb2-ts*

Fig 1C	D4107	*MATa CDC28*
	D2395	*MATa cdc28-as1*
Fig 2B	D1	*MATa SMC4 YCS4 SMC2 YCG1*
	D2565	*MATa smc4-10A(702)::3xSTII::HIS3MX6*
	D3317	*MATa ycs4-6A::13xMYC::kanMX6*
	D3334	*MATa smc2-2A::caURA3MX6*
	D3347	*MATa ycg1-4A::TRP1*
	D3349	*MATa smc4-10A(702)::3xSTII::HIS3MX6 ycs4-6A ::13xMYC::kanMX6*
	D3384	*MATa smc4-10A(702)::3xSTII::HIS3MX6 ycs4 6A ::13xMYC::kanMX6 smc2-2A::caURA3MX6*
	D3421	*MATa smc4-10A(702)::3xSTII::HIS3MX6 ycs4-6A ::13xMYC::kanMX6 smc2-2A::caURA3MX6 ycg1-4A::TRP1*
Fig 2D	D3321	*MATa/MATα SMC4/SMC4::3xSTII::HIS3MX6*
	D3727	*MATa/MATα SMC4/smc4-ΔNT(1011)::3xSTII::HIS3MX6*
Fig 3A & B	D2832	*MATa YCG1::3xFLAG::kanMX6 cdc15-2 [YCplac111-SMC4-NT::NLS::13xMYC]*
Fig 3C	D2963	*MATa SMC4::3xSTII::HIS3MX6*
	D2563	*MATa smc4-7A(601)::3xSTII::HIS3MX6*
	D1868	*MATa smc4-128A::3xSTII::HIS3MX6*
Fig 3D	D2969	*MATa SMC4::3xSTII::HIS3MX6 YCG1::3xFLAG::kanMX6 cdc15-2*
	D3265	*MATa SMC4::3xSTII::HIS3MX6 YCG1::3xFLAG::kanMX6 cdc15-2 [YCplac111-SMC4-NT::NLS::13xMYC]*
Fig 3E	D3265	*MATa SMC4::3xSTII::HIS3MX6 YCG1::3xFLAG::kanMX6*

		cdc15-2 [YCplac111-SMC4-NT::NLS::13xMYC]
	D3267	*MATa SMC4::3xSTII::HIS3MX6 YCG1::3xFLAG::kanMX6 cdc15-2 [YCplac111-smc4-NT-7A::NLS::13xMYC]*
Fig 3F	D4022	*MATa CLB1 CLB2 CLB3 CLB4 [YCplac111-SMC4-NT::NLS::13xMYC]*
	D4024	*MATa clb1Δ clb3Δ::TRP1 clb4Δ::HIS3 clb2-ts [YCplac111-SMC4-NT::NLS::13xMYC]*
Fig 3G	D2832	*MATa YCG1::3xFLAG::kanMX6 cdc15-2 [YCplac111-SMC4-NT::NLS::13xMYC]*
	D4020	*MATa YCG1::3xFLAG::kanMX6 cdc15-2 [YCplac111-SMC4-rxl-NT::NLS::13xMYC]*
Fig 4A	D2963	*MATa SMC4::3xSTII::HIS3MX6*
	D2563	*MATa smc4-7E(757)::3xSTII::HIS3MX6*
Fig 4B & C	D3272	*MATa SMC4::3xSTII::HIS3MX6*
	D2563	*MATa smc4-7E(757)::3xSTII::HIS3MX6*
	D3692	*MATa SMC4::3xSTII::AID::HIS3MX6 ura3-1::ADH1::OsTIR1::9xMYC::URA3*
Fig 4D	D1	*MATa SMC4 YCG1*
	D2969	*MATa SMC4::3xSTII::HIS3MX6 YCG1::3xFLAG::kanMX6 cdc15-2*
	D3192	*MATa smc4-7A(601)::3xSTII::HIS3MX6 YCG1::3xFLAG::kanMX6 cdc15-2*
Fig 4E & F	D3882	*MATa SMC4::3xSTII::HIS3MX6 HTA1-mCherry::URA3 SPC42-GFP::TRP1*

	D3884	*MATa smc4-7A(601)::3xSTII::HIS3MX6 HTA1-mCherry::URA3 SPC42-GFP::TRP1*
Fig 4G & H	D2963	*MATa SMC4::3xSTII::HIS3MX6*
	D1817	*MATa smc4-82::HIS3MX6*
	D2563	*MATa smc4-7E(757)::3xSTII::HIS3MX6*
Fig 5B	D3321	*MATa/MATα SMC4/SMC4::3xSTII::HIS3MX6*
	D1652	*MATa/MATα SMC4/smc4-7AP(601)::3xSTII::HIS3MX6*
	D2452	*MATa/MATα SMC4/smc4-7EP(757)::3xSTII::HIS3MX6*
	D3919	*MATa/MATα SMC4/smc4-7AE(1061)::3xSTII::HIS3MX6*
	D3471	*MATa/MATα SMC4/smc4-7AA(969)::3xSTII::HIS3MX6*
	D3226	*MATa/MATα SMC4/smc4-7EE(879)::3xSTII::HIS3MX6*
	D3921	*MATa/MATα SMC4/smc4-7QQ(1075)::3xSTII::HIS3MX6*
	D3928	*MATa/MATα SMC4/CLB2::SMC4::3xSTII::HIS3MX6*
	D3971	*MATa/MATα SMC4/clb2-CycBoxΔ::SMC4::3xSTII::HIS3MX6*
	D4218	*MATa/MATα SMC4/CLB2::smc4-7A(601)::3xSTII::HIS3MX6*
Fig 5D	D3940	*MATa SMC4::3xSTII::HIS3MX6 ura3-1::Pgal1::URA3*
	D3941	*MATa SMC4::3xSTII::HIS3MX6 ura3-1::Pgal1::SMC4::3xSTII::URA3*
	D3966	*MATa SMC4::3xSTII::HIS3MX6 ura3-1::Pgal1::smc4-1::3xSTII::URA3*
	D3942	*MATa SMC4::3xSTII::HIS3MX6 ura3-1::Pgal1::smc4-7EE(879)::3xSTII::URA3*
	D4219	*MATa SMC4::3xSTII::HIS3MX6 ura3-1::Pgal1::smc4-7EE-1()::3xSTII::URA3*

Fig 5E	D4364	*MATa SMC4::3xSTII::HIS3MX6 ura3-1::Pgal1::URA3*
	D4341	*MATa SMC4::3xSTII::HIS3MX6 ura3-1::Pgal1::smc4-7EE-NT::NLS::13xMyc::URA3*
	D4366	*MATa smc4-7A(601)::3xSTII::HIS3MX6 ura3-1::Pgal1::URA3*
	D4345	*MATa smc4-7A(601)::3xSTII::HIS3MX6 ura3-1::Pgal1::smc4-7EE-NT::NLS::13xMyc::URA3*
Fig 6	D3471	*MATa/MATα SMC4/smc4-969::3xSTII::HIS3MX6*
	D3226	*MATa/MATα SMC4/smc4-879::3xSTII::HIS3MX6*
	D3319	*MATa/MATα SMC4/smc4-927::3xSTII::HIS3MX6*
	D3567	*MATa/MATα SMC4/smc4-983::3xSTII::HIS3MX6*
	D3406	*MATa/MATα SMC4/smc4-928::3xSTII::HIS3MX6*
	D3405	*MATa/MATα SMC4/smc4-929::3xSTII::HIS3MX6*
	D3880	*MATa/MATα SMC4/smc4-1051::3xSTII::HIS3MX6*
	D3578	*MATa/MATα SMC4/smc4-988::3xSTII::HIS3MX6*
	D3654	*MATa/MATα SMC4/smc4-1002::3xSTII::HIS3MX6*
	D3576	*MATa/MATα SMC4/smc4-986::3xSTII::HIS3MX6*
	D3639	*MATa/MATα SMC4/smc4-997::3xSTII::HIS3MX6*
	D3563	*MATa/MATα SMC4/smc4-982::3xSTII::HIS3MX6*
	D3684	*MATa/MATα SMC4/smc4-995::3xSTII::HIS3MX6*
	D3637	*MATa/MATα SMC4/smc4-996::3xSTII::HIS3MX6*
	D3567	*MATa/MATα SMC4/smc4-984::3xSTII::HIS3MX6*
	D3566	*MATa/MATα SMC4/smc4-930::3xSTII::HIS3MX6*
	D3729	*MATa/MATα SMC4/smc4-1013::3xSTII::HIS3MX6*
Fig 7A, B & C	D3980	*MATa/MATα SMC4::3xGFP::kanMX6/SMC4 ::3xGFP::kanMX6 [pASZ11]*
	D3978	*MATa/MATα smc4-7A(601)::3xGFP::kanMX6/ smc4-7A(601)::3xGFP::kanMX6 [pASZ11]*

	D3993	*MATa Pbzz1::GFP::Tadh1::kanMX6::bzz1 [pASZ11]*
Fig S1	D390	*MATa clb1Δ clb3Δ::TRP1 clb4Δ::HIS3 clb2-ts*
Fig S3A	D2969	*MATa SMC4::3xSTII::HIS3MX6 YCG1::3xFLAG::kanMX6 cdc15-2*
	D3265	*MATa SMC4::3xSTII::HIS3MX6 YCG1::3xFLAG::kanMX6 cdc15-2 [YCplac111-SMC4-NT::NLS::13xMYC]*
Fig S3B	D3265	*MATa SMC4::3xSTII::HIS3MX6 YCG1::3xFLAG::kanMX6 cdc15-2 [YCplac111-SMC4-NT::NLS::13xMYC]*
	D3267	*MATa SMC4::3xSTII::HIS3MX6 YCG1::3xFLAG::kanMX6 cdc15-2 [YCplac111-smc4-NT-7A::NLS::13xMYC]*
Fig S3C	D4022	*MATa [YCplac111-SMC4-NT::NLS::13xMYC]*
	D4040	*MATa clb5Δ::URA3 clb6Δ::LEU2 [YCplac111-SMC4-NT::NLS::13xMYC]*
Fig S3D	D4022	*MATa CLB1 CLB2 CLB3 CLB4 [YCplac111-SMC4-NT::NLS::13xMYC]*
	D4024	*MATa clb1Δ clb3Δ::TRP1 clb4Δ::HIS3 clb2-ts [YCplac111-SMC4-NT::NLS::13xMYC]*
Fig S3E	D2832	*MATa YCG1::3xFLAG::kanMX6 cdc15-2 [YCplac111-SMC4-NT::NLS::13xMYC]*
	D4020	*MATa YCG1::3xFLAG::kanMX6 cdc15-2 [YCplac111-SMC4-rxl-NT::NLS::13xMYC]*
Fig S4A	D2963	*MATa SMC4::3xSTII::HIS3MX6*
	D2563	*MATa smc4-7E(757)::3xSTII::HIS3MX6*

	D1863	*MATa smc4-S4A::3xSTII::HIS3MX6*
	D1864	*MATa smc4-T43A::3xSTII::HIS3MX6*
	D1865	*MATa smc4-T60A::3xSTII::HIS3MX6*
	D1866	*MATa smc4-S109A::3xSTII::HIS3MX6*
	D4026	*MATa smc4-S113A::3xSTII::HIS3MX6*
	D1867	*MATa smc4-S117A::3xSTII::HIS3MX6*
	D1868	*MATa smc4-S128A::3xSTII::HIS3MX6*
	D1869	*MATa smc4-T757A::3xSTII::HIS3MX6*
	D1870	*MATa smc4-T847A::3xSTII::HIS3MX6*
	D1871	*MATa smc4-T1345A::3xSTII::HIS3MX6*
Fig S4B	D3272	*MATa SMC4::3xSTII::HIS3MX6 YCG1*
	D1868	*MATa smc4-S128A::3xSTII::HIS3MX6 YCG1*
	D834	*MATa SMC4 ycg1-2::3xHA::TRP1*
Fig S5A	D4334	*h+/h- ade6-210/ade6-216 cut3/cut3::kanMX6*
	D4336	*h+/h- ade6-210/ade6-216 cut3/cut3-T19V::kanMX6*
Fig S5B	D4188	*h+/h- ade6-210/ade6-216 cut3/cut3*
	D4334	*h+/h- ade6-210/ade6-216 cut3/cut3::kanMX6*
	D4336	*h+/h- ade6-210/ade6-216 cut3/cut3-T19V::kanMX6*
Fig S5C	D1	*MATa SAN1 SMC4*
	D3272	*MATa SAN1 SMC4::3xSTII::HIS3MX6*
	D2563	*MATa SAN1 smc4-7A(601)::3xSTII::HIS3MX6*
	D1849	*MATα san1Δ::HIS3MX6 SMC4*
	D3739	*MATa san1Δ::HIS3MX6 SMC4::3xSTII::HIS3MX6*
	D3737	*MATa san1Δ::HIS3MX6 smc4-7A(601)::3xSTII::HIS3MX6*
Fig S6D	D3321	*MATa/MATα SMC4/SMC4::3xSTII::HIS3MX6*

	D3471	*MATa/MATα SMC4/smc4-7AA(969)::3xSTII::HIS3MX6*
	D3226	*MATa/MATα SMC4/smc4-7EE(879)::3xSTII::HIS3MX6*
Fig S7A	D3928	*MATa/MATα SMC4/CLB2::SMC4::3xSTII::HIS3MX6*
	D3971	*MATa/MATα SMC4/clb2-CycBoxΔ::SMC4::3xSTII::HIS3MX6*
	D4218	*MATa/MATα SMC4/CLB2::smc4-7A(601)::3xSTII::HIS3MX6*
Fig S7B,C,D&E		
	D3641	*MATa SMC4 ura3-1::Pgal1::SMC4::3xSTII::URA3*
	D3645	*MATa SMC4 ura3-1::Pgal1::smc4-7EE(879)::3xSTII::URA3*
Fig S7F	D3980	*MATa/MATα SMC4::3xGFP::kanMX6/SMC4 ::3xGFP::kanMX6 [pASZ11]*
	D3978	*MATa/MATα smc4-7A(601)::3xGFP::kanMX6/ smc4-7A(601)::3xGFP::kanMX6 [pASZ11]*
	D3993	*MATa Pbzz1::GFP::Tadh1::kanMX6::bzz1 [pASZ11]*

2.11 Supplemental Figures and Legends:

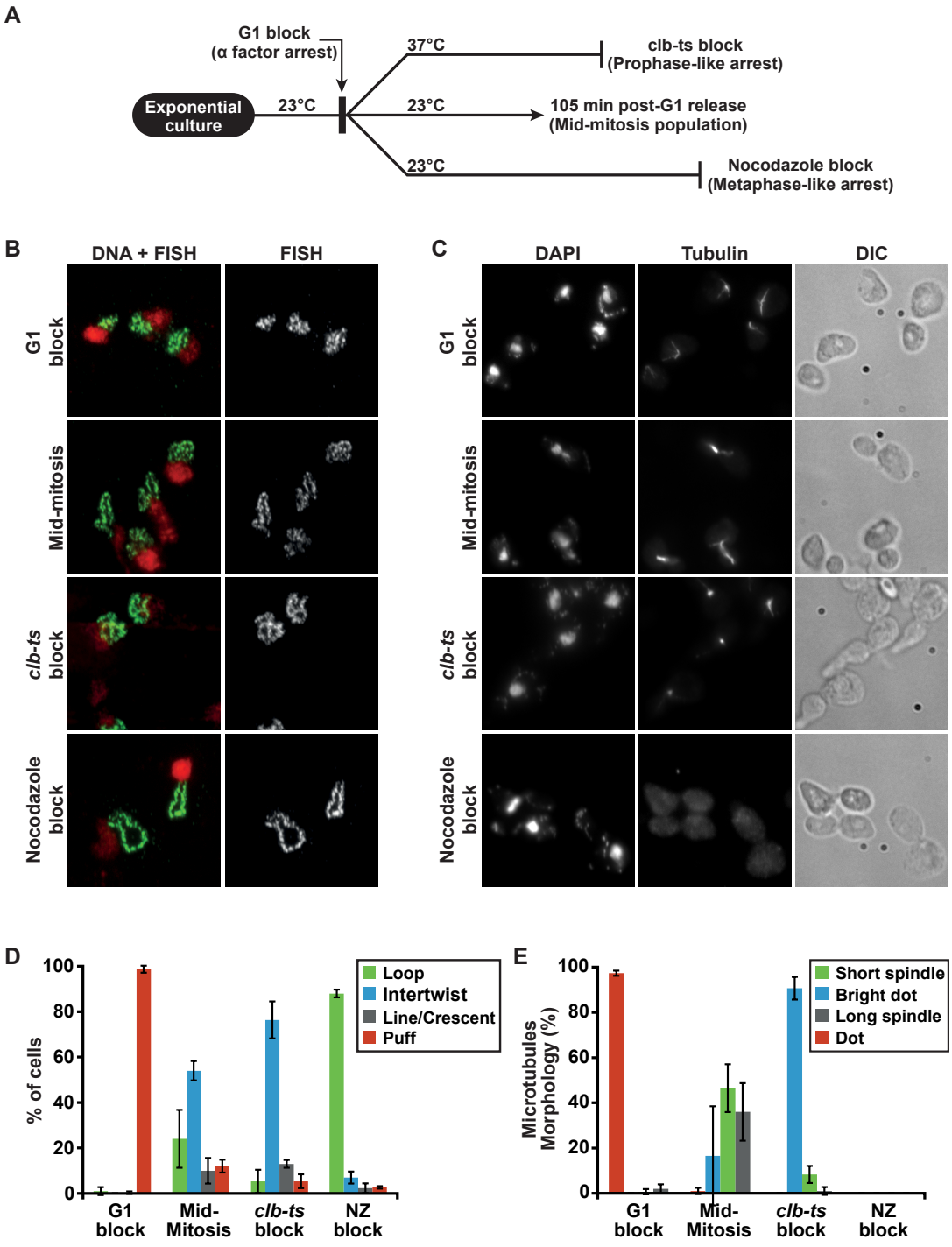

Figure S1. Microtubule, nucleus, and rDNA morphology in cells arrested at different stages of interphase and mitosis.

(**A**) Schematic representation of the experimental set up. Cells carrying *clb1 clb3 clb4 clb2-VI* mutations (Amon et al., 1993) (*i.e.*, *clb-ts* mutants) were arrested in G1 with α-factor, split into four cultures, and released from the arrest. The first culture was shifted at 37 °C and allowed to grow for 135 min to generate a prophase-like *clb-ts* arrest. The second culture was grown at 23 °C for 105 min to allow most cells in the culture to reach mitosis naturally. The third culture was released into medium containing nocodazole for 150 min at 23 °C to generate a metaphase-like arrest. The fourth culture was harvested immediately after the G1 release. Samples of each culture were collected and processed for rDNA FISH analysis or indirect immunofluorescence to detect α-tubulin. It was necessary to perform FISH and immunofluorescence staining in different cells because the conditions for staining the rDNA and tubulin are incompatible. (**B**) Morphology of the rDNA locus as detected by FISH. A representative micrograph of the dominant rDNA species for each condition is shown. Propidium iodide (PI; red) and fluorescein isothiocyanate (FITC; green) were used to label the nucleus and rDNA locus, respectively. (**C**) Cell morphology (differential interference contrast [DIC] microscopy), nuclei morphology (4',6-diamidino-2-phenylindole; DAPI) and mitotic spindle length/tubulin staining have been determined in the cells described above. (**D–E**) Quantification of the rDNA and spindle/tubulin morphologies observed in cells described in panels B and C, respectively (n = 3; error bars represent S.D.). At least, 100 nuclei or cells were counted per condition. The categories "bright spot" and "dot" in panel e refer to duplicated and unduplicated SPB, as previously described (Fitch et al., 1992; Yin et al., 2002).

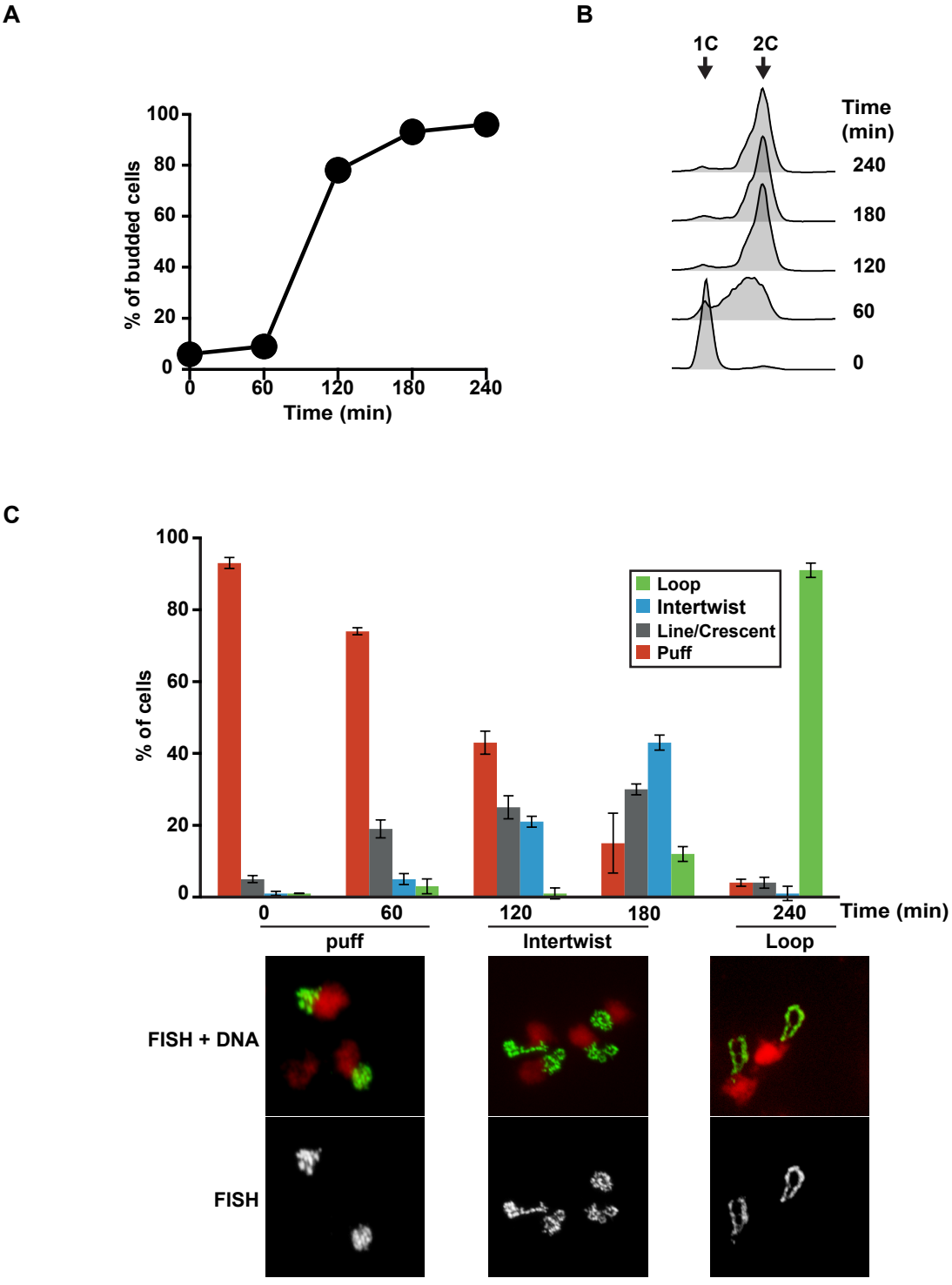
A
% of budded cells
100
80
60
40
20
0
0
60
120
180
240
Time (min)
B
1C
2C
Time (min)
240
180
120
60
0
C
% of cells
100
80
60
40
20
0
Loop
Intertwist
Line/Crescent
Puff
0
60
120
180
240
Time (min)
puff
Intertwist
Loop
FISH + DNA
FISH

Figure S2. The intertwist rDNA morphology is revealed in cells undergoing chromosome morphogenesis at low temperatures.

(**A-C**). Cells were synchronized in G1 using α-factor and released into a fresh medium containing nocodazole at 16˚C for 240 minutes. Samples were collected every 60 minutes and processed for visualization of the budding index, DNA content analysis and rDNA morphology. (**A**) Budding index of the cell population examined during the time-course. At least 100 cells were scored per time point (**B**) Flow cytometry analysis of cellular DNA content at various time points during the experiment. (**C**) Morphology of the yeast rDNA locus revealed by FISH. Quantification of each rDNA species is shown on the top. At least one hundred nuclei were counted per condition. (n=3 and error bars represent S.D.). Representative micrographs of the most prominent rDNA morphology observed during the time course is shown below the graph. PI (red) and FITC (green) were used to label the nucleus and rDNA locus, respectively.

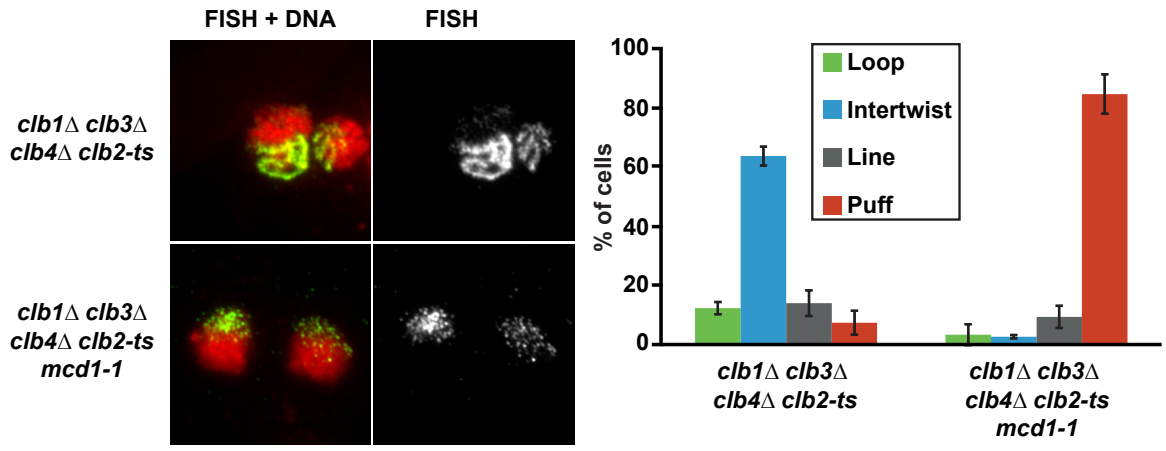

Figure S3. The formation of the intertwist rDNA morphology requires cohesin activity.

clb-ts or *clb-ts mcd1-1* cells growing asynchronously at 23°C were arrested in early mitosis by shifting the culture at 37°C for 135 min. Samples were then fixed and the morphology of the rDNA locus was monitored by FISH. Representative micrographs of the most prominent rDNA morphology observed for each condition is shown on the left. PI (red) and FITC (green) were used to label the nucleus and rDNA locus, respectively. Quantification of each rDNA species is shown on the right. At least one hundred nuclei were counted per condition. (n=3 and error bars represent S.D.).

A

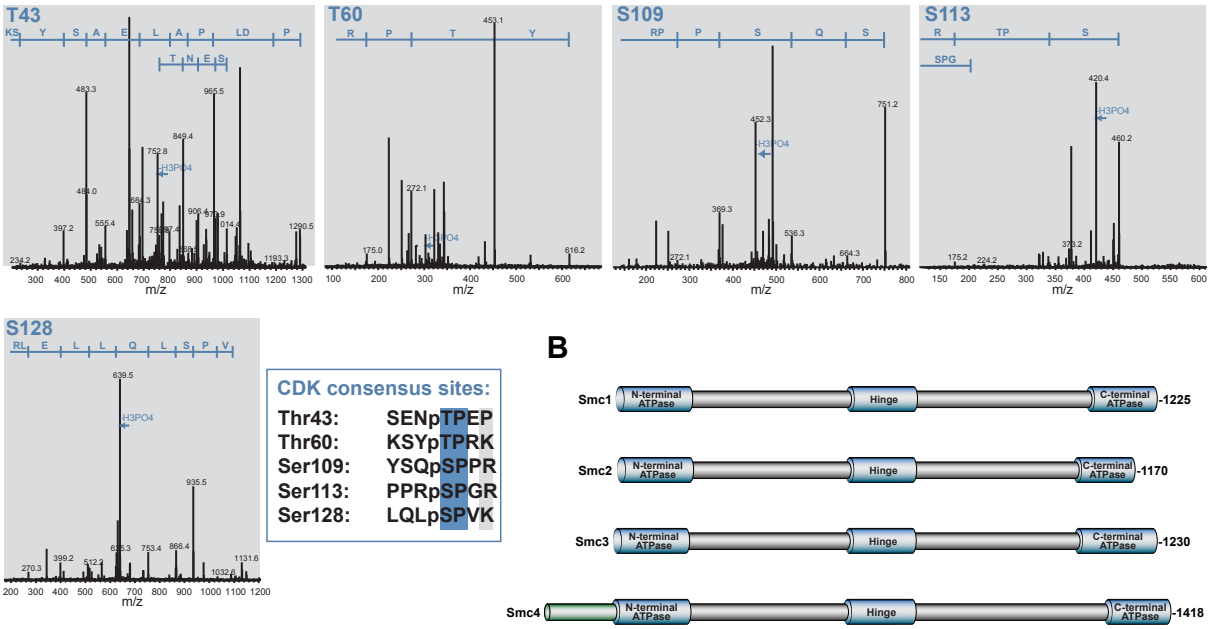
T43
S109
S113
S128
CDK consensus sites:
Thr43: SENpTPEP
Thr60: KSYpTPRK
Ser109: YSQpSPPR
Ser113: PPRpSPGR
Ser128: LQLpSPVK
m/z

B

Smc1
Smc2
Smc3
Smc4
N-terminal ATPase
Hinge
C-terminal ATPase
-1225
-1170
-1230
-1418

C

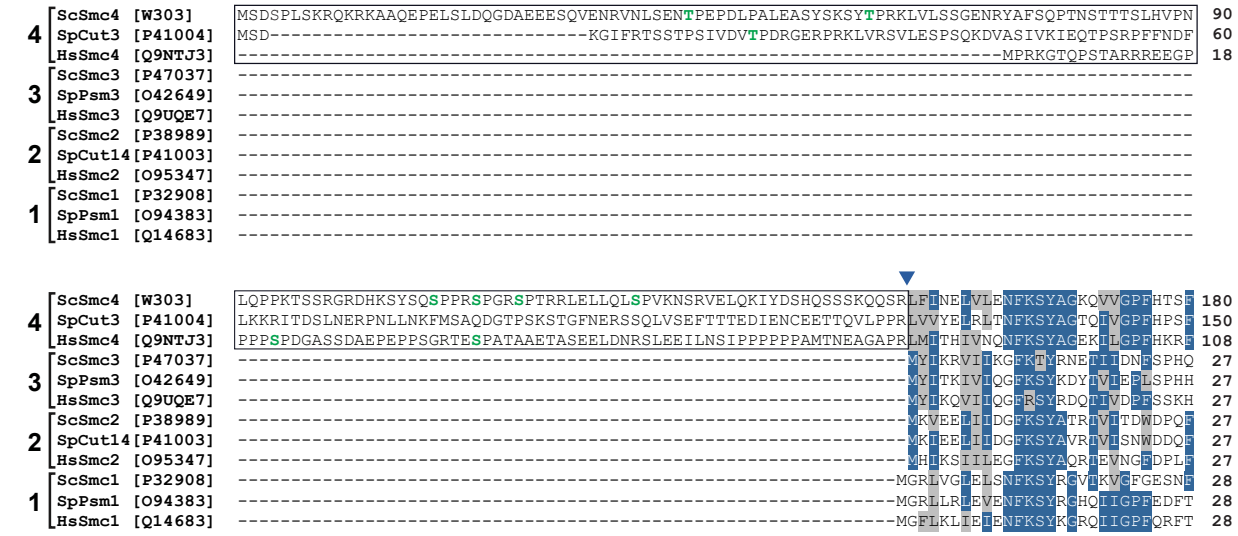
4
3
2
1
ScSmc4 [W303]
SpCut3 [P41004]
HsSmc4 [Q9NTJ3]
ScSmc3 [P47037]
SpPsm3 [O42649]
HsSmc3 [Q9UQE7]
ScSmc2 [P38989]
SpCut14 [P41003]
HsSmc2 [O95347]
ScSmc1 [P32908]
SpPsm1 [O94383]
HsSmc1 [Q14683]

Figure S4. Cdk1 targets the evolutionarily-conserved N-terminus of Smc4.

(**A**) Mass spectra of Cdk1 phosphorylation sites identified in Smc4 immuno-purified from mitotic cell extracts. Spectra are shown for phospho-residues Thr43, Thr60, Ser109, Ser113 and Ser128 in the N-terminal extension of Smc4. The blue box at the bottom right corner of this panel highlights the amino-acid sequence surrounding the phosphorylation sites. Most of the phospho-sites conform to the optimal consensus sequence for Cdk1 phosphorylation (*i.e.*, Ser/Thr-Pro-X-Arg/Lys) (Koivomagi et al., 2011), whereas one conforms to the core Cdk1 consensus (*i.e.*, Ser/Thr-Pro; Thr43) (Holt et al., 2009; Rudner & Murray, 2000). Note that several of those sites, together with Ser117, were found to be phosphorylated in a Cdk1-dependent manner in proteome-wide screens that aimed to identify mitotic phosphorylation sites (Bazile et al., 2010; Holt et al., 2009; Kao et al., 2014). Interestingly, Cdk1 phospho-sites were not identified in other condensin subunits in the course of our mass spectrometry analysis. (**B**) Schematic representation of the SMC subunits of cohesin (Smc1 and Smc3) and condensin (Smc2 and Smc4) complexes from budding yeast. The conserved functional domains of SMC family members are drawn to approximate scale. Note that only Smc4 carry an N-terminal extension among this group of SMC proteins. (**C**) Conservation of the N-terminal extension among Smc4 family members in eukaryotes. A multiple local alignment of the primary amino-acid sequence corresponding to the N-terminal portion of *H. sapiens* (Hs), *S. pombe* (Sp) and *S. cerevisiae* (Sc) Smc1-4 homologs is shown. The blue arrow indicates the start of the ATPase domain, whereas the boxed sequences correspond to the N-terminal extension specific to the Smc4 family members. Known phospho-sites that conform to the Cdk1 consensus sequence in the N-terminal extensions of budding yeast, fission yeast and human Smc4 are highlighted in green (Bazile et al., 2010; Holt et al., 2009; Kao et al., 2014; Sutani et al., 1999).

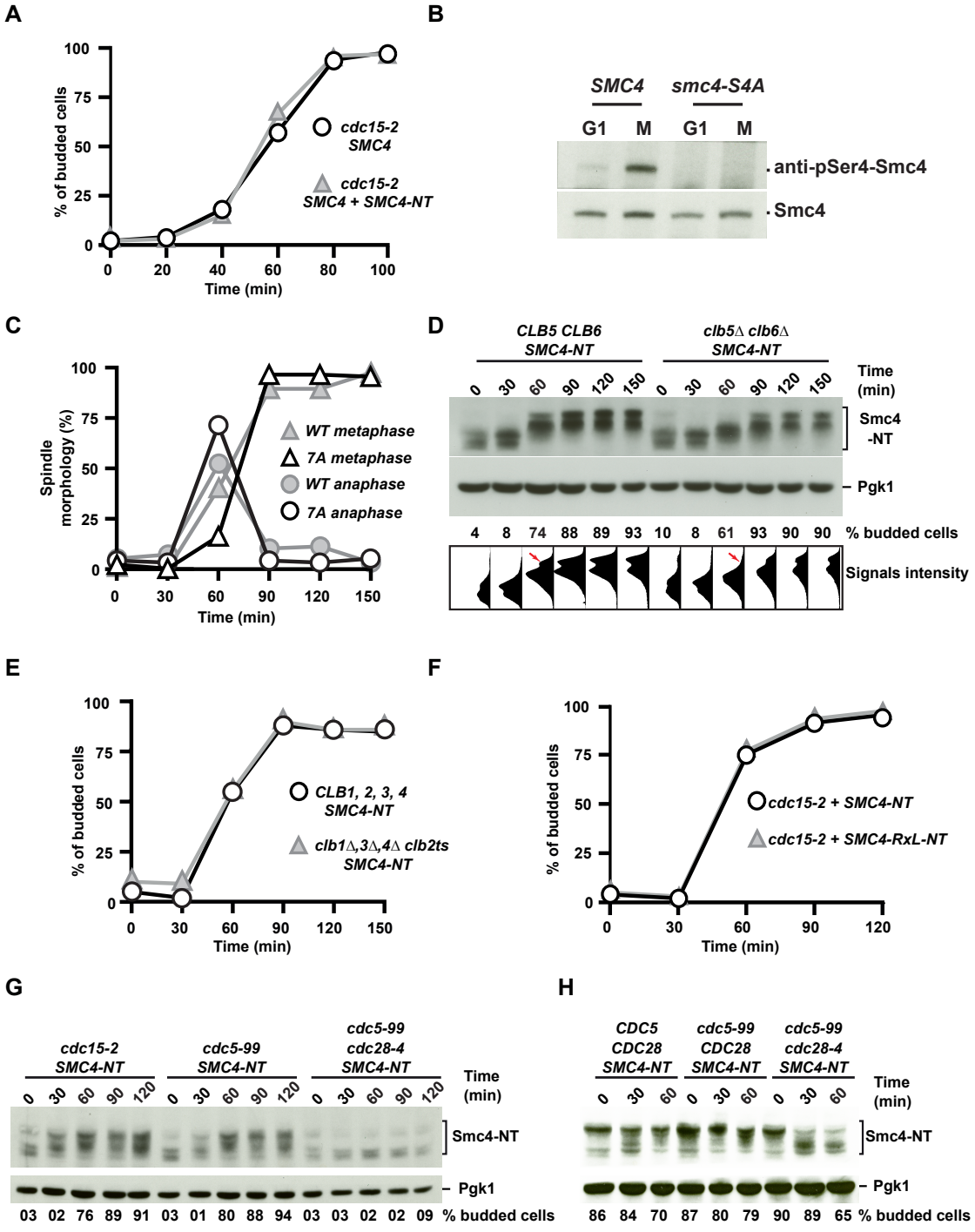
A
% of budded cells
Time (min)
cdc15-2 SMC4
cdc15-2 SMC4 + SMC4-NT
B
SMC4
smc4-S4A
G1
M
G1
M
anti-pSer4-Smc4
Smc4
C
Spindle morphology (%)
Time (min)
WT metaphase
7A metaphase
WT anaphase
7A anaphase
D
CLB5 CLB6 SMC4-NT
clb5Δ clb6Δ SMC4-NT
Time (min)
Smc4 -NT
Pgk1
4 8 74 88 89 93 10 8 61 93 90 90 % budded cells
Signals intensity
E
% of budded cells
Time (min)
CLB1, 2, 3, 4 SMC4-NT
clb1Δ,3Δ,4Δ clb2ts SMC4-NT
F
% of budded cells
Time (min)
cdc15-2 + SMC4-NT
cdc15-2 + SMC4-RxL-NT
G
cdc15-2 SMC4-NT
cdc5-99 SMC4-NT
cdc5-99 cdc28-4 SMC4-NT
Time (min)
Smc4-NT
Pgk1
03 02 76 89 91 03 01 80 88 94 03 03 02 02 09 % budded cells
H
CDC5 CDC28 SMC4-NT
cdc5-99 CDC28 SMC4-NT
cdc5-99 cdc28-4 SMC4-NT
Time (min)
Smc4-NT
Pgk1
86 84 70 87 80 79 90 89 65 % budded cells

Figure S5. Cdk1 regulation of Smc4 phosphorylation in mitosis.

(**A**) Budding index and mitotic spindle length of the cell populations examined in the time-courses presented in Figures 3D. (**B**) Validation of antibodies against phosphoserine 4 (pSer4) of Smc4. Protein samples from interphase (G1) and mitotic (M) cells of the indicated genotypes were probed by immunoblot analysis for the presence of phosphorylated Smc4. The Smc4-3xSTII signal serves as loading control (**C**) Budding index and mitotic spindle length of the cell populations examined in the time-courses presented in Figures 3E. (**D**) Smc4 phosphorylation is delayed and reduced in strains carrying *clb5Δ clb6Δ* mutations. Cells expressing the Smc4-NT fragment were released from a G1 arrest into fresh medium containing nocodazole at 37 °C. Samples were collected every 30 minutes and processed for immunoblotting. The intensity of the signal for the electrophoretically-retarded phospho-species of Smc4 was quantified using ImageJ software, and is shown below the gels. A red arrow indicates the peaks corresponding to the most retarded phospho-species of Smc4. These species usually appear 60 minutes after release in the control wild-type situation, but is significantly delayed and reduced in the *clb5Δ clb6Δ* mutant. Percentages of budded cells are shown below the gels. We noticed, as previously observed (Schwob and Nasmyth 1993), that *clb5 clb6* mutants show delayed kinetics of cell cycle entry and that this may indirectly affect the appearance of Smc4 phospho-species in these mutants. This limitation can be addressed by testing for Smc4 phosphorylation in a mutant lacking its RxL docking sites, as shown in Figure 3G. These motifs are used by early B-type cyclins to selectively target their substrates *in vivo*, and removal of RxL motifs has been shown to reduce phosphorylation of Clb5 substrates in yeast (Archambault et al. 2005; Loog and Morgan 2005). (**E–F**) Budding indexes of the cell populations examined in the time-courses presented in Figures 3F and G, respectively. (**G-H**) Smc4 phosphorylation is not dependent on Cdc5 activity. (**G**) Cells expressing the Smc4-NT fragment were released from a G1 arrest at 23°C into fresh medium at 37°C. Samples were collected every 30 minutes and processed for immunoblot analysis and budding index. Pgk1 serves as loading control. (**H**) Cells expressing the Smc4-NT fragment were arrested in metaphase (nocodazole) at 23°C, shifted to 37°C maintaining nocodazole arrest for 1 hour. Samples

were collected every 30 minutes and processed for immunoblot analysis and budding index. Pgk1 serves as loading control. Note how removal of Cdk1 activity in the *cdc5-99 cdc28-4* double mutant leads to a rapid dephosphorylation of Smc4 in dividing cells. In contrast, the *cdc5-99* single mutant maintains full Smc4-NT phosphorylation under the same conditions.

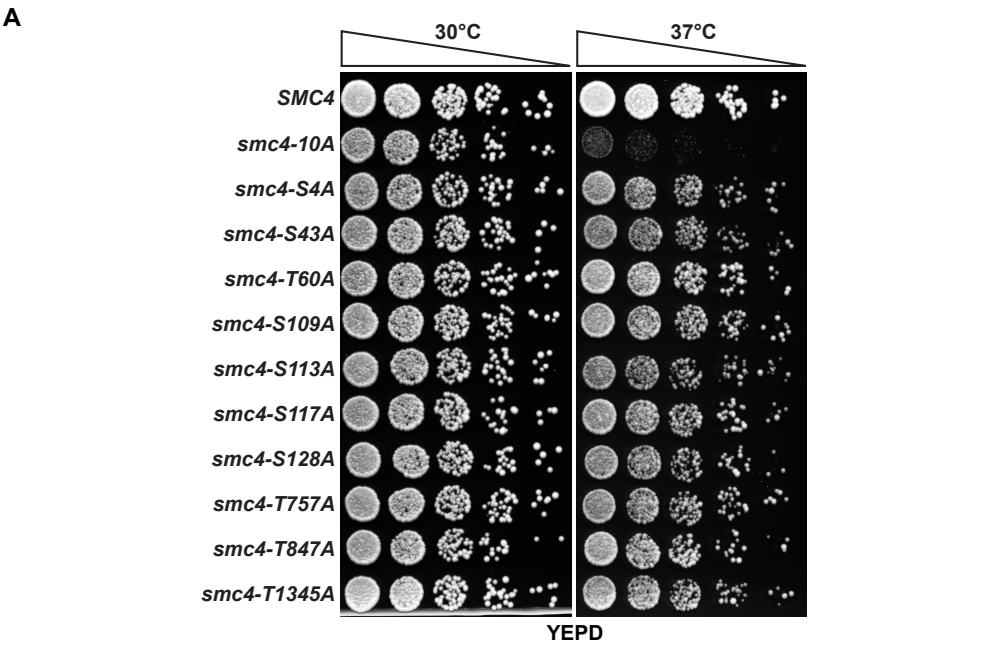
A
30°C
37°C
SMC4
smc4-10A
smc4-S4A
smc4-S43A
smc4-T60A
smc4-S109A
smc4-S113A
smc4-S117A
smc4-S128A
smc4-T757A
smc4-T847A
smc4-T1345A
YEPD

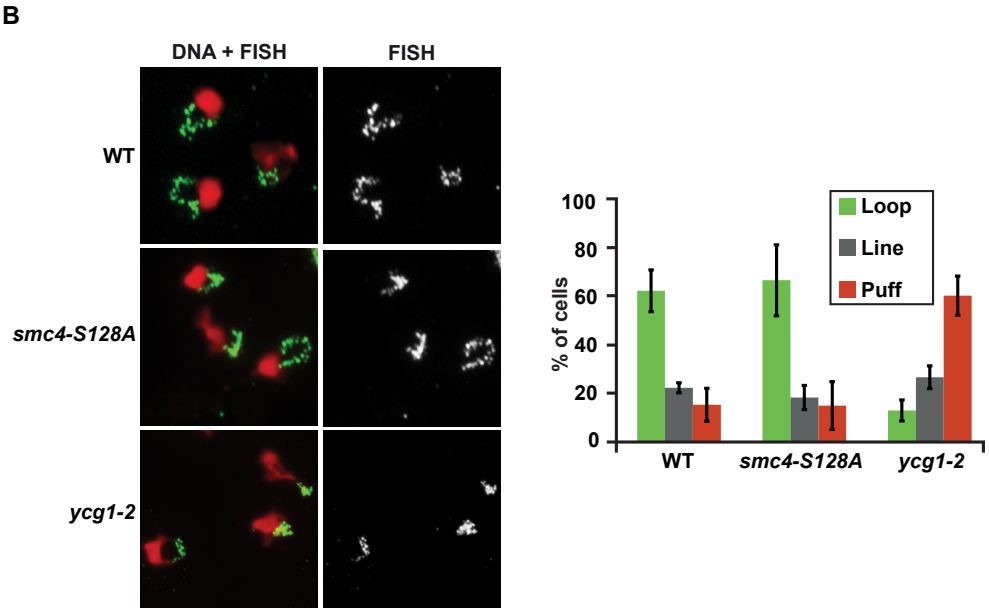
B
DNA + FISH
FISH
WT
smc4-S128A
ycg1-2
% of cells
100
80
60
40
20
0
Loop
Line
Puff
WT
smc4-S128A
ycg1-2

Figure S6. Phenotype of yeast carrying single-mutations in condensin phosphosites.

(**A**) Loss of individual Cdk1 sites in Smc4 does not affect cell proliferation. Five-fold dilution series of wild-type and *smc4* mutant yeast strains defective in single Cdk1 phosphorylation sites were spotted on solid medium to evaluate growth at different temperatures. Plates were grown 2-3 days until individual colonies were clearly visible. (**B**) Morphology of the yeast rDNA locus at 37 °C in the *smc4-S128A* mutant as revealed by FISH. Representative micrographs of the most prominent rDNA morphology observed for each condition is shown on the left. Propidium iodide (PI; red) and fluorescein isothiocyanate (FITC; green) were used to label the nucleus and rDNA locus, respectively. Quantification of each rDNA species is shown on the right. At least one hundred nuclei were counted per condition. (n=3 for all experiments and error bars represent S.D.) The *ycg1-2* mutant was used as positive control to induce a typical chromosome condensation defect (Lavoie et al. 2002). The lack of condensation defect in our FISH experiment with the *smc4-S128A* single mutant is consistent with a previous analysis showing no increase in cells showing decondensed DNA (*i.e.*, "2-dot phenotype" using the dual LacO repeats system) in the absence of Ser128 phosphorylation (Kao et al. 2014). We note that the modest ~20% increase in "3-dot phenotype" previously linked with loss of Ser128 phosphorylation (Kao et al. 2014) likely reflects difference in the timing of sister-chromatid segregation at different loci, as previously shown (Straight et al. 1997). Indeed, condensin is a known regulator of chromosome arm cohesion (Lam et al. 2006), and the simplest interpretation of a 3-dot phenotype in this context is that it reflects a cohesion defect. Interestingly, the strong condensin mutant *smc2-8* (Freeman et al. 2000) did not exhibit any chromosome condensation defects in the assays performed by Kao and collaborators.

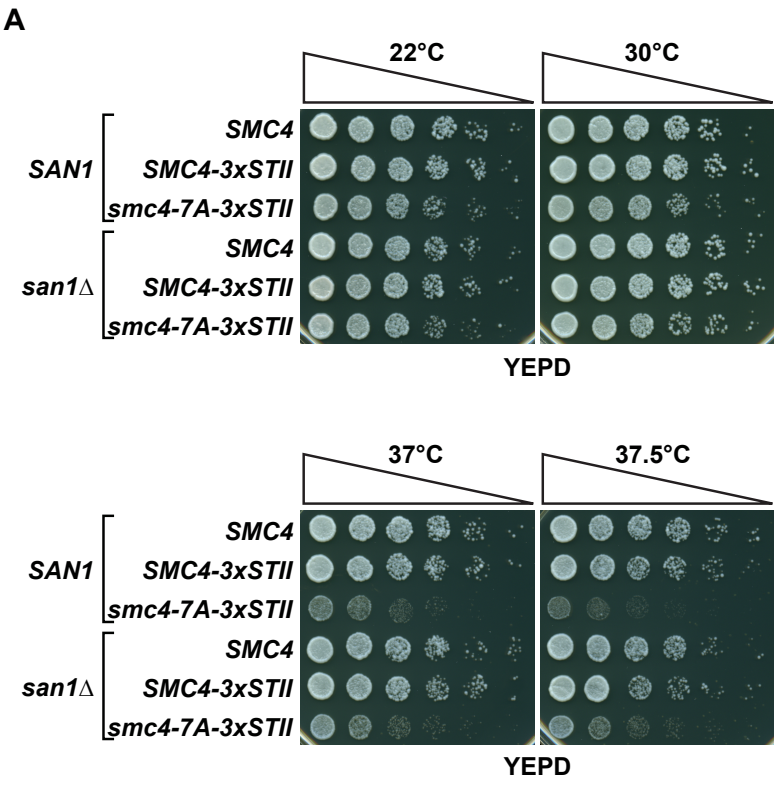
A
22°C
30°C
SAN1
SMC4
SMC4-3xSTII
smc4-7A-3xSTII
san1Δ
SMC4
SMC4-3xSTII
smc4-7A-3xSTII
YEPD
37°C
37.5°C
SAN1
SMC4
SMC4-3xSTII
smc4-7A-3xSTII
san1Δ
SMC4
SMC4-3xSTII
smc4-7A-3xSTII
YEPD

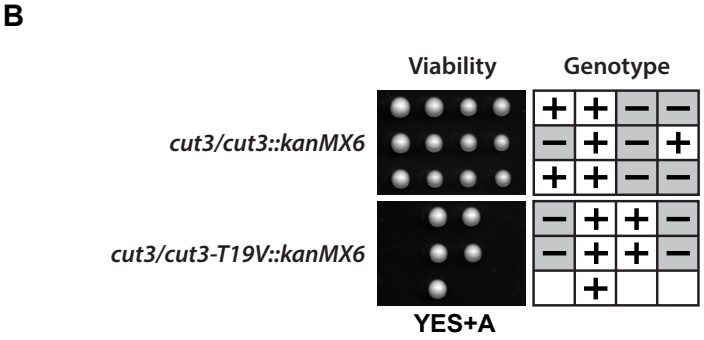
B
Viability
Genotype
cut3/cut3::kanMX6
cut3/cut3-T19V::kanMX6
YES+A

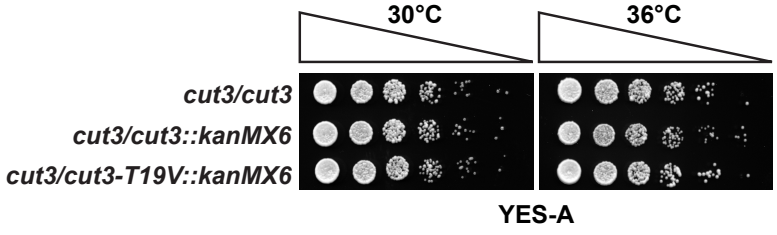
C
30°C
36°C
cut3/cut3
cut3/cut3::kanMX6
cut3/cut3-T19V::kanMX6
YES-A

Figure S7. Genetic analysis of phosphorylation mutants of Smc4/Cut3 in budding and fission yeasts.

(**A**) Inactivation of the protein quality control pathway does not rescue the temperature-sensitive (ts) growth phenotype of *smc4-7A* mutants. Five-fold dilution series of *SMC4*, *SMC4-3xSTII* and *smc4-7A-3xSTII* strains carrying either *san1Δ* or wild-type *SAN1* were spotted on solid medium to evaluate growth at different temperatures. Loss of the protein quality control pathway in *san1Δ* cells did not suppress the ts phenotype of the *smc4-7A-3xSTII* mutant, thereby indicating that the phenotype of this strain is not due to protein instability (Gardner et al. 2005). (**B**) A heterozygous diploid fission yeast strain carrying the *cut3-T19V:Tadh1:kanMX6* phosphomutant allele was induced to sporulate and the viability of the resulting haploid spores was determined after 3 days of growth on solid medium. Three typical tetrads of spores are shown. The genotype of spores was deduced using the *kanMX6* marker associated with the *cut3* locus (*i.e.*, + sign indicate spores that have inherited the wild-type *cut3+* allele). Note that the *cut3-T19V* allele also has a weak meiotic effect, thereby causing some tetrads to exhibit less than 2 live spores. A heterozygous wild-type *cut3*/*cut3:Tadh1:kanMX6* strain was included as control. Haploid G418-resistant (*i.e.*, *kanMX6* positive) spores were never recovered after sporulation of the mutant, whereas the *kanMX*-linked wild-type *cut3* allele segregated in a perfect Mendelian manner after sporulation. (**C**) Five-fold dilution series of the *cut3-T19V:Tadh1:kanMX6/ cut3* heterozygous diploid and control strains were spotted on solid YES-A medium to evaluate growth at different temperatures. Note the absence of dominant growth defect associated with the *cut3-T19V:Tadh1:kanMX6* allele.

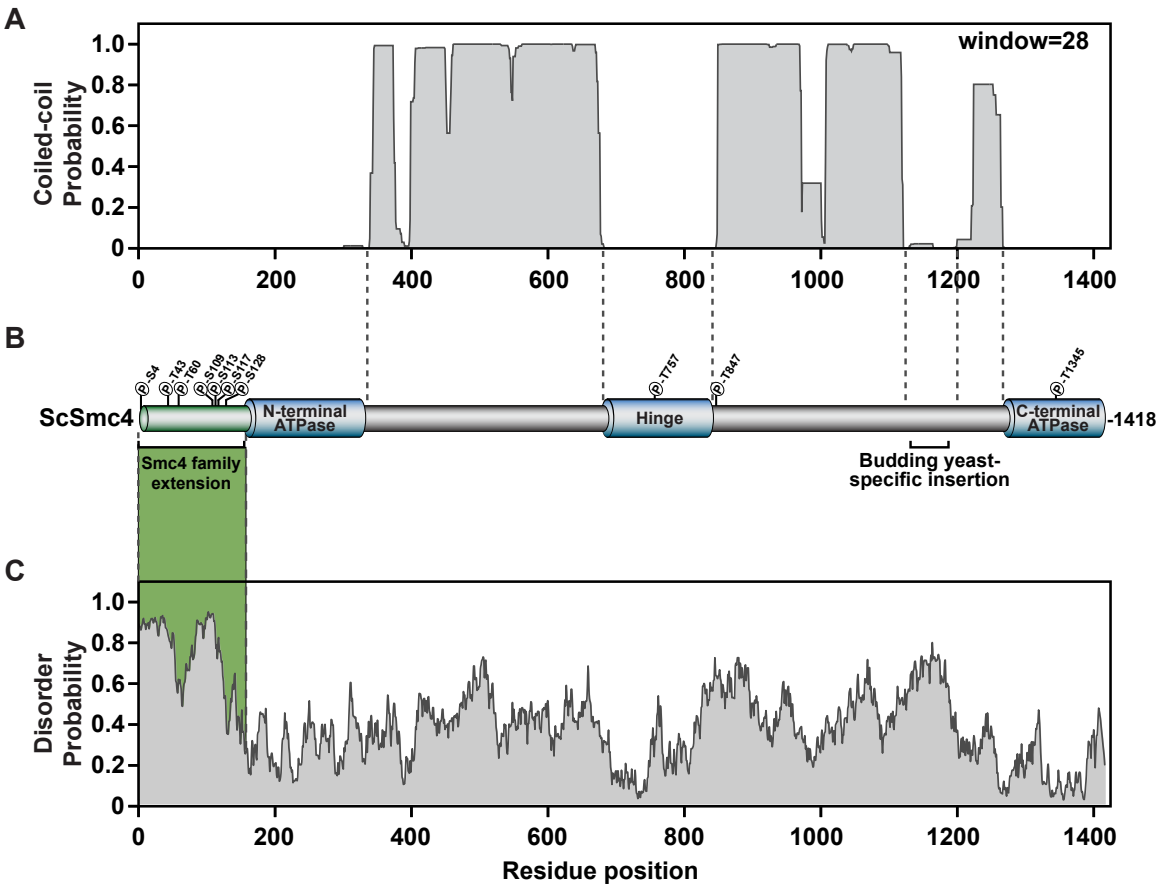
A
window=28
Coiled-coil Probability
1.0
0.8
0.6
0.4
0.2
0
0
200
400
600
800
1000
1200
1400
B
ScSmc4
N-terminal ATPase
Hinge
C-terminal ATPase
-1418
Smc4 family extension
Budding yeast-specific insertion
C
Disorder Probability
Residue position

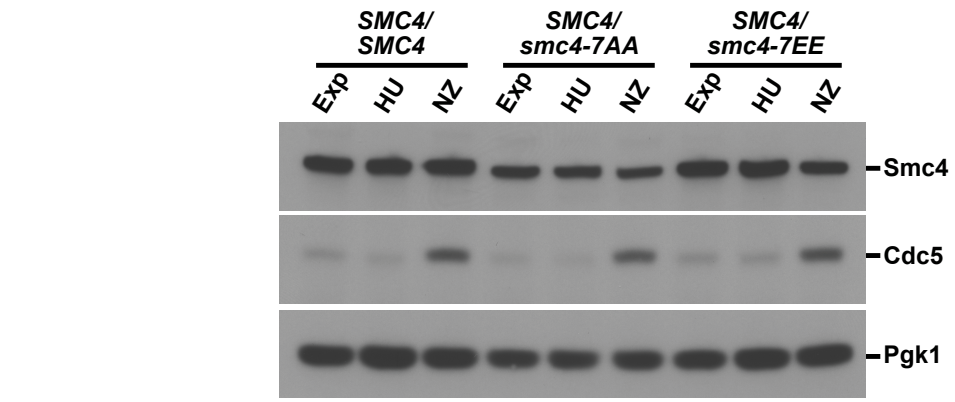
D
SMC4/ SMC4
SMC4/ smc4-7AA
SMC4/ smc4-7EE
Exp
HU
NZ
Smc4
Cdc5
Pgk1

Figure S8. Constitutive phosphorylation of Smc4 – Structural implications and effects.

Secondary structure analysis of Smc4 N-terminal extension. Smc4 primary amino-acid sequence was analyzed *in silico* to determine the position and nature of structural landmarks in the protein. The presence of extended antiparallel coiled-coil regions in Smc4 was determined using the COILS program (Lupas et al. 1991), whereas the propensity of particular regions of the protein to adopt an unstructured conformation was determined using IUPred (Dosztanyi et al. 2005). (**A**) The graph on top shows the regions of Smc4 predicted to adopt a coiled-coil structure. (**B**) The secondary structure prediction is consistent with the known boundaries of the ATPase and hinge domains of SMC family members (Hirano and Mitchison 1994; Saitoh et al. 1994; Saka et al. 1994; Strunnikov et al. 1995), as highlighted in the protein schematic. (**C**) This graph shows the propensity of the various regions of Smc4 to adopt an unstructured conformation. According to this analysis, the N-terminal extension of Smc4 shows a very high probability of being unstructured relative to other parts of the protein. This property correlates well with the observation that most Cdk1 sites in cells are found within unstructured parts of proteins (Holt et al. 2009). (**D**) The lethality of Smc4 charge-mimetic mutations is not due to lower protein abundance. A culture of heterozygous diploid cells expressing Smc4-7EE-3xSTII/Smc4 where grown at 23 °C and split into three subcultures. The first subculture was grown for an additional 120 min at 23 °C and corresponds to an exponential population of cells (Exp). The second subculture was blocked in metaphase using nocodozole for 150 min (NZ). The third subculture was blocked in S phase using 0.2M hydroxyurea for 120 min (HU). Samples were taken and analysed by immunoblot with an anti-STII antibody. Cdc5 serves as marker for mitotic cells and Pgk1 levels are used as loading control.

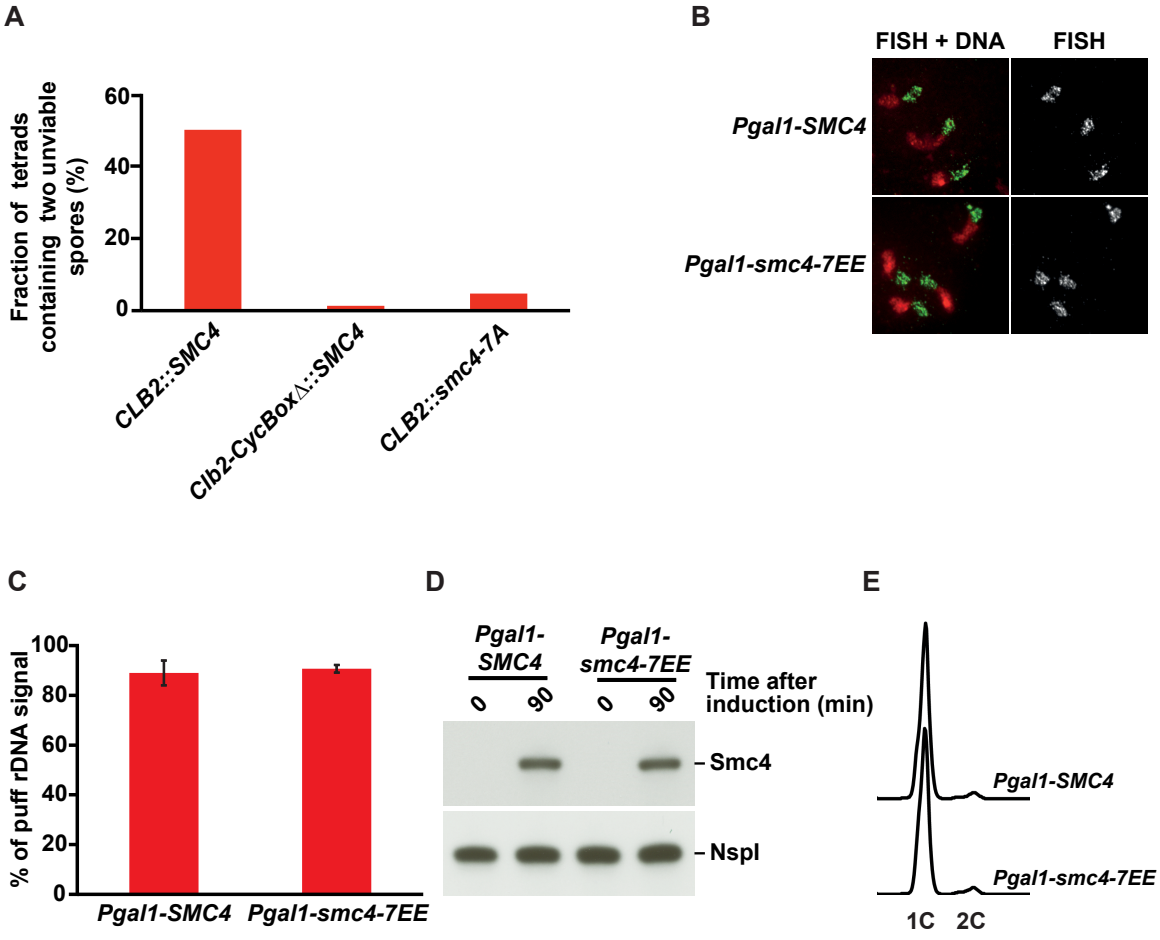
A
Fraction of tetrads containing two unviable spores (%)
60
40
20
0
CLB2::SMC4
Clb2-CycBoxΔ::SMC4
CLB2::smc4-7A
B
FISH + DNA
FISH
Pgal1-SMC4
Pgal1-smc4-7EE
C
% of puff rDNA signal
100
80
60
40
20
0
Pgal1-SMC4
Pgal1-smc4-7EE
D
Pgal1-SMC4
Pgal1-smc4-7EE
0
90
0
90
Time after induction (min)
Smc4
NspI
E
Pgal1-SMC4
Pgal1-smc4-7EE
1C
2C

Figure S9. Phenotypes of phospho-defective and charge-mimetic mutants of Smc4.
(**A**) Quantification of the fraction of tetrads showing a 2:2 lethality phenotype co-segregating with *smc4* fusion alleles. Tetrads were derived from the dissection of heterozygous diploid strains expressing Clb2-Smc4 fusion derivatives that drives constitutive phosphorylation of Smc4 by Cdk1 (*i.e.*, *CLB2::SMC4::HIS3MX6/SMC4*). The *clb2-CycBoxΔ::SMC4::HIS3MX6* and *CLB2::smc4-7A::HIS3MX6* alleles are used as negative controls since the former lacks part of the cyclin box region necessary for its interaction with Cdk1 (Lees and Harlow 1993), whereas the latter lacks the N-terminal Cdk1 phospho-sites of Smc4. The ability of cells to grow on solid medium lacking histidine (*i.e.*, HIS+ phenotype) was used to score the segregation of the fusion alleles after meiosis and sporulation. The genotype of unviable spores was deduced based on Mendelian inheritance of *SMC4* alleles. At least 70 tetrads were counted for each genotype. (**B–E**) Overexpression of the charge-mimetic mutant of Smc4 does not induce unscheduled condensation of chromosomes in interphase. Strains containing inducible ectopic copies of *SMC4* or *smc4-7EE* were synchronized in G1 with alpha-factor in raffinose-containing media. Overexpression of *SMC4* or *smc4-7EE* was induced by adding 2% galactose in medium for 90 min. (**B**) FISH analysis of rDNA locus morphology after *SMC4* overexpression. Representative micrographs of G1-arrested cells are shown after 90 min of overexpression of *smc4-7EE* or *SMC4*. (**C**) Quantification of rDNA locus morphology after *smc4-7EE* or *SMC4* overexpression. Most cells show the typical uncondensed "puff" rDNA morphology in G1 despite *SMC4* overexpression. (**D**) Immunoblot analysis of Smc4 abundance before and after induction with galactose in G1. Nsp1 protein levels are used as loading control. (**E**) Flow cytometry analysis of cellular DNA content after 90 min overexpression of *smc4-7EE* or *SMC4*. Most cells show a typical 1C DNA content under these experimental conditions.

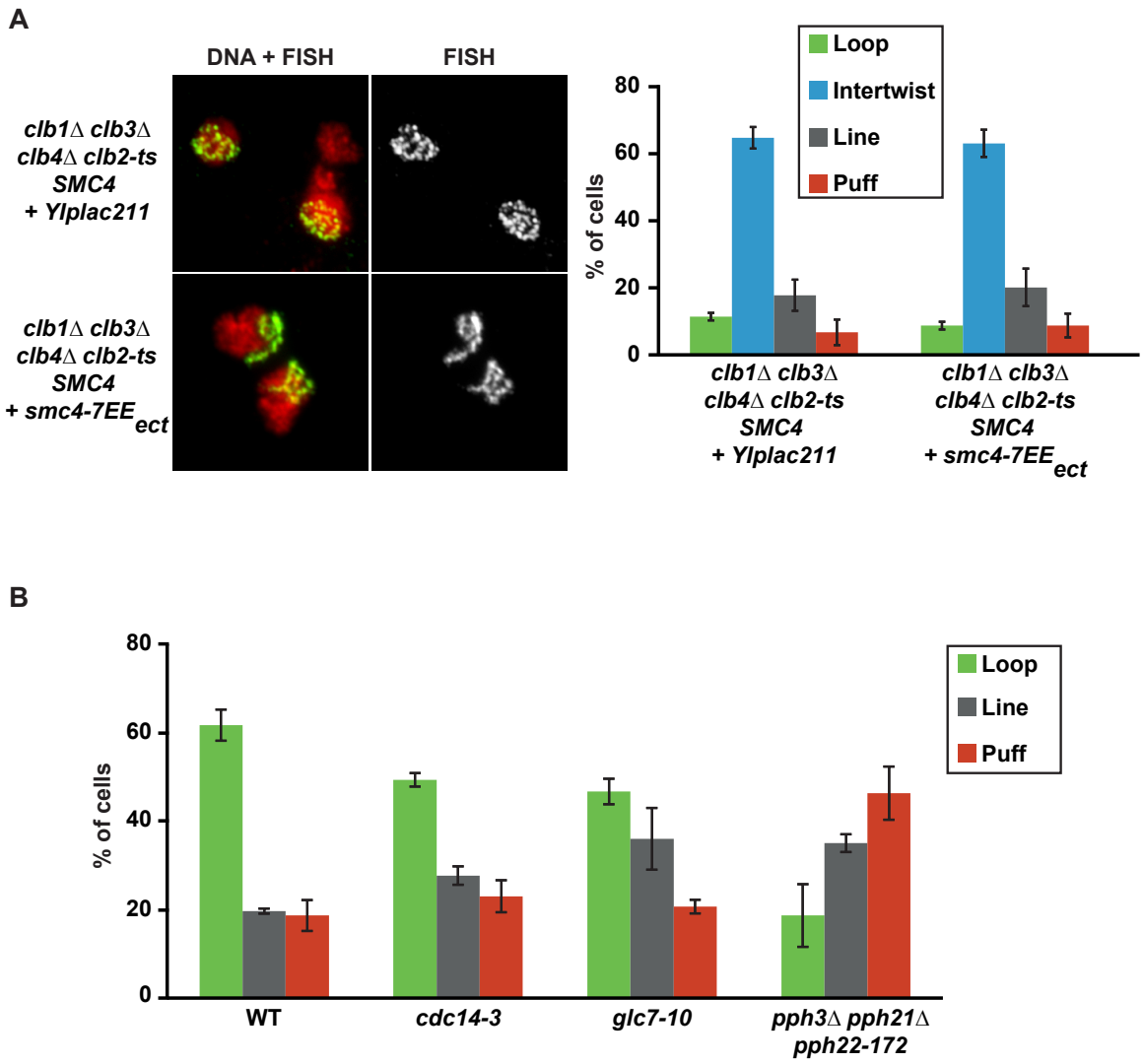
A
DNA + FISH
FISH
clb1Δ clb3Δ clb4Δ clb2-ts SMC4 + Ylplac211
clb1Δ clb3Δ clb4Δ clb2-ts SMC4 + smc4-7EE ect
Loop
Intertwist
Line
Puff
% of cells
80
60
40
20
0
clb1Δ clb3Δ clb4Δ clb2-ts SMC4 + Ylplac211
clb1Δ clb3Δ clb4Δ clb2-ts SMC4 + smc4-7EE ect
B
80
60
40
20
0
% of cells
Loop
Line
Puff
WT
cdc14-3
glc7-10
pph3Δ pph21Δ pph22-172

Figure S10. Impact of the *smc4* charge mimetic mutant on the intertwist morphology.

(**A**) *clb-ts* cells expressing *smc4-7EE* (or an empty vector) from an ectopic locus were grown asynchronously at 23°C before being arrested in early mitosis by shifting the culture at 37°C for 135 min. The morphology of the yeast rDNA locus was revealed by FISH. Representative micrographs of the most prominent rDNA morphology observed for each condition is shown on the left. PI (red) and FITC (green) were used to label the nucleus and rDNA locus, respectively. Quantification of each rDNA species is shown on the right. At least one hundred nuclei were counted per condition. (n=3 and error bars represent S.D.). (**B**) Turnover of phosphorylation sites on condensin regulates rDNA condensation. Quantification of rDNA morphologies in yeast phosphatase mutants grown at non-permissive temperature. Cells were grown asynchronously at 23°C until exponential phase and subsequently shifted at 37°C for 150 min. Nocodazole was used to block cells in metaphase**.** At least 100 cells have been counted for each genotype in 3 independent experiments (error bars are S.D.).

A

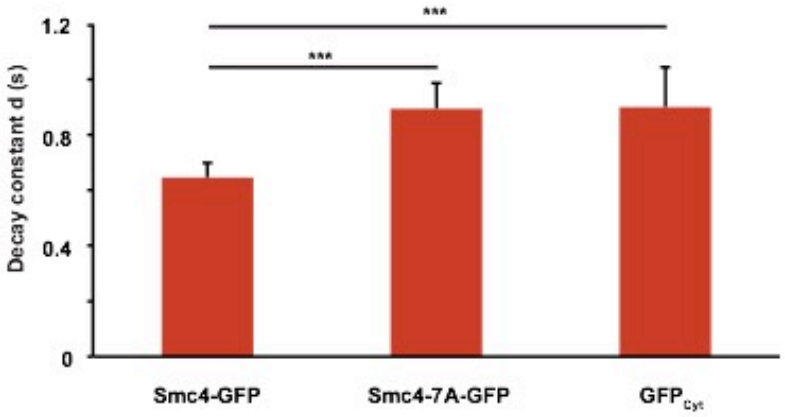
***
***
1.2
0.8
0.4
0
Decay constant d (s)
Smc4-GFP
Smc4-7A-GFP
GFP Cyt

B

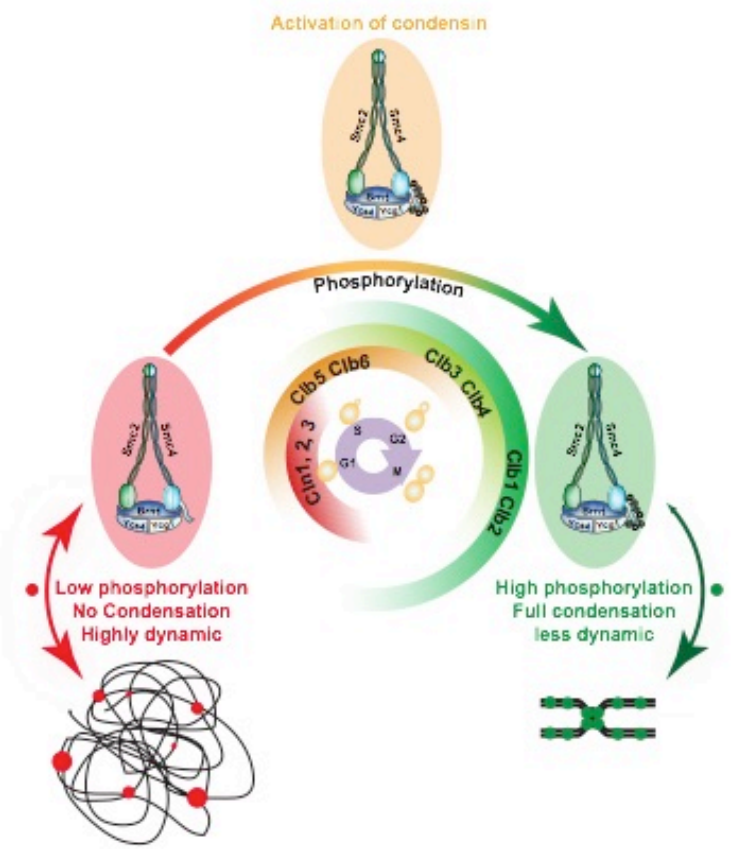
Activation of condensin
Smc2
Smc4
Phosphorylation
Clb5 Clb6
Clb3 Clb4
Clb1 Clb2
Cln1, 2, 3
S
G2
G1
M
Low phosphorylation
No Condensation
Highly dynamic
High phosphorylation
Full condensation
less dynamic

Figure S11. Loss of Cdk1 phosphorylation in the *smc4-7A* phosphomutant affects its interaction with chromatin.

(**A**) Decay of fluorescence after photobleaching of cells expressing Smc4-3xGFP. Histogram showing the calculated decay constant *d* of wild-type Smc4, Smc4-7A mutant and cytosolic GFP (*c.f.*, Equation 1 above). Data for this decay constant comes from the experiment shown in Fig. 7. Triple star symbols indicate a significant difference in decay constant for cells expressing Smc4-3xGFP relative to cells expressing cytosolic GFP or the Smc4-7A-3xGFP mutant (***$p < 0.001$). Error bars indicate S.D. over three independent experiments ($n \geq 12$ cells per experiment). (**B**) Expended model for the role of Cdk1 in the activation of condensin during early mitosis. During interphase, the condensin complex is not targeted for phosphorylation by cyclin-dependent kinases and remains inactive. Upon mitotic entry, the progressive activation of Cdk1 activity leads to Smc4 phosphorylation and initial formation of condensed chromosomes (Figs. 1–3). We propose that condensin responds to Cdk1 activity in a sensitive and proportional manner due to the multisite nature of this phosphoregulatory event (Figs. 2, S4A, S6A). The relative hypersensitivity of condensin to low levels of Cdk1 activity explains why the process of chromosome condensation occurs earlier in the mitotic program than other processes that require more Cdk1 activity for completion (Figs. 1, 6, S1). From a molecular perspective, the phosphorylation of N-terminal part of Smc4 by Cdk1 leads to a change in condensin dynamic interaction with chromatin. The phosphorylation slows down the interactions between condensin and chromatin, effectively stabilizing condensin on chromosomes for longer periods of time (Fig. 7). Ultimately, this increased residency time allows condensin to act on its substrate more effectively, thereby triggering chromosome condensation.

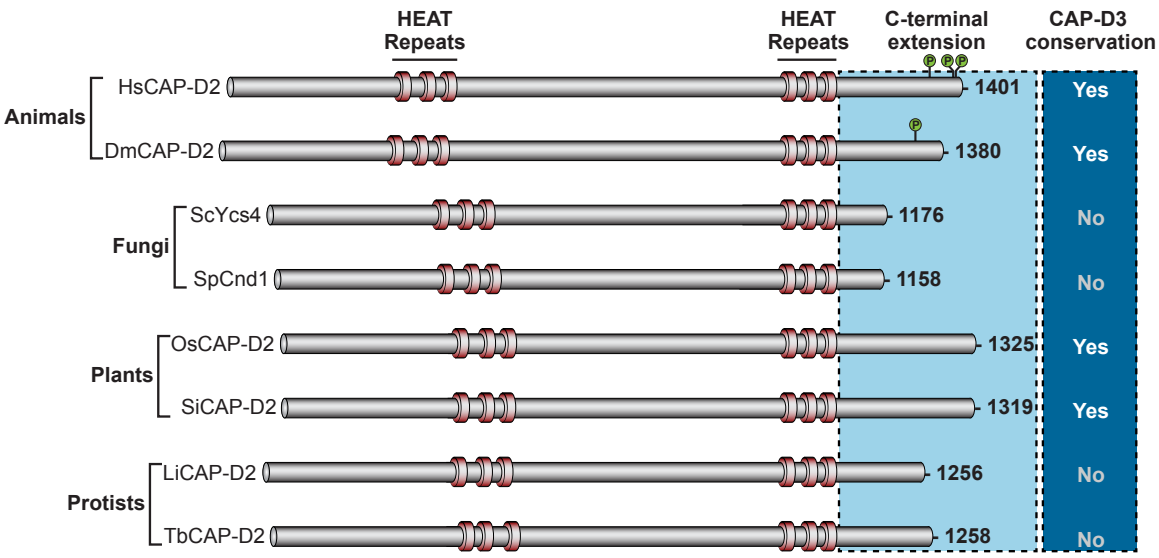

Figure S12. Conservation of the C-terminal extensions of CAP-D2 family members from various eukaryotes.

Schematic representation of CAP-D2/Ycs4 proteins from different species. Clusters of HEAT domains conserved in all eukaryotic members of the CAP-D2 family (Onn et al. 2007) are shown in red. The light blue box marks the boundaries of the C-terminal extension in CAP-D2 homologs, whereas the dark blue box indicates the presence of condensin II/CAP-D3 in the selected species. Known or putative (Holt et al. 2009) Cdk1 phosphorylation sites located in the C-terminal extension of CAP-D2 homologs are represented as green circles above the protein schematics. In human CAP-D2, Thr1339 is a putative Cdk1 site whereas Thr1384 and Thr1389 are likely Cdk1 phospho-sites (Bazile et al. 2010), while in *drosophila*, Thr1328 is a putative Cdk1 site. HEAT domain positions and phospho-residue locations within CAP-D2 homologs are drawn to approximate scale. Note the absence of putative Cdk1 consensus sites in the C-terminal extensions of a number of important exemplar species found within 4 kingdoms of the eukaryotic domain. In some of these species, condensin is monomorphic as evidenced by the absence of CAP-D3 homologs (Hirano 2012). Species names are abbreviated as follows: Hs, *Homo sapiens*; Dm, *Drosophila melanogaster*; Sc, *Saccharomyces cerevisiae*; Sp, *Schizosaccharomyces pombe*; Os, *Oryza sativa*; Si, *Setaria italica*; Li, *Leishmania infantum*; and Tb, *Trypanosoma brucei brucei*.

2.12 Supplemental References:

Amon, A., Tyers, M., Futcher, B., & Nasmyth, K. (1993). Mechanisms that help the yeast cell cycle clock tick: G2 cyclins transcriptionally activate G2 cyclins and repress G1 cyclins. *Cell, 74*(6), 993-1007.

Bazile, F., St-Pierre, J., & D'Amours, D. (2010). Three-step model for condensin activation during mitotic chromosome condensation. *Cell Cycle, 9*(16), 3243-3255. doi:10.4161/cc.9.16.12620

Bishop, A. C., Ubersax, J. A., Petsch, D. T., Matheos, D. P., Gray, N. S., Blethrow, J., Shimizu, E., Tsien, J. Z., Schultz, P. G., Rose, M. D., Wood, J. L., Morgan, D. O., & Shokat, K. M. (2000). A chemical switch for inhibitor-sensitive alleles of any protein kinase. *Nature, 407*(6802), 395-401. doi:10.1038/35030148

Fitch, I., Dahmann, C., Surana, U., Amon, A., Nasmyth, K., Goetsch, L., Byers, B., & Futcher, B. (1992). Characterization of four B-type cyclin genes of the budding yeast Saccharomyces cerevisiae. *Mol Biol Cell, 3*(7), 805-818.

Foiani, M., Marini, F., Gamba, D., Lucchini, G., & Plevani, P. (1994). The B subunit of the DNA polymerase alpha-primase complex in Saccharomyces cerevisiae executes an essential function at the initial stage of DNA replication. *Mol Cell Biol, 14*(2), 923-933.

Gasser, S. M., Laroche, T., Falquet, J., Boy de la Tour, E., & Laemmli, U. K. (1986). Metaphase chromosome structure. Involvement of topoisomerase II. *J Mol Biol, 188*(4), 613-629.

Guacci, V., Hogan, E., & Koshland, D. (1994). Chromosome condensation and sister chromatid pairing in budding yeast. *J Cell Biol, 125*(3), 517-530.

Gutherie, G. R. F. a. C. (1991). Guide to yeast Genetics and Molecular Biology. *Acedemic Press, San Diego*.

Holt, L. J., Tuch, B. B., Villen, J., Johnson, A. D., Gygi, S. P., & Morgan, D. O. (2009). Global analysis of Cdk1 substrate phosphorylation sites provides insights into evolution. *Science, 325*(5948), 1682-1686. doi:10.1126/science.1172867

Kalderon, D., Roberts, B. L., Richardson, W. D., & Smith, A. E. (1984). A short amino acid sequence able to specify nuclear location. *Cell, 39*(3 Pt 2), 499-509.

Kao, L., Wang, Y. T., Chen, Y. C., Tseng, S. F., Jhang, J. C., Chen, Y. J., & Teng, S. C. (2014). Global analysis of cdc14 dephosphorylation sites reveals essential regulatory role in mitosis and cytokinesis. *Mol Cell Proteomics, 13*(2), 594-605. doi:10.1074/mcp.M113.032680

Kinoshita, E., Kinoshita-Kikuta, E., Takiyama, K., & Koike, T. (2006). Phosphate-binding tag, a new tool to visualize phosphorylated proteins. *Mol Cell Proteomics, 5*(4), 749-757. doi:10.1074/mcp.T500024-MCP200

Koivomagi, M., Valk, E., Venta, R., Iofik, A., Lepiku, M., Morgan, D. O., & Loog, M. (2011). Dynamics of Cdk1 substrate specificity during the cell cycle. *Mol Cell, 42*(5), 610-623. doi:10.1016/j.molcel.2011.05.016

Lavoie, B. D., Hogan, E., & Koshland, D. (2004). In vivo requirements for rDNA chromosome condensation reveal two cell-cycle-regulated pathways for mitotic chromosome folding. *Genes Dev, 18*(1), 76-87. doi:10.1101/gad.1150404

Lees, E. M., & Harlow, E. (1993). Sequences within the conserved cyclin box of human cyclin A are sufficient for binding to and activation of cdc2 kinase. *Mol Cell Biol, 13*(2), 1194-1201.

Moreno, S., Klar, A., & Nurse, P. (1991). Molecular genetic analysis of fission yeast Schizosaccharomyces pombe. *Methods Enzymol, 194*, 795-823.

Nasmyth, K., Stillman, D., & Kipling, D. (1987). Both positive and negative regulators of HO transcription are required for mother-cell-specific mating-type switching in yeast. *Cell, 48*(4), 579-587.

Nishimura, K., Fukagawa, T., Takisawa, H., Kakimoto, T., & Kanemaki, M. (2009). An auxin-based degron system for the rapid depletion of proteins in nonplant cells. *Nat Methods, 6*(12), 917-922. doi:10.1038/nmeth.1401

Ratsima, H., Ladouceur, A. M., Pascariu, M., Sauve, V., Salloum, Z., Maddox, P. S., & D'Amours, D. (2011). Independent modulation of the kinase and polo-box activities of Cdc5 protein unravels unique roles in the maintenance of genome

stability. *Proc Natl Acad Sci U S A, 108*(43), E914-923. doi:10.1073/pnas.1106448108

Rudner, A. D., & Murray, A. W. (2000). Phosphorylation by Cdc28 activates the Cdc20-dependent activity of the anaphase-promoting complex. *J Cell Biol, 149*(7), 1377-1390.

Sheff, M. A., & Thorn, K. S. (2004). Optimized cassettes for fluorescent protein tagging in Saccharomyces cerevisiae. *Yeast, 21*(8), 661-670. doi:10.1002/yea.1130

St-Pierre, J., Douziech, M., Bazile, F., Pascariu, M., Bonneil, E., Sauve, V., Ratsima, H., & D'Amours, D. (2009). Polo kinase regulates mitotic chromosome condensation by hyperactivation of condensin DNA supercoiling activity. *Mol Cell, 34*(4), 416-426. doi:10.1016/j.molcel.2009.04.013

Sutani, T., Yuasa, T., Tomonaga, T., Dohmae, N., Takio, K., & Yanagida, M. (1999). Fission yeast condensin complex: essential roles of non-SMC subunits for condensation and Cdc2 phosphorylation of Cut3/SMC4. *Genes Dev, 13*(17), 2271-2283.

Yin, H., You, L., Pasqualone, D., Kopski, K. M., & Huffaker, T. C. (2002). Stu1p is physically associated with beta-tubulin and is required for structural integrity of the mitotic spindle. *Mol Biol Cell, 13*(6), 1881-1892. doi:10.1091/mbc.01-09-0458

Chapter III: Cdc48/VCP promotes chromosome morphogenesis by releasing condensin from self-entrapment in chromatin

Yogitha Thattikota[1], Sylvain Tollis[1 & 3], Mike Tyers[1], and Damien D'Amours[1, 2 & 4]

[1]Institute for Research in Immunology and Cancer
[2]Département de Pathologie et Biologie Cellulaire
Université de Montréal
C.P. 6128, succursale Centre-ville
Montréal, QC, H3C 3J7
CANADA
[3]Wellcome Trust Centre for Cell Biology
University of Edinburgh,
Edinburgh, EH93BF,
United Kingdom

[4]Corresponding author: Damien D'Amours

3.1 Summary

The morphological transformation of amorphous chromatin into distinct chromosomes is a hallmark of mitosis. To achieve this, chromatin must be compacted and remodeled by a ring-shaped enzyme complex known as condensin. However, the mechanistic basis underpinning condensin's role in chromosome remodeling has remained elusive. Here we show that condensin has a strong tendency to trap itself in its own reaction product during chromatin compaction, and yet is capable of interacting with chromatin in a highly-dynamic manner *in vivo*. To resolve this apparent paradox, we identified specific chromatin remodelers and AAA-class ATPases that act in a coordinated manner to release condensin from chromatin entrapment. The Cdc48 segregase is the central linchpin of this regulatory mechanism and promotes ubiquitin-dependent cycling of condensin on mitotic chromatin as well as effective chromosome condensation. Collectively, our results show that condensin inhibition by its own reaction product is relieved by forceful enzyme extraction from chromatin.

3.2 Introduction

Faithful transmission of genetic material during sister-chromatid separation is essential for cell survival. Errors in the segregation of sister chromatids lead to aneuploidy and genome instability, key features associated with pathologies in humans (Pfau & Amon, 2012). During cell division, chromatin undergoes major structural changes that are responsible for the formation of visible chromosomes, a process known as chromosome morphogenesis (Robellet et al., 2015; van Heemst et al., 1999; Yu & Koshland, 2005). To achieve this higher-order reorganization, chromatin must be compacted by the condensin complex, a highly conserved ring-shaped ATPase (Bazile et al., 2010; Hirano, 2016; Piskadlo & Oliveira, 2016). In *Saccharomyces cerevisiae*, the condensin complex is composed of the two ATPases Smc2 and Smc4, the heat repeat proteins Ycs4 and Ycg1 and the kleisin subunit Brn1. Condensin is associated with chromatin throughout the cell cycle (D'Ambrosio et al., 2008) and its loading on chromatin is promoted by several factors, including Scc2/4, TFIIIC, and Monopolin (D'Ambrosio et al., 2008; Johzuka & Horiuchi, 2009). At the onset of mitosis, the condensin enzyme is activated by Cdk1 phosphorylation of the Smc4 and CapD2/3 subunits, which leads to the initial stages of chromosome condensation (Ono et al., 2004; Robellet et al., 2015). When Cdk1 becomes inactive later in mitosis, Cdc5/Polo kinase assumes the role of condensin phosphorylation and promoting condensation (Lavoie et al., 2004; St-Pierre et al., 2009). Once activated by phosphorylation, however, it is unclear how condensin catalyzes the compaction of chromatin into visible chromosomes. Recent proposals for the mode of action of this enzyme include topological entrapment of DNA (Cuylen et al., 2011; Cuylen et al., 2013) and chromatin loop extrusion models (Goloborodko et al., 2016).

Many proposals for the mechanism of action of condensin are focused on structural considerations and how the relationship of the complex to DNA could explain its chromosome compaction activity. However, condensin function also depends on its ATPase activity, since abrogation of ATP hydrolysis by Smc2 or Smc4 is incompatible with chromosome segregation and cell viability (Hudson et al., 2008; Kinoshita et al.,

2015). Consistent with this view, recent evidence shows that condensin binding to mitotic chromosome is highly dynamic, suggesting that it is not merely a static scaffold (Gerlich et al., 2006; Oliveira et al., 2007; Robellet et al., 2015). Rather, condensin promotes chromosome condensation through repeated cycles of binding to, and release from its chromatin substrate. This implies the existence of an active unloading mechanism that ensures condensin can dissociate effectively from chromatin once its enzymatic cycle of compaction is completed. Interestingly, the nature of the chromatin product generated by a cycle of condensin activity –namely, highly condensed chromatin– and the need for condensin to be unloaded efficiently from its reaction product to engage in a subsequent catalytic cycle may be incompatible. Indeed, condensin initially binds to uncondensed chromatin that is highly accessible to other DNA binding proteins (reviewed in (Bell et al., 2011)). In contrast, after condensin completes its condensation cycle, the chromatin reaction product is rendered inaccessible to other DNA binding factors (Fig. 1a) (Chen et al., 2005; Chen et al., 2002; Cheutin et al., 2003; Martin & Cardoso, 2010). How condensin is extracted from the compact chromatin environment that it generates is currently unknown but likely represents a critical regulatory step in the process of chromosome condensation.

The observations highlighted above hint that specific chromatin-associated factors, such as remodelers or chaperones, may assist in the process of chromosome morphogenesis by promoting the removal of condensin from chromatin, and thereby allow on-going rounds of condensin activity during mitosis. Here, we test this hypothesis by conducting a genetic screen to identify chromatin-associated proteins that promote a dynamic condensin state on mitotic chromosomes. This screen uncovered the Cdc48 segregase, also known as Vasolin-containing protein (VCP)/p97 in humans (Barthelme & Sauer, 2016; Franz et al., 2016; Meyer & Weihl, 2014), as a critical new effector of chromosome condensation. We show that Cdc48 acts together with its Ufd1-Npl4 co-factor to stimulate dynamic cycles of condensin loading and unloading on compacted chromatin in order to promote chromosome condensation in mitosis.

3.3 Results

3.3.1 A candidate-based screen for novel regulators of condensin mobility on chromatin

To identify effectors of condensin dynamics in chromatin, we performed a candidate-based genetic screen for mutants that show defects in chromosome morphology specifically in mitosis. We focused our screen on known effectors of chromatin transactions, including chromatin remodelers, chaperones, and other regulators of nucleosome behavior. Yeast cells carrying temperature sensitive or deletion mutants for candidate genes were synchronized in metaphase at 37 °C and the morphology of the ribosomal DNA (rDNA) repeat locus was monitored by fluorescence *in situ* hybridization (FISH). This assay takes advantage of a well-defined series of condensin-induced changes in rDNA shape that reflect functional or dysfunctional chromosome condensation, namely the "loop" and "puff" phenotypes, as defined by Guacci and Koshland (Guacci et al., 1994) (Fig 1b). The screen uncovered 4 novel effectors of chromosome condensation, namely *CDC48*, *RVB2*/reptin, *SWR1* and *ESA1*. Cells carrying mutations in these genes showed various degrees of abnormality in chromosome morphology, from a mild increase in puff/uncondensed phenotype (*swr1Δ*) to completely defective loop/condensed chromosome formation (*cdc48-3* and *esa1-L327L*; Fig 1b). *ESA1* and *SWR1* encode components of the NuA4 and SWR complexes, which have previously-described roles in sister-chromatid cohesion (Sharma et al., 2013). These genes were not studied further because the condensation defect could be secondary to effects on sister-chromatid cohesion. However, one very interesting candidate identified in our screen is Cdc48, an AAA-type ATPase known for its role in extracting proteins from chromatin (Franz et al., 2016). Cdc48 has been predominantly studied for its role in the ERAD pathway, but is also involved in other cellular functions including cell cycle regulation and organelle biogenesis (Barthelme & Sauer, 2016; Meyer & Weihl, 2014). Because Cdc48 has not been previously connected with chromosome morphogenesis in early

mitosis, we decided to focus further analyses on this protein.

Since the *cdc48* mutants were not identified in previous screens for chromosome condensation effectors, we wondered whether the defect we observed in *cdc48-3* mutants was allele specific. Assessment of chromosome morphology in two other mutants, *cdc48-6* and *cdc48-9* arrested in metaphase at 37°C (Fig 2a) confirmed that defects in chromosome condensation were a general phenotype associated with *cdc48* inactivation (Fig 2b). A previous study reported that unloading of the CMG replicative helicase from chromatin after completion of DNA replication is dependent on Cdc48 (Maric et al., 2014), providing a possible cause for the condensation defects observed in *cdc48* mutants. However, inactivating CMG disassembly in a *dia2D* mutant (Maric et al., 2014) did not lead to condensation defects (Fig S1a), whereas inactivating *cdc48* after CMG unloading had occurred (Maric et al., 2014) did not suppress the chromosome condensation phenotype (Fig S1b).

Cdc48 is known to promote multiple cellular functions through interactions with a variety of substrate-recruiting or substrate-processing co-factors (Jentsch & Rumpf, 2007). To address this, we constructed an isogenic collection of 15 mutants defective in known Cdc48 substrate-recruiting cofactors (Ufd1, Shp1/Ubx1, Ubx2-7 and Npl4), substrate-processing cofactors (Ufd2, Ufd3 and Otu1), the SUMO specific cofactor (Wss1), the mitochondrial associated cofactor (Vms1), and screened these mutants for defects in chromosome morphology during mitosis. We found that *ufd1-2* and *npl4-1* mutants showed strong defects in chromosome morphology in mitosis (Fig 2c). Interestingly, Ufd1 interacts with Cdc48 as a heterodimer with Npl4 (Pye et al., 2007), consistent with the fact that both mutants phenocopied the *cdc48-3* mutant in our assay. The rDNA morphology defects observed in *ubx7Δ* and *ufd3Δ* mutants (Fig 2c) were not studied further since these mutants could not be synchronized effectively in metaphase (*ubx7Δ*; our unpublished observation) or had abnormal levels of ubiquitin (*ufd3Δ*; (Mullally et al., 2006)). We concluded from the above results that the Ufd1-Npl4 dimer is the specific co-factor that assists Cdc48 in the regulation of chromosome morphogenesis

in mitosis.

3.3.2 Cdc48$^{Ufd1\text{-}Npl4}$ regulates chromosome condensation through a novel mechanism

We next asked if condensation defects identified in *cdc48* mutants were due to defects in sister chromatid cohesion, since a previous report indicated that Cdc48 stabilizes Cut1/separase in fission yeast (Ikai & Yanagida, 2006) and cohesion defects can lead to indirect effects on condensation (Guacci et al., 1997). To test this, we assayed for sister chromatid cohesion defects in *cdc48-3* mutant arrested in metaphase with nocodazole using tetO arrays integrated adjacent to *CEN4* and *RDN1* loci (D'Amours et al., 2004). We scored cohesion defects by monitoring one or two GFP spots in those strains, and observed that the *cdc48-3* mutant did not show any cohesion defects at *CEN4* and *RDN1* (Fig 3a). In contrast, the cohesin mutant *mcd1-1* showed the expected *CEN4* cohesion defect in this assay. Together, these results indicated that chromosome condensation defects observed in *cdc48-3* were not due to impaired cohesion in this strain.

Cdc48 has many substrates and is implicated in numerous cellular processes (Barthelme & Sauer, 2016; Franz et al., 2016; Meyer & Weihl, 2014). We next asked whether any known Cdc48 substrates could explain its involvement in chromosome condensation. In particular, it has been previously shown that Cdc48 can regulate late mitotic steps, including nuclear envelope reformation and chromatin decompaction, by controlling Aurora B kinase association with chromosomes (Ramadan et al., 2007). To examine whether Cdc48 might regulate chromosome morphogenesis through Aurora B in yeast, we monitored rDNA morphology in strong Aurora B (*ipl1*) mutants arrested in mitosis by nocodazole. FISH analysis did not reveal any rDNA morphological defects in *ipl1-2* and *ipl1-85* strains at the restrictive temperature of 32 °C for these mutant alleles (Fig 3b & Fig 3c). This result is consistent with an earlier report showing no impact of *ipl1-321* (a weaker allele of yeast Aurora B) on rDNA morphology in early mitosis (Lavoie et al., 2004). Since none of the other known substrates of Cdc48 could readily explain the

changes we observed in chromosome morphology, our results suggested a novel role for Cdc48 in chromosome condensation.

3.3.3 Chromosome condensation is ubiquitin-dependent

It is known that substrate recognition by Cdc48 depends on SUMOylation or ubiquitylation (Franz et al., 2016), raising the possibility that condensin is modified by ubiquitin or SUMO moieties *in vivo*. We investigated these modifications might be important for chromosome condensation in metaphase. To test this, we monitored rDNA morphology by FISH in *uba1-204* and *ubc9-1* mutants arrested in metaphase. These two conditional mutants encode the sole E1 activating and E2 conjugating enzymes for ubiquitylation and SUMOylation of proteins in yeast, respectively (Ghaboosi & Deshaies, 2007; Seufert et al., 1995). General disruption of ubiquitylation caused severe chromosome condensation defects, whereas loss of SUMOylation has no detectable effect in our assay (Fig 4a & 4b). This result was consistent with the condensation defect associated with the loss of *UFD3* (Fig 2c), which is known to reduce ubiquitin levels *in vivo* (Mullally et al., 2006). These observations prompted us to investigate whether any subunit of condensin complex was ubiquitylated *in vivo*. We expressed His-tagged ubiquitin from the *GAL1* promoter on a high copy plasmid and subsequently purified ubiquitylated proteins from cell lysates using nickel-conjugated beads. Immunoblot analysis for condensin subunits revealed the presence of Brn1-HA in the ubiquitylated fraction (Fig 4c). We also investigated whether we could detect condensin modification without ubiquitin overexpression. We immunoprecipitated epitope-tagged Ycs4 from wild-type and *cdc48-3* mutant cells followed by immunoblot with an anti-ubiquitin antibody on denatured membrane. Although we did not detect a significant ubiquitin signal on Ycs4 from wild-type cells, we observed a robust signal for high-molecular weight ubiquitin conjugates Ycs4 from the *cdc48-3* strain (Fig 4d). Together, these results indicate that condensin subunits are either ubiquitylated and/or associate with an ubiquitylated protein, and that the process of ubiquitylation is essential for chromosome morphogenesis. These results are consistent with proteome-wide mass

spectrometry analyses that have found condensin subunits to be ubiquitylated *in vivo* in yeast (Kim et al., 2011; Oshikawa et al., 2012; Povlsen et al., 2012; Swaney et al., 2013; Wagner et al., 2011).

3.3.4 Condensin interacts with Cdc48 during mitosis

Could condensin be a direct substrate for Cdc48 in mitosis? To address this possibility, we tested if an interaction between condensin and Cdc48 could be detected by co-immunoprecipitation. Lysates were prepared from mitotic cells expressing unmodified or epitope tagged Ycs4 and/or *cdc48-3*. We used *cdc48-3* mutants rather than the wild-type protein for this analysis because previous studies indicated that it has properties of substrate-trapping mutant (Nakatsukasa et al., 2013). Remarkably, Cdc48-3 protein was found to specifically co-precipitate with Ycs4 in mitotic cells (Fig 5a). These results are consistent with earlier proteome-wide studies that documented an interaction between condensin subunits and Cdc48/p97 in humans (Hein et al., 2015; Raman et al., 2015; Yu et al., 2013). These results imply that the condensin complex may be a substrate of Cdc48 during mitosis.

We then investigated whether Cdc48 might regulate condensin abundance since some of its known substrates are targeted for degradation by the proteasome (Barthelme & Sauer, 2016; Franz et al., 2016; Meyer & Weihl, 2014). Each subunit of the condensin complex was epitope-tagged and protein abundance monitored by immunoblot analysis of cell lysates. Wild-type and *cdc48-3* mutant cells were synchronized at G1 and released into fresh medium containing nocodazole at 37 °C. Analysis of protein samples at various time points after G1 release revealed similar protein levels for condensin subunits in *cdc48-3* mutant and control cells (Fig 5b). Cdc48 thus did not appear to modulate condensin protein abundance or stability in mitosis.

3.3.5 Cdc48 drives dynamic binding of condensin on chromatin during mitosis

Unlike the cohesin complex, condensins in yeast, flies and humans are known to interact dynamically with metaphase chromatin (Gerlich et al., 2006; Oliveira et al., 2007; Robellet et al., 2015). This evolutionarily conserved behavior suggests that high mobility on chromatin is an important feature for condensin function *in vivo*. Given that compacted chromatin is an inherently low accessibility/mobility environment (Chen et al., 2005; Chen et al., 2002; Cheutin et al., 2003; Martin & Cardoso, 2010), it seemed plausible that other factors might be required for the highly dynamic interactions of condensin with mitotic chromatin. As Cdc48 has been shown to extract DNA-binding factors from chromosomal regions with hard-to-access chromatin configurations (Franz et al., 2016), we therefore asked if Cdc48 could promote condensin mobility on mitotic chromatin. We investigated the dynamics of condensin in live yeast cells using raster image correlation spectroscopy (RICS), a variant of fluorescence correlation spectroscopy, in which space-time fluorescence correlations are analyzed in order to quantify the mobility of fluorescent molecules at a subcellular resolution (Brown et al., 2008; Digman et al., 2009). Metaphase cells expressing triple GFP-tagged Smc4 were subjected to RICS imaging in wild type and mutant *cdc48* strains (Figs 6a,b & S2). As expected, Smc4-3GFP from wild-type cells showed mobile behavior on mitotic chromatin on the millisecond (ms) timescale, such that correlated motion could be fitted with an effective free diffusion model (Fig 6a). Importantly, Smc4-3GFP showed a significantly slower effective diffusion in the *cdc48-3* mutant (0.75 $\mu m^2/s$, N=31) compared to wild-type cells (1.16 $\mu m^2/s$, N=32, Mann-Whitney-Wilcoxon rank test p-value < 0.01) (Fig 6b). As a control, we performed similar imaging experiments and analysis in cells expressing cytoplasmic GFP (Fig 6a & S3a), and we found a median diffusion coefficient of 8.98 $\mu m^2/s$ (N=35), in agreement with an earlier study (Slaughter et al., 2007).

Complex microscopic dynamics including binding/unbinding of freely diffusing molecules to immobile target sites often result in an effective free diffusion regime at larger timescales. The effective diffusion coefficient (as measured by RICS) depends on both the free diffusion coefficient and the relative fractions of bound and free molecules (Pando et al., 2006; Sigaut et al., 2014). Hence, the apparent slower Smc4-3GFP mobility

in *cdc48-3* vs wild-type cells could be a passive consequence of an overall slower diffusion in the nuclei of the mutant cells. To rule out this possibility, we performed identical experiments and analyses on wild-type and *cdc48-3* strains expressing 3xGFP fused to a NLS (nuclear localization signal). The analysis of the diffusion dynamics of NLS-3GFP provides a reasonable measure of free diffusion in the nucleus (Fig 6a). We saw no significant difference between NLS-3GFP diffusion coefficient in wild-type (2.73 $\mu m^2/s$, N=56) and *cdc48-3* cells (3.23 $\mu m^2/s$, N=56, MWW rank test *p*-value > 0.01), indicating that the slower Smc4-3GFP mobility in the *cdc48-3* strain was due to an increased fraction of chromatin-bound condensin, or equivalently of condensin residency time on chromatin (Fig 6c).

If more condensin interacts with compacted chromatin at any given time, one prediction would be that it should be possible to detect increased abundance of the complex on mitotic chromosomes. This is a strong prediction because such behavior would represent a gain-of-function from a DNA-binding perspective. To test this, we performed chromatin immunoprecipitation (ChIP) experiments to assess the abundance of condensin at the *rDNA* and *CEN6* loci. The Smc4 subunit of condensin showed an increased enrichment at these two chromosomal binding sites in *cdc48-3* mutant cells relative to wild-type cells synchronized in metaphase (Fig 6d). We also observed a similar increase in condensin chromosomal occupancy by analysis of chromatin spreads from cells arrested at metaphase (Fig S3b). Collectively, these results indicated that Cdc48 governs the dynamic interactions of condensin with mitotic chromatin in live cells.

3.4 Discussion

The mechanistic basis for the compaction of chromatin into visible chromosomes remains one of the most enduring mysteries of mitosis. Specifically, how condensin promotes chromosome remodeling and how chromatin is folded in condensed chromosomes represent outstanding questions (Hirano, 2016; Piskadlo & Oliveira,

2016). In this study, we address the mechanism of chromosome condensation by condensin. Previous work on this enzyme has focused on its regulation by different kinases, on the nature of its chromatin loading factors, and on its topological relationship with DNA during the chromosome condensation process (Bazile et al., 2010; Hirano, 2016; Piskadlo & Oliveira, 2016). By analogy with cohesin, it has been recently proposed that condensin acts as a molecular ring (Cuylen et al., 2011; Cuylen et al., 2013) that traps distant chromosomal regions and promotes compaction of chromatin via a loop extrusion mechanism (Goloborodko et al., 2016). However, once it completes its loading and activation in S-phase, cohesin remains associated with chromosomes and show very little net dissociation from chromatin until anaphase, despite its evident dynamic interaction with chromatin (Haering et al., 2004; Yeh et al., 2008). This particular dynamic aspect is unlikely to apply to condensin and prompted us to ask: What happens with condensin when its first cycle of chromatin compaction is completed? Considering the mechanism of action of condensin from an enzymatic standpoint requires one to explain how multiple rounds of chromatin compaction might occur in mitosis, and how this enzyme might be efficiently unloaded from compacted chromatin at each catalytic cycle. This question is mechanistically relevant for at least three reasons. First, we now know that the condensin complex shows highly dynamic chromatin binding behavior in many eukaryotes during mitosis (Gerlich et al., 2006; Oliveira et al., 2007; Robellet et al., 2015), which require effective loading and unloading of the enzyme from chromosomes. Second, the sparse abundance of condensin in relationship with chromosomal DNA (~1 complex per 5-10 kb DNA; (MacCallum et al., 2002; Wang et al., 2005)) makes it unlikely that condensin can provide sufficient structural constraint to compact chromatin when acting at a single chromosomal locus throughout mitosis, as implied by a purely static mode of action. Finally, by its fundamental nature, the product of the condensin reaction –compacted chromatin– significantly reduces the effectiveness with which proteins can exchange in and out of this dense macromolecular assembly (Chen et al., 2005; Chen et al., 2002; Cheutin et al., 2003; Martin & Cardoso, 2010). This contrast with the easy access condensin has with its substrate –open/uncondensed chromatin– at mitotic onset. As such, the product of the condensin reaction has the potential to inhibit reaction

progression by local trapping of condensin and preventing effective catalytic turnover.

The observations highlighted above led us to speculate about the existence of a previously unanticipated activity that might release of condensin from chromatin entrapment (Fig. 7). We show herein that the Cdc48 segregase, together with its ubiquitin-adaptor complex Ufd1-Npl4, is a condensin "extractase" that acts on compacted chromatin in early mitosis. Importantly, this chromatin extraction mechanism is essential for chromosome morphogenesis as inactivation of any component of this pathway (Cdc48, its co-factors, or ubiquitylation) abrogates chromatin compaction and reduces condensin mobility on chromosomes in live cells. Disruption of Cdc48 function consequently leads to the entrapment of condensin on its preferred chromosomal binding sites (rDNA array and CEN) in an inactive sequestered state. Our results illustrate the physiological relevance of promoting high mobility of condensin on mitotic chromosomes, as previously observed in yeast, flies, and humans (for condensin I) (Gerlich et al., 2006; Oliveira et al., 2007; Robellet et al., 2015). Our results are not inconsistent with the notion that some fraction of condensin might still act in a static manner to provide structural constrains important for maintenance of chromosome condensation. Indeed, it has been observed that a pool of human condensin II is less dynamic on chromosomes in mitosis (Gerlich et al., 2006) and we envision that his may represent a specialized pool contributing a qualitatively different function to chromosome condensation than the dynamic pool of condensin.

The mode of action we propose for Cdc48 in condensin dynamics is consistent with its role in the unloading of other chromatin-bound proteins from chromosomes (reviewed in (Franz et al., 2016)). However, there is a major distinction between condensin and other substrates of Cdc48 in that the latter are passively trapped into chromatin, whereas condensin engenders its own steric entrapment by virtue of its chromatin condensation activity. Without an active release mechanism, this self-entrapment would effectively freeze the compaction cycle at an early stage due to the limiting abundance of condensin. In this sense, the mode of action of condensin and

cohesin diverge, since cohesin binds stably to its chromosomal substrate from S-phase to mid-mitosis (Haering et al., 2004; Yeh et al., 2008). In the absence of Cdc48 activity, the unloading of condensin from chromatin becomes markedly slower, as evidenced by the reduced diffusion rates of the enzyme in *cdc48-3* mutants, consistent with observations that compacted chromosomes impede the unloading of other DNA binding proteins (Chen et al., 2005; Chen et al., 2002; Cheutin et al., 2003; Martin & Cardoso, 2010).

The mechanism of condensin unloading revealed in this study is likely to be conserved throughout eukaryotic evolution since the homologs of $Cdc48^{Ufd1\text{-}Npl4}$, VCP/p97 and its Ufd1L-Npl4 cofactors, are present in humans and also implicated in the extraction of chromatin-associated proteins (reviewed in (Barthelme & Sauer, 2016; Franz et al., 2016; Meyer & Weihl, 2014)). Consistently, unbiased proteome-wide mass spectrometry analyses have identified condensin subunits as interactors of human VCP (Hein et al., 2015; Raman et al., 2015; Yu et al., 2013). The ubiquitin-dependent extraction mechanism we propose also explains the observation that condensin subunits are heavily ubiquitylated in humans (65 sites identified; see Table S1) and yet appear to be stable throughout the cell cycle (Takemoto et al., 2004). The identity of the ubiquitin ligases that modify condensin subunits, the deubiquitinating enzymes that may reverse this modification, and the precise role that these enzymes play in facilitating Cdc48-dependent extraction of condensin from compacted chromatin remain to be determined. Given that Cdc48/VCP inhibitors hold promise in cancer therapy (Ramadan et al., 2007), it will be important to consider the effect of these agents on the condensin catalytic cycle and mitotic chromosome compaction.

3.5 Methods

Methods, including statements of data availability and associated references, are available in the Supplementary Information.

3.6 Acknowledgments

We would like to thank Dr. Julie St-Pierre for her comments on the manuscript, and Drs. Susan R Wente, Toshio Tsukiyama, Mark Hochstrasser, Raymond Deshaies, & Rey-Huei Chen for providing yeast strains. This work was supported by grants from the Canadian Institutes of Health Research to DD (CIHR; MOP 82912, MOP 136788, PJT 148969) and MT (MOP 126129, MOP 366608). DD is a recipient of a FRQ-S Senior Research Scholar career award and MT holds a Canada Research Chair in Systems and Synthetic Biology. ST is funded by the Wellcome Trust Centre for Cell Biology.

3.7 Author Contributions

Conceived and designed the experiments: YT, ST, DD. Performed the experiments: YT, ST. Analyzed the data: YT, ST, DD. Wrote the paper: YT, ST, MT, DD.

3.8 Figure Legends

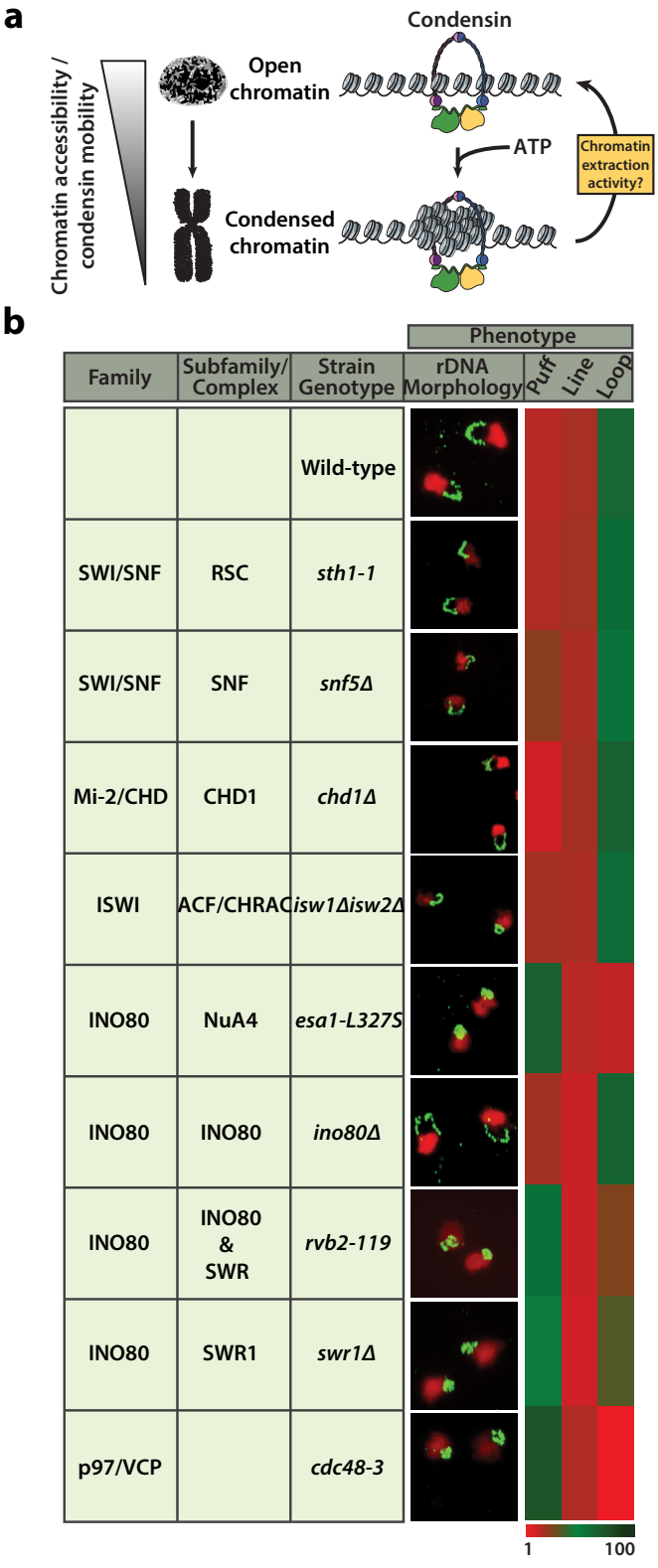

Figure 1. A candidate-based genetic screen for mutants that traps condensin in an inactive state in chromatin. a. Chromatin compaction and its effect on condensin mobility hypothesis. Dynamic behavior of condensin complex results in multiple cycles of binding and release from the chromatin during mitosis and it catalyzes chromatin compaction reaction upon ATP hydrolysis. The model depicts the process of chromatin compaction, which makes the immediate chromatin environment less accessible and eventually trap condensin onto chromatin. To resume the next cycle of condensation, condensin extraction from compacted chromatin environment is essential. **b.** Chromosome condensation defects of *esa1*, *swr1*, *rvb2* and *cdc48* mutants. The heat map depicts the frequencies of specific rDNA morphology classes observed in yeast mutants, from low (red) to high (green). Mutants used in the screen are described in the table on the left. Micrographs show the most prominent rDNA morphology observed with each mutant. Cells were grown asynchronously until exponential phase at 23°C and shifted to 37°C to block in metaphase by nocodazole for 150 min. Samples were processed for FISH analysis, as described previously (Robellet et al., 2015). Nuclei were strained with propidium iodide (PI; red), whereas the rDNA locus was labelled using a probe conjugated to fluorescein isothiocyanate (FITC; green). At least 100 cells were counted for each mutant (n=3; error bars represent standard error of the mean).

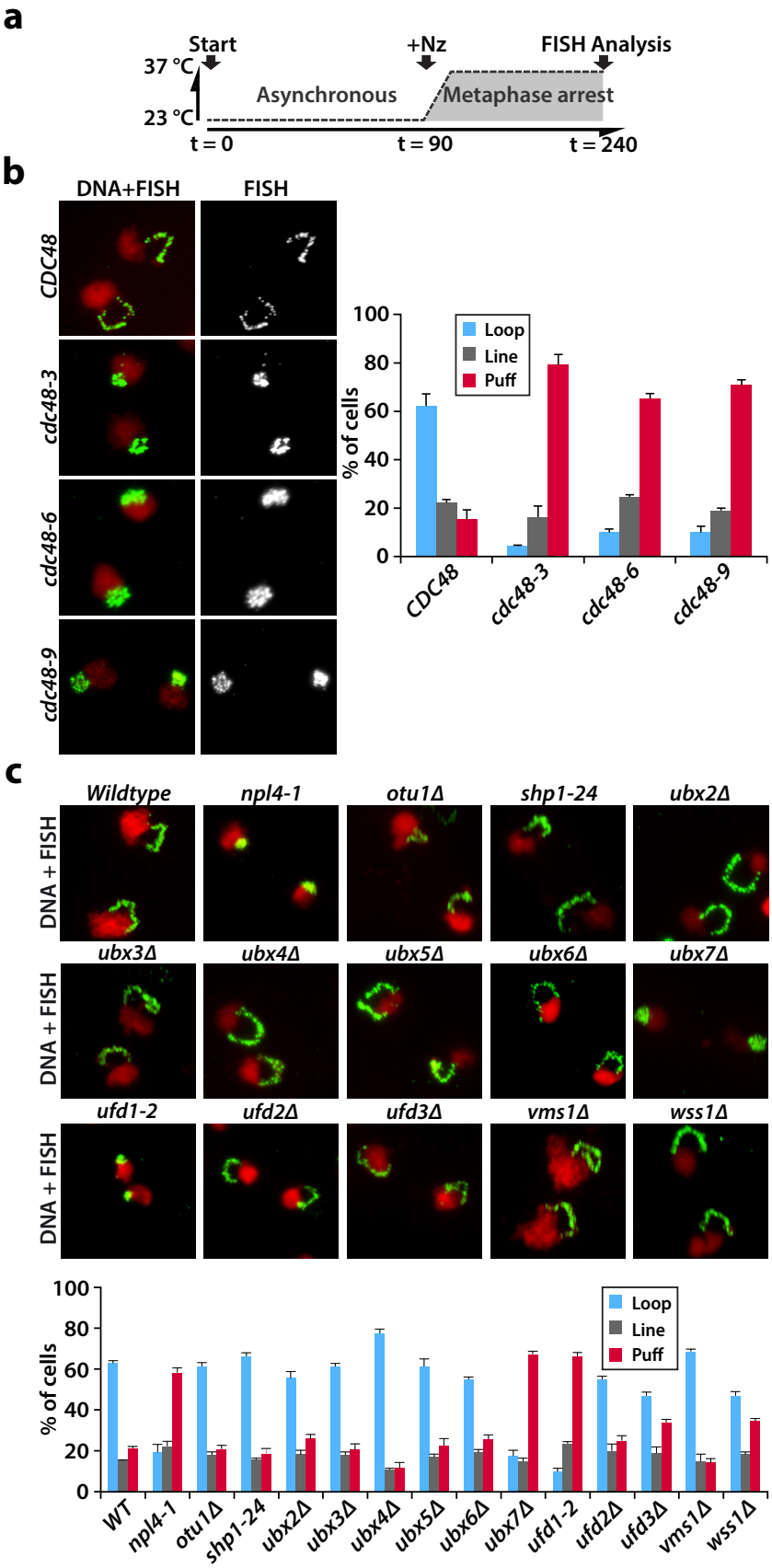
a
Start
+Nz
FISH Analysis
37 °C
23 °C
Asynchronous
Metaphase arrest
t = 0
t = 90
t = 240
b
DNA+FISH
FISH
CDC48
cdc48-3
cdc48-6
cdc48-9
100
80
60
40
20
0
% of cells
Loop
Line
Puff
CDC48
cdc48-3
cdc48-6
cdc48-9
c
Wildtype
npl4-1
otu1Δ
shp1-24
ubx2Δ
ubx3Δ
ubx4Δ
ubx5Δ
ubx6Δ
ubx7Δ
ufd1-2
ufd2Δ
ufd3Δ
vms1Δ
wss1Δ
DNA + FISH
DNA + FISH
DNA + FISH
100
80
60
40
20
0
% of cells
Loop
Line
Puff
WT
npl4-1
otu1Δ
shp1-24
ubx2Δ
ubx3Δ
ubx4Δ
ubx5Δ
ubx6Δ
ubx7Δ
ufd1-2
ufd2Δ
ufd3Δ
vms1Δ
wss1Δ

Figure 2. The Cdc48$^{Ufd1\text{-}Npl4}$ complex is a novel chromosome condensation effector. **a.** Experimental set up for FISH analysis. Cells were grown asynchronously at 23°C and then shifted to 37°C with nocodazole for 150 min to arrest the cells at metaphase and proceeded to FISH analysis. **b-c**. Cells were processed for rDNA morphology analysis as described before. **a**. Chromosome condensation defects observed in *cdc48* mutants are not allele-specific. Micrographs on the left represent the most prominent rDNA morphology class for each mutant, whereas the graph on the right reports morphology quantification. **b.** The Ufd1-Npl4 heterodimer is essential for chromosome condensation. Micrographs on the top panel illustrate the most frequent rDNA morphology for each genotype and graph on the lower panel represents the quantification of rDNA morphologies. At least 100 cells were counted for each genotype (n=3; error bars represent standard error to mean).

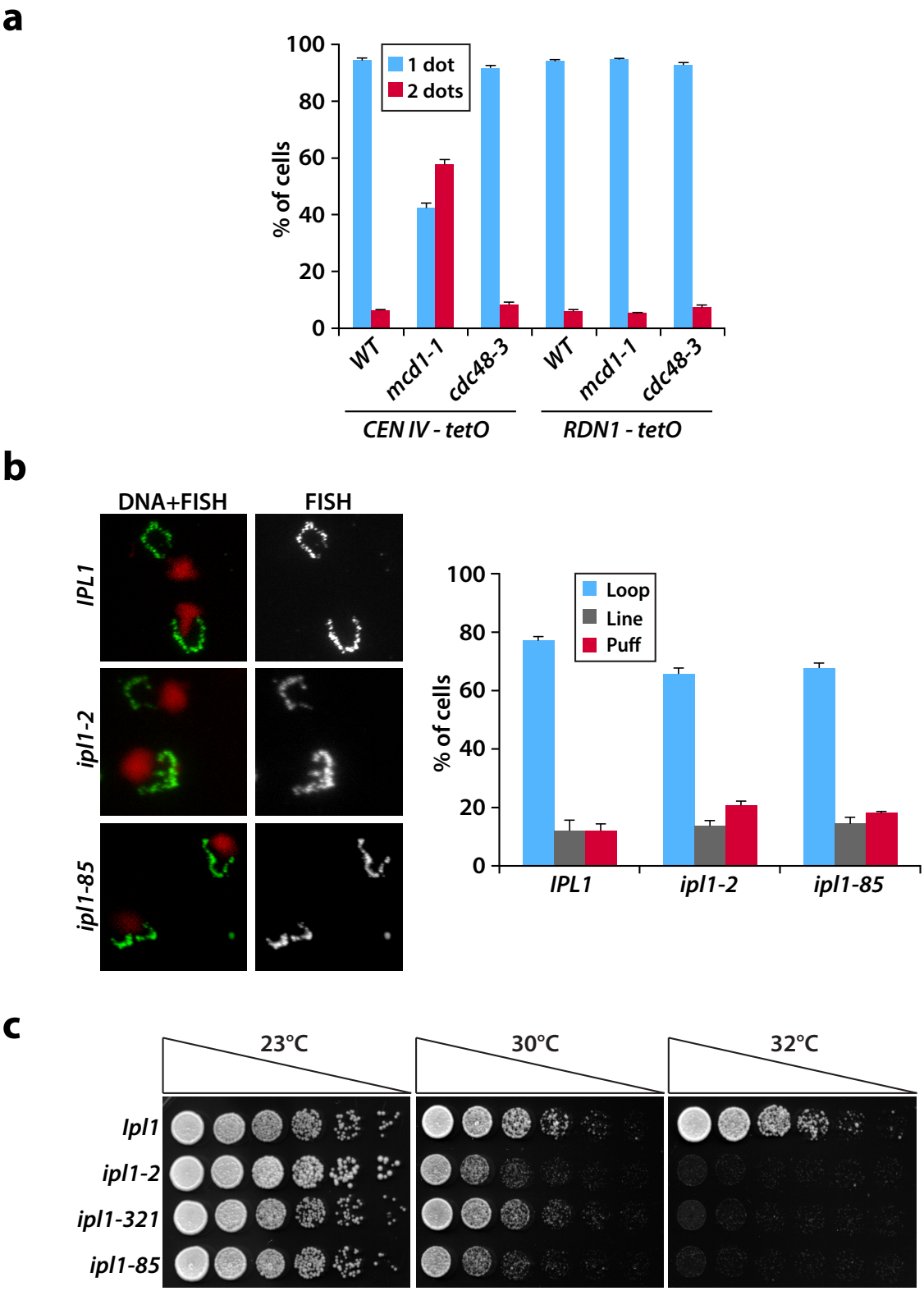
a
100
80
60
40
20
0
% of cells
1 dot
2 dots
WT
mcd1-1
cdc48-3
WT
mcd1-1
cdc48-3
CEN IV - tetO
RDN1 - tetO
b
DNA+FISH
FISH
IPL1
ipl1-2
ipl1-85
100
80
60
40
20
0
% of cells
Loop
Line
Puff
IPL1
ipl1-2
ipl1-85
c
23°C
30°C
32°C
Ipl1
ipl1-2
ipl1-321
ipl1-85

Figure 3. Condensation defects observed in Cdc48 are independent of Ipl1 and sister chromatid cohesion defects. a. The *cdc48-3* mutant does not show defects in sister chromatid cohesion. Wild-type, *cdc48-3* and *mcd1-1* mutants carrying a tetR-GFP fusion and tetO repeats adjacent to *CEN4* and/or rDNA array were synchronized in G1 with alpha-factor treatment at 23 °C. Next, cells were released into medium containing nocodazole at 37 °C to arrest at metaphase. Samples were collected at 150 min and large budded cells were analyzed for the presence of one or two GFP spots. For each genotype, at least 100 cells were counted (n=3; error bars are represented in standard error to mean). **b.** FISH analysis of rDNA morphology in *ipl1* mutants. Cells were grown at 23°C and shifted to 32 °C to synchronize at metaphase with nocodazole treatment for 150 min. Nuclei and rDNA were labelled with PI (red) and FITC (green) respectively. The micrograph on the left represents most prominent rDNA morphology observed in each mutant and graph on the right reports the quantification of rDNA morphology classes. For each genotype, 100 cells were counted. **c.** Phenotype of strong *ipl1* mutants. Fivefold serial dilutions of yeast culture were spotted on solid media and grown at 23°C, 30°C and 32°C for 2-3 days.

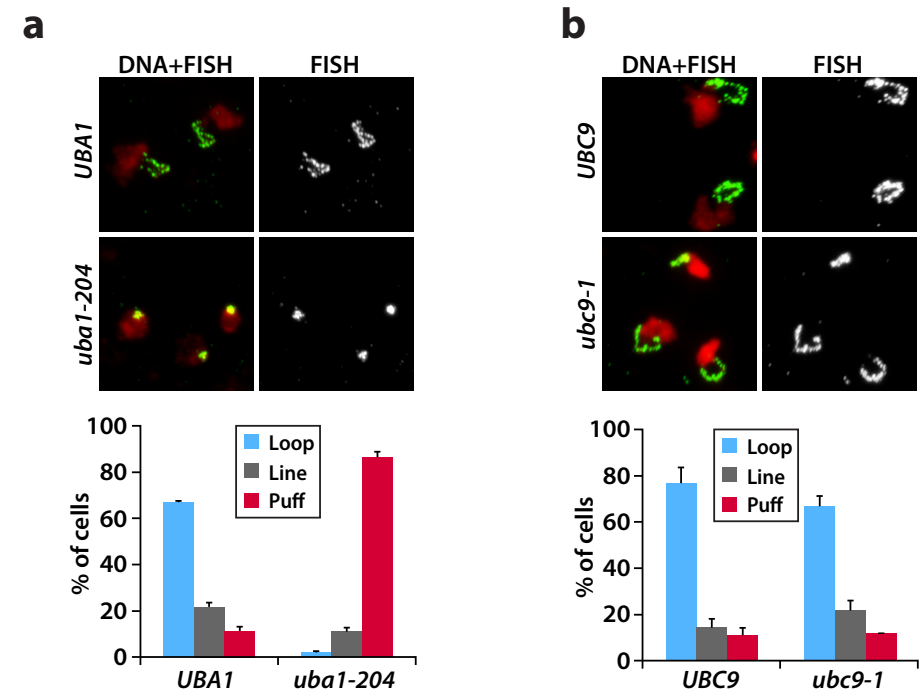
a
DNA+FISH
FISH
UBA1
uba1-204
100
80
60
40
20
0
% of cells
Loop
Line
Puff
UBA1
uba1-204
b
DNA+FISH
FISH
UBC9
ubc9-1
100
80
60
40
20
0
% of cells
Loop
Line
Puff
UBC9
ubc9-1

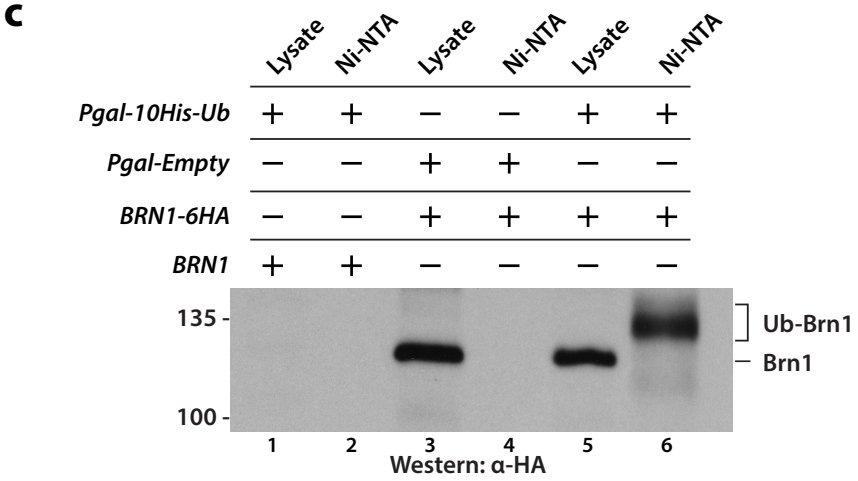
c
Lysate
Ni-NTA
Lysate
Ni-NTA
Lysate
Ni-NTA
Pgal-10His-Ub + + – – + +
Pgal-Empty – – + + – –
BRN1-6HA – – + + + +
BRN1 + + – – – –
135
100
Ub-Brn1
Brn1
1 2 3 4 5 6
Western: α-HA

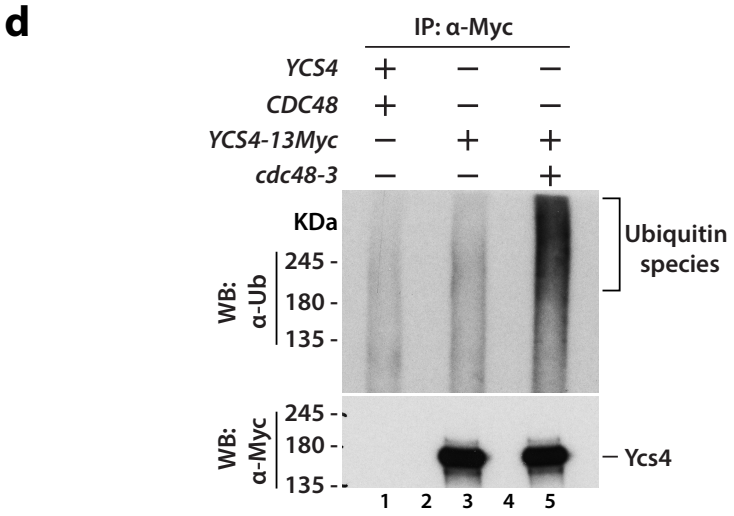
d
IP: α-Myc
YCS4 + – –
CDC48 + – –
YCS4-13Myc – + +
cdc48-3 – – +
KDa
WB: α-Ub
245
180
135
Ubiquitin species
WB: α-Myc
245
180
135
Ycs4
1 2 3 4 5

Figure 4. Chromosome condensation requires active ubiquitylation. a-b. rDNA morphology was analyzed by FISH in ubiquitylation- and sumoylation-deficient mutants. At least 100 cells were counted for each experiment (n=3; error bars represent standard error to mean). Upper panels show pictures of the most prominent rDNA morphology for each genotype, whereas lower panels report morphology quantification. **a.** Ubiquitylation-defective E1 mutant, *uba1-204*, shows strong chromosome condensation defects. **b.** Sumoylation-defective E2 mutant, *uba9-1*, does not show detectable condensation defects. **c.** Cells carrying HA-tagged Brn1 and galactose-inducible 6xHIS-ubiquitin were grown until exponential phase before adding 2% galactose to the medium to induce ubiquitin overexpression for 4 hours. The ubiquitylated proteins were then enriched by Ni-NTA affinity chromatography and analyzed for the presence of Brn1 by immonoblotting with an anti-HA antibody. **d.** Asynchronously-growing cultures of wild-type and *cdc48-3* mutant cells carrying Myc-tagged Ycs4 were shifted to 37 °C and synchronized at metaphase using nocodazole treatment for 150 min. Ycs4 was immunoprecipitated from cell lysates with an anti-Myc tag antibody and the purified material analyzed by western blotting using an anti-ubiquitin antibody.

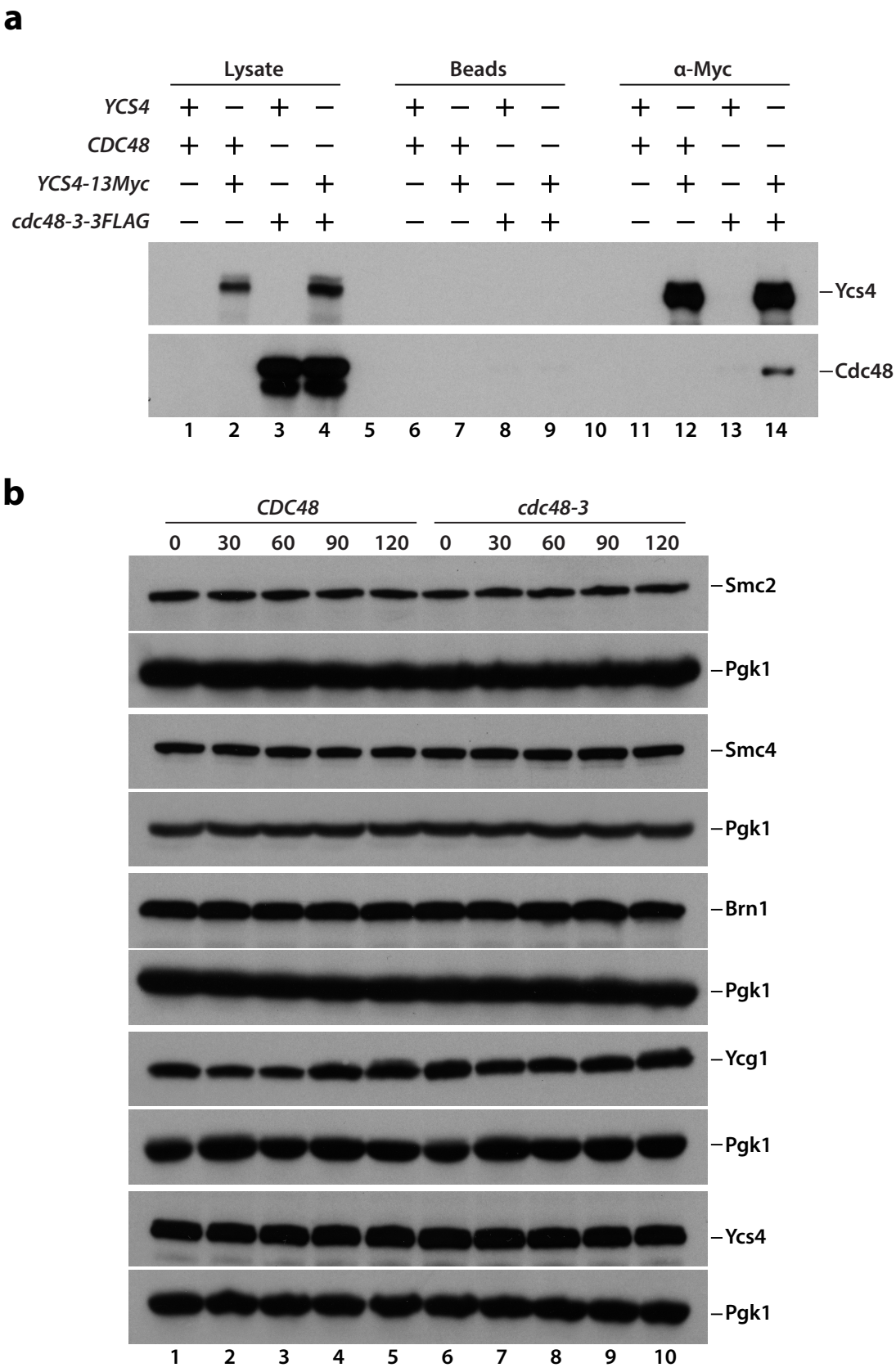
a
Lysate
Beads
α-Myc
YCS4
CDC48
YCS4-13Myc
cdc48-3-3FLAG
Ycs4
Cdc48
1 2 3 4 5 6 7 8 9 10 11 12 13 14
b
CDC48
cdc48-3
0 30 60 90 120 0 30 60 90 120
Smc2
Pgk1
Smc4
Pgk1
Brn1
Pgk1
Ycg1
Pgk1
Ycs4
Pgk1
1 2 3 4 5 6 7 8 9 10

Figure 5. Condensin interacts with Cdc48 *in vivo*. a. Condensin complex interacts with Cdc48. Cultures of cells carrying *YCS4-13Myc* with or without *cdc48-3FLAG* were grown at 23 °C until exponential phase and shifted to 37 °C to block at metaphase with nocodazole treatment for 150 min. Ycs4 was immunoprecipitated with an anti-Myc antibody and the purified material analyzed by immunoblotting with anti-FLAG/Myc antibodies. Untagged cells and beads serve as negative controls. **b.** Condensin subunits levels are not influenced by Cdc48. Cells carrying epitope-tagged condensin subunits were synchronized in G1 with alpha-factor treatment and released into medium containing nocodazole at 37°C. Samples were collected at every 30 min and protein abundance was monitored by immunoblotting. Pgk1 serves as a loading control.

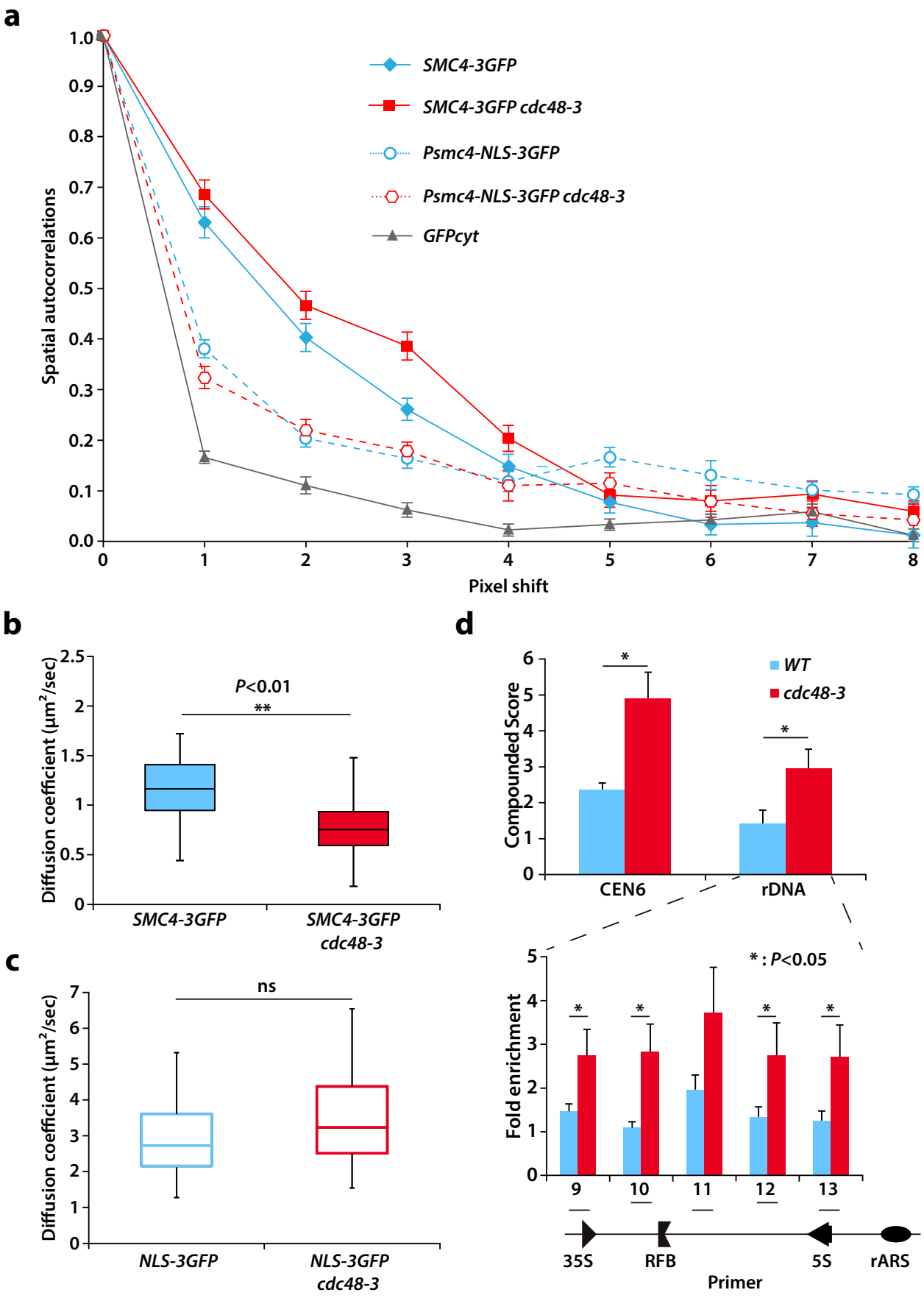
a
Spatial autocorrelations
Pixel shift
SMC4-3GFP
SMC4-3GFP cdc48-3
Psmc4-NLS-3GFP
Psmc4-NLS-3GFP cdc48-3
GFPcyt
b
Diffusion coefficient (μm²/sec)
P<0.01
**
SMC4-3GFP
SMC4-3GFP cdc48-3
c
Diffusion coefficient (μm²/sec)
ns
NLS-3GFP
NLS-3GFP cdc48-3
d
Compounded Score
WT
cdc48-3
CEN6
rDNA
Fold enrichment
* : P<0.05
9
10
11
12
13
35S
RFB
5S
rARS
Primer

Figure 6. Cdc48 promotes condensin turnover on chromatin. a. RICS analysis of condensin mobility on mitotic chromatin. Fluorescence spatial auto-correlations were normalized to the 0-shift correlation as a function of the pixel shift along the vertical axis (ms timescale). Fluorophores were Smc4-3GFP (*CDC48*: blue and *cdc48-3*: red), NLS-3GFP (*CDC48*: dashed blue line and *cdc48-3*: dashed red line) and cytosolic GFP (grey). Data points and error bars correspond respectively to average and standard error over >20 individual cells imaged under the same conditions in the same experiment. **b-c.** Box and whisker plots of the distribution of fitted diffusion coefficients over >30 *CDC48* (solid blue box) and *cdc48-3* (solid red box) metaphase cells expressing Smc4-3GFP (B), and >50 *CDC48* (open blue box) and *cdc48-3* (open red box) metaphase cells expressing NLS-3GFP (C). The box is defined by the first and third quartiles of the distributions (Q1, Q3), while lower and upper whiskers were respectively set to Q1-3 (median-Q1) and Q3+3 (Q3-median). **d.** Condensin occupancy on mitotic chromosomes. Wild type and *cdc48-3* mutant strains were synchronized in metaphase at 37°C for 150 min and processed for chromatin immunoprecipitation (Johzuka & Horiuchi, 2009). Top panel shows enrichment of Smc4 at the *CEN6* and *rDNA* loci (compounded score), as revealed by ChIP and qPCR analysis of wild-type and mutant cells ($p>0.05$; error bars represent standard error on the mean). Lower panel indicates enrichment of Smc4 at different positions along the rDNA array repeat. The location of primers used for qPCR analysis are indicated as black bars.

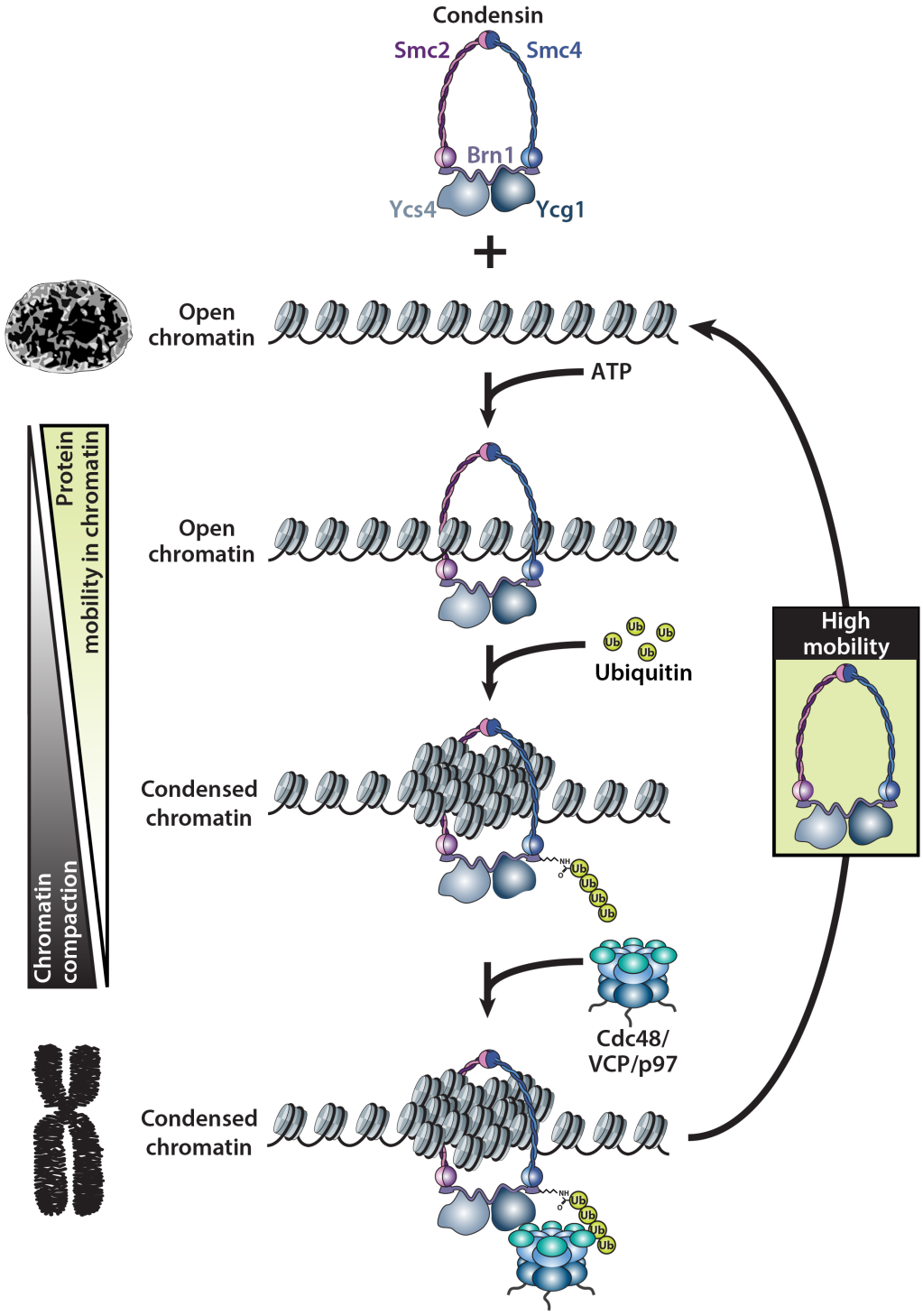
Condensin
Smc2
Smc4
Brn1
Ycs4
Ycg1
+
Open chromatin
ATP
Open chromatin
Ubiquitin
Condensed chromatin
Cdc48/ VCP/p97
Condensed chromatin
High mobility
Protein mobility in chromatin
Chromatin compaction

Figure 7. Model of the mechanism of chromosome condensation by condensin and Cdc48. a. Upon ATP hydrolysis, condensin encompasses its substrate to catalyze the compaction of proximal chromatin, thereby restricting its mobility. After a compaction cycle, condensin is ubiquitylated by an uncharacterized ubiquitin ligase, which recruits the Cdc48-Ufd1-Npl4 complex for condensin extraction. The release of free condensin enables a new cycle of chromosome condensation process.

3.9 References

Barthelme, D., & Sauer, R. T. (2016). Origin and Functional Evolution of the Cdc48/p97/VCP AAA+ Protein Unfolding and Remodeling Machine. *J Mol Biol, 428*(9 Pt B), 1861-1869. doi:10.1016/j.jmb.2015.11.015

Bazile, F., St-Pierre, J., & D'Amours, D. (2010). Three-step model for condensin activation during mitotic chromosome condensation. *Cell Cycle, 9*(16), 3243-3255. doi:10.4161/cc.9.16.12620

Bell, O., Tiwari, V. K., Thoma, N. H., & Schubeler, D. (2011). Determinants and dynamics of genome accessibility. *Nat Rev Genet, 12*(8), 554-564. doi:10.1038/nrg3017

Brown, C. M., Dalal, R. B., Hebert, B., Digman, M. A., Horwitz, A. R., & Gratton, E. (2008). Raster image correlation spectroscopy (RICS) for measuring fast protein dynamics and concentrations with a commercial laser scanning confocal microscope. *J Microsc, 229*(Pt 1), 78-91. doi:10.1111/j.1365-2818.2007.01871.x

Chen, D., Dundr, M., Wang, C., Leung, A., Lamond, A., Misteli, T., & Huang, S. (2005). Condensed mitotic chromatin is accessible to transcription factors and chromatin structural proteins. *J Cell Biol, 168*(1), 41-54. doi:10.1083/jcb.200407182

Chen, D., Hinkley, C. S., Henry, R. W., & Huang, S. (2002). TBP dynamics in living human cells: constitutive association of TBP with mitotic chromosomes. *Mol Biol Cell, 13*(1), 276-284. doi:10.1091/mbc.01-10-0523

Cheutin, T., McNairn, A. J., Jenuwein, T., Gilbert, D. M., Singh, P. B., & Misteli, T. (2003). Maintenance of stable heterochromatin domains by dynamic HP1 binding. *Science, 299*(5607), 721-725. doi:10.1126/science.1078572

Cuylen, S., Metz, J., & Haering, C. H. (2011). Condensin structures chromosomal DNA through topological links. *Nat Struct Mol Biol, 18*(8), 894-901. doi:10.1038/nsmb.2087

Cuylen, S., Metz, J., Hruby, A., & Haering, C. H. (2013). Entrapment of chromosomes by condensin rings prevents their breakage during cytokinesis. *Dev Cell, 27*(4), 469-478. doi:10.1016/j.devcel.2013.10.018

D'Ambrosio, C., Schmidt, C. K., Katou, Y., Kelly, G., Itoh, T., Shirahige, K., & Uhlmann, F. (2008). Identification of cis-acting sites for condensin loading onto budding yeast chromosomes. *Genes Dev, 22*(16), 2215-2227. doi:10.1101/gad.1675708

D'Amours, D., Stegmeier, F., & Amon, A. (2004). Cdc14 and condensin control the dissolution of cohesin-independent chromosome linkages at repeated DNA. *Cell, 117*(4), 455-469.

Digman, M. A., Wiseman, P. W., Horwitz, A. R., & Gratton, E. (2009). Detecting protein complexes in living cells from laser scanning confocal image sequences by the cross correlation raster image spectroscopy method. *Biophys J, 96*(2), 707-716. doi:10.1016/j.bpj.2008.09.051

Franz, A., Ackermann, L., & Hoppe, T. (2016). Ring of Change: CDC48/p97 Drives Protein Dynamics at Chromatin. *Front Genet, 7*, 73. doi:10.3389/fgene.2016.00073

Gerlich, D., Hirota, T., Koch, B., Peters, J. M., & Ellenberg, J. (2006). Condensin I stabilizes chromosomes mechanically through a dynamic interaction in live cells. *Curr Biol, 16*(4), 333-344. doi:10.1016/j.cub.2005.12.040

Ghaboosi, N., & Deshaies, R. J. (2007). A conditional yeast E1 mutant blocks the ubiquitin-proteasome pathway and reveals a role for ubiquitin conjugates in targeting Rad23 to the proteasome. *Mol Biol Cell, 18*(5), 1953-1963. doi:10.1091/mbc.E06-10-0965

Goloborodko, A., Marko, J. F., & Mirny, L. A. (2016). Chromosome Compaction by Active Loop Extrusion. *Biophys J, 110*(10), 2162-2168. doi:10.1016/j.bpj.2016.02.041

Guacci, V., Hogan, E., & Koshland, D. (1994). Chromosome condensation and sister chromatid pairing in budding yeast. *J Cell Biol, 125*(3), 517-530.

Guacci, V., Koshland, D., & Strunnikov, A. (1997). A direct link between sister chromatid cohesion and chromosome condensation revealed through the analysis of MCD1 in S. cerevisiae. *Cell, 91*(1), 47-57.

Haering, C. H., Schoffnegger, D., Nishino, T., Helmhart, W., Nasmyth, K., & Lowe, J. (2004). Structure and stability of cohesin's Smc1-kleisin interaction. *Mol Cell, 15*(6), 951-964. doi:10.1016/j.molcel.2004.08.030

Hein, M. Y., Hubner, N. C., Poser, I., Cox, J., Nagaraj, N., Toyoda, Y., Gak, I. A., Weisswange, I., Mansfeld, J., Buchholz, F., Hyman, A. A., & Mann, M. (2015). A human interactome in three quantitative dimensions organized by stoichiometries and abundances. *Cell, 163*(3), 712-723. doi:10.1016/j.cell.2015.09.053

Hirano, T. (2016). Condensin-Based Chromosome Organization from Bacteria to Vertebrates. *Cell, 164*(5), 847-857. doi:10.1016/j.cell.2016.01.033

Hudson, D. F., Ohta, S., Freisinger, T., Macisaac, F., Sennels, L., Alves, F., Lai, F., Kerr, A., Rappsilber, J., & Earnshaw, W. C. (2008). Molecular and genetic analysis of condensin function in vertebrate cells. *Mol Biol Cell, 19*(7), 3070-3079. doi:10.1091/mbc.E08-01-0057

Ikai, N., & Yanagida, M. (2006). Cdc48 is required for the stability of Cut1/separase in mitotic anaphase. *J Struct Biol, 156*(1), 50-61. doi:10.1016/j.jsb.2006.04.003

Jentsch, S., & Rumpf, S. (2007). Cdc48 (p97): a "molecular gearbox" in the ubiquitin pathway? *Trends Biochem Sci, 32*(1), 6-11. doi:10.1016/j.tibs.2006.11.005

Johzuka, K., & Horiuchi, T. (2009). The cis element and factors required for condensin recruitment to chromosomes. *Mol Cell, 34*(1), 26-35. doi:10.1016/j.molcel.2009.02.021

Kim, W., Bennett, E. J., Huttlin, E. L., Guo, A., Li, J., Possemato, A., Sowa, M. E., Rad, R., Rush, J., Comb, M. J., Harper, J. W., & Gygi, S. P. (2011). Systematic and quantitative assessment of the ubiquitin-modified proteome. *Mol Cell, 44*(2), 325-340. doi:10.1016/j.molcel.2011.08.025

Kinoshita, K., Kobayashi, T. J., & Hirano, T. (2015). Balancing acts of two HEAT subunits of condensin I support dynamic assembly of chromosome axes. *Dev Cell, 33*(1), 94-106. doi:10.1016/j.devcel.2015.01.034

Lavoie, B. D., Hogan, E., & Koshland, D. (2004). In vivo requirements for rDNA chromosome condensation reveal two cell-cycle-regulated pathways for mitotic chromosome folding. *Genes Dev, 18*(1), 76-87. doi:10.1101/gad.1150404

MacCallum, D. E., Losada, A., Kobayashi, R., & Hirano, T. (2002). ISWI remodeling complexes in Xenopus egg extracts: identification as major chromosomal

components that are regulated by INCENP-aurora B. *Mol Biol Cell, 13*(1), 25-39. doi:10.1091/mbc.01-09-0441

Maric, M., Maculins, T., De Piccoli, G., & Labib, K. (2014). Cdc48 and a ubiquitin ligase drive disassembly of the CMG helicase at the end of DNA replication. *Science, 346*(6208), 1253596. doi:10.1126/science.1253596

Martin, R. M., & Cardoso, M. C. (2010). Chromatin condensation modulates access and binding of nuclear proteins. *FASEB J, 24*(4), 1066-1072. doi:10.1096/fj.08-128959

Meyer, H., & Weihl, C. C. (2014). The VCP/p97 system at a glance: connecting cellular function to disease pathogenesis. *J Cell Sci, 127*(Pt 18), 3877-3883. doi:10.1242/jcs.093831

Mullally, J. E., Chernova, T., & Wilkinson, K. D. (2006). Doa1 is a Cdc48 adapter that possesses a novel ubiquitin binding domain. *Mol Cell Biol, 26*(3), 822-830. doi:10.1128/MCB.26.3.822-830.2006

Nakatsukasa, K., Brodsky, J. L., & Kamura, T. (2013). A stalled retrotranslocation complex reveals physical linkage between substrate recognition and proteasomal degradation during ER-associated degradation. *Mol Biol Cell, 24*(11), 1765-1775, S1761-1768. doi:10.1091/mbc.E12-12-0907

Oliveira, R. A., Heidmann, S., & Sunkel, C. E. (2007). Condensin I binds chromatin early in prophase and displays a highly dynamic association with Drosophila mitotic chromosomes. *Chromosoma, 116*(3), 259-274. doi:10.1007/s00412-007-0097-5

Ono, T., Fang, Y., Spector, D. L., & Hirano, T. (2004). Spatial and temporal regulation of Condensins I and II in mitotic chromosome assembly in human cells. *Mol Biol Cell, 15*(7), 3296-3308. doi:10.1091/mbc.E04-03-0242

Oshikawa, K., Matsumoto, M., Oyamada, K., & Nakayama, K. I. (2012). Proteome-wide identification of ubiquitylation sites by conjugation of engineered lysine-less ubiquitin. *J Proteome Res, 11*(2), 796-807. doi:10.1021/pr200668y

Pando, B., Dawson, S. P., Mak, D. O., & Pearson, J. E. (2006). Messages diffuse faster than messengers. *Proc Natl Acad Sci U S A, 103*(14), 5338-5342. doi:10.1073/pnas.0509576103

Pfau, S. J., & Amon, A. (2012). Chromosomal instability and aneuploidy in cancer: from yeast to man. *EMBO Rep, 13*(6), 515-527. doi:10.1038/embor.2012.65

Piskadlo, E., & Oliveira, R. A. (2016). Novel insights into mitotic chromosome condensation. *F1000Res, 5*. doi:10.12688/f1000research.8727.1

Povlsen, L. K., Beli, P., Wagner, S. A., Poulsen, S. L., Sylvestersen, K. B., Poulsen, J. W., Nielsen, M. L., Bekker-Jensen, S., Mailand, N., & Choudhary, C. (2012). Systems-wide analysis of ubiquitylation dynamics reveals a key role for PAF15 ubiquitylation in DNA-damage bypass. *Nat Cell Biol, 14*(10), 1089-1098. doi:10.1038/ncb2579

Pye, V. E., Beuron, F., Keetch, C. A., McKeown, C., Robinson, C. V., Meyer, H. H., Zhang, X., & Freemont, P. S. (2007). Structural insights into the p97-Ufd1-Npl4 complex. *Proc Natl Acad Sci U S A, 104*(2), 467-472. doi:10.1073/pnas.0603408104

Ramadan, K., Bruderer, R., Spiga, F. M., Popp, O., Baur, T., Gotta, M., & Meyer, H. H. (2007). Cdc48/p97 promotes reformation of the nucleus by extracting the kinase Aurora B from chromatin. *Nature, 450*(7173), 1258-1262. doi:10.1038/nature06388

Raman, M., Sergeev, M., Garnaas, M., Lydeard, J. R., Huttlin, E. L., Goessling, W., Shah, J. V., & Harper, J. W. (2015). Systematic proteomics of the VCP-UBXD adaptor network identifies a role for UBXN10 in regulating ciliogenesis. *Nat Cell Biol, 17*(10), 1356-1369. doi:10.1038/ncb3238

Robellet, X., Thattikota, Y., Wang, F., Wee, T. L., Pascariu, M., Shankar, S., Bonneil, E., Brown, C. M., & D'Amours, D. (2015). A high-sensitivity phospho-switch triggered by Cdk1 governs chromosome morphogenesis during cell division. *Genes Dev, 29*(4), 426-439. doi:10.1101/gad.253294.114

Seufert, W., Futcher, B., & Jentsch, S. (1995). Role of a ubiquitin-conjugating enzyme in degradation of S- and M-phase cyclins. *Nature, 373*(6509), 78-81. doi:10.1038/373078a0

Sharma, U., Stefanova, D., & Holmes, S. G. (2013). Histone variant H2A.Z functions in sister chromatid cohesion in Saccharomyces cerevisiae. *Mol Cell Biol, 33*(17), 3473-3481. doi:10.1128/MCB.00162-12

Sigaut, L., Pearson, J. E., Colman-Lerner, A., & Ponce Dawson, S. (2014). Messages do diffuse faster than messengers: reconciling disparate estimates of the morphogen bicoid diffusion coefficient. *PLoS Comput Biol, 10*(6), e1003629. doi:10.1371/journal.pcbi.1003629

Slaughter, B. D., Schwartz, J. W., & Li, R. (2007). Mapping dynamic protein interactions in MAP kinase signaling using live-cell fluorescence fluctuation spectroscopy and imaging. *Proc Natl Acad Sci U S A, 104*(51), 20320-20325. doi:10.1073/pnas.0710336105

St-Pierre, J., Douziech, M., Bazile, F., Pascariu, M., Bonneil, E., Sauve, V., Ratsima, H., & D'Amours, D. (2009). Polo kinase regulates mitotic chromosome condensation by hyperactivation of condensin DNA supercoiling activity. *Mol Cell, 34*(4), 416-426. doi:10.1016/j.molcel.2009.04.013

Swaney, D. L., Beltrao, P., Starita, L., Guo, A., Rush, J., Fields, S., Krogan, N. J., & Villen, J. (2013). Global analysis of phosphorylation and ubiquitylation cross-talk in protein degradation. *Nat Methods, 10*(7), 676-682. doi:10.1038/nmeth.2519

Takemoto, A., Kimura, K., Yokoyama, S., & Hanaoka, F. (2004). Cell cycle-dependent phosphorylation, nuclear localization, and activation of human condensin. *J Biol Chem, 279*(6), 4551-4559. doi:10.1074/jbc.M310925200

van Heemst, D., James, F., Poggeler, S., Berteaux-Lecellier, V., & Zickler, D. (1999). Spo76p is a conserved chromosome morphogenesis protein that links the mitotic and meiotic programs. *Cell, 98*(2), 261-271.

Wagner, S. A., Beli, P., Weinert, B. T., Nielsen, M. L., Cox, J., Mann, M., & Choudhary, C. (2011). A proteome-wide, quantitative survey of in vivo ubiquitylation sites reveals widespread regulatory roles. *Mol Cell Proteomics, 10*(10), M111 013284. doi:10.1074/mcp.M111.013284

Wang, B. D., Eyre, D., Basrai, M., Lichten, M., & Strunnikov, A. (2005). Condensin binding at distinct and specific chromosomal sites in the Saccharomyces cerevisiae genome. *Mol Cell Biol, 25*(16), 7216-7225. doi:10.1128/MCB.25.16.7216-7225.2005

Yeh, E., Haase, J., Paliulis, L. V., Joglekar, A., Bond, L., Bouck, D., Salmon, E. D., & Bloom, K. S. (2008). Pericentric chromatin is organized into an intramolecular loop in mitosis. *Curr Biol, 18*(2), 81-90. doi:10.1016/j.cub.2007.12.019

Yu, C. C., Yang, J. C., Chang, Y. C., Chuang, J. G., Lin, C. W., Wu, M. S., & Chow, L. P. (2013). VCP phosphorylation-dependent interaction partners prevent apoptosis in Helicobacter pylori-infected gastric epithelial cells. *PLoS One, 8*(1), e55724. doi:10.1371/journal.pone.0055724

Yu, H. G., & Koshland, D. (2005). Chromosome morphogenesis: condensin-dependent cohesin removal during meiosis. *Cell, 123*(3), 397-407. doi:10.1016/j.cell.2005.09.014

3.10 Supplemental materials and methods

3.10.1 Yeast strains, plasmids and growth conditions:

All yeast strains used in this study are derived from the W303/K699 background. Standard conditions were used to grow yeast (Gutherie, 1991). For the construction of deletion strains, a PCR-based method was used as described previously (Longtine et al., 1998). Cell synchronization in G1 (50 ng/ml of alpha factor for 180 min) at 23 °C; in metaphase (30 µg/ml of nocodazole for 150 min) at 23 °C, 32 °C and 37 °C were performed as described earlier (Robellet et al., 2015). Five-fold serial dilution was performed on solid media as described earlier (Ratsima et al., 2011). For overexpression of ubiquitin, cells were grown in synthetic media containing 2% galactose. For fluorescence correlation spectroscopy experiments, cells were grown in synthetic complete media.

For the construction of a ubiquitin overexpression plasmid (YEpFAT4-10His-UBI), a fragment encoding one copy of ubiquitin (*i.e.*, one repeat of 76 amino acids) with an N-terminal His-tag was subcloned into a YEp-based plasmid carrying a galactose-inducible promoter. The temperature sensitive allele *rvb2-119* was constructed by random mutagenesis (GeneMorph II Kit from Agilent).

3.10.2 Fluorescence *in situ* hybridization (FISH):

Fluorescence *in situ* hybridization was performed as described previously (Guacci et al., 1994; Lavoie et al., 2004; Robellet et al., 2015). For all experiments, cells were fixed (3.7% formaldehyde in 0.1M KPO_4 pH 6.4) for 2 hours at 23°C and then spheroplasted. For probe preparation, a rDNA sequence (~9.1 Kb) was amplified and labelled with digoxigenin using BioNick labeling system (Invitrogen). The rDNA probes were detected using a mouse anti-digoxigenin antibody (Boeheringer Manheim Biochemicals), FITC-conjugated goat anti-mouse (Jackson Immunoresearch Laboratories) and Alexa Fluor 488-conjugated swine anti-goat antibodies. All three antibodies were diluted in 10%

horse serum (1:250). Nucleus was counter-stained with propidium iodide (5 mg/ml; Sigma). For visualizing rDNA morphology, DeltaVision microscopy was used. Images were acquired using oil immersion 60x objective.

3.10.3 Chromatin spreads:

Chromatin spreads were performed as described previously (Grubb et al., 2015; Lavoie et al., 2002) with some modifications. Briefly, cells were washed in 1 ml solution-I (0.1M KPO_4 pH7.4, 0.5mM $MgCl_2$, 1.2M sorbitol) and were resuspended in solution-I with 1M DTT. Spheroplasting of cells was achieved by the addition of Zymolase (10mg/ml) and incubation at 30°C with gentle rotation. Subsequently, spheroplasted cells were centrifuged (2000 rpm/2min) at room temperature and resuspended in Solution-II (0.1M MES pH6.4, 0.5mM $MgCl_2$, 1mM EDTA, 1M sorbitol). Next, cells were added to the glass slide (Corning) and immediately were fixed and lysed by addition of a fixative solution (4% paraformaldehyde in 3.4% sucrose) and 1% NP-40 solution. Cells were spread using a plastic pipette rolled from one end of the slide to the other end. Slides with chromatin spreads were dried for overnight. Next day, slides were washed with 1x PBS for 10 min and blocked for 15 min with 10% BSA (Bovine serum albumin) in 1xPBS (Phosphate buffer solution). Chromatin spreads were incubated with mouse monoclonal anti-Myc 9E10 antibody (1:250; Genetex) for 2 hours and Alexa Fluor 488-conjugated goat anti-mouse antibody (1:250; Invitrogen) for 2 hours. Nuclei were counter-stained with DAPI (4',6-diamidino-2-phenylindole). Images were acquired using DeltaVision microscopy with an oil immersion 60x objective. Fluorescence intensity of Smc4 was measured using the ImageJ software.

3.10.4 Sister-chromatid cohesion assay:

Sister-chromatid cohesion was monitored using the tetO/tetR-GFP dot system, as described previously (D'Amours et al., 2004; Michaelis et al., 1997). Cells were synchronized in G1 with alpha factor and released into fresh media containing

nocodazole at 37 °C for 180 min. Cells were then fixed with 3.7% formaldehyde in 0.1M KPO_4 pH-7 for 10 min and centrifuged (2000rpm/2min) at room temperature. Later, cells were resuspended in 0.1M KPO_4 pH-7 and images were acquired using Zeiss LSM 700 Laser scanning microscope with oil immersion 63x objective.

3.10.5 Chromatin immunoprecipitation:

Chromatin immunoprecipitation (ChIP) by anti-Myc antibodies followed by qPCR analysis was carried as described before (Chatterjee et al., 2016; Villeneuve, 2015). For this, cells were cross-linked with 1% formaldehyde at room temperature for 15 min. Then the reaction was quenched by addition of 2.5 M glycine (final concentration 125 mM). Subsequently, the cells were lysed with glass beads containing lysis buffer (50mM HEPES KOH pH 7.5, 140mM NaCl, 1% Triton X-100, 0.1% Sodium deoxycholate, 1mM EDTA pH-8, 1mM AEBSF and protease inhibitors). The lysate was sonicated to get chromatin fragments of an average size of 300-500 bp using a Diagenode bioruptor (Thermo Scientific). Later, the sonicated lysate was centrifuged at 13000rpm/30 min/4 °C.

Input DNA: Approximately $1/10^{th}$ of lysate (for Input DNA) was diluted in TE buffer (10mM Tris-HCl, pH-8 and 1mM EDTA) with 1% SDS and incubated at 65°C overnight for reverse cross-linking. The lysate was incubated with TE buffer, RNase-A and Glycogen (10mg/ml) for 2 hours at 37 °C. Next, the lysate was treated with proteinase-K (20mg/ml) and incubated at 37 °C for 3 hours. The sample was extracted with an equal volume of phenol-chloroform-isoamyl alcohol (25:24:1). Input DNA was precipitated by addition of 5M NaCl (final concentration 200mM) and ice-cold 100% ethanol and centrifuge for 13000rpm/10 min/4 °C. The DNA pellet was washed with 70% alcohol, dried and resuspended in TE buffer.

Immunoprecipitated fraction (IP DNA): Dynabeads (Invitrogen) were incubated with anti-Myc 9E10 antibody (Genetex) at 4 °C for 2 hours. Antibody bound beads were washed with 1xPBS-BSA and incubated with remaining sonicated lysate at 4°C for

overnight. IP bound beads were recovered using magnetic stand system. These beads were sequentially washed with lysis buffer, lysis buffer containing NaCl (final concentration 360mM), LiCl wash buffer (10mM Tris-Cl pH-8, 250mM LiCl, 0.5% NP40, 0.5% Sodium dexoycholate, 1mM EDTA pH-8) and TE buffer. Finally, the beads were reverse cross-linked and processed as Input DNA to isolate IP DNA.

3.10.6 Quantitative PCR

The real time quantitative PCR (qPCR) was performed using iQ SyBr green mix (BioRad) on the iQ5 multi-colour real time PCR detection system (BioRad). The data was analysed by iQ5 software. The graph was plotted according to the fold enrichment method (Mukhopadhyay et al., 2008).

3.10.7 Immunoprecipitation:

Immunoprecipitation was carried as previously described (St-Pierre et al., 2009). Cell were synchronized in metaphase with nocodazole at 37°C for 150 min and were centrifuged (3000 rpm/10 min), resuspended in lysis buffer (50mM Tris-HCl pH-8, 150mM KCl, 100mM NaF, 10% glycerol, 0.1% tween-20, 1mM tungstate, 1mM DTT, 10µM AEBSF, 10µM pepstatin A, 10µM E-64). The lysate was incubated with anti-Myc 9E10 antibody (Genetex) and GammaBind Plus Sepharose beads (GE healthcare). Beads were washed five times with lysis buffer and resuspended in sample buffer for SDS-PAGE analysis.

3.10.8 Detection of ubiquitination:

In vivo detection of ubiquitination: Immunoprecipitation of epitope-tagged Ycs4 was performed as described above in the presence of 10mM N-ethyl-maleimide (Sigma). After SDS-PAGE, proteins were transferred onto nitrocellulose membrane. Denaturation of proteins on the membrane was performed as described earlier (Penengo et al., 2006).

The membrane was treated with denaturation buffer (6M Guanidine chloride, 20mM Tris-Cl pH-7.4, 5 µM beta mercaptoethanol, 1mM AEBSF) for 30 min at 4 °C. Subsequently, membrane was washed five times with Tris buffer saline (TBS) and blocked with 5% BSA in TBS and subjected to western blotting.

Overexpression of ubiquitin: Cells were washed in ice-cold water and incubated with 1.85 M NaOH and 7% beta-mercaptoethanol for 10min at room temperature with gentle rotation. Cells were then incubated with 50% TCA (Trichloro acetic acid) on ice for 10 min. After centrifugation (3000rpm/10min/4 ˚C), the protein pellet was washed with 70% acetone and air-dried. Proteins pellet was resuspended in denaturation buffer (8M Guanidine chloride, 10mM Tris-cl pH-8) containing 10mM N-ethyl-maleimide (Sigma) and incubated at 30˚C for 30 min. The lysate was separated by centrifugation (15000rpm/20min/4 ˚C) and incubated with Ni-NTA beads (Qiagen) at 4 ˚C for overnight on a rotator. Then, Ni-NTA beads were washed three times with wash buffer-I (8M Urea, 50mM NaHPO4, 10mM Tris-Cl pH-8, 20mM Imidazole) and two times with wash buffer-II (500mM NaCl, 10% Glycerol). Ni-NTA beads were then resuspended in sample buffer for SDS-PAGE analysis.

3.10.9 Western blotting:

Proteins extracts were electrophoresed using 8% SDS-PAGE or precast gels (Biorad) and gels were transferred by the iBlot system (Invitrogen). Following antibodies were used for immunoblotting: mouse monoclonal anti-Myc 9E-10 antibody (1:1000; Genetex), mouse monoclonal anti-FLAG antibody (1:1000; Sigma), mouse monoclonal anti-HA 12CA5 antibody (1:1000; Sigma), mouse monoclonal anti-HA 16B12 antibody (1:1000; BioLegend), mouse polyclonal anti-ubiquitin antibody (1:500; Millipore), mouse monoclonal anti-Pgk1 antibody (1:1000; Abcam), HRP conjugated anti-mouse IgG antibody (1:10000). Proteins were detected using ECL plus chemiluminescence kit (Perkin-Elmers). Anti-ubiquitin antibodies were prepared in 5% BSA and remaining all antibodies were prepared in 2% milk and 1% BSA.

3.10.10 Raster image correlation spectroscopy (RICS):

Principle: RICS is a variant of conventional Fluctuation Correlation Spectroscopy developed to extract molecular dynamics features at the subcellular level using space- and time- dependent fluctuations of fluorescence intensity in 2D confocal images (Brown et al., 2008). Briefly, the same field of view (FOV) is imaged multiple times using a fast scanning device and the space-dependent fluorescence correlations are averaged over multiple time frames with or without removal of the time-invariant contribution to the signal (immobile fluorescent elements), yielding information on molecular dynamics.

Sample preparation: Cells were grown at 23 °C and then shifted to 37 °C for 150 min. Cells were centrifuged (2000rpm/2min/room temperature) and resuspended in fresh media. Then cells were placed on pads made of circular coverslips (Fisher Scientific) topped with 70 µl of 2% low-melting agarose (Bio-Rad) prepared in synthetic media and incubated for 4min at room temperature for drying. Cells were then immobilized by placing another coverslip on top of the agarose pad, coated with 2mg/mL Concanavalin A (Sigma), and gripping the "sandwich" with a metallic nut and bolt system. Finally, the pads were transferred to a 37 °C incubator before imaging.

Image acquisition: Images were acquired using an ISS Alba scanning mirror FCS system coupled to a Nikon confocal microscope equipped with a 60x water objective, and to APD single-photon detectors. Fluorescent samples were excited with a 40MHz pulse-picked white laser (Fianium/NKT Photonics) through 488nm selective bandpass dichroic filters. 6.25µm*6.25µm FOVs were scanned at 256*256 pixel resolution, yielding a 48.8nm pixel size, with 20 microseconds (µs) dwell time on each pixel (duration of photon counting) and 50 frames per sample (Brown et al., 2008). With such a choice of parameters, the line scan time was 6.24ms (characteristic timescale of vertical correlations) and the frame scan time was about 1.60s. Excitation power was tuned to detect 1-8 photons per pixel per frame (depending on samples), maximizing the capture of intensity fluctuations. Each agarose pad was imaged at 6-10 different FOVs (1-2 metaphase cells per FOV, 20-30 min total acquisition time) at room temperature before being stored again at 37°C for further imaging 40min-1h later. Images were saved as time stacked TIFF files.

Raw data analysis: Analysis of the raw stacks was performed using the commercially available software SimFCS (http://www.lfd.uci.edu/globals) as follows: For each sample, the contribution of fluorescent elements that are immobile over very large timescales (tens of seconds) was subtracted by removing, on each image, the 10 timeframes running average. This step allowed filtering out auto-fluorescent bright spots/blobs that are sometimes visible under these imaging conditions in yeast. Then, RICS correlations were computed on the background-filtered image, and correlations along both the horizontal and vertical lines of the 2D-RICS function were fitted with a simple free diffusion model in SimFCS with pixel size and dwell time, line/frame scan times, and actual size of the Point Spread Function (PSF) were fixed prior to fitting, yielding the zero-shift correlation G0 and the effective diffusion coefficient D as the only remaining fitting parameters (see Fig S2). Specifically, G0 was inferred from horizontal correlations and was fixed before fitting vertical correlations to get the effective diffusion coefficient. Note that the PSF size was computed before each experiment by fitting FCS data acquired on a 1.2nM Rhodamine110 solution with conventional FCS formulas in the ISS Alba software. The goodness of fit was visually checked and cells for which either horizontal of vertical correlations could not be fitted accurately were removed from further analysis.

3.11 Supplemental figures and legends:

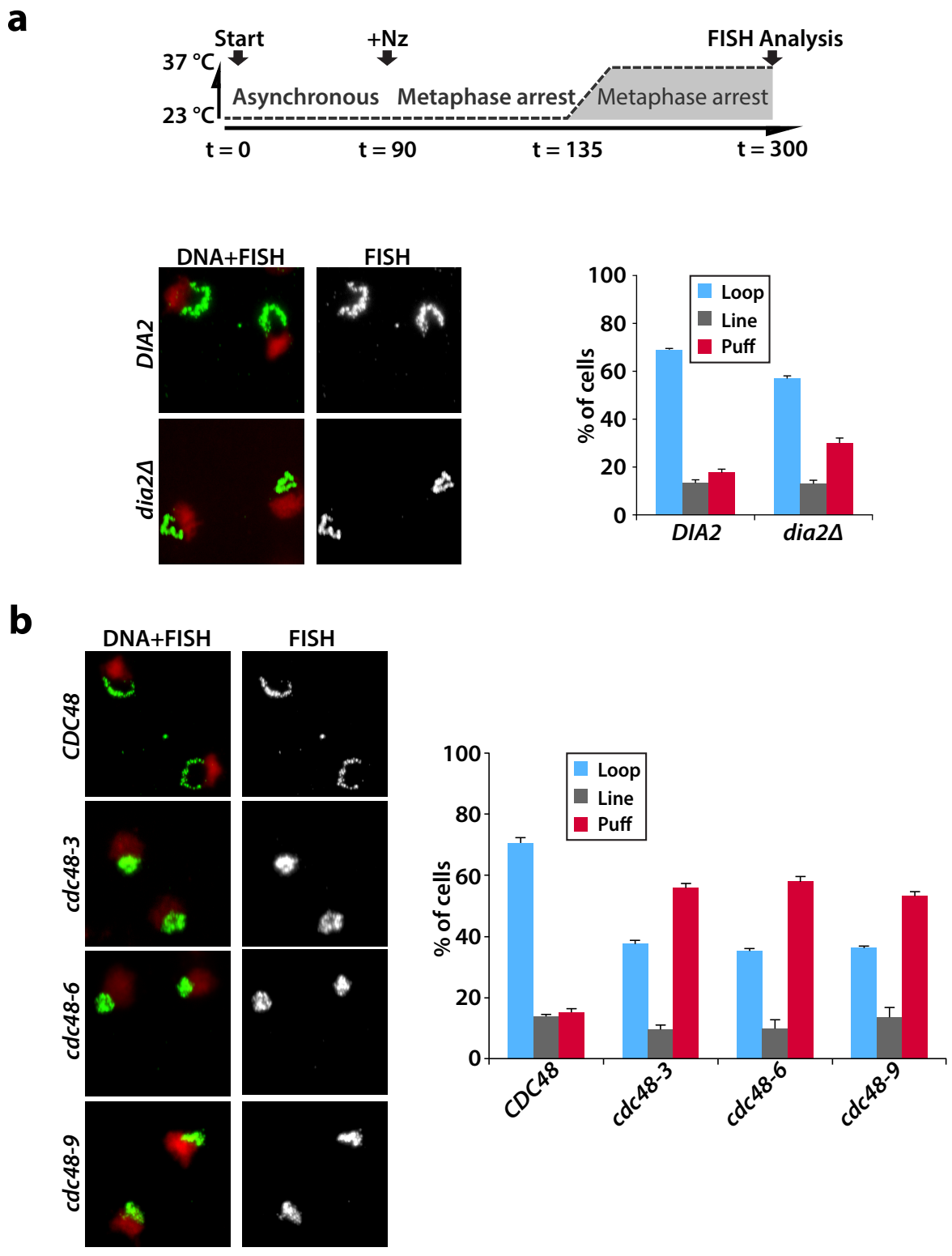

Figure S1: **a.** The chromosome condensation process is not dependent on Dia2. **b.** The chromosome condensation defects of *cdc48* mutants do not depend on S-phase events. **a-b.** Cells were arrested metaphase at 23°C for 45 min and shifted to 37 °C and continue to synchronize at metaphase with nocodazole treatment for 120 min and proceeded for FISH analysis. Nucleus and rDNA were labelled with PI (red) and FITC (green) respectively. The micrographs on the left represent the most relevant rDNA morphology observed in each mutant, whereas the graph on the right shows the quantification of the results. At least 100 cells were counted for each genotype.

a

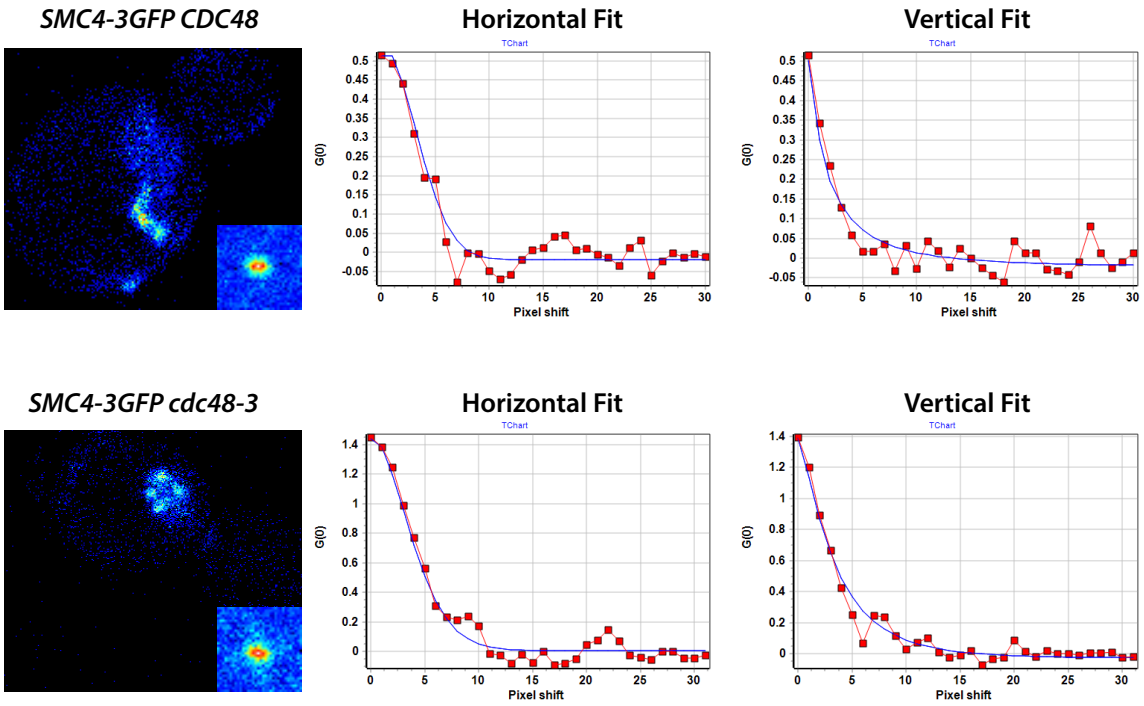

Figure S2. a. Left: Typical RICS individual frame for Smc4-3GFP in *CDC48* (top) and *cdc48-3* (bottom) cells in metaphase. The color map represents the number of individual photons counted from each pixel for this frame (dark blue: 1 photon, to red: 7-10 photons). Inset: Color-coded two-dimensional RICS autocorrelation function for the same cell. Middle, right: spatial auto-correlation as a function of the pixel shift along the horizontal (middle - µs tmescale) and vertical (right - ms timescale) axes, in *CDC48* (top) and *cdc48-3* (bottom) cells shown on the left panel. Red squares and line represent the raw data, while the least squares fit from which the diffusion coefficient is computed is shown in blue

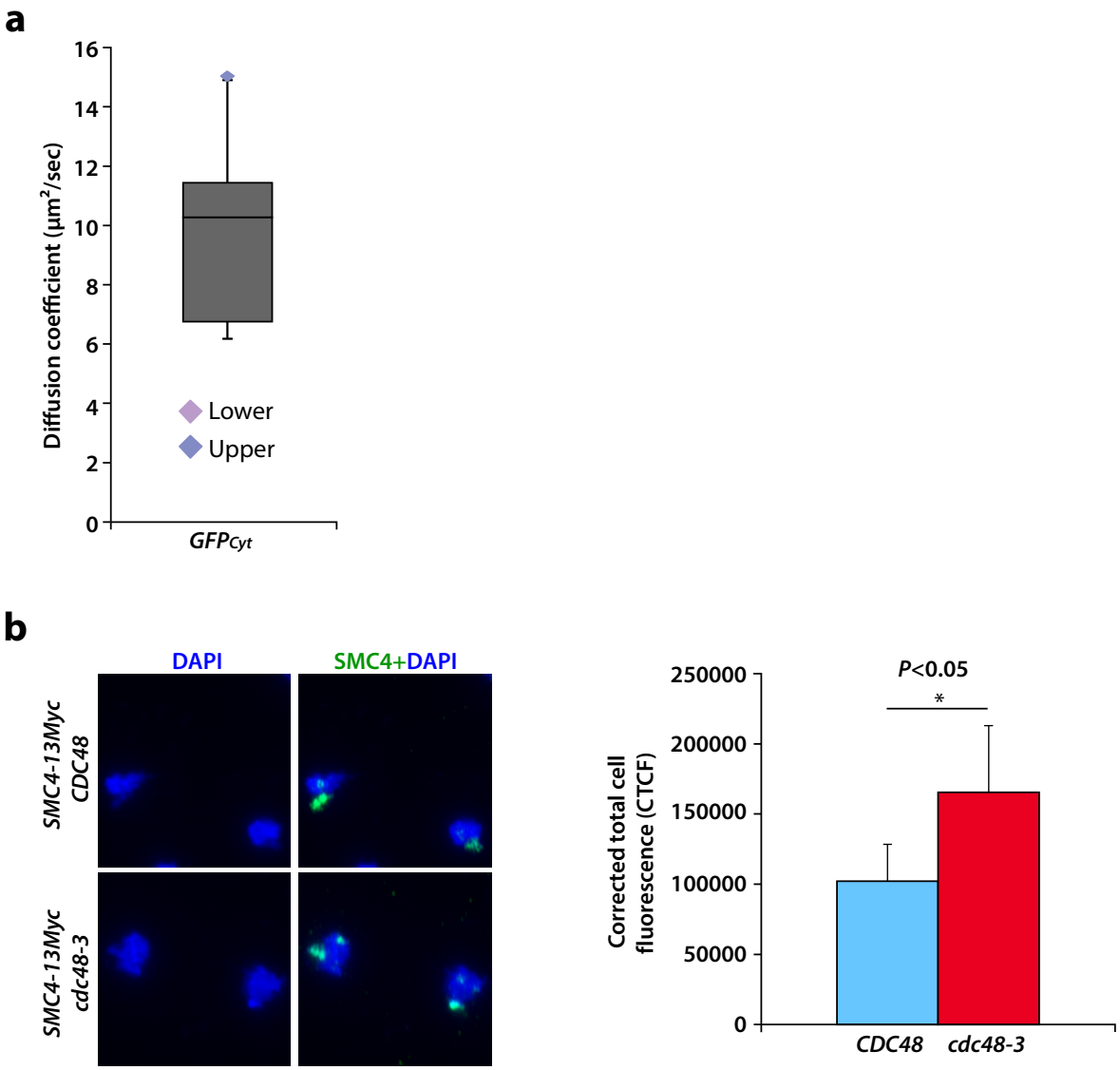
a
Diffusion coefficient (μm²/sec)
16
14
12
10
8
6
4
2
0
Lower
Upper
GFPCyt
b
DAPI
SMC4+DAPI
SMC4-13Myc CDC48
SMC4-13Myc cdc48-3
P<0.05
*
Corrected total cell fluorescence (CTCF)
250000
200000
150000
100000
50000
0
CDC48
cdc48-3

Figure S3. a. Box and whisker plots showing the distribution of fitted cytosolic diffusion coefficient over >35 wild-type metaphase cells expressing P_{BZZ1}-*GFP*. Box and whiskers were defined as in Figure 6. **b.** Chromatin spreads of Myc-tagged Smc4. Fluorescence intensity of Smc4 is increased in *cdc48-3* mutant compared to wild-type cells. Cells were synchronized in G1 and released into medium containing nocodazole to block at metaphase for 150 min. Cells were spheroplasted and processed for chromatin spread analysis. The micrographs on the left represent typical chromatin spreads whereas the graph on the right represents a quantification of fluorescence intensity. Nuclei were stained by 4',6-diamidino-2-phenylindole (DAPI-blue) and Smc4 was labelled with FITC (green). At least 100 cells were processed for each experiment (n=4; $p>0.05$; and error bars are represented in standard error to mean).

Table S1. Ubiquitylation sites in the subunits of human condensins. Data is from the mUbiSiDa database.

Complex	SMC2	SMC4	NCAPH	NCAPD2	NCAPG
Condensin I	K12 K68 K677 K1025 K1160	K202 K207 K389 K413 K607 K1187 K1112 K1267 K1273 K1280 K1285	K41 K126 K142 K359 K484 K495	K35 K78 K148 K298 K452 K517 K580 K616 K685 K705 K749 K785 K855 K962 K969 K1065 K1201 K1288 K1301	K142 K262 K522 K537 K690 K852 K899
	SMC2	SMC4	NCAPH2	NCAPD3	NCAPG2
Condensin II	K12 K68 K677 K1025	K202 K207 K389 K413	K92	K1246 K1258	K159 K164 K332 K422 K474 K601 K641 K650 K660 K796 K809 K871 K940 K1025

Table S2: Yeast strains used in this study

Figure	Strain number	Relevant genotype
Fig 1b	D4107	*MATa*
	D4988	*MATx sth1-1*
	D5980	*MATa snf5::HIS3MX6*
	D5555	*MATa chd1::TRP1*
	D5557	*MATa isw1::ADE2 isw2::LEU2*
	D5739	*MATa esa1-L327S::URA3MX6*
	D5674	*MATa ino80[1-300Δ]::TRP1*
	D5431	*MATa rvb2-119::HIS3MX6*
	D5676	*MATa swr1::URA3MX6*
	D93	*MATa cdc48-3*
Fig 2a	D4107	*MATa*
	D93	*MATa cdc48-3*
	D4804	*MATa cdc48-6*
	D5855	*MATa cdc48-9::3FLAG::URA3MX6*
Fig 2b	D4107	*MATa*
	D4457	*MATa npl4-1*
	D5443	*MATa otu1::URA3MX6*
	D5974	*MATa shp1-24::HIS3MX6*
	D5845	*MATa ubx2::HIS3MX6*
	D5445	*MATa ubx3::URA3MX6*
	D5847	*MATa ubx4::URA3MX6*
	D5849	*MATa ubx5::HIS3MX6*
	D5851	*MATa ubx6::HIS3MX6*

	D5853	*MATa ubx7::HIS3MX6*
	D4455	*MATa ufd1-2*
	D4460	*MATa ufd2::HIS3MX6*
	D4462	*MATa ufd3::HIS3MX6*
	D5916	*MATa vms1::HIS3MX6*
	D5381	*MATa wss1::URA3MX6*
Fig 3a	D4107	*MATa*
	D141	*MATa ipl1-2*
	D1015	*MATa ipl1-85::HIS3MX6*
Fig 3b	D4107	*MATa*
	D141	*MATa ipl1-2*
	D1015	*MATa ipl1-85::HIS3MX6*
	D6166	*MATa ipl1-321*
Fig 3c	D299	*MATa leu2-3, 112::Pura3:tetR:GFP::LEU2 CENIV::teto448::URA3*
	D6224	*MATa leu2-3, 112::Pura3:tetR:GFP::LEU2 CENIV::teto448::URA3 mcd1-1*
	D6154	*MATa leu2-3, 112::Pura3:tetR:GFP::LEU2 CENIV::teto448::URA3 cdc48-3*
	D331	*MATa leu2-3, 112::Pura3:tetR:GFP::LEU2 RDN1::teto112::URA3*
	D338	*MATa leu2-3, 112::Pura3:tetR:GFP::LEU2 RDN1::teto112::URA3 mcd1-1*
	D6156	*MATa leu2-3, 112::Pura3:tetR:GFP::LEU2 RDN1::teto112::URA3 cdc48-3*
Fig 4a	D4138	*MATa ura3-1::Pgal-SIC::HA::URA3 uba1::kanMx6 pRS313-UBA1::HIS3*

	D4139	*MATa ura3-1::Pgal-SIC::HA::URA3 uba1::kanMx6 pRS313-uba1-204::HIS3*
Fig 4b	D4107	*MATa*
	D369	*MATa ubc9-1*
Fig 4c	D5863	*MATa YepFAT-Pgal10::10His-Ub*
	D6111	*MATa YepFAT::Pgal10-1 Brn1::6HA::HIS3*
	D6113	*MATa YepFAT::Pgal10-1::10His-Ub Brn1::6HA::HIS3*
Fig 4d	D4107	*MATa*
	D268	*MATa YCS4::13Myc::kanMX6*
	D5823	*MATa YCS4::13Myc::kanMX6 cdc48-3*
Fig 5a	D5830	*MATa SMC2::3HA-12His::leu2*
	D5831	*MATa SMC2::3HA-12His::leu2 cdc48-3*
	D3749	*MATa SMC4::13Myc::HIS3MX6*
	D4476	*MATa SMC4::13Myc::HIS3MX6 cdc48-3*
	D5825	*MATa BRN1:: 3HA-12His::URA3*
	D5826	*MATa BRN1:: 3HA-12His::URA3 cdc48-3*
	D268	*MATa YCS4::13Myc::kanMX6*
	D5823	*MATa YCS4::13Myc::kanMX6 cdc48-3*
	D5828	*MATa YCG1::3FLAG::kanMX6*
	D5829	*MATa YCG1::3FLAG::kanMX6 cdc48-3*
Fig 5b	D4107	*MATa*
	D268	*MATa YCS4::13Myc::kanMX6*
	D4400	*MATa YCS4::13Myc::kanMX6 cdc48-3::3FLAG::URA3MX6*
	D5932	*MATa YCS4::13Myc::kanMX6 cdc48-3::3FLAG::URA3MX6*
Fig 6a	D6158	*MATa SMC4::3GFP::kanMX6*
	D5330	*MATa SMC4::3GFP::kanMX6 cdc48-3*

	D3987	*MATa Pbzz1-GFP::Tadh1::kanMX6::bzz1*
	D6249	*MATa ura3-1::NLS-3GFP::kanMX6::URA3*
	D6251	*MATa ura3-1::NLS-3GFP::kanMX6::URA3*
Fig 6b	D6158	*MATa SMC4::3GFP::kanMX6*
	D5330	*MATa SMC4::3GFP::kanMX6 cdc48-3*
Fig 6c	D6249	*MATa ura3-1::NLS-3GFP::kanMX6::URA3*
	D6251	*MATa ura3-1::NLS-3GFP::kanMX6::URA3*
Fig 6d	D4107	*MATa*
	D3749	*MATa SMC4::13Myc::HIS3MX6*
	D4476	*MATa SMC4::13Myc::HIS3MX6 cdc48-3*
Fig S1a	D4107	*MATa*
	D93	*MATa cdc48-3*
	D4804	*MATa cdc48-6*
	D5855	*MATa cdc48-9::3FLAG::URA3MX6*
Fig S1b	D4107	*MATa*
	D6247	*MATa dia2::HIS3MX6*
Fig S2a	D6158	*MATa SMC4::3GFP::kanMX6*
	D5330	*MATa SMC4::3GFP::kanMX6 cdc48-3*
Fig S3a	D3987	*MATa Pbzz1-GFP::Tadh1::kanMX6::bzz1*
Fig S3b	D3749	*MATa SMC4::13myc::HIS3MX6*
	D4476	*MATa SMC4::13myc::HIS3MX6 cdc48-3*

3.12 References:

Brown, C. M., Dalal, R. B., Hebert, B., Digman, M. A., Horwitz, A. R., & Gratton, E. (2008). Raster image correlation spectroscopy (RICS) for measuring fast protein dynamics and concentrations with a commercial laser scanning confocal microscope. *J Microsc, 229*(Pt 1), 78-91. doi:10.1111/j.1365-2818.2007.01871.x

Chatterjee, G., Sankaranarayanan, S. R., Guin, K., Thattikota, Y., Padmanabhan, S., Siddharthan, R., & Sanyal, K. (2016). Repeat-Associated Fission Yeast-Like Regional Centromeres in the Ascomycetous Budding Yeast Candida tropicalis. *PLoS Genet, 12*(2), e1005839. doi:10.1371/journal.pgen.1005839

D'Amours, D., Stegmeier, F., & Amon, A. (2004). Cdc14 and condensin control the dissolution of cohesin-independent chromosome linkages at repeated DNA. *Cell, 117*(4), 455-469.

Grubb, J., Brown, M. S., & Bishop, D. K. (2015). Surface Spreading and Immunostaining of Yeast Chromosomes. *J Vis Exp*(102), e53081. doi:10.3791/53081

Guacci, V., Hogan, E., & Koshland, D. (1994). Chromosome condensation and sister chromatid pairing in budding yeast. *J Cell Biol, 125*(3), 517-530.

Gutherie, G. R. F. a. C. (1991). Guide to yeast Genetics and Molecular Biology. *Acedemic Press, San Diego*.

Lavoie, B. D., Hogan, E., & Koshland, D. (2002). In vivo dissection of the chromosome condensation machinery: reversibility of condensation distinguishes contributions of condensin and cohesin. *J Cell Biol, 156*(5), 805-815. doi:10.1083/jcb.200109056

Lavoie, B. D., Hogan, E., & Koshland, D. (2004). In vivo requirements for rDNA chromosome condensation reveal two cell-cycle-regulated pathways for mitotic chromosome folding. *Genes Dev, 18*(1), 76-87. doi:10.1101/gad.1150404

Longtine, M. S., McKenzie, A., 3rd, Demarini, D. J., Shah, N. G., Wach, A., Brachat, A., Philippsen, P., & Pringle, J. R. (1998). Additional modules for versatile and economical PCR-based gene deletion and modification in Saccharomyces cerevisiae. *Yeast, 14*(10), 953-961. doi:10.1002/(SICI)1097-0061(199807)14:10<953::AID-YEA293>3.0.CO;2-U

Michaelis, C., Ciosk, R., & Nasmyth, K. (1997). Cohesins: chromosomal proteins that prevent premature separation of sister chromatids. *Cell, 91*(1), 35-45.

Mukhopadhyay, A., Deplancke, B., Walhout, A. J., & Tissenbaum, H. A. (2008). Chromatin immunoprecipitation (ChIP) coupled to detection by quantitative real-time PCR to study transcription factor binding to DNA in Caenorhabditis elegans. *Nat Protoc, 3*(4), 698-709. doi:10.1038/nprot.2008.38

Penengo, L., Mapelli, M., Murachelli, A. G., Confalonieri, S., Magri, L., Musacchio, A., Di Fiore, P. P., Polo, S., & Schneider, T. R. (2006). Crystal structure of the ubiquitin binding domains of rabex-5 reveals two modes of interaction with ubiquitin. *Cell, 124*(6), 1183-1195. doi:10.1016/j.cell.2006.02.020

Ratsima, H., Ladouceur, A. M., Pascariu, M., Sauve, V., Salloum, Z., Maddox, P. S., & D'Amours, D. (2011). Independent modulation of the kinase and polo-box activities of Cdc5 protein unravels unique roles in the maintenance of genome stability. *Proc Natl Acad Sci U S A, 108*(43), E914-923. doi:10.1073/pnas.1106448108

Robellet, X., Thattikota, Y., Wang, F., Wee, T. L., Pascariu, M., Shankar, S., Bonneil, E., Brown, C. M., & D'Amours, D. (2015). A high-sensitivity phospho-switch triggered by Cdk1 governs chromosome morphogenesis during cell division. *Genes Dev, 29*(4), 426-439. doi:10.1101/gad.253294.114

St-Pierre, J., Douziech, M., Bazile, F., Pascariu, M., Bonneil, E., Sauve, V., Ratsima, H., & D'Amours, D. (2009). Polo kinase regulates mitotic chromosome condensation by hyperactivation of condensin DNA supercoiling activity. *Mol Cell, 34*(4), 416-426. doi:10.1016/j.molcel.2009.04.013

Villeneuve, V. (2015). *Homéostasie des histones en réponse au dommage à l'ADN et étude d'inhibiteurs de désacétylases d'importance clinique.* (PhD), University de Montreal, Montreal.

Chapter IV: Discussion:

During cell division, the ultimate goal of a cell is to segregate the genome equally into two daughter cells. One of the early cytologically visible step during cell division is the condensation of chromosomes. It is a vital process required for sister chromatid separation during cell division and for maintaining the structural integrity of the chromatin. Chromosome condensation involves removing the tangles between different chromosomes after replication, the compaction of interphase chromatin and maintaining proper rigidity and flexibility of sister chromatids. Several models were proposed to explain this highly essential process, including the hierarchical model, loops on a scaffold model and the chromatin network model (Maeshima & Eltsov, 2008; Swedlow & Hirano, 2003). One of the key players involved in mediating the chromosome condensation process is the condensin complex. Any erroneous events in this process may lead to aneuploidy and cancer. In consistence with this, it is well recognized that condensin subunits are either over-expressed or mutated in many cancers (De Keersmaecker et al., 2014; Ham et al., 2007; Zhang et al., 2016; Zhou et al., 2012). Condensin requirement in chromosome condensation is well established. However, the molecular mechanism underlying the compaction of interphase chromatin into mitotic chromosomes remains an enigma in the field.

Condensin's role in mitotic chromosomes is well established from experiments in *Xenopus* egg extracts (Hirano & Mitchison, 1994). Since then, many studies further emphasized its different functions such as inducing positive supercoils in DNA, removing catenates, ATPase activity to compact the chromosomes (Hirano 2016). Besides, several studies focused on condensin regulation by different kinases (Bazile et al., 2010; Hirano, 2012). But most of these studies were carried under *in vitro* conditions and activation of condensin by kinases do not completely explain how condensin achieve this compaction process during mitosis.

One such important question is how mitotic chromosome condensation is

initiated and how it is achieved during metaphase. Earlier studies have shown that Cdk1 phosphorylation of condensin complex is required for its transportation from cytoplasm to nucleus (Bazile et al., 2010; Hirano, 2012, 2016) but it does not explain how chromosome condensation is activated during early mitosis. Especially, the lack of mutants that show intermediate stages of chromosome compaction makes it difficult to know how the condensin complex mediates the activation of compaction.

Here, in my thesis, I try to answer some of these important questions about how the condensin complex triggers the chromosome condensation process during early mitosis and any further consequences of this activation. We hypothesized that Cdk1 phosphorylates condensin and initiates the chromosome condensation process during early mitosis. The presence of many substrates for Cdk1 during mitosis makes it difficult to define it's precise role in activating chromosome condensation.

4.1 Identification of an intermediate stage during chromosome condensation:

In budding yeast, chromosome condensation is studied mostly using the rDNA locus, taking advantage of its visible morphological changes from uncondesed state (puff) to condensed state (loop) (Guacci et al., 1994; Lavoie et al., 2004). Here, in my thesis, we determined for the first time that Cdk1 is important for chromosome condensation in budding yeast. Altering Cdk1 levels using *clb2-t*s mutant, we identified a twisted thread like phenotype at the rDNA locus, an important intermediate stage previously not described in the chromosome condensation process. We termed this intermediate stage "intertwist" and found that it is stabilized at low temperature (at 16°C) in wildtype cells suggesting that it is not merely a consequence of mutant phenotype. We determined that formation of intertwist is also dependent on cohesion.

A subunit of condensin was previously identified as a target for Cdk1 in *S. pombe* and vertebrates. Interestingly, our studies in budding yeast revealed Smc4 as the key substrate for Cdk1 in condensin complex and, most prominently, we observed seven

Cdk1 consensus phosphosites (S/T-P) clustered in the N-terminal region of Smc4. We also identified many of these sites by mass spectrometry. Chromosome condensation defects observed in *smc4* phospho-mutant further established Smc4 as the potential substrate for Cdk1. Our analysis showed that constitutive Smc4 phosphorylation is lethal and 3-4 phospho-sites are enough to mediate chromosome condensation. We further showed that constitutive phosphorylation creates a dominant negative phenotype leading to impairment in the phosphorylation-dephosphorylation cycles. Additionally, we identified PP2A as a major phosphatase important for regulating chromosome condensation during mitosis. These results emphasize that phosphorylation of Smc4 at its N-terminal extension by Cdk1 is indispensable for condensin activation.

4.2 Cdk1 phosphorylation is important for condensin dynamic binding onto chromatin:

Recent models on condensin function propose that the condensin complex first binds on chromatin followed by the ATP hydrolysis, which promotes the opening of arms. Subsequently, head to head interaction between different condensin molecules either assemble a DNA-condensin network or forms a chiral loop structure which trap the condensin complex on the chromatin (Hirano, 2006). These models suggest that condensin binding onto chromatin might be stable. However, this is not the case as recent studies point out to a dynamic mode of condensin binding to chromatin rather than a stable binding (Gerlich et al., 2006). In our studies (Chapter II) we anticipated Smc4 phosphorylation might regulate condensin binding to chromatin in a dynamic manner. Concomitantly, our results supported this idea of Cdk1 phosphorylation of condensin is as an important step for its dynamic binding onto chromatin during mitosis. The abrogation of this dynamic binding of condensin to chromatin in *smc4* phospho-mutant further confirms our hypothesis.

Our study for the first time presented how chromosome condensation is initiated during early mitosis and also revealed a novel pathway where Cdk1 promotes condensin

dynamic binding to chromatin to facilitate proper chromosome condensation during mitosis. The above findings suggest that condensin undergoes repeated cycles of binding and release from chromatin to mediate proper chromatin compaction. It is intriguing to predict as how condensin can be extracted from compacted chromatin generated by its own reaction. We think that phosphorylation alone cannot regulate both loading and unloading of condensin from compacted environment. Previous studies have shown that various factors such as Scc2-4, TFIIIC and Monopolin regulate condensin loading onto chromatin (D'Ambrosio et al., 2008; Johzuka & Horiuchi, 2009). However, condensin removal from the chromatin during this repeated cycles of dynamic binding are not well established yet. Thus, we speculated the existence of other chromatin factors or regulators, which might assist condensin unloading from chromatin as any unwanted accumulation of condensin on chromatin might lead to lethal consequences. This prompted us to study the factors required to regulate condensin mobility on chromatin during mitosis (in chapter III).

To address this, we carried out a candidate-based screen to identify factors that regulate condensin mobility on chromatin. We screened known chromatin regulators such as chromatin remodelers and molecular chaperons. Our analysis identified Cdc48, Esa1, Rvb2/Reptin and Swr1 complex as important regulators of chromosome condensation. Primarily, we focused our study on Cdc48 because of its role as segregase in the removal of chromatin bound proteins (Franz et al., 2016; Jentsch & Rumpf, 2007; Meyer & Weihl, 2014). This observation of condensation defects was further confirmed using other *cdc48* mutant alleles. We also excluded other mechanisms such as sister chromatid cohesion or regulators (Ipl1) as the cause for these defects in *cdc48* mutant, thus validating the role of Cdc48 in chromosome condensation. Previous studies in yeast have shown that Cdc48 is important for the removal of CMG helicase at the end of DNA replication (Maric et al., 2014) and interestingly, CMG helicase components were stabilized under Cdc48 depletion during S-phase. Therefore, this raises an important question whether the condensation defects observed in *cdc48* mutant are due to incomplete DNA replication, as this is an important step before chromosome

condensation in early mitosis (Dulev et al., 2008). Nevertheless, this is not the case as DNA replication is completed in *cdc48* depleted cells (Maric et al., 2014). Our findings confirm that the observed condensation defects in *cdc48* mutant are not due to improper DNA replication (chapter III; Figure S1b), therefore suggesting these defects are specific to disruption in chromosome condensation process.

4.3 Cdc48 regulates dynamic binding of condensin complex to facilitate proper chromosome condensation:

Cdc48 was initially identified in yeast as factor required for cell cycle progression (Moir et al., 1982). Cdc48 has been implicated in many cellular activities (Franz et al., 2016; Jentsch & Rumpf, 2007; Meyer & Weihl, 2014). This AAA-ATPase usually recognizes ubiquitylated or SUMOylated substrates and processes them with the help of a specific cofactor via proteasome dependent or independent mechanisms. Here, in our study (chapter III) we focused on exploring this pathway of how Cdc48 might extract the condensin from chromatin to regulate condensation process.

Cdc48 has several cofactors such as substrate recruiting and substrate processing and each cellular process has specific cofactor(s) associated with Cdc48 (Jentsch & Rumpf, 2007). Our analysis identified Ufd1-Npl4 complex as the cofactor required for chromosome condensation and a recent study showed that Ufd1 forms heterodimer with Npl4 in yeast (Pye et al., 2007). It is also interesting to note that Ufd1-Npl1 dimer is a cofactor for many cell cycle events regulated by Cdc48 (Franz et al., 2016; Jentsch & Rumpf, 2007; Meyer & Weihl, 2014). Our study identified that the process of chromosome condensation is ubiquitin dependent and, interestingly, we also observed condensation defects to a lesser extent in *ufd3* deletion mutant, which is another cofactor for Cdc48 (Chapter III-Figure 2b). This could be due to the previously reported low ubiquitin pool in *ufd3* deletion mutant (Mullally et al., 2006) and further supports our results that ubiquitin depletion leads to condensation defects. Previous studies show that condensin subunits undergo ubiquitylation (Kim et al., 2011; Oshikawa et al., 2012;

Povlsen et al., 2012; Swaney et al., 2013; Wagner et al., 2011) and consistent with this, our study identified two non-SMC subunits: Brn1 and Ycs4 undergoes ubiquitylation *in vivo*. But it is also likely possible that other subunits of condensin might be ubiquitylated *in vivo*.

Ubiquitylation is an important posttranslational modification of proteins, which is carried out by a set of conserved enzymes: E1 (activating), E2 (conjugating) and E3 (ligase). These modifications regulate proteins via proteolytic or non-proteolytic mechanisms (Finley et al., 2012; Kerscher et al., 2006). However, we do not know the E2 or E3 enzymes that catalyze the condensin ubiquitylation at this time. Earlier report in *Drosophila* showed SCF-mediated ubiquitin dependent degradation of CAP-H2 subunit in condensin II to maintain interphase chromatin (Buster et al., 2013). Instead, our studies pointed out that Cdc48 regulates the ubiquitylated condensin via proteasome independent mechanism.

Cdc48 removes many chromatin bound substrates via its segregase activity in various processes such as DNA replication, DNA repair or at the end of mitosis (Franz et al., 2016; Meyer & Weihl, 2014). Our study showed that kinetics of condensin mobility is slower in *cdc48* mutant resulting in enrichment of condensin on chromatin. Interestingly, we observed that ubiquitylated Ycs4 is stabilized in *cdc48* mutant compared to wildtype. These data further confirm that condensin is extracted from chromatin network by Cdc48-Ufd1-Npl4 in an ubiquitin dependent and proteasome independent manner.

In yeast, condensin is always localized in the nucleus and from this thesis (chapter III) it is now evident that Cdc48 removes condensin from chromatin during mitosis to facilitate chromosome condensation. During the process of cell division, any perturbations in the DNA due to external or internal factors lead to the activation of damage and repair pathways. To enable the repair mechanisms, the chromatin bound proteins must undergo disassembly (Linger & Tyler, 2007) and it is interesting to speculate if Cdc48, in such scenario, might play a similar role in extracting condensin

from damaged DNA prior to the loading of repair proteins.

4.4 Conclusions and future perspectives:

Our study was initially carried out to understand how chromosome condensation is initiated in early mitosis. These studies lead us to identify novel mechanisms involved in the regulation of chromosome condensation during mitosis. In chapter II, we demonstrated the Cdk1-dependent chromosome condensation activation in early mitosis. This study further led us to identify the dynamic behavior of condensin in budding yeast. In chapter III, we have determined the consequences of dynamic binding of condensin onto chromatin and demonstrated the Cdc48-dependent condensin extraction from chromatin that facilitates the chromosome compaction during mitosis. The study also identified new players involved in the regulation of chromosome condensation process. Mutations in condensin subunits are known in many cancers and neurodevelopmental diseases like microcephaly. Understanding the regulation of condensin complex functions is important to identify the pathology of these diseases.

In the chapter II, we identified that Cdk1 phosphorylates Smc4 during mitosis and most phosphosites are present on its N-terminal extension. It will be interesting to study if this N-terminal extension can act as scaffold for other proteins to interact with condensin complex. Also, it will be important to understand whether condensin is a target of other important kinases like CKII (casein kinase) as CKII was previously shown to negatively regulating condensin complex.

Finally, a genetic screen I analyzed in chapter III identified three new regulators of chromosome condensation apart from Cdc48. It would be interesting to understand whether these new effectors of chromosome morphology have any direct role in regulating chromosome condensation or condensin complex function. NuA4 and Swr1 complexes have a role in sister chromatid cohesion, so the condensation defects observed here might be an apparent consequence of cohesion defects. But, we cannot

rule out completely their direct role in chromosome condensation. Especially, Esa1 is a subunit of NuA4, a histone acetyl transferase (HAT) complex that also has many non-histone substrates (Lee & Workman, 2007; Lin et al., 2009). Hence, there is a possibility that condensin complex can be a target of this acetyl transferase. Previously it has been shown that condensin is acetylated and it is important for its loading onto chromatin (Choudhary et al., 2009). Interestingly, NuA4 and SAGA complexes were previously shown to be implicated in condensin binding onto chromatin in *S. pombe* (Tanaka et al., 2012; Toselli-Mollereau et al., 2016).

Another attractive candidate in our screen was Rvb2/Reptin. This is AAA+ type ATPase and found in both INO80 and SWR complexes (Nano & Houry, 2013). Our analysis shows condensation defects with *swr1* deletion mutant, which suggests that the defects in Rvb2 are most likely due to SWR complex function. Rvb2/Reptin has been associated with regulating several processes like spindle assembly, chromatin remodeling, telomerase function (Nano & Houry, 2013). Also, recent studies on *C. elegans* and *Xenopus* demonstrated Rvb2 role in chromatin decondensation at the end of mitosis (Magalska et al., 2014). Further, it will be interesting to understand if Rvb2 has any direct role in chromosome condensation in yeast.

My thesis addressed several key questions in the chromosome condensation field but also at same time unraveled a new set of questions, which need to be answered for a better understanding of chromosome condensation process. This knowledge will allow us to identify possible new therapeutic targets, as well as the development of novel strategies to fight cancer.

Bibliography:

Abe, S., Nagasaka, K., Hirayama, Y., Kozuka-Hata, H., Oyama, M., Aoyagi, Y., Obuse, C., & Hirota, T. (2011). The initial phase of chromosome condensation requires Cdk1-mediated phosphorylation of the CAP-D3 subunit of condensin II. *Genes Dev, 25*(8), 863-874. doi:10.1101/gad.2016411

Amon, A. (1999). The spindle checkpoint. *Curr Opin Genet Dev, 9*(1), 69-75.

Anderson, D. E., Losada, A., Erickson, H. P., & Hirano, T. (2002). Condensin and cohesin display different arm conformations with characteristic hinge angles. *J Cell Biol, 156*(3), 419-424. doi:10.1083/jcb.200111002

Aono, N., Sutani, T., Tomonaga, T., Mochida, S., & Yanagida, M. (2002). Cnd2 has dual roles in mitotic condensation and interphase. *Nature, 417*(6885), 197-202. doi:10.1038/417197a

Bardin, A. J., & Amon, A. (2001). Men and sin: what's the difference? *Nat Rev Mol Cell Biol, 2*(11), 815-826. doi:10.1038/35099020

Baxter, J., Sen, N., Martinez, V. L., De Carandini, M. E., Schvartzman, J. B., Diffley, J. F., & Aragon, L. (2011). Positive supercoiling of mitotic DNA drives decatenation by topoisomerase II in eukaryotes. *Science, 331*(6022), 1328-1332. doi:10.1126/science.1201538

Bazile, F., St-Pierre, J., & D'Amours, D. (2010). Three-step model for condensin activation during mitotic chromosome condensation. *Cell Cycle, 9*(16), 3243-3255. doi:10.4161/cc.9.16.12620

Bhalla, N., Biggins, S., & Murray, A. W. (2002). Mutation of YCS4, a budding yeast condensin subunit, affects mitotic and nonmitotic chromosome behavior. *Mol Biol Cell, 13*(2), 632-645. doi:10.1091/mbc.01-05-0264

Bhat, M. A., Philp, A. V., Glover, D. M., & Bellen, H. J. (1996). Chromatid segregation at anaphase requires the barren product, a novel chromosome-associated protein that interacts with Topoisomerase II. *Cell, 87*(6), 1103-1114.

Bhavsar-Jog, Y. P., & Bi, E. (2016). Mechanics and regulation of cytokinesis in budding yeast. *Semin Cell Dev Biol*. doi:10.1016/j.semcdb.2016.12.010

Booher, R. N., Deshaies, R. J., & Kirschner, M. W. (1993). Properties of Saccharomyces cerevisiae wee1 and its differential regulation of p34CDC28 in response to G1 and G2 cyclins. *EMBO J, 12*(9), 3417-3426.

Burrack, L. S., Applen Clancey, S. E., Chacon, J. M., Gardner, M. K., & Berman, J. (2013). Monopolin recruits condensin to organize centromere DNA and repetitive DNA sequences. *Mol Biol Cell, 24*(18), 2807-2819. doi:10.1091/mbc.E13-05-0229

Buster, D. W., Daniel, S. G., Nguyen, H. Q., Windler, S. L., Skwarek, L. C., Peterson, M., Roberts, M., Meserve, J. H., Hartl, T., Klebba, J. E., Bilder, D., Bosco, G., & Rogers, G. C. (2013). SCFSlimb ubiquitin ligase suppresses condensin II-mediated nuclear reorganization by degrading Cap-H2. *J Cell Biol, 201*(1), 49-63. doi:10.1083/jcb.201207183

Callegari, A. J., & Kelly, T. J. (2007). Shedding light on the DNA damage checkpoint. *Cell Cycle, 6*(6), 660-666. doi:10.4161/cc.6.6.3984

Choudhary, C., Kumar, C., Gnad, F., Nielsen, M. L., Rehman, M., Walther, T. C., Olsen, J. V., & Mann, M. (2009). Lysine acetylation targets protein complexes and co-regulates major cellular functions. *Science, 325*(5942), 834-840. doi:10.1126/science.1175371

Collette, K. S., Petty, E. L., Golenberg, N., Bembenek, J. N., & Csankovszki, G. (2011). Different roles for Aurora B in condensin targeting during mitosis and meiosis. *J Cell Sci, 124*(Pt 21), 3684-3694. doi:10.1242/jcs.088336

Coudreuse, D., & Nurse, P. (2010). Driving the cell cycle with a minimal CDK control network. *Nature, 468*(7327), 1074-1079. doi:10.1038/nature09543

Cross, F. R. (1995). Starting the cell cycle: what's the point? *Curr Opin Cell Biol, 7*(6), 790-797.

Csankovszki, G., Collette, K., Spahl, K., Carey, J., Snyder, M., Petty, E., Patel, U., Tabuchi, T., Liu, H., McLeod, I., Thompson, J., Sarkeshik, A., Yates, J., Meyer, B. J., & Hagstrom, K. (2009). Three distinct condensin complexes control C. elegans chromosome dynamics. *Curr Biol, 19*(1), 9-19. doi:10.1016/j.cub.2008.12.006

Cuylen, S., Metz, J., & Haering, C. H. (2011). Condensin structures chromosomal DNA through topological links. *Nat Struct Mol Biol, 18*(8), 894-901. doi:10.1038/nsmb.2087

D'Ambrosio, C., Schmidt, C. K., Katou, Y., Kelly, G., Itoh, T., Shirahige, K., & Uhlmann, F. (2008). Identification of cis-acting sites for condensin loading onto budding yeast chromosomes. *Genes Dev, 22*(16), 2215-2227. doi:10.1101/gad.1675708

D'Amours, D., Stegmeier, F., & Amon, A. (2004). Cdc14 and condensin control the dissolution of cohesin-independent chromosome linkages at repeated DNA. *Cell, 117*(4), 455-469.

De Keersmaecker, K., Porcu, M., Cox, L., Girardi, T., Vandepoel, R., de Beeck, J. O., Gielen, O., Mentens, N., Bennett, K. L., & Hantschel, O. (2014). NUP214-ABL1-mediated cell proliferation in T-cell acute lymphoblastic leukemia is dependent on the LCK kinase and various interacting proteins. *Haematologica, 99*(1), 85-93. doi:10.3324/haematol.2013.088674

Diffley, J. F. (2004). Regulation of early events in chromosome replication. *Curr Biol, 14*(18), R778-786. doi:10.1016/j.cub.2004.09.019

Dulev, S., Aragon, L., & Strunnikov, A. (2008). Unreplicated DNA in mitosis precludes condensin binding and chromosome condensation in S. cerevisiae. *Front Biosci, 13*, 5838-5846.

Earnshaw, W. C., Halligan, B., Cooke, C. A., Heck, M. M., & Liu, L. F. (1985). Topoisomerase II is a structural component of mitotic chromosome scaffolds. *J Cell Biol, 100*(5), 1706-1715.

Espinoza, F. H., Farrell, A., Erdjument-Bromage, H., Tempst, P., & Morgan, D. O. (1996). A cyclin-dependent kinase-activating kinase (CAK) in budding yeast unrelated to vertebrate CAK. *Science, 273*(5282), 1714-1717.

Finley, D., Ulrich, H. D., Sommer, T., & Kaiser, P. (2012). The ubiquitin-proteasome system of Saccharomyces cerevisiae. *Genetics, 192*(2), 319-360. doi:10.1534/genetics.112.140467

Flemming, W. (1882). Zellsubstanz, kern und zelltheilung. *F.C.W Vogel, Leipzig*.

Franz, A., Ackermann, L., & Hoppe, T. (2016). Ring of Change: CDC48/p97 Drives Protein Dynamics at Chromatin. *Front Genet, 7*, 73. doi:10.3389/fgene.2016.00073

Freeman, L., Aragon-Alcaide, L., & Strunnikov, A. (2000). The condensin complex governs chromosome condensation and mitotic transmission of rDNA. *J Cell Biol, 149*(4), 811-824.

Gasser, S. M., Laroche, T., Falquet, J., Boy de la Tour, E., & Laemmli, U. K. (1986). Metaphase chromosome structure. Involvement of topoisomerase II. *J Mol Biol, 188*(4), 613-629.

Gerlich, D., Hirota, T., Koch, B., Peters, J. M., & Ellenberg, J. (2006). Condensin I stabilizes chromosomes mechanically through a dynamic interaction in live cells. *Curr Biol, 16*(4), 333-344. doi:10.1016/j.cub.2005.12.040

Giet, R., & Glover, D. M. (2001). Drosophila aurora B kinase is required for histone H3 phosphorylation and condensin recruitment during chromosome condensation and to organize the central spindle during cytokinesis. *J Cell Biol, 152*(4), 669-682.

Graumann, P. L., & Knust, T. (2009). Dynamics of the bacterial SMC complex and SMC-like proteins involved in DNA repair. *Chromosome Res, 17*(2), 265-275. doi:10.1007/s10577-008-9014-x

Guacci, V., Hogan, E., & Koshland, D. (1994). Chromosome condensation and sister chromatid pairing in budding yeast. *J Cell Biol, 125*(3), 517-530.

Guertin, D. A., Trautmann, S., & McCollum, D. (2002). Cytokinesis in eukaryotes. *Microbiol Mol Biol Rev, 66*(2), 155-178.

Gurley, L. R., D'Anna, J. A., Barham, S. S., Deaven, L. L., & Tobey, R. A. (1978). Histone phosphorylation and chromatin structure during mitosis in Chinese hamster cells. *Eur J Biochem, 84*(1), 1-15.

Haering, C. H., Lowe, J., Hochwagen, A., & Nasmyth, K. (2002). Molecular architecture of SMC proteins and the yeast cohesin complex. *Mol Cell, 9*(4), 773-788.

Ham, M. F., Takakuwa, T., Rahadiani, N., Tresnasari, K., Nakajima, H., & Aozasa, K. (2007). Condensin mutations and abnormal chromosomal structures in

pyothorax-associated lymphoma. *Cancer Sci, 98*(7), 1041-1047. doi:10.1111/j.1349-7006.2007.00500.x

Heale, J. T., Ball, A. R., Jr., Schmiesing, J. A., Kim, J. S., Kong, X., Zhou, S., Hudson, D. F., Earnshaw, W. C., & Yokomori, K. (2006). Condensin I interacts with the PARP-1-XRCC1 complex and functions in DNA single-strand break repair. *Mol Cell, 21*(6), 837-848. doi:10.1016/j.molcel.2006.01.036

Herskowitz, I. (1988). Life cycle of the budding yeast Saccharomyces cerevisiae. *Microbiol Rev, 52*(4), 536-553.

Hiraga, S. (2000). Dynamic localization of bacterial and plasmid chromosomes. *Annu Rev Genet, 34*, 21-59. doi:10.1146/annurev.genet.34.1.21

Hirano, M., Anderson, D. E., Erickson, H. P., & Hirano, T. (2001). Bimodal activation of SMC ATPase by intra- and inter-molecular interactions. *EMBO J, 20*(12), 3238-3250. doi:10.1093/emboj/20.12.3238

Hirano, T. (2005). Condensins: organizing and segregating the genome. *Curr Biol, 15*(7), R265-275. doi:10.1016/j.cub.2005.03.037

Hirano, T. (2006). At the heart of the chromosome: SMC proteins in action. *Nat Rev Mol Cell Biol, 7*(5), 311-322. doi:10.1038/nrm1909

Hirano, T. (2012). Condensins: universal organizers of chromosomes with diverse functions. *Genes Dev, 26*(15), 1659-1678. doi:10.1101/gad.194746.112

Hirano, T. (2016). Condensin-Based Chromosome Organization from Bacteria to Vertebrates. *Cell, 164*(5), 847-857. doi:10.1016/j.cell.2016.01.033

Hirano, T., Kobayashi, R., & Hirano, M. (1997). Condensins, chromosome condensation protein complexes containing XCAP-C, XCAP-E and a Xenopus homolog of the Drosophila Barren protein. *Cell, 89*(4), 511-521.

Hirano, T., & Mitchison, T. J. (1994). A heterodimeric coiled-coil protein required for mitotic chromosome condensation in vitro. *Cell, 79*(3), 449-458.

Hudson, D. F., Ohta, S., Freisinger, T., Macisaac, F., Sennels, L., Alves, F., Lai, F., Kerr, A., Rappsilber, J., & Earnshaw, W. C. (2008). Molecular and genetic analysis of condensin function in vertebrate cells. *Mol Biol Cell, 19*(7), 3070-3079. doi:10.1091/mbc.E08-01-0057

Jentsch, S., & Rumpf, S. (2007). Cdc48 (p97): a "molecular gearbox" in the ubiquitin pathway? *Trends Biochem Sci, 32*(1), 6-11. doi:10.1016/j.tibs.2006.11.005

Jenuwein, T., & Allis, C. D. (2001). Translating the histone code. *Science, 293*(5532), 1074-1080. doi:10.1126/science.1063127

Joglekar, A. P. (2016). A Cell Biological Perspective on Past, Present and Future Investigations of the Spindle Assembly Checkpoint. *Biology (Basel), 5*(4). doi:10.3390/biology5040044

Johzuka, K., & Horiuchi, T. (2009). The cis element and factors required for condensin recruitment to chromosomes. *Mol Cell, 34*(1), 26-35. doi:10.1016/j.molcel.2009.02.021

Kagami, Y., Nihira, K., Wada, S., Ono, M., Honda, M., & Yoshida, K. (2014). Mps1 phosphorylation of condensin II controls chromosome condensation at the onset of mitosis. *J Cell Biol, 205*(6), 781-790. doi:10.1083/jcb.201308172

Kaitna, S., Pasierbek, P., Jantsch, M., Loidl, J., & Glotzer, M. (2002). The aurora B kinase AIR-2 regulates kinetochores during mitosis and is required for separation of homologous Chromosomes during meiosis. *Curr Biol, 12*(10), 798-812.

Kaldis, P., Sutton, A., & Solomon, M. J. (1996). The Cdk-activating kinase (CAK) from budding yeast. *Cell, 86*(4), 553-564.

Karve, T. M., & Cheema, A. K. (2011). Small changes huge impact: the role of protein posttranslational modifications in cellular homeostasis and disease. *J Amino Acids, 2011*, 207691. doi:10.4061/2011/207691

Kerscher, O., Felberbaum, R., & Hochstrasser, M. (2006). Modification of proteins by ubiquitin and ubiquitin-like proteins. *Annu Rev Cell Dev Biol, 22*, 159-180. doi:10.1146/annurev.cellbio.22.010605.093503

Kim, J. H., Shim, J., Ji, M. J., Jung, Y., Bong, S. M., Jang, Y. J., Yoon, E. K., Lee, S. J., Kim, K. G., Kim, Y. H., Lee, C., Lee, B. I., & Kim, K. T. (2014). The condensin component NCAPG2 regulates microtubule-kinetochore attachment through recruitment of Polo-like kinase 1 to kinetochores. *Nat Commun, 5*, 4588. doi:10.1038/ncomms5588

Kim, W., Bennett, E. J., Huttlin, E. L., Guo, A., Li, J., Possemato, A., Sowa, M. E., Rad, R., Rush, J., Comb, M. J., Harper, J. W., & Gygi, S. P. (2011). Systematic and quantitative assessment of the ubiquitin-modified proteome. *Mol Cell, 44*(2), 325-340. doi:10.1016/j.molcel.2011.08.025

Kimura, K., Hirano, M., Kobayashi, R., & Hirano, T. (1998). Phosphorylation and activation of 13S condensin by Cdc2 in vitro. *Science, 282*(5388), 487-490.

Kimura, K., & Hirano, T. (1997). ATP-dependent positive supercoiling of DNA by 13S condensin: a biochemical implication for chromosome condensation. *Cell, 90*(4), 625-634.

King, R. W., Peters, J. M., Tugendreich, S., Rolfe, M., Hieter, P., & Kirschner, M. W. (1995). A 20S complex containing CDC27 and CDC16 catalyzes the mitosis-specific conjugation of ubiquitin to cyclin B. *Cell, 81*(2), 279-288.

Kinoshita, K., Kobayashi, T. J., & Hirano, T. (2015). Balancing acts of two HEAT subunits of condensin I support dynamic assembly of chromosome axes. *Dev Cell, 33*(1), 94-106. doi:10.1016/j.devcel.2015.01.034

Koivomagi, M., Valk, E., Venta, R., Iofik, A., Lepiku, M., Morgan, D. O., & Loog, M. (2011). Dynamics of Cdk1 substrate specificity during the cell cycle. *Mol Cell, 42*(5), 610-623. doi:10.1016/j.molcel.2011.05.016

Kong, X., Stephens, J., Ball, A. R., Jr., Heale, J. T., Newkirk, D. A., Berns, M. W., & Yokomori, K. (2011). Condensin I recruitment to base damage-enriched DNA lesions is modulated by PARP1. *PLoS One, 6*(8), e23548. doi:10.1371/journal.pone.0023548

Kornberg, R. D. (1974). Chromatin structure: a repeating unit of histones and DNA. *Science, 184*(4139), 868-871.

Kornberg, R. D., & Thomas, J. O. (1974). Chromatin structure; oligomers of the histones. *Science, 184*(4139), 865-868.

Lammens, A., Schele, A., & Hopfner, K. P. (2004). Structural biochemistry of ATP-driven dimerization and DNA-stimulated activation of SMC ATPases. *Curr Biol, 14*(19), 1778-1782. doi:10.1016/j.cub.2004.09.044

Lavoie, B. D., Hogan, E., & Koshland, D. (2004). In vivo requirements for rDNA chromosome condensation reveal two cell-cycle-regulated pathways for

mitotic chromosome folding. *Genes Dev, 18*(1), 76-87. doi:10.1101/gad.1150404

Lavoie, B. D., Tuffo, K. M., Oh, S., Koshland, D., & Holm, C. (2000). Mitotic chromosome condensation requires Brn1p, the yeast homologue of Barren. *Mol Biol Cell, 11*(4), 1293-1304.

Lee, K. K., & Workman, J. L. (2007). Histone acetyltransferase complexes: one size doesn't fit all. *Nat Rev Mol Cell Biol, 8*(4), 284-295. doi:10.1038/nrm2145

Lin, Y. Y., Lu, J. Y., Zhang, J., Walter, W., Dang, W., Wan, J., Tao, S. C., Qian, J., Zhao, Y., Boeke, J. D., Berger, S. L., & Zhu, H. (2009). Protein acetylation microarray reveals that NuA4 controls key metabolic target regulating gluconeogenesis. *Cell, 136*(6), 1073-1084. doi:10.1016/j.cell.2009.01.033

Linger, J. G., & Tyler, J. K. (2007). Chromatin disassembly and reassembly during DNA repair. *Mutat Res, 618*(1-2), 52-64. doi:10.1016/j.mrfmmm.2006.05.039

Lipp, J. J., Hirota, T., Poser, I., & Peters, J. M. (2007). Aurora B controls the association of condensin I but not condensin II with mitotic chromosomes. *J Cell Sci, 120*(Pt 7), 1245-1255. doi:10.1242/jcs.03425

Liu, W., Tanasa, B., Tyurina, O. V., Zhou, T. Y., Gassmann, R., Liu, W. T., Ohgi, K. A., Benner, C., Garcia-Bassets, I., Aggarwal, A. K., Desai, A., Dorrestein, P. C., Glass, C. K., & Rosenfeld, M. G. (2010). PHF8 mediates histone H4 lysine 20 demethylation events involved in cell cycle progression. *Nature, 466*(7305), 508-512. doi:10.1038/nature09272

Lupo, R., Breiling, A., Bianchi, M. E., & Orlando, V. (2001). Drosophila chromosome condensation proteins Topoisomerase II and Barren colocalize with Polycomb and maintain Fab-7 PRE silencing. *Mol Cell, 7*(1), 127-136.

Maeshima, K., & Eltsov, M. (2008). Packaging the genome: the structure of mitotic chromosomes. *J Biochem, 143*(2), 145-153. doi:10.1093/jb/mvm214

Maeshima, K., Hihara, S., & Eltsov, M. (2010). Chromatin structure: does the 30-nm fibre exist in vivo? *Curr Opin Cell Biol, 22*(3), 291-297. doi:10.1016/j.ceb.2010.03.001

Magalska, A., Schellhaus, A. K., Moreno-Andres, D., Zanini, F., Schooley, A., Sachdev, R., Schwarz, H., Madlung, J., & Antonin, W. (2014). RuvB-like ATPases

function in chromatin decondensation at the end of mitosis. *Dev Cell, 31*(3), 305-318. doi:10.1016/j.devcel.2014.09.001

Maric, M., Maculins, T., De Piccoli, G., & Labib, K. (2014). Cdc48 and a ubiquitin ligase drive disassembly of the CMG helicase at the end of DNA replication. *Science, 346*(6208), 1253596. doi:10.1126/science.1253596

Marston, A. L. (2014). Chromosome segregation in budding yeast: sister chromatid cohesion and related mechanisms. *Genetics, 196*(1), 31-63. doi:10.1534/genetics.112.145144

McKinley, K. L., & Cheeseman, I. M. (2016). The molecular basis for centromere identity and function. *Nat Rev Mol Cell Biol, 17*(1), 16-29. doi:10.1038/nrm.2015.5

Meyer, H., & Weihl, C. C. (2014). The VCP/p97 system at a glance: connecting cellular function to disease pathogenesis. *J Cell Sci, 127*(Pt 18), 3877-3883. doi:10.1242/jcs.093831

Michaelis, C., Ciosk, R., & Nasmyth, K. (1997). Cohesins: chromosomal proteins that prevent premature separation of sister chromatids. *Cell, 91*(1), 35-45.

Moir, D., Stewart, S. E., Osmond, B. C., & Botstein, D. (1982). Cold-sensitive cell-division-cycle mutants of yeast: isolation, properties, and pseudoreversion studies. *Genetics, 100*(4), 547-563.

Moreno, S., & Nurse, P. (1990). Substrates for p34cdc2: in vivo veritas? *Cell, 61*(4), 549-551.

Morgan, D. O. (2007). The Cell Cycle: Principles of Control. *New Science Press, London*.

Morgan, T. H. (1915). Localization of the Hereditary Material in the Germ Cells. *Proc Natl Acad Sci U S A, 1*(7), 420-429.

Mullally, J. E., Chernova, T., & Wilkinson, K. D. (2006). Doa1 is a Cdc48 adapter that possesses a novel ubiquitin binding domain. *Mol Cell Biol, 26*(3), 822-830. doi:10.1128/MCB.26.3.822-830.2006

Nakazawa, N., Mehrotra, R., Ebe, M., & Yanagida, M. (2011). Condensin phosphorylated by the Aurora-B-like kinase Ark1 is continuously required

until telophase in a mode distinct from Top2. *J Cell Sci, 124*(Pt 11), 1795-1807. doi:10.1242/jcs.078733

Nano, N., & Houry, W. A. (2013). Chaperone-like activity of the AAA+ proteins Rvb1 and Rvb2 in the assembly of various complexes. *Philos Trans R Soc Lond B Biol Sci, 368*(1617), 20110399. doi:10.1098/rstb.2011.0399

Nasmyth, K., & Haering, C. H. (2005). The structure and function of SMC and kleisin complexes. *Annu Rev Biochem, 74*, 595-648. doi:10.1146/annurev.biochem.74.082803.133219

Nasmyth, K., & Haering, C. H. (2009). Cohesin: its roles and mechanisms. *Annu Rev Genet, 43*, 525-558. doi:10.1146/annurev-genet-102108-134233

Nigg, E. A. (1993). Cellular substrates of p34(cdc2) and its companion cyclin-dependent kinases. *Trends Cell Biol, 3*(9), 296-301.

Nitiss, J. L. (2009). DNA topoisomerase II and its growing repertoire of biological functions. *Nat Rev Cancer, 9*(5), 327-337. doi:10.1038/nrc2608

Nurse, P., Masui, Y., & Hartwell, L. (1998). Understanding the cell cycle. *Nat Med, 4*(10), 1103-1106. doi:10.1038/2594

Nyberg, K. A., Michelson, R. J., Putnam, C. W., & Weinert, T. A. (2002). Toward maintaining the genome: DNA damage and replication checkpoints. *Annu Rev Genet, 36*, 617-656. doi:10.1146/annurev.genet.36.060402.113540

Oliveira, R. A., Heidmann, S., & Sunkel, C. E. (2007). Condensin I binds chromatin early in prophase and displays a highly dynamic association with Drosophila mitotic chromosomes. *Chromosoma, 116*(3), 259-274. doi:10.1007/s00412-007-0097-5

Oshikawa, K., Matsumoto, M., Oyamada, K., & Nakayama, K. I. (2012). Proteome-wide identification of ubiquitylation sites by conjugation of engineered lysine-less ubiquitin. *J Proteome Res, 11*(2), 796-807. doi:10.1021/pr200668y

Ouspenski, II, Cabello, O. A., & Brinkley, B. R. (2000). Chromosome condensation factor Brn1p is required for chromatid separation in mitosis. *Mol Biol Cell, 11*(4), 1305-1313.

Paulson, J. R., & Taylor, S. S. (1982). Phosphorylation of histones 1 and 3 and nonhistone high mobility group 14 by an endogenous kinase in HeLa metaphase chromosomes. *J Biol Chem, 257*(11), 6064-6072.

Peters, J. M., Tedeschi, A., & Schmitz, J. (2008). The cohesin complex and its roles in chromosome biology. *Genes Dev, 22*(22), 3089-3114. doi:10.1101/gad.1724308

Povlsen, L. K., Beli, P., Wagner, S. A., Poulsen, S. L., Sylvestersen, K. B., Poulsen, J. W., Nielsen, M. L., Bekker-Jensen, S., Mailand, N., & Choudhary, C. (2012). Systems-wide analysis of ubiquitylation dynamics reveals a key role for PAF15 ubiquitylation in DNA-damage bypass. *Nat Cell Biol, 14*(10), 1089-1098. doi:10.1038/ncb2579

Pye, V. E., Beuron, F., Keetch, C. A., McKeown, C., Robinson, C. V., Meyer, H. H., Zhang, X., & Freemont, P. S. (2007). Structural insights into the p97-Ufd1-Npl4 complex. *Proc Natl Acad Sci U S A, 104*(2), 467-472. doi:10.1073/pnas.0603408104

Rhind, N., & Russell, P. (1998). Mitotic DNA damage and replication checkpoints in yeast. *Curr Opin Cell Biol, 10*(6), 749-758.

Saitoh, N., Goldberg, I. G., Wood, E. R., & Earnshaw, W. C. (1994). ScII: an abundant chromosome scaffold protein is a member of a family of putative ATPases with an unusual predicted tertiary structure. *J Cell Biol, 127*(2), 303-318.

Saka, Y., Sutani, T., Yamashita, Y., Saitoh, S., Takeuchi, M., Nakaseko, Y., & Yanagida, M. (1994). Fission yeast cut3 and cut14, members of a ubiquitous protein family, are required for chromosome condensation and segregation in mitosis. *EMBO J, 13*(20), 4938-4952.

Shintomi, K., & Hirano, T. (2011). The relative ratio of condensin I to II determines chromosome shapes. *Genes Dev, 25*(14), 1464-1469. doi:10.1101/gad.2060311

Shintomi, K., Takahashi, T. S., & Hirano, T. (2015). Reconstitution of mitotic chromatids with a minimum set of purified factors. *Nat Cell Biol, 17*(8), 1014-1023. doi:10.1038/ncb3187

Smoyer, C. J., & Jaspersen, S. L. (2014). Breaking down the wall: the nuclear envelope during mitosis. *Curr Opin Cell Biol, 26*, 1-9. doi:10.1016/j.ceb.2013.08.002

St-Pierre, J., Douziech, M., Bazile, F., Pascariu, M., Bonneil, E., Sauve, V., Ratsima, H., & D'Amours, D. (2009). Polo kinase regulates mitotic chromosome condensation by hyperactivation of condensin DNA supercoiling activity. *Mol Cell, 34*(4), 416-426. doi:10.1016/j.molcel.2009.04.013

Stegmeier, F., & Amon, A. (2004). Closing mitosis: the functions of the Cdc14 phosphatase and its regulation. *Annu Rev Genet, 38*, 203-232. doi:10.1146/annurev.genet.38.072902.093051

Stern, B., & Nurse, P. (1996). A quantitative model for the cdc2 control of S phase and mitosis in fission yeast. *Trends Genet, 12*(9), 345-350.

Straight, A. F., Marshall, W. F., Sedat, J. W., & Murray, A. W. (1997). Mitosis in living budding yeast: anaphase A but no metaphase plate. *Science, 277*(5325), 574-578.

Strunnikov, A. V., Hogan, E., & Koshland, D. (1995). SMC2, a Saccharomyces cerevisiae gene essential for chromosome segregation and condensation, defines a subgroup within the SMC family. *Genes Dev, 9*(5), 587-599.

Sutani, T., & Yanagida, M. (1997). DNA renaturation activity of the SMC complex implicated in chromosome condensation. *Nature, 388*(6644), 798-801. doi:10.1038/42062

Sutani, T., Yuasa, T., Tomonaga, T., Dohmae, N., Takio, K., & Yanagida, M. (1999). Fission yeast condensin complex: essential roles of non-SMC subunits for condensation and Cdc2 phosphorylation of Cut3/SMC4. *Genes Dev, 13*(17), 2271-2283.

Swaney, D. L., Beltrao, P., Starita, L., Guo, A., Rush, J., Fields, S., Krogan, N. J., & Villen, J. (2013). Global analysis of phosphorylation and ubiquitylation cross-talk in protein degradation. *Nat Methods, 10*(7), 676-682. doi:10.1038/nmeth.2519

Swedlow, J. R., & Hirano, T. (2003). The making of the mitotic chromosome: modern insights into classical questions. *Mol Cell, 11*(3), 557-569.

Tada, K., Susumu, H., Sakuno, T., & Watanabe, Y. (2011). Condensin association with histone H2A shapes mitotic chromosomes. *Nature, 474*(7352), 477-483. doi:10.1038/nature10179

Takemoto, A., Kimura, K., Yanagisawa, J., Yokoyama, S., & Hanaoka, F. (2006). Negative regulation of condensin I by CK2-mediated phosphorylation. *EMBO J, 25*(22), 5339-5348. doi:10.1038/sj.emboj.7601394

Tanaka, A., Tanizawa, H., Sriswasdi, S., Iwasaki, O., Chatterjee, A. G., Speicher, D. W., Levin, H. L., Noguchi, E., & Noma, K. (2012). Epigenetic regulation of condensin-mediated genome organization during the cell cycle and upon DNA damage through histone H3 lysine 56 acetylation. *Mol Cell, 48*(4), 532-546. doi:10.1016/j.molcel.2012.09.011

Toselli-Mollereau, E., Robellet, X., Fauque, L., Lemaire, S., Schiklenk, C., Klein, C., Hocquet, C., Legros, P., N'Guyen, L., Mouillard, L., Chautard, E., Auboeuf, D., Haering, C. H., & Bernard, P. (2016). Nucleosome eviction in mitosis assists condensin loading and chromosome condensation. *EMBO J, 35*(14), 1565-1581. doi:10.15252/embj.201592849

Tsang, C. K., & Zheng, X. F. (2009). Opposing role of condensin and radiation-sensitive gene RAD52 in ribosomal DNA stability regulation. *J Biol Chem, 284*(33), 21908-21919. doi:10.1074/jbc.M109.031302

Uemura, T., Ohkura, H., Adachi, Y., Morino, K., Shiozaki, K., & Yanagida, M. (1987). DNA topoisomerase II is required for condensation and separation of mitotic chromosomes in S. pombe. *Cell, 50*(6), 917-925.

Uhlmann, F. (2016). SMC complexes: from DNA to chromosomes. *Nat Rev Mol Cell Biol, 17*(7), 399-412. doi:10.1038/nrm.2016.30

Uhlmann, F., Lottspeich, F., & Nasmyth, K. (1999). Sister-chromatid separation at anaphase onset is promoted by cleavage of the cohesin subunit Scc1. *Nature, 400*(6739), 37-42. doi:10.1038/21831

Van Hooser, A., Goodrich, D. W., Allis, C. D., Brinkley, B. R., & Mancini, M. A. (1998). Histone H3 phosphorylation is required for the initiation, but not maintenance, of mammalian chromosome condensation. *J Cell Sci, 111 (Pt 23)*, 3497-3506.

Venema, J., & Tollervey, D. (1999). Ribosome synthesis in Saccharomyces cerevisiae. *Annu Rev Genet, 33*, 261-311. doi:10.1146/annurev.genet.33.1.261

Verma, R., Annan, R. S., Huddleston, M. J., Carr, S. A., Reynard, G., & Deshaies, R. J. (1997). Phosphorylation of Sic1p by G1 Cdk required for its degradation and entry into S phase. *Science, 278*(5337), 455-460.

Wagner, S. A., Beli, P., Weinert, B. T., Nielsen, M. L., Cox, J., Mann, M., & Choudhary, C. (2011). A proteome-wide, quantitative survey of in vivo ubiquitylation sites reveals widespread regulatory roles. *Mol Cell Proteomics, 10*(10), M111 013284. doi:10.1074/mcp.M111.013284

Weber, C. M., & Henikoff, S. (2014). Histone variants: dynamic punctuation in transcription. *Genes Dev, 28*(7), 672-682. doi:10.1101/gad.238873.114

Wei, Y., Yu, L., Bowen, J., Gorovsky, M. A., & Allis, C. D. (1999). Phosphorylation of histone H3 is required for proper chromosome condensation and segregation. *Cell, 97*(1), 99-109.

Winey, M., & O'Toole, E. T. (2001). The spindle cycle in budding yeast. *Nat Cell Biol, 3*(1), E23-27. doi:10.1038/35050663

Wood, J. L., Liang, Y., Li, K., & Chen, J. (2008). Microcephalin/MCPH1 associates with the Condensin II complex to function in homologous recombination repair. *J Biol Chem, 283*(43), 29586-29592. doi:10.1074/jbc.M804080200

Zhang, C., Kuang, M., Li, M., Feng, L., Zhang, K., & Cheng, S. (2016). SMC4, which is essentially involved in lung development, is associated with lung adenocarcinoma progression. *Sci Rep, 6*, 34508. doi:10.1038/srep34508

Zhou, B., Yuan, T., Liu, M., Liu, H., Xie, J., Shen, Y., & Chen, P. (2012). Overexpression of the structural maintenance of chromosome 4 protein is associated with tumor de-differentiation, advanced stage and vascular invasion of primary liver cancer. *Oncol Rep, 28*(4), 1263-1268. doi:10.3892/or.2012.1929